

REPORT NO.  
UCB/EERC-89/05  
JULY 1989

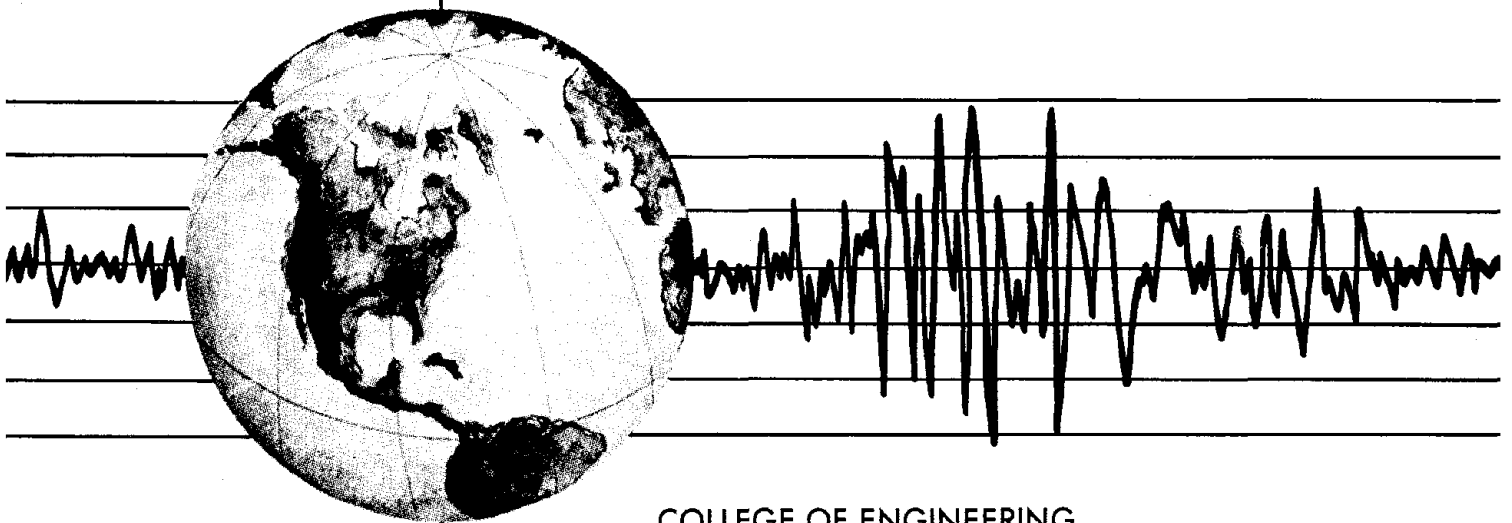
EARTHQUAKE ENGINEERING RESEARCH CENTER

# THE 1985 CHILE EARTHQUAKE: AN EVALUATION OF STRUCTURAL REQUIREMENTS FOR BEARING WALL BUILDINGS

by

JOHN W. WALLACE  
JACK P. MOEHLE

Report to the National Science Foundation



COLLEGE OF ENGINEERING

UNIVERSITY OF CALIFORNIA AT BERKELEY

REPRODUCED BY  
U.S. DEPARTMENT OF COMMERCE  
NATIONAL TECHNICAL  
INFORMATION SERVICE  
SPRINGFIELD, VA 22161

For sale by the National Technical Information Service, U.S. Department of Commerce, Springfield, Virginia 22161

See back of report for up to date listing of EERC reports.

**DISCLAIMER**

Any opinions, findings, and conclusions or recommendations expressed in this publication are those of the authors and do not necessarily reflect the views of the National Science Foundation or the Earthquake Engineering Research Center, University of California at Berkeley.

*i.a*

**THE 1985 CHILE EARTHQUAKE:  
AN EVALUATION OF STRUCTURAL REQUIREMENTS  
FOR BEARING WALL BUILDINGS**

by

John W. Wallace

and

Jack P. Moehle

**A Report to Sponsor:  
National Science Foundation**

**Report No. UCB/EERC-89/05  
Earthquake Engineering Research Center  
College of Engineering  
University of California at Berkeley**

**July 1989**



## ABSTRACT

Detailing requirements for bearing wall buildings were evaluated based on data obtained from the 3 March 1985 Chile earthquake. The epicenter of the surface magnitude 7.8 earthquake was located approximately 80 km from the city of Viña del Mar, where more than 400 modern reinforced concrete buildings existed. A strong-motion instrument recorded the ground motion in Viña del Mar. Four buildings in Viña del Mar were selected to study building performance during the 3 March 1985 earthquake.

The buildings were analyzed to compare Chilean and U.S. code requirements and to estimate deformation demands. Response spectrum and response history analyses were conducted to investigate building performance for the recorded earthquake ground motions. The effects of soil-structure interaction were addressed using detailed and simplified procedures. Performance of bearing wall buildings subjected to a spectrum of recorded U.S. ground motions is evaluated.

This report documents the study and makes recommendations for the design of bearing wall buildings.

## ACKNOWLEDGEMENTS

The work in this report was funded by the National Science Foundation under Grant No. ECE 86-06089. Opinions, findings, conclusions, and recommendations in this report are those of the authors, and do not necessarily represent those of the sponsor. The work was part of a cooperative project that included participants from the University of Illinois, the University of Michigan, and the Pontificia Universidad Católica de Chile.

Professors Vitelmo V. Bertero and Rene DeVogelaere are thanked for their advice and comments on this report. Professor Edward L. Wilson is thanked for assistance in the use of the SAP80 computer program.

Professor H. Bolton Seed is thanked for his valuable assistance in evaluating soil properties and site response. The time spent by his graduate student, Joseph Sun, is appreciated.

Mete A. Sozen, Sharon L. Wood, James K. Wight, Rafael Riddell and Roberto Stark are thanked for their valuable discussion and suggestions during the study. Special thanks are expressed to Shyh-Jiann Hwang, Stavroula Pantazopoulou, Bahram Shahrooz, and Rochus Bergmann for providing valuable advice and encouragement throughout this project.

# TABLE OF CONTENTS

ABSTRACT .....	i
ACKNOWLEDGMENTS .....	ii
TABLE OF CONTENTS .....	iii
LIST OF TABLES .....	vi
LIST OF FIGURES .....	vii
1. INTRODUCTION .....	1
1.1 Introduction .....	1
1.2 Objectives and Scope .....	2
2. STRUCTURAL ENGINEERING PRACTICE IN CHILE .....	5
2.1 Design Philosophy .....	5
2.2 Seismic Code Requirements .....	6
2.3 Reinforced Concrete Construction .....	8
2.4 Construction and Inspection .....	11
2.5 Summary .....	12
3. THE 3 MARCH 1985 CHILE EARTHQUAKE .....	13
3.1 General Information and Characteristics .....	13
3.2 Strong-Motion Instrumentation .....	14
3.2.1 The Recorded Ground Motions .....	15
3.2.2 Intensities .....	16
3.2.3 Response Spectra .....	17
3.3 Summary .....	20
4. SOIL EFFECTS ON GROUND MOTIONS .....	22
4.1 Soil Characteristics and Engineering Properties .....	22
4.1.1 General Geological Characteristics .....	22
4.1.2 Engineering Properties of the Foundation Materials .....	23
4.2 Geologic Effects on Ground Motions .....	26
4.2.1 Recorded 3 March 1985 Earthquake Ground Motions .....	26
4.2.2 Recorded Aftershock Ground Motions .....	27
4.2.3 Analysis and Interpretation of the Recorded Data .....	28
4.3 Site Response Analysis Using Horizontally Layered Soils .....	30
4.4 Summary .....	32

5. ELEMENT MODELING TECHNIQUES .....	33
5.1 Elastic Modeling Techniques .....	33
5.1.1 Beam and Slab Elements .....	33
5.1.2 Wall Elements .....	34
5.2 Inelastic Modeling Techniques .....	35
5.2.1 Beam and Slab Elements .....	36
5.2.2 Wall Elements .....	39
5.3 Strength Analysis Modeling .....	40
6. EFFECT OF FOUNDATION MATERIALS ON BUILDING RESPONSE .....	41
6.1 Soil-Structure Interaction Effects .....	41
6.2 Linear Soil-Structure Interaction Analysis .....	42
6.3 Simplified Procedures .....	43
6.3.1 Elastic Half Space .....	44
6.3.2 ATC-3-06 Procedure .....	44
6.4 Recorded Information on Soil-Structure Interaction .....	47
6.5 Analysis of Torres del Miramar Building .....	48
6.5.1 Building Model .....	48
6.5.2 Soil Model .....	49
6.5.3 Analysis Results .....	50
6.6 Simplified Analysis Using ATC-3-06 Procedure .....	53
6.7 Summary .....	53
7. EVALUATION OF FOUR BUILDINGS IN VIÑA DEL MAR .....	55
7.1 Description of Buildings Studied .....	55
7.2 Construction Materials .....	56
7.3 General Design Considerations .....	57
7.4 Results of Elastic Building Analyses .....	59
7.4.1 Periods and Mode Shapes .....	60
7.4.2 Code Analysis .....	61
7.5 Strength Analysis .....	63
7.5.1 Plaza del Mar Building .....	65
7.5.2 Festival Building .....	66
7.5.3 Acapulco Building .....	68
7.5.4 Torres de Miramar Building .....	71
7.6 Dynamic Response Analysis for 3 March 1985 Earthquake .....	72
7.6.1 Elastic Response Spectrum Analysis .....	72

7.6.2 Inelastic Response History Analysis .....	74
7.7 Summary Evaluation .....	75
7.7.1 Plaza del Mar Building .....	75
7.7.2 Festival Building .....	76
7.7.3 Acapulco Building .....	78
7.7.4 Miramar Building .....	79
8. IMPLICATIONS FOR DESIGN OF BEARING WALL BUILDINGS .....	80
8.1 Code Strength Requirements for Structural Wall Buildings .....	81
8.1.1 Minimum Base Shear Strength for Code Requirements .....	81
8.1.2 Comparison of Code Strength Requirements .....	82
8.2 Comparison of Spectra for U.S. and Chilean Motions .....	84
8.3 Building Response Characteristics .....	87
8.3.1 Roof Drift .....	87
8.3.2 Displacement Ductility Requirements .....	89
8.4 Detailing Requirements for Bearing Wall Buildings .....	92
8.4.1 Required Curvature Ductility .....	93
8.4.2 Available Curvature Ductility .....	95
8.5 Summary .....	98
9. SUMMARY AND CONCLUSIONS .....	100
9.1 Summary .....	100
9.2 Conclusions .....	102
TABLES .....	104
FIGURES .....	120
APPENDIX A - Geotechnical Characteristics of Soil in Viña del Mar .....	255
APPENDIX B - Building Descriptions and Observed Damage .....	266
APPENDIX C - Material Properties .....	272
REFERENCES .....	274

## LIST OF TABLES

Table 2.1	Summary of Strong Earthquakes in Chile .....	104
Table 3.1	Strong-Motion Instrument Data .....	105
Table 3.2	Housner and Arias Intensities .....	105
Table 4.1	Typical Engineering Properties of Foundation Materials in Viña del Mar .....	106
Table 4.2	Computed Shear Wave Velocity from SPT Tests .....	107
Table 4.3	Computed Shear Wave Velocity for Eq. 4.5.2 .....	107
Table 4.4	Shear Wave Velocity for Site Response Analyses .....	108
Table 6.1	Soil Stiffness Modification .....	109
Table 6.2	Building Model Properties .....	109
Table 6.3	Soil Properties and Computed Periods .....	109
Table 6.4	Response Characteristics .....	110
Table 7.1	Computed Building Periods - 3D Models .....	111
Table 7.2	Computed Periods Including Soil-Structure Interaction .....	111
Table 7.3	Computed Damping Ratios Including Soil-Structure Interaction .....	112
Table 7.4	Code Design Requirements .....	112
Table 7.5	Strength Ratios for Several Chilean Walls .....	113
Table 7.6	Computed Base Shear Strengths .....	113
Table 7.7	Plaza del Mar Building Strength Calculations .....	114
Table 7.8	Festival Building Strength Calculations .....	115
Table 7.9	Acapulco Building Strength Calculations .....	116
Table 7.10	Computed Response Spectrum Drift Ratios .....	117
Table 7.11	Computed 3D Model Response Characteristics .....	117
Table 7.12	Computed SDOF Model Response Characteristics .....	118
Table 7.13	Effect of Torsion on Wall Forces – Acapulco Building .....	118
Table 8.1	Building Characteristics .....	119
Table 8.2	Recorded U.S. Ground Motions .....	119

## LIST OF FIGURES

Figure 2.1	Average Percent Wall Area Versus Building Height .....	120
Figure 2.2	Measured Periods for Chilean Buildings .....	121
Figure 2.3	Comparison of Code Spectra .....	122
Figure 2.4	Typical Wall Reinforcement .....	123
Figure 2.5	Typical Column Reinforcement – Plaza del Mar Building .....	124
Figure 2.6	Typical Beam Reinforcement – Plaza del Mar Building .....	125
Figure 2.7	Coupling Girder Reinforcement – Acapulco Building .....	126
Figure 2.8	Typical Slab Reinforcement – Festival Building .....	127
Figure 3.1	Epicenter and Intensity Map for 3 March 1985 Earthquake .....	128
Figure 3.2	Location of Strong-Motion Instruments in the Epicentral Region of 3 March 1985 Earthquake .....	129
Figure 3.3.a	Strong-Motion Record – Lloleco .....	130
Figure 3.3.b	Strong-Motion Record – Viña del Mar .....	131
Figure 3.3.c	Strong-Motion Record – Valparaíso .....	132
Figure 3.3.d	Strong-Motion Record – El Almendral .....	133
Figure 3.4	Strong-Motion Record – El Centro 1940 NS .....	134
Figure 3.5	Evolutionary Arias Intensity .....	135
Figure 3.6.a	Elastic Response Spectra – Lloleco .....	136
Figure 3.6.b	Elastic Response Spectra – Viña del Mar .....	137
Figure 3.6.c	Elastic Response Spectra – Valparaíso .....	138
Figure 3.6.d	Elastic Response Spectra – El Almendral .....	139
Figure 3.7	Elasto-Plastic Response Spectra .....	140
Figure 3.8	Bilinear Response Spectra .....	141
Figure 3.9	Comparison of Elastic Response Spectra from the 1940 El Centro and 1985 Viña del Mar Records (2% Damping) .....	142
Figure 3.10	Inelastic Response Spectra for the 1940 El Centro Record .....	143
Figure 4.1	Shear Modulus of Sand as a Function of Shear Strain .....	144
Figure 4.2	Three Estimates for Shear Wave Velocity .....	145
Figure 4.3.a	Comparison of Response Spectra for Rock and Soil Sites Valparaíso and Viña del Mar .....	146
Figure 4.3.b	Comparison of Response Spectra for Rock and Soil Sites Valparaíso and El Almendral .....	147

Figure 4.4	Building and Instrument Locations in Viña del Mar .....	148
Figure 4.5.a	Ratios of Fourier Spectral Velocity for Two Events Municipal Building (Viña del Mar) over Valparaíso .....	149
Figure 4.5.b	Ratios of Fourier Spectral Velocity for Two Events Edificio Acapulco (Viña del Mar) over Valparaíso .....	150
Figure 4.5.c	Ratios of Fourier Spectral Velocity for Two Events Torres de Miramar (Viña del Mar) over Valparaíso .....	151
Figure 4.6	Spectra for Site Response Analyses – Municipal Building .....	152
Figure 4.7	Spectra for Site Response Analyses – Beach Locations .....	153
Figure 5.1	Beam Effective Slab Width .....	154
Figure 5.2	Wide-Column Analogy for Slender Structural Walls .....	155
Figure 5.3	Structural Walls with Flange Sections .....	156
Figure 5.4	Connected Wide-Column Model for Slender Structural Walls .....	157
Figure 5.5	Three-Dimensional Frame-Wall Interaction .....	158
Figure 5.6	Definition of Section Properties for Inelastic Modeling .....	159
Figure 5.7	Procedure to Compute Properties of Trilinear Member End Springs ...	160
Figure 5.8	Model to Compute Fixed End Rotation due to Reinforced Slip .....	161
Figure 5.9	Bilinear Member End Springs for DRAIN-2D Program Modeling .....	162
Figure 6.1	Effect of Soil Flexibility on Building Response .....	163
Figure 6.2.a	Floor Plan of Torres de Miramar – Level 1 .....	164
Figure 6.2.b	Floor Plan of Torres de Miramar – Levels 3 and 5 .....	165
Figure 6.2.c	Elevation of Torres de Miramar – Axis a .....	166
Figure 6.2.d	Elevation of Torres de Miramar – Axis A .....	167
Figure 6.3	Torres de Miramar – Response History Characteristics Fixed and Flexible Bases .....	168
Figure 6.4	Torres de Miramar – Response History Characteristics Proportional and nonproportional Damping .....	169
Figure 6.5	Response Spectra – Viña del Mar S20W .....	170
Figure 6.6	Effect of Base Flexibility on Displacement .....	171
Figure 6.7	Effect of Base Flexibility on Base Shear .....	172
Figure 7.1	Locations of Buildings in Viña del Mar .....	173
Figure 7.2.a	Floor Plan of Plaza del Mar Building .....	174
Figure 7.2.b	Elevation of Plaza del Mar Building .....	175
Figure 7.3.a	First Floor Plan of Festival Building .....	176
Figure 7.3.b	Typical Floor Plan of Festival Building .....	177

Figure 7.3.c	Elevation of Festival Building .....	178
Figure 7.4.a	Typical Floor Plan of Acapulco Building .....	179
Figure 7.4.b	Elevation of Acapulco Building .....	180
Figure 7.5	Mode Shapes – Plaza del Mar Building .....	181
Figure 7.6	Mode Shapes – Festival Building .....	182
Figure 7.7	Mode Shapes – Acapulco Building .....	183
Figure 7.8	Mode Shapes – Torres de Miramar Building .....	184
Figure 7.9	Factored Code Spectra .....	185
Figure 7.10	Drift Ratios for Code Loads – Plaza del Mar Building .....	186
Figure 7.11	Drift Ratios for Code Loads – Festival Building .....	187
Figure 7.12	Drift Ratios for Code Loads – Acapulco Building .....	188
Figure 7.13	Drift Ratios for Code Loads – Torres de Miramar Building .....	189
Figure 7.14	Structural Walls Constructed in Chile .....	190
Figure 7.15	Code Comparison of Design Requirements for Structural Walls .....	191
Figure 7.16	Collapse Mechanisms .....	192
Figure 7.17	Plaza del Mar Building – Geometry and Steel Quantities .....	193
Figure 7.18	Festival Building – Geometry and Steel Quantities .....	194
Figure 7.19.a	Acapulco Building – Beam Designations for Strength Calculations ....	195
Figure 7.19.b	Acapulco Building – Beam Geometry and Steel Ratios .....	196
Figure 7.20	Collapse Mechanism for Wall Yielding .....	197
Figure 7.21.a	Acapulco Building – Wall Designations for Strength Calculations ....	198
Figure 7.21.b	Acapulco Building – Wall Geometry and Steel Quantities Wall A .....	199
Figure 7.21.c	Acapulco Building – Wall Geometry and Steel Quantities Walls B, D1, G, H, and I (assumed for D2) .....	200
Figure 7.21.d	Acapulco Building – Wall Geometry and Steel Quantities Wall C .....	201
Figure 7.21.e	Acapulco Building – Wall Geometry and Steel Quantities Walls D3 and D4 .....	202
Figure 7.21.f	Acapulco Building – Wall Geometry and Steel Quantities Wall E1 .....	203
Figure 7.21.g	Acapulco Building – Wall Geometry and Steel Quantities Walls E2 and E3 .....	204
Figure 7.21.h	Acapulco Building – Wall Geometry and Steel Quantities Wall F1 .....	205

Figure 7.21.i	Acapulco Building – Wall Geometry and Steel Quantities Walls F2 and F3 .....	206
Figure 7.21.j	Acapulco Building – Wall Geometry and Steel Quantities Wall J .....	207
Figure 7.21.k	Acapulco Building – Wall Geometry and Steel Quantities Wall K .....	208
Figure 7.21.l	Acapulco Building – Wall Geometry and Steel Quantities Wall L .....	209
Figure 7.21.m	Acapulco Building – Wall Geometry and Steel Quantities Wall M .....	210
Figure 7.21.n	Acapulco Building – Wall Geometry and Steel Quantities Wall Y1 .....	211
Figure 7.21.o	Acapulco Building – Wall Geometry and Steel Quantities Wall Y2 .....	212
Figure 7.21.p	Acapulco Building – Wall Geometry and Steel Quantities Wall P1 .....	213
Figure 7.21.q	Acapulco Building – Wall Geometry and Steel Quantities Wall P2 .....	214
Figure 7.21.r	Acapulco Building – Wall Geometry and Steel Quantities Wall R .....	215
Figure 7.21.s	Acapulco Building – Wall Geometry and Steel Quantities Wall S .....	216
Figure 7.22	Torres de Miramar – Core Wall Geometry and Steel Quantities .....	217
Figure 7.23	Acapulco Building – Strength Distribution versus Height Wall M .....	218
Figure 7.24	Drift Ratios for Response Spectrum Analysis Plaza del Mar Building .....	219
Figure 7.25	Drift Ratios for Response Spectrum Analysis Festival Building .....	220
Figure 7.26	Drift Ratios for Response Spectrum Analysis Acapulco Building .....	221
Figure 7.27	Drift Ratios for Response Spectrum Analysis Torres de Miramar Building .....	222
Figure 7.28	Response History Characteristics – Festival Building .....	223
Figure 7.29	Drift Ratios for Inelastic Analysis – Festival Building .....	224

Figure 7.30	Yielding Pattern for Inelastic Analysis – Festival Building .....	225
Figure 8.1	Minimum U.S. Code Strength – $A_w/A_b=0.005$ .....	226
Figure 8.2	Minimum Chilean Code Strength – $A_w/A_b=0.025$ .....	227
Figure 8.3	Minimum U.S. Code Strength – $A_w/A_b=0.025$ .....	228
Figure 8.4	Shear Strength versus Wall Area to Floor Area Ratio .....	229
Figure 8.5.a	Acceleration Response Spectrum – Viña del Mar S20W .....	230
Figure 8.5.b	Displacement Response Spectrum – Viña del Mar S20W .....	231
Figure 8.6.a	Acceleration Response Spectrum – Recorded U.S. Motions .....	232
Figure 8.6.b	Displacement Response Spectrum – Recorded U.S. Motions .....	233
Figure 8.7.a	Comparison of Acceleration Response Spectra Recorded U.S. Motions – Viña del Mar S20W .....	234
Figure 8.7.b	Comparison of Displacement Response Spectra Recorded U.S. Motions – Viña del Mar S20W .....	235
Figure 8.8.a	Comparison of Acceleration Response Spectra ATC-3-06 (1978) – Viña del Mar S20W .....	236
Figure 8.8.b	Comparison of Displacement Response Spectra ATC-3-06 (1978) – Viña del Mar S20W .....	237
Figure 8.9.a	Comparison of Acceleration Response Spectra Newmark-Hall (1982) – Viña del Mar S20W .....	238
Figure 8.9.b	Comparison of Displacement Response Spectra Newmark-Hall (1982) – Viña del Mar S20W .....	239
Figure 8.10	Comparison of Roof Drift Versus Number of Floors – Wall Buildings ATC-3-06 (1978) – Viña del Mar S20W .....	240
Figure 8.11	Comparison of Roof Drift Versus Number of Floors – Wall Buildings Newmark-Hall (1982) – Viña del Mar S20W .....	241
Figure 8.12	Comparison of Roof Drift Versus Number of Floors – Frame Buildings Newmark-Hall (1982) – Viña del Mar S20W .....	242
Figure 8.13	Base Shear Versus Period – Viñs del Mar S20W Displacement Ductilities, $\mu_\delta = 1,2,3$ .....	243
Figure 8.14	Base Shear Versus Period – ATC-3-06 (1978) Soil Type 1 Displacement Ductilities, $\mu_\delta = 1,2,3$ .....	244
Figure 8.15	Base Shear Versus Period – ATC-3-06 (1978) Soil Type 2 Displacement Ductilities, $\mu_\delta = 1,2,3$ .....	245
Figure 8.16	Base Shear Versus Period – ATC-3-06 (1978) Soil Type 3 Displacement Ductilities, $\mu_\delta = 1,2,3$ .....	246

Figure 8.17	Base Shear Versus Period (Firm Ground) - Newmark-Hall (1982) Displacement Ductilities, $\mu_\delta = 1,2,3$ .....	247
Figure 8.18	Base Shear Versus Period (Flexible Ground) - Newmark-Hall (1982) Displacement Ductilities, $\mu_\delta = 1,2,3$ .....	248
Figure 8.19	Required Wall Curvature Ductility Displacement Ductilities, $\mu_\delta = 2,3,4,5$ .....	249
Figure 8.20.a	Effect of Anchorage Pullout on Required Wall Curvature Ductility 10 ft Wall - Displacement Ductilities, $\mu_\delta = 2,3,4,5$ .....	250
Figure 8.20.b	Effect of Anchorage Pullout on Required Wall Curvature Ductility 20 ft Wall - Displacement Ductilities, $\mu_\delta = 2,3,4,5$ .....	251
Figure 8.21	Wall Geometry and Reinforcing Details .....	252
Figure 8.22.a	Computed Wall Curvature - 10 ft Wall Steel Ratios - 0.25%, 0.50%, 1.00%, 2.00% .....	253
Figure 8.22.b	Computed Wall Curvature - 20 ft Wall Steel Ratios - 0.25%, 0.50%, 1.00%, 2.00% .....	254
Figure A.1	Locations of Soil Borings .....	257
Figure A.2	Soil Profile and Standard Penetration Test Data for Boring #1 .....	258
Figure A.3	Soil Profile and Standard Penetration Test Data for Boring #2 .....	259
Figure A.4	Soil Profile and Standard Penetration Test Data for Boring #3 .....	260
Figure A.5	Soil Profile and Standard Penetration Test Data for Boring #4 .....	261
Figure A.6	Soil Profile and Standard Penetration Test Data for Boring #5 .....	262
Figure A.7	Soil Profile and Standard Penetration Test Data for Boring #6 .....	263
Figure A.8	Soil Profile and Standard Penetration Test Data for Boring #7 .....	264
Figure A.9	Soil Profile and Standard Penetration Test Data for Boring #8 .....	265

# CHAPTER 1

## 1.1 Introduction

The development of codes for earthquake resistant design of buildings parallels major earthquakes causing damage and loss of life. Post earthquake studies to evaluate reasons for poor building performance during earthquakes are instrumental in the development and improvement of building codes. Good building performance during earthquakes, although often overlooked, instills confidence that provisions are adequate, and may even lead to relaxations in certain code requirements. Because of variations between U.S. and foreign code practices, evaluations of building behavior for earthquakes outside of the U.S. provide valuable insight into both U.S. and foreign code practices.

On 3 March 1985, a strong earthquake of surface magnitude 7.8 occurred near the central coast of Chile [Wyllie et al. (1986)]. The region affected included the city of Viña del Mar, where approximately 400 modern, reinforced concrete buildings exist. Most of the buildings were designed for lateral forces comparable to those used in high seismic areas in the United States. Recorded ground motions in Viña del Mar revealed a relatively long duration (45 sec between first and last peak of 0.05g), and a peak ground acceleration of 0.36g. Peak spectral accelerations for the recorded ground motions exceed 1.0g for 5% damping.

Reconnaissance reports [Wyllie et al. (1986)] indicated that the stiff, shear wall structures constructed in Chile “performed extremely well”, with little to no apparent damage in the majority of buildings. Later investigations [Wood et al. (1987)] revealed that although

the seismic code requirements in Chile are similar to those used for high seismic risk regions in the U.S., detailing requirements are less stringent. In addition, inspection and quality control are lax by U.S. standards.

Current U.S. seismic design codes typified by the Uniform Building Code (1988), classify Chilean structures as "bearing wall buildings". Design forces for such structures are substantially higher compared with ductile moment-resisting frames, or dual systems. Furthermore, ductile detailing and inspection are required to the same degree as for moment resisting and dual systems. The requirements appear to be inconsistent with observations from the 3 March 1985 Chile earthquake.

## **1.2 Objectives and Scope**

Because of the good building performance in Viña del Mar, and the inconsistency of the performance with U.S. code requirements, a detailed study of the structural requirements for bearing wall buildings is undertaken. Specific objectives of this study are (1) to evaluate the reasons for good and poor behavior of the buildings in Viña del Mar, Chile, (2) to evaluate the performance of similarly constructed buildings in the U.S., and (3) to evaluate current U. S. code seismic requirements for strength, stiffness and detailing practice for bearing wall buildings.

In an effort to achieve the aforementioned objectives, detailed analytical studies were conducted for four buildings in Viña del Mar. All four buildings were all located within a few blocks of one another, and range in height from 15 to 23 stories. One of the buildings was constructed in 1964, whereas the other three were constructed between 1975 and 1982.

Four additional buildings, evaluated in detail in companion studies [Stark (1988), Wight (1988)], are also studied. The buildings suffered varied degrees of damage.

A brief discussion of Chilean code development and design philosophy is presented in Chapter 2. Seismic code requirements, and typical details of reinforced concrete construction, are also presented. Chapter 3 discusses the general characteristics of the 3 March 1985 earthquake, and presents engineering features of the recorded ground motions. Chapter 4 presents engineering properties for the soils in Viña del Mar, and addresses effects of local soil conditions on the recorded ground motions.

Elastic and inelastic modeling techniques and results are presented in Chapters 5, 6, and 7. A detailed investigation of soil-structure interaction for one of the buildings is presented in Chapter 6. The results are compared with available data from free vibration tests and recorded aftershock data. ATC-3-06 (1978) recommendations for soil-structure interaction are also evaluated. Chapter 7 presents the detailed analyses of four buildings. The analyses include comparisons of UBC and Chilean code requirements, calculations of stiffness and base shear strengths, and evaluations of elastic and inelastic dynamic responses for the recorded earthquake ground motions. Effects of soil-structure interaction and correlation with observed damage are also addressed.

In Chapter 8, the analytical findings from Chapter 7 are extended to U.S. practice. A simplified procedure is used to evaluate deformation demands for "Chilean type" structures for three characterizations of U.S. ground motions. Estimates of global deformation demands are used to compute local deformation demands. Requirements for member detailing are evaluated by comparing required and available curvature ductility.

A summary and conclusions of the study are presented in Chapter 9. Recommendations are made for the development of code requirements for bearing wall buildings.

## CHAPTER 2

### STRUCTURAL ENGINEERING PRACTICE IN CHILE

An overview of structural engineering practice in Chile is presented. The first section describes the Chilean design philosophy, followed by a brief outline of the seismic code requirements. The final section discusses multi-story reinforced concrete construction in Chile and presents typical structural details.

#### 2.1 Design Philosophy

The Chilean design philosophy [Wood et al. (1987)] with respect to acceptable damage and safety for earthquake resistant design and construction is the same as that commonly expressed in the United States: to prevent structural and non-structural damage in frequent minor intensity earthquakes; to prevent structural damage and minimize non-structural damage in the occasional moderate intensity earthquake; and to prevent the collapse of the building in the rare high intensity earthquake. However, what constitutes a minor, moderate, or high intensity earthquake in Chile differs considerably from that in the United States. Although no explicit bounds are established, earthquakes with magnitudes of 6.0 to 7.0 (close to urban areas) are considered as minor intensity in Chile due to their frequent occurrence (Table 2.1) [Lomnitz (1970)]. Earthquakes with magnitudes of 7.0 to 7.5 are generally considered to be moderate. Earthquakes with magnitudes greater than 7.5 are considered strong, and occur approximately every 20–25 years (Table 2.1). This philosophy

developed to limit excessive repair costs and risk to human safety in the frequent earthquakes in Chile.

The Chilean experience with frequent strong earthquakes has led to a construction practice that differs from that used in the United States. In the early 1900's both frame and wall construction were common. The failure of some frame buildings during earthquakes in the 1930's led subsequently to the almost exclusive use of structural walls for lateral load resistance [Wood et al. (1987)]. Chilean engineers, architects, and occupants became accustomed to the liberal use of structural walls in buildings. As multi-story construction began to evolve in the 1960's the liberal use of structural walls continued. Typical moderate-rise Chilean buildings have wall to floor areas of 5 to 6% (Fig. 2.1) [Riddell et al. (1987)], resulting in relatively stiff buildings (Fig. 2.2) [Wood et al. (1987)]. Figure 2.2 reveals that a good estimate of the fundamental period of a typical Chilean building on firm soil is  $N/20$ , where  $N$  is the number of stories. In contrast, for a U.S. frame building a commonly accepted estimate of the fundamental period is  $N/10$ .

## 2.2 Seismic Code Requirements

Development of the Chilean practice for earthquake resistant design and construction closely parallels major seismic events in the history of the country. The Talca earthquake of 1 December 1928 initiated the development of seismic regulations in Chile [Bertling (1956), Flores and Jimenez (1986)], resulting in *Ley Ordenanza General de Construcciones y Urbanización* (1949). The General Ordinance, endorsed in 1931, became law in 1935. It governed until the adoption of the current code, NCh 433: *Cálculo Antisísmico de Edificios* (1974). The following paragraphs present a brief outline of the current seismic code. A

complete English translation is contained in *Earthquake Resistant Regulations—A World List* (1980).

The format of the Chilean seismic code and the resulting design forces are very similar to those used in areas of high seismic activity in the United States. The base shear force is computed from the following relationship:

$$V = K_1 K_2 C P \quad (2.1)$$

Where:  $K_1$  = occupancy factor

$K_2$  = building system factor

$$C = 0.10 \frac{2T_0 T}{T_0^2 + T^2} \geq 0.06 \quad \text{for } T > T_0 \quad (2.2.a)$$

$$C = 0.10 \quad \text{for } T < T_0 \quad (2.2.b)$$

$P$  = building weight + minimum of 25% of live load

$T_0$  is a factor relating to the type of soil, and is taken as 0.2 for rock, dense gravel, or dense sandy gravel, 0.3 for dense sand or firm cohesive soils, and 0.9 for granular or soft cohesive soils.

For most of the buildings in Viña del Mar, the appropriate values for  $K_1$  and  $K_2$  are 1.0, therefore:

$$V = (1.0) (1.0) C P = 1.0 C P \quad (2.3)$$

Equation (2.3) can be used directly to produce a equivalent code acceleration spectrum. The spectrum is plotted in Fig. 2.3 for  $T_0=0.3$ . The spectra for the Uniform Building Code (1985) and (1988) are also plotted. For the UBC-85 Z, I, and K were assumed to be equal to one, and S equal to 1.2. For the UBC-88 the following values were assumed:

$I=1$ ,  $Z=0.4$ ,  $S=1.2$ , and  $R_w=6$ . Load factors of 1.40 and 1.70 were used for the UBC and Chilean code, respectively. A higher value is used for the Chilean code because the allowable concrete strength is 49% of the cylinder strength compared with an equivalent value of 60% ( $=0.85/1.4$ ) for the UBC (A similar factor is obtained by comparing steel stresses). The spectra indicate that the code strength requirements for most Chilean buildings are similar to those for U.S. buildings in areas of high seismic risk.

The Chilean code allows both an equivalent static lateral force procedure, or a modal analysis. For the equivalent lateral force procedure the distribution of base shear over the height is similar to that used in the UBC.

Drift limits for the Chilean code are more restrictive than the UBC limits. Lateral displacements for the Chilean code forces are limited to 0.2% of the story height. If partitions are separated from the structural elements 0.4% drift is allowed. Gross sections are commonly used for the drift calculations.

### **2.3 Reinforced Concrete Construction**

The detailed development of reinforced concrete building construction in Chile has been influenced by procedures used in the U.S., Japan, and Germany. The current building code for reinforced concrete [Hormigón Armado—Part I, II (1965)] is based on the 1952 German DIN standard [DIN 1045 (1952)], which was developed primarily for gravity loads. Because the detailing requirements for anchorage and transverse reinforcement specified by the 1952 German DIN do not apply for seismic construction in Chile, the manufacturer of reinforcing bars, CAP, publishes a set of recommended details [*Barras para Hormigón*

Armado]. The recommended details for development length, lap splices, hooks, and bar spacing are the same as the ACI-318 (1983) requirements for regions with low seismic risk. One notable deviation from the ACI requirements is the required cover. Apparently the cover requirements are taken from the German DIN, and are approximately equal to the ACI requirements in cm rather than inches. Although no special ductile detailing requirements are required, some engineers follow the provisions in Appendix A of ACI-318 (1977).

No uniform set of detailing recommendations is followed in Chile. Reinforcement is fabricated at the construction site directly from the structural drawings. In general, the contractor is not provided with detailed drawings for the placement of steel in the slabs, beams, and walls. Although standard details are recommended [*Barras para Hormigón Armado*], the details vary with contractor and modifications during construction are made at the contractors discretion. Typical details for structural elements are discussed in the following sections. The details were taken from the structural drawings of the buildings described in Chapter 7.

(i) *Structural Walls*

The typical structural wall in a Chilean building does not have boundary elements or special transverse reinforcement, although longitudinal steel may be concentrated at the edge (Fig. 2.4). A minimum wall thickness of 20 cm (8 in.) is specified [*Hormigón Armado-Part II* (1965)]. No limit is placed on the amount of flexural reinforcement in a wall. Lap splices for the boundary bars are typically located at or immediately above the level of the floor slab. Two curtains of shear reinforcement are required by the code with 0.1% vertical and horizontal in each face (0.2% horizontal and 0.2% vertical). The shear reinforcement may be either welded wire fabric or individual tied

bars. The maximum spacing is limited to 30 cm (12 in.), and a hoop not less than 6 mm (#2) in diameter must be provided at least every 50 cm (20 in.) to tie the two curtains of wall reinforcement. Diagonal shear reinforcement was used in some cases. Shear reinforcement in excess of the code minimum is generally not provided.

(ii) *Columns*

Columns are sparsely used in most Chilean buildings and typically carry only gravity loads. The flexural reinforcement ratio for columns must be between 0.8 and 6%. The locations of lap splices for the longitudinal bars generally occur near or at the beam-column joint (Fig. 2.5). The location of ties are usually specified on the structural drawings. Spiral reinforcement is not common. Figure 2.5 presents typical reinforcing for a column (taken from the Plaza del Mar building).

(iii) *Beams and Slabs*

No limit is placed on the flexural reinforcement that can be placed in beams; however, steel ratios rarely exceed 0.75%. Shear reinforcement is required for beams when the working stress exceeds  $8 \text{ kg/cm}^2$  for  $f'_c = 255 \text{ kg/cm}^2$  ( $1.90\sqrt{f'_c}$  psi). Bending of longitudinal reinforcement in beams to provide shear reinforcement is recommended; however, vertical stirrups are allowed. The design procedure for shear in beams does not, in general, account for the flexural overstrength due to actual steel yield strength or contribution of slab steel. Figure 2.6 presents typical reinforcing for a beam not designed to couple walls (taken from the Plaza del Mar drawings). Beams over doorways that couple walls sometimes have diagonal steel to resist shear. Figure 2.7 presents a wall coupling beam (from the Acapulco building drawings).

Slabs are typically designed for gravity loads. The minimum slab thickness is 12 cm (4.8 in.), and slab thickness between 12 and 20 cm (4.8 and 8 in.) is common. Where slabs are used to couple walls additional reinforcement is typically provided. Slab shear reinforcement is not common. Typical slab reinforcement is shown in Fig. 2.8 (from the Festival Building drawings).

(iv) *Foundations*

Three types of foundations are used in Viña del Mar. The most common type being a mat or cellular mat foundation. The cellular mat foundations are sometimes filled with soil-cement to anchor the building against overturning. Continuous footings are common for buildings founded on rock. A few buildings in Reñaca are supported on wood piles. On the coast the foundations are typically 5–8 m below grade to avoid undercutting by storms.

## **2.4 Construction and Inspection**

Construction and inspection practices in Chile are loosely regulated. Prior to 1981 all drawings and design calculations were checked by the municipal office before a construction permit was issued. On-site inspection was not required. Due to the lack of technical support design checks were discontinued. Present regulations only require the engineer to review and stamp the structural drawings. Some engineers make site inspections, but they are not required.

The architect is responsible for building construction and inspection. The progress and problems of the project are recorded in a log book, and serves as the contractor's proof that

the building was constructed according to the drawings. Deviations must be approved by the architect or engineer. The municipality requires that the architect and engineer accept the building before a certificate of occupancy is issued. The municipality also checks the building to ensure that it agrees with the drawings.

Controls on the construction materials appear to be adequate. The concrete is frequently and well tested during construction with samples collected by the contractor. The reinforcing steel has reliable mechanical properties. However, very little control is exercised on the construction process. Construction errors, poor placement of materials, and poor detailing practices often go unchecked. Remarkably, building damage in the 3 March 1985 earthquake was relatively light [Wood et al. (1987), Bonelli (1986), Wyllie et al. (1986)]. Some Chilean engineers maintain that the damage from the 3 March 1985 earthquake could have been reduced if adequate regulations concerning design review by qualified engineers and construction inspection by independent parties had been in force [Flores and Jimenez (1986)].

## **2.5 Summary**

The liberal use of structural walls in Chilean buildings developed to limit damage in the frequent moderate to strong earthquakes that effect the region. The Chilean seismic code requirements are similar to those used in regions of high seismic risk in the United States; however, detailing requirements are less stringent. Experience has led to the conclusion that careful detailing and construction inspection are, in most cases, unnecessary for this type of construction.

## CHAPTER 3

### THE 3 MARCH 1985 CHILE EARTHQUAKE

On 3 March 1985, a major earthquake occurred near the coast of central Chile [Wyllie et al. (1986)]. The region affected included the port city of Valparaíso and the resort community of Viña del Mar. These cities contained buildings of modern construction that have been designed for lateral forces comparable to those used for high seismic areas in the United States. General characteristics of the earthquake and engineering features of the recorded ground motions are presented in this chapter. Chapter 4 addresses variations from the recorded motions at building locations due to geologic conditions of the site.

#### 3.1 General Information and Characteristics

The earthquake occurred at 7:27 p.m. local time on Sunday, 3 March 1985. The epicenter was located approximately 10 km off the coast of central Chile (Fig. 3.1), approximately 80 km from the Municipality of Viña del Mar [Saragoni et al. (1985)], with an estimated focal depth of 33 km [Bonelli (1986)]. Communities affected by the earthquake included Viña del Mar, Valparaíso, Reñaca, Melipilla, and Santiago. The earthquake consisted of two events. The main event had a surface magnitude of  $M_s = 7.8$ , and a P-wave magnitude of  $M_b = 6.9$  [Wyllie et al. (1986)]. A smaller event with  $M_b = 5.2$  preceded the main event by approximately ten seconds, making it difficult to accurately locate the epicenter of the main event [Wyllie et al. (1986)]. Modified Mercalli Intensities were VIII in the epicentral

regions and VII and VIII in Viña del Mar and Santiago. Several significant aftershocks were recorded [Celebi, ed. (1986)].

The earthquake resulted in significant damage in Chile [Wyllie, et al. (1986), Bonelli (1986)]. According to Chilean government statistics [Wyllie et al. (1986)] 45,000 homes were destroyed and another 76,000 were damaged. Approximately 10,000 people were injured during the earthquake, while another 2,500 required hospitalization. Approximately 180 deaths were recorded from the 6.8 million population of the region affected by the earthquake. In the communities of Viña del Mar and Valparaíso approximately 40 deaths were reported from the population of 550,000 [Wyllie et al. (1986)].

Observed damage was not universal to all construction types. Adobe houses throughout the region were severely damaged with many in a state of partial or total collapse. Wood and reinforced masonry structures performed quite well. No significant damage was observed in steel structures, which are not common in Chile. Damage to industrial facilities and bridges was generally light. Many modern reinforced concrete structures existed in the community of Viña del Mar and Valparaíso at the time of the earthquake. Although several of these buildings were damaged, most performed well, with little to no apparent damage [Wyllie et al. (1986), Wood et al. (1987)].

### **3.2 Strong-Motion Instrumentation**

A strong motion instrument has been in operation in Santiago since approximately 1940, and has recorded seven earthquakes between 1945 and 1971. More recently, the departments of Geology and Geophysics and Civil Engineering at the University of Chile

have assembled a network of more than 60 analog strong-motion instruments [Wyllie et al. (1986)]. Most of the instruments in the network are SMA-1 accelerometers [Wyllie, et al. (1986)]. The instruments are typically placed in small buildings so that recorded motions resemble free-field motions. It is not common to instrument buildings other than at the base.

A significant engineering feature of the 3 March 1985 Chile earthquake was that more than 30 strong motion instruments recorded the event [Wyllie et al. (1986), Saragoni et al. (1985)]. Approximately 15 high quality records were obtained from stations located within 150 km of the epicenter (Fig. 3.2). Important characteristics from the recordings are listed in Table 3.1 [Wyllie et al. (1986), Wood et al. (1987)]. The instrument in Santiago that had recorded previous earthquakes did not function during the 3 March 1985 earthquake, so no direct comparison with previously recorded events is possible.

### **3.2.1 The Recorded Ground Motions**

Only the recordings at Llole, Viña del Mar, and Valparaíso (at El Almendral and the Universidad Técnica Federico Santa María) are presented and discussed in the following sections. For simplicity the record obtained at the University will be denoted Valparaíso, whereas the other will be referred to as El Almendral. Additional information on the seismicity of the region and the instrumental records obtained during the 3 March 1985 earthquake is given in References [Wyllie et al. (1986), Bonelli (1986), Celebi, ed. (1986), Wood et al. (1987), and Saragoni et al. (1985)].

Acceleration records obtained at the four locations are presented in Figure 3.3.a-d. Three components of motion, two horizontal and a vertical, were obtained for all records

except El Almendral, which lacks a vertical component. For comparison, the NS component of the El Centro record obtained in the 1940 Imperial Valley earthquake is plotted in Figure 3.4. The figures reveal a relatively long duration of strong ground motion in Chile compared with the El Centro record. The long duration associated with the 3 March 1985 earthquake is due in part to the sub-event which preceded the main shock by about ten seconds [Wyllie et al. (1986)]. In some locations more than two minutes of ground motion were recorded [Saragoni et al. (1985)]. Due to uncertainties associated with arrival times of P-waves (because the sub-event that preceded the main shock triggered the strong motion instruments) there is not an accurate location for the epicenter of the main event [Wyllie et al. (1986)].

The peak acceleration recorded during the earthquake was 0.67g at Llolleo and Melipilla. The instrument at Llolleo was approximately 40 km from the epicenter (hypocentral distance of 45 km [Saragoni et al. (1985)]), and was located in the basement of a 1-story building founded on firm soil deposits [Wood et al. (1987)]. The peak accelerations recorded at Valparaíso were 0.29 and 0.18g for the instruments at El Almendral and Valparaíso, respectively. The El Almendral instrument was located in a 1-story building supported on soft soil. The Valparaíso instrument was self contained (free field) and was located on volcanic rock. Compared with the record obtained on rock in Valparaíso (0.18g) the recorded acceleration at Viña del Mar (0.36g) and El Almendral (0.29g) indicate that the local geological conditions affected the motions.

### 3.2.2 Intensities

Modified Mercalli Intensities of VII and VIII were assigned to the Viña del Mar and

Valparaíso areas (Fig. 3.1) [Wyllie et al. (1986)]. Less subjective intensities based on analytical procedures are presented in Table 3.2, and discussed in the following paragraphs.

Housner Spectrum Intensities [Housner (1959)] are presented in Table 3.2 for the records presented in Fig. 3.3 and 3.4. Housner Intensities are computed as the area under the five percent damped spectral pseudo-velocity curve between periods of 0.1 and 2.5 seconds. Duration of ground motion is not included in the Housner Intensity. Intensities for the Viña del Mar and El Almendral records are comparable to that for the NS component of the 1940 El Centro record. The intensities for the Lolleo records are higher than the El Centro record, while those recorded at Valparaíso are the lowest.

Arias Intensities [Hansen, ed. (1970)] are also presented in Table 3.2 for the ground motions records presented in Fig. 3.3 and 3.4. The intensity is computed as a constant times the integral over the duration of the ground motion of the acceleration squared. Figure 3.5 plots the evolutionary Arias Intensity for the records obtained at Viña del Mar and the 1940 Imperial Valley Earthquake. The Arias intensities for the Chilean ground motions are considerably higher than that for the El Centro record, because of the relatively long duration of the Chilean motions.

### **3.2.3 Response Spectra**

Response spectra for an elastic system and displacement ductility spectra for inelastic systems were computed for the horizontal components of ground motion. Numerical integration employing Newmark's Beta Method [Newmark (1959)] for constant acceleration was used to compute the maximum response quantities. A maximum time step of 0.01 seconds was used.

### (a) Elastic Response Spectra

Elastic response spectra for viscous damping of 2, 5, and 10 percent of critical were computed. Figures 3.6.a-d present the calculated spectral displacement and spectral pseudo-acceleration for the horizontal components of the four Chilean records presented in Fig. 3.3. Figure 3.9 compares elastic 2 percent damped spectra for the El Centro and Viña del Mar S20W records. The ordinates are plotted to a common scale except for the Llolleo records, which showed significantly higher response quantities. Significant aspects revealed in Fig. 3.6.a-d and 3.9 are:

#### (i) *Spectral Acceleration:*

The spectral shapes for the Viña del Mar (Fig. 3.6.b) and El Almendral (Fig. 3.6.d) records are similar, and indicate a characteristic ground period of approximately 0.7 seconds. Peaks of 2.00g and 1.25g were calculated for the Viña del Mar S20W and El Almendral N50E records, respectively. Peak ordinates occur between periods of 0.4 to 1.0 seconds for the Viña del Mar spectra, and between 0.2 to 1.0 seconds for the El Almendral spectra. The 1940 NS component of the El Centro record has similar frequency content to the Viña del Mar and El Almendral records, with spectral ordinates comparable to the El Almendral spectra.

The Llolleo spectra exhibit significantly higher spectral ordinates than the other records for periods less than 0.5 sec. Above 0.5 sec the ordinates for the Llolleo records are similar to those for the Viña del Mar S20W spectra. The El Almendral and Valparaíso spectra have lower ordinates, with Valparaíso being the lowest.

(ii) *Spectral Displacement:*

In general, ordinates increase rapidly above periods of 0.5 seconds, and peak for periods from 0.75 to 1.0 seconds. The ordinates remain relatively constant or diminish for periods beyond 0.75 to 1.0 seconds. Peak values of 15 cm (6 in.) are computed for Viña del Mar and El Almendral (for 5% damping). The displacement response spectra for the NS component of the 1940 El Centro record have similar ordinates below a period of 1.5 sec, but have greater ordinates for longer periods.

**(b) Inelastic Displacement Ductility Spectra**

Inelastic response spectra displaying displacement ductilities for the Viña del Mar and El Almendral records were computed for base shear yield strengths of 10, 20, 30, 40, and 50 percent of building weight. Viscous damping was taken as 5 percent of critical for the elastic structure. Two models were considered for post-yield behavior. The first model used perfectly plastic yielding, while the second assumed a strain hardening ratio of twenty percent of the elastic stiffness. To achieve moderate strain hardening in a building system requires either a material with inherent strain hardening or a structural system with several yielding elements in which the elements do not yield simultaneously. When yielding was detected, iterations were made within the time step to ensure that the yield point was not exceeded by more than one percent. Similar iterations to determine precise unloading points were not made. Stiffness degradation was not accounted for in either model.

The displacement ductility spectra are presented in Fig. 3.8. For comparison, corresponding spectra for the NS component of the 1940 El Centro record are plotted in Fig. 3.10. Important observations revealed in Fig. 3.8 and 3.10 are:

- (i) The elasto-plastic spectra suggest that significant inelastic responses occurred over a broad period range. For systems with moderate strength ( $0.20W - 0.30W$ ), displacement ductility as high as ten are required. Local demand for curvature ductility would be approximately three times the displacement ductility demand [Paulay (1986)]. The low level of damage observed in the moderate-rise buildings (5-23 stories) after the earthquake suggests that typical Chilean buildings possess considerable strength based on elasto-plastic spectra.
  
- (ii) The spectra for the bilinear model with 20 percent strain hardening show a substantial reduction in the required displacement ductility relative to the elasto-plastic model. The reduction in required displacement ductility is pronounced in the low period range. For example, the displacement ductility demand for a structure with a base shear strength of 20 percent of its weight and a period of about 0.5 sec is only four, compared to a value of twenty for the elasto-plastic spectra.
  
- (iii) Displacement ductility requirements for the Viña del Mar, El Almendral, and Lolleo records are generally higher than those required for the NS component of the 1940 El Centro record, whereas those for Valparaíso are lower.

### **3.3 Summary**

The preceding sections presented general characteristic and engineering features for the ground motions recorded in Chile during the 3 March 1985 earthquake. Modified Mercalli Intensities of VII to VIII were assigned to the epicentral region. Computed Housner Spectrum Intensities, which do not account for duration, were similar for the Chilean and

El Centro earthquakes. Due to the long duration of the Chilean motions, Arias intensities, which account for duration, indicate the Chilean motions were more severe. A comparison of spectral relations revealed that the frequency content for the Viña del Mar and El Almendral records was similar to the frequency content for the 1940 El Centro NS component. Local geological conditions apparently affected ground motions in Valparaíso and Viña del Mar. Ordinates of spectral acceleration for these records were slightly higher than those for the 1940 El Centro NS record. Inelastic displacement ductility spectra for an elasto-plastic system indicate that significant demands for ductility existed over a broad range of periods and strengths.

# CHAPTER 4

## SOIL EFFECTS ON GROUND MOTIONS

Many of the buildings selected for study later in this report are located along the beach in Viña del Mar. Unfortunately, no strong-motion instruments were located in this area during the 3 March 1985 earthquake. The closest instrument was located approximately 1300 m away. Soil conditions and the depth of the soil deposits are known to vary between the two sites. This chapter investigates the effects of the varying soil conditions on the intensity and frequency content of the ground motions at the two locations.

### 4.1 Soil Characteristics and Engineering Properties

The following sections present general characteristics and engineering properties for the soils in Viña del Mar.

#### 4.1.1 General Geological Characteristics

The general topography and geology of the coastal region of Valparaíso and Viña del Mar are presented in Reference [Wood et al. (1987)]. The foundation conditions in the region have been divided into five categories: (1) fresh rock, (2) weathered rock, (3) cemented sand and gravel, (4) uncemented sand and gravel, and (5) artificial fill. Four of these foundation materials are found in Viña del Mar. Unsaturated, weathered rock is found in the hills surrounding the city. The cemented sand and gravel is located to the

north in the dunes around Reñeca. The majority of the city rests on uncemented sand and gravel. The artificial fill exists along the coast. The depth of this fill varies from 2–4 meters in Viña del Mar.

Some soft-soil regions of fluvial and colluvial deposits are found along the Marga-Marga River. The soil to the south of the river and the top 25 to 35 m of soil north of the river are medium grained fluvial sands. The soil north of the river below 25 to 35 m to bedrock is a very compact silty marine sand [Petersen (1986)].

#### 4.1.2 Engineering Properties of the Foundation Materials

Engineering properties for the top 25 to 35 m of soil in Viña del Mar are presented in the following subsections. Essentially no data are available for the soil below 35 m. Table 4.1 [Wood et al. (1987)] presents typical engineering properties for the foundation materials in Viña del Mar. A majority of the buildings in Viña del Mar are founded on the uncemented sand and gravel; therefore, the remainder of this section focuses on this material.

The shear modulus is commonly used to describe the strength of soils. Three methods are presented for estimating the shear modulus for the uncemented sand and gravel deposits in Viña del Mar. The first method is an empirical relation used by Chilean engineers. The second method is based on experimentally obtained data from the site, whereas the third method is an empirical relation often used in the U.S..

**Method 1:** The shear modulus can be estimated from Young's modulus and Poisson's ratio using the following equation:

$$G = \frac{E}{2(1 + \mu)} \quad (4.1)$$

Poisson's ratio is typically taken to be between 0.25 to 0.40 for dense sands [Holtz and Kovacs (1981)]. To estimate Young's Modulus,  $E$ , Chilean engineers often use the following relationship [Poblete (1982)]:

$$E_{static} = 450Z \quad (4.2.1)$$

$$E_{dynamic} = \alpha E_{static} \quad (4.2.2)$$

Where  $Z$  is the depth in meters, and  $E$  is Young's modulus in metric tons per square meter, and  $\alpha$  typically ranges between 4 and 5.

**Method 2:** An alternative method to estimate the shear modulus is based on measurements of the shear wave velocity. The following equation can be used [Seed et al. (1984)]:

$$G_{dynamic} = V_s^2 \frac{\gamma}{g} \quad (4.3)$$

Where  $V_s$  is the shear wave velocity,  $\gamma$  is the unit weight of soil, and  $g$  is the acceleration due to gravity. The unit weights for the soils in Viña del Mar are as follows: The artificial fill at the surface has a unit weight of approximately  $1.75\text{t/m}^3$  with a relative density of about 40 % [Petersen and Donoso (1980)]. The unit weight of the cohesionless sand and gravel varies from  $1.9$  to  $2.2 \text{ t/m}^3$ .

Unfortunately, field recorded shear wave velocities are not available for Viña del Mar; however, standard penetration test (SPT) data can be used with the following equation to estimate the shear wave velocity [Seed, Idriss, and Arango (1981)].

$$V_s = 200\sqrt{N_1} \quad (fps) \quad (4.4)$$

Where  $N_1$  is the number of blows per foot. Appendix A presents the results of SPT data obtained at eight sites in Viña del Mar [Herrera (1977), Petersen and Donoso

(1980)]. The borings vary in depth from 10–25 m. Table 4.2 presents estimates made by University of California Professor H. Bolton Seed of shear wave velocity for two of the sites using Eq. 4.4. The average shear wave velocity is approximately 275 m/sec (900 ft/sec) indicating that the soils are relatively dense.

**Method 3:** Seed et al. (1984) recommend the following equation to estimate the shear modulus versus depth for cohesionless soils:

$$G_{max} = 1000K_2(\sigma'_m)^{1/2} \quad (psf) \quad (4.5.1)$$

$$G_{max} = 70K_2(\sigma'_m)^{1/2} \quad (tsm) \quad (4.5.2)$$

The coefficient  $K_2$  depends primarily on the relative density of the material, and varies from 40 to 60 for relatively dense soils (at low soil strain). The mean effective stress,  $\sigma'_m$ , is calculated from the following relation:

$$\sigma'_m = \frac{1}{3}(\sigma'_v + 2\sigma'_h) \quad (4.6)$$

Where  $\sigma'_v$  is the effective vertical stress, and  $\sigma'_h$  is the effective horizontal stress. The effective horizontal stress is typically taken as  $\sigma'_h = K_o\sigma'_v$ , with  $K_o = 0.40$  to  $0.45$ ; therefore,  $\sigma'_m \approx 0.60\sigma'_v$ . Shear modulus and shear wave velocity for free field conditions are presented in Table 4.3 for Eq. 4.5.

The shear modulus predicted by Eq. 4.5 is for dynamic response at relatively low levels of soil strain. The parameter,  $K_2$ , is a function of soil strain, and reduces the shear modulus as soil strains increase [Seed et al. (1984)]. Figure 4.1 plots the variation of  $K_2$  versus soil strain for a cohesionless soil with a relative density of 70%.

A direct comparison of the preceding relationships can be made in for approximately the top 30 m of soil in Viña del Mar. Figure 4.2 plots the three estimates of shear modulus

versus depth. The figure reveals that the relation used by the Chilean engineers (Eq. 4.2) and the relation recommended by Seed (Eq. 4.5) underestimate the modulus estimated using the SPT data (Eq. 4.3). All estimates converge to approximately 325 m/sec for a depth of 30 meters.

## **4.2 Geologic Effects on Ground Motions**

The effect of local geology on earthquake ground motions is an important factor in the distribution of building damage [Seed and Alonso (1974), Steinbrugge and Schader (1973), Seed (1987)]. The following sections address these effects in Viña del Mar using both empirical relations and experimentally obtained data. Spectra for use along the beach in Viña del Mar are postulated.

### **4.2.1 Recorded 3 March 1985 Earthquake Ground Motions**

The ground motions recorded at Viña del Mar were obtained in the basement of a 10-story building founded on medium-grained fluvial sand. The Valparaíso instrument, located approximately 3.5 km southwest of the Viña del Mar instrument, is supported on rock. The ground motions recorded at El Almendral (also in Valparaíso) were obtained in the basement of a 1-story building founded on artificial fill. About 1200 m separates the instruments in Valparaíso. All three instruments were approximately 80 km from the epicenter of the 3 March 1985 earthquake [Calcagni (1987)].

The recorded motions at Viña del Mar and El Almendral indicate significant site amplification for some periods. The peak accelerations recorded at these soil sites were 0.36g

and 0.29g, respectively, compared with a peak acceleration of 0.18g on rock at Valparaíso. Figures 4.3.a-b plot the 5% damped spectral acceleration for the Viña del Mar and El Almendral records. For comparison, the spectra for the Valparaíso records are also plotted. Spectral ordinates are amplified by approximately three for periods between 0.5 and 1.0 sec for the Viña del Mar records.

#### 4.2.2 Recorded Aftershock Ground Motions

Due to the likelihood of aftershocks a group from the United States Geological Survey (USGS) went to Chile soon after the 3 March 1985 earthquake. Several significant aftershocks occurred, and instrumental recordings were obtained to address local variations in the ground motions due to soil and topographical conditions [Celebi, ed. (1986)]. Instruments were also placed in several buildings to evaluate the influence of soil-structure interaction [Bongiovanni et al. (1987)].

The locations of the strong-motion instruments for the site response study conducted by the USGS are shown in Fig. 4.4. The USGS study used an instrument on rock at the Universidad Técnica Federico Santa María as the reference station. This is the same location as the Valparaíso instrument in the 3 March 1985 earthquake. An instrument was also located near the instrument in Viña del Mar that recorded the 3 March 1985 earthquake. This instrument was placed in a 2-story building (instead of the 10-story building). Instruments were also placed in the basements of several buildings along the beach.

Data obtained for two aftershocks by Celebi, ed. (1986) are presented in Fig. 4.5. The recorded frequency dependent variations are presented in the form of ratios of Fourier

amplitude velocity spectra. The ratios plotted are the Fourier amplitude at the various sites divided by the Fourier amplitude at the reference station (Valparaíso). The plots are discussed in the following paragraphs.

Figures 4.5.a plot the Fourier amplitude ratios for the Viña del Mar instrument location (designated MUN in the USGS study). Amplification occurred for periods between 0.50 and 0.70 seconds, with the peaks at about 0.55 seconds. The peak spectral ratios are from 40–50. Amplification for periods between 0.125 and 0.18 is also evident, with peak ratios of 8 to 12.

Figures 4.5.b–c plot the Fourier amplitude ratios for the beach locations (designated EAC and TRA in the USGS study). Amplification occurred for periods between 0.80 and 1.20 seconds, with the peaks at about 1.00 second. The peak spectral ratios were from 18 to 25, or about one-half of those at the Municipal station. No clear trends are apparent for lesser periods.

The recorded aftershock data suggest that the ground motions at the beach area (where many of the modern buildings are located) were different than those recorded on the Viña del Mar instrument during the 3 March 1985 earthquake. Earthquake demands on shorter buildings (less than 15 stories) may not have been as high as indicated by the recording obtained during the 3 March 1985 earthquake. Demands for taller buildings may have been greater.

#### **4.2.3 Analysis and Interpretation of the Recorded Data**

The important parameters affecting the intensity and frequency content of ground motions at a soil site are the depth of the soil deposit and the properties of the soil. If these

quantities are known the characteristic period of the soil deposit can be computed from the relation [Seed (1975)]:

$$T_s = \frac{4H}{V_s} \quad (4.7)$$

Where  $H$  is the depth of the soil,  $V_s$  is the shear wave velocity, and  $T_s$  is the characteristic site period. The shear wave velocity of the soil varies with ground motion intensity. ATC-3-06 (1978) recommends reductions of shear wave velocity of 10 to 20% for moderate ground motions and 35% for intense ground motions. The following paragraphs evaluate the recorded data.

The response and Fourier spectra for the Viña del Mar instrument (Fig. 4.3 and 4.5.a) revealed characteristic site periods of 0.70 and 0.55 sec, respectively. The ratio of the characteristic soil periods for these different intensity ground motions is 1.27 (0.70/0.55). This is consistent (according to Eq. 4.7) with the ratio of shear wave velocities for moderate and intense ground motions ( $0.85/0.65 = 1.31$ ). This suggests that the 10-story building did not significantly affect the predominant period of the recording obtained at Viña del Mar in the 3 March 1985 earthquake. However, because the period of the building would also be approximately 0.5 sec, some interaction still may have occurred.

The depth to bedrock at the Viña del Mar instrument is not well known; however, it can be estimated from Eq. 4.7. The shear wave velocity at the Municipal building can be estimated using boring and standard penetration test data. Table 4.2 presents estimated shear wave velocities based for a boring taken just north of the Marga-Marga River (Appendix A - Boring # 8). The table indicates an average shear wave velocity of approximately 325 m/sec. The Viña del Mar recording was obtained 400 m away, just south of the river. Using either the data from the 3 March 1985 earthquake ( $T_s = 0.7$  sec,

$V_s = 0.65(325) = 210$  m/sec) or the aftershocks ( $T_s = 0.55$  sec,  $V_s = 0.85(325) = 275$  m/sec) a depth of 37 m is computed using Eq. 4.7. The depth to bedrock is estimated to be between 30 and 50 m [Crempien (1987), Petersen (1986)].

The depth of the sand at the beach is estimated to be 100 m [Grimme and Alvarez (1964), Petersen (1986)]. The characteristic soil period can be estimated using the standard penetration test results in Appendix A. The method used to compute the characteristic site period is also summarized in Appendix A. Average shear wave velocities of 400 and 475 m/sec were computed for two sites in Viña del Mar (using borings #1 and #2, and #3). Assuming a 10% reduction in shear wave velocity for the moderate intensity aftershocks results in characteristic site periods of 0.93 and 1.10 sec. These periods are consistent with the 1.00 sec site period recorded in the aftershocks. For the more intense 3 March 1985 ground motions, the reduction in soil stiffness increases the characteristic site period to 1.20 sec (assuming a 30% reduction in  $V_s$ ). This is a significant increase compared with the characteristic soil period of 0.70 sec at the Viña del Mar instrument location.

### 4.3 Site Response Analysis Using Horizontally Layered Soils

Because of the significant variation in characteristic site period in Viña del Mar, the motions recorded during the 3 March 1985 may not be representative for all locations. Therefore, a site response analysis for an equivalent linear, horizontally layered soil was conducted to calculate an acceleration spectrum for the buildings located along the beach. The analyses were conducted by Professor H. B. Seed and one of his research assistants, Joseph Sun. The motions recorded during the 3 March 1985 earthquake at Valparaíso were used to represent the base rock motion; thus, topographical and spatial effects were

neglected. Soil properties for low soil strain were computed using the standard penetration test data. Equation 4.5 was used to account for reduced soil shear modulus at higher strains.

Two analyses were considered. The first analysis was for the site of the Viña del Mar instrument during the 3 March 1985 earthquake. Various soil depths were assumed. The objective of the analysis was to gage the accuracy of the computation procedure to reproduce the spectrum computed from the motions recorded during the 3 March 1985 earthquake. An acceleration spectrum representative of the beach area was computed in the second analysis. Shear wave velocities for the analyses were based on data presented in Appendix A, and presented in Tables 4.2 and 4.4.

**(a) Viña del Mar – Municipal Building**

The analyses by Seed and Sun indicate soil a characteristic soil period of approximately 0.7 sec for a soil depth of 35 to 40 meters. Figure 4.6 plots the computed acceleration spectrum. The spectrum for the Viña del Mar S20W component is also plotted. Relatively good agreement is obtained between the predicted spectrum and that computed from the recorded motions.

**(b) Viña del Mar – Beach Locations**

Because soil properties for depths below 30 m were not available, three analyses were considered. The first analysis used a “best estimate” of the shear wave velocities. Shear wave velocities for the second analysis were increased relative to the first analysis, whereas those for the third analysis were decreased. The estimated shear wave velocities for the analyses are presented in Table 4.4. Low strain site periods of 0.93, 0.74, and

0.94 were computed for the three profiles. The low strain site periods were compared with those measured by Celebi (1986) (Figures 4.5.b-c). The low strain site periods were approximately equal to those recorded.

The analyses by Seed and Sun indicate a range of soil periods depending on the assumptions made for the soils below a depth of 30 m. Figure 4.7 plots the computed acceleration response spectra. The spectrum for recorded Viña del Mar S20W component is also plotted. The spectra for the beach location have lower ordinates compared with the recorded motion, especially for periods between 0.5 and 1.0 seconds. For periods greater than 1.0 sec, the computed spectral ordinates exceed those for recorded motion.

#### 4.4 Summary

General characteristics and engineering properties for the cohesionless sand and gravel in Viña del Mar were presented. Spectra for the motions recorded during the 3 March 1985 earthquake revealed that soil conditions amplified motions at approximately 0.7 seconds. Investigation of recorded site amplification revealed that the characteristic period for the beach area was significantly greater than that for the recorded ground motions during the 3 March 1985. Site response analyses predicted relatively good agreement between spectra for the computed and recorded ground motions. Several spectra were computed for the beach area because soil properties for depths below 30 m were not available. The analyses revealed that the ground motions for the beach area less intense for periods less than one second, but more intense for greater periods. Measured periods of Chilean buildings (Fig. 2.2) indicated that this variation could effect building damage.

# CHAPTER 5

## ELEMENT MODELING TECHNIQUES

To understand the behavior of buildings subjected to the 3 March 1985 earthquake several buildings were analyzed. Modeling techniques for the elastic and inelastic analyses of the buildings are described in this chapter. Elastic techniques are described first, followed by the inelastic techniques. Analyses of the buildings are presented in Chapters 6 and 7.

### 5.1 Elastic Modeling Techniques

The following sections discuss the modeling techniques used for the elastic analysis of the Chilean buildings. Emphasis was placed on modeling techniques that could be used readily in design-office practice. Flexural and shear deformations were included for all members. Axial deformations were included only in the column and wall elements. Element lengths were defined by centerline-to-centerline dimensions. Stiffness calculations were based on concrete gross sections.

#### 5.1.1 Beam and Slab Elements

Beams were modeled by assuming an effective flange width (Fig. 5.1) as specified in Section 8.10 of ACI-318 (1983). The joint region of the beam was assumed to be infinitely rigid.

Slabs were modeled by assuming an effective slab width as defined for interior slab-column connections by Pecknold (1975). The effective slab width varies depending on the

ratio of the width of the supporting member (column or wall) to the length of slab in the direction of loading,  $c_2/l_1$ . Because of the liberal use of structural walls in Chilean buildings, slabs rarely span greater than 7 m (20 ft). Therefore,  $c_2/l_1$  ratios are typically greater than 0.10, and effective slab widths of 60 to 75% of the maximum result. If cracking effects are included the effective slab width is reduced to one-third to one-half of the gross section value [Moehle and Diebold (1985)]. Cracking effects were not included in the elastic analysis.

### 5.1.2 Wall Elements

Chilean buildings rely mainly on structural walls to provide vertical and lateral load resistance. The type of wall model to be used is a function of the relative importance of flexural and shear deformations. For slender walls the wide-column analogy (a column with the inertia of the wall and rigid beams at each story extending to the wall boundary, Fig. 5.2) can be used. This analogy has been shown to work well for wall height to length ratio greater than 5:1 [Smith and Girgis (1984)]. For the buildings studied, wall height to length ratios generally exceeded 4:1; therefore, the wide-column analogy was used.

In some buildings several walls adjoined to form T-shaped, L-shaped, or irregular-shaped walls (Fig. 5.3). For T-shaped or L-shaped walls it is common practice to calculate the inertia of the wall by neglecting the flange, or assuming an effective flange width. ACI requirements for T-beams can be used for flanged wall sections if the span length (for the T-beam) is interpreted as twice the height of the wall [Paulay (1986)]. The wall could then be modeled by using a wide-column located in plan at the centroid of the flanged wall

section. For irregular shaped walls the code requirements for effective flange width are not well defined. Modeling procedures for such walls are addressed later in this chapter.

For slender walls an effective flange width of eight times the flange thickness usually results from the ACI requirements; however, this is believed to be quite conservative (for stiffness). Therefore, this requirement was ignored for all elastic analyses herein, and overhanging flange widths were estimated using the minimum of  $h_w/4$  and one-half the clear distance to the next wall web. For most walls this resulted in the entire flange being effective.

For three-dimensional analysis of building systems the calculation of wall inertia and neutral axis location for T or L-shaped walls is somewhat cumbersome. The computations for irregular shaped walls are even more intensive. Therefore an alternative modeling approach was used. Each rectangular section of the wall was modeled as a wide-column (Fig. 5.4). For slender walls plane sections can be assumed to remain plane; therefore, a rigid connection is required between the walls (Fig. 5.4). Three-dimensional effects, such as racking of beams (Fig. 5.5), are included for rotation about the centerline of the wall; however, migration of the neutral axis towards the compression zone of the wall is not. Although modeling of this type is convenient for stiffness calculations, and was found by finite element studies to be accurate, it has the drawback that forces on each element must be combined to compute the resultant forces on a wall (Fig. 5.4); therefore, it is not recommended for design purposes.

## 5.2 Inelastic Modeling Techniques

The following sections discuss the modeling techniques used for the inelastic analysis of the buildings in Chile. Element lengths were defined by centerline-to-centerline dimensions.

Flexural and shear deformations were included for all members; however, axial deformations were included only in the wall elements.

### 5.2.1 Beam and Slab Elements

A modified version of Takeda's model was used to approximate the behavior of beams [Kannan and Powell (1973)]. For this model beams are represented by elastic line segments connected to nodes by bilinear springs at the member ends. The initial stiffness and strain hardening ratio of the bilinear springs are determined from monotonic loading conditions for flexural deformations only. Degrading stiffness of the spring is introduced when reversed loading is applied. Effects of gravity loads on beam strength were considered by initializing the member end forces to those under gravity loads.

Yield moments and stiffness properties for the bilinear springs at the member ends were based on moment-rotation relations obtained from moment-curvature relationships. The moment-curvature relations were computed using the **BIA X2** computer program [Wallace (1989)] accounting for probable material strengths, steel strain-hardening effects, and floor slab contribution. The concrete strengths were based on 28 day cube tests done during construction of the buildings (Appendix C). The modified Kent and Park model [Park et al. (1982)] was used to describe the concrete stress-strain curve. The steel model incorporated elastic, plastic, and strain-hardening that closely follows observed behavior. ACI-318 (1983) requirements were used for both negative and positive bending to estimate the slab contribution to beams. Slabs were modeled by assuming an uncracked effective slab width as defined for interior slab-column connections by Pecknold (1975).

A trilinear curve was used to approximate the moment–curvature relation (Fig. 5.6). The two breakpoints correspond to cracking and yielding of the section, respectively. The ultimate moment and curvature were taken as the computed values for a compressive strain at the extreme compression fiber of 0.003. The beam was segmented (Fig. 5.7), with the moment–curvature relation for each segment defined by the approximate trilinear curve. The moment–rotation relation was computed by applying equal and opposite end rotations and using an event–to–event solution strategy to integrate the moment–curvature responses over the length of beams. A trilinear curve was used to approximate the computed moment–rotation relation.

Slip of the rebar at the member ends was considered by an approximate procedure similar to the one suggested by Takeda et al. (1970). According to the model (Fig. 5.8), the increase in member rotation due to reinforcement slip at each end can be expressed as:

$$\Theta = \frac{f_s^2 d_b}{8\bar{u}j d E_s} \quad (5.1)$$

Where  $f_s$  is the steel stress,  $d_b$  the diameter of the reinforcing bar,  $jd$  is the distance between the tension–compression couple,  $E_s$  is steel modulus of elasticity, and  $\bar{u}$  is the average bond stress.

Member end rotation due to reinforcing slip was computed for the breakpoints of the trilinear moment–rotation curve (cracking, yielding, and ultimate). Bertero et al. (1978) suggest an average bond stress of 70 kg/cm<sup>2</sup> (1000 psi) for well confined joints. Although not well confined, beam and slab reinforcement were typically well anchored in structural walls; therefore, an average bond stress of 50 kg/cm<sup>2</sup> (715 psi) was assumed.

The **DRAIN-2D** computer program requires that the properties of the nonlinear

springs at the member ends are based on bilinear moment-rotation relations (Fig. 5.9). Several methods of fitting a bilinear relation to a trilinear curve are available. One method involves the use of the concept of "equal areas". In this approach the area under the bilinear curve is equated to the area under the trilinear curve, producing equal energy dissipation capacities for the two curves. The ACI-318 code (1983) suggests an empirical relation (Eq. 9-7) using a weighted inertia that depends on the relative values of the cracking moment to the applied moment. An equation similar to the ACI equation suggested by Pantazopoulou (1987) was used. The relation uses a weighted average of cracking and applied moments as follows:

$$\frac{1}{E} = \left[ \frac{M_{cr}}{M_a} \right]^3 \frac{1}{E_{cr}} + \left( 1 - \left[ \frac{M_{cr}}{M_a} \right]^3 \right) \frac{1}{E_t} \quad (5.2)$$

Where  $M_{cr}$  and  $M_a$  are the cracking and applied moments, respectively,  $E_{cr}$  is uncracked modulus of elasticity, and  $E_t$  is the tangent modulus to the level of the applied moment. The stiffness computed from Eq. 5.2 was used with the line describing the post yield behavior to calculate the yield moment and rotation (Fig. 5.9.b).

To evaluate the effective stiffness, the level of moment that the element will undergo must be assumed. For the initial analysis, it was assumed that all the beams would reach yield. Several analyses were required to obtain convergence between the assumed and calculated level of moment. The beam initial stiffness and strain hardening ratio were determined by averaging the bilinear stiffness curves for positive and negative bending. Different yield moments were used for the positive and negative bending.

For some short wall coupling beams, shear failure controlled the yield strength of the element. Equation 11-6 of the ACI-318 (1983) code was used to calculate the shear strength of the coupling beams. The properties of the nonlinear flexural springs at the ends of the

members were computed assuming equal and opposite shears acting on the member ends, and considering flexural and shear deformations. Slip of reinforcing was ignored. A strain-hardening ratio of 5% was arbitrarily assumed.

### 5.2.2 Wall Elements

Axial load-moment interaction was not considered due to the unavailability of an appropriate element; therefore, the wall elements were modeled with the same element used for the beams. Yield moments and stiffness properties for the bilinear springs at the member ends were based on moment-rotation relations obtained from moment-curvature relationships. The moment-curvature relations were computed using the same procedures described for the beam elements. Axial loads were taken equal to the product of tributary area and  $1000 \text{ kg/cm}^2$ . Effective flange widths were based on the same procedures used for the elastic analyses. Typically this resulted in the entire flange considered as effective. Moment-rotation relations were derived by assuming that the wall was under constant moment, and therefore, constant curvature within each story. The effect of reinforcing slip was considered only at the base of the building. The base wall rotation was computed by Eq. 5.1. The wall stiffness and strength were varied over the height of the building. The bending stiffness was defined by using a secant to the maximum level of moment attained (Eq. 5.2 is not valid because constant moment is assumed for each story). Several analyses were required to obtain convergence between the assumed and calculated level of moment.

### **5.3 Strength Analysis Modeling**

Calculations of element flexural strengths to determine base shear strength of the buildings were based on the same element cross-sections and material properties used for the inelastic analysis.

# CHAPTER 6

## EFFECT OF FOUNDATION MATERIALS ON BUILDING RESPONSE

Because of the relatively deep, flexible soil deposits in Viña del Mar and apparent soil heaving at the base of several buildings after the 3 March 1985 earthquake [Wyllie et al. (1986)], the effect of the foundation materials on the building response is investigated. Linear elastic methods and simplified code procedures are presented and compared.

### 6.1 Soil-Structure Interaction Effects

For structures supported on rock or stiff soil, the ground motion at the base of the structure is essentially the same as the free field ground motion. The deformation in the foundation material due to the motion of the structure is negligible under the earthquake induced stress.

For structures supported on flexible soil, the ground motion at the base of the structure is significantly influenced by the presence of the structure. This feedback or interaction between the vibrating structure and the underlying soil must be considered to properly predict the response levels of the structure [Veletsos (1977)].

## 6.2 Linear Soil-Structure Interaction Analysis

The equations for linear analysis of a discretized model of the complete structure, foundation, and soil system can be simplified so that the effective force-vector is a function of only the contact degrees of freedom between the structure and soil systems [Clough and Penzien (1975)]. The equation of motion that describes the complete system in this simplified form is

$$[m^b + m^s]\ddot{v} + [c^b + c^s]\dot{v} + [k^b + k^s]v = - \left\{ [m^b + m^s]r + \begin{bmatrix} m_{gb}^b \\ m_{gg}^b \\ 0 \end{bmatrix} \right\} \ddot{v}_g \quad (6.1)$$

where the superscripts and subscripts **b** and **s** refer to the building and the soil system, respectively. The subscript **g** refers to the free-field (or ground) motions at the contact surface between the two systems. The equation results from partitioning the building and free-field displacements as follows

$$\mathbf{v}^t = \begin{bmatrix} v_b^t \\ v_g^t \\ v_s^t \end{bmatrix} \quad \mathbf{v}^s = \begin{bmatrix} 0 \\ v_g^s \\ v_s^s \end{bmatrix} \quad (6.2)$$

where the three partitions refer to the degrees of freedom associated with the building, the contact surface, and the soil. The response is expressed as the sum of the dynamic and pseudostatic components as:

$$\mathbf{v}^{total} = \mathbf{v}^{dynamic} + (\mathbf{r}\mathbf{v}_g)^{pseudostatic} \quad (6.3)$$

Where:

$$\mathbf{r} = -[k^b + k^s]^{-1} \begin{bmatrix} k_{bg}^b \\ k_{gg}^b \\ 0 \end{bmatrix} \quad (6.4)$$

The mass matrices defining the physical properties of the building, foundation, and soil systems have been partitioned as follows:

$$\mathbf{m}^b = \begin{bmatrix} m_{bb}^b & m_{bg}^b & 0 \\ m_{gb}^b & m_{gg}^b & 0 \\ 0 & 0 & 0 \end{bmatrix} \quad \mathbf{m}^s = \begin{bmatrix} 0 & 0 & 0 \\ 0 & m_{gg}^s & m_{sg}^s \\ 0 & m_{gs}^s & m_{ss}^s \end{bmatrix} \quad (6.5)$$

Similar expressions can be written for the damping and stiffness matrices.

The response of the mathematical model to earthquake motions can be evaluated by transforming the general equations of motion to normal coordinates and using numerical integration [Clough and Penzien (1975)]. If damping properties of the building and of the soil differ, the generalized damping matrix is not diagonal; therefore, the modal equations typically cannot be solved independently.

The complete discretized model of the soil-structure system can be used to calculate system response; however, due to the large problem size, and uncertainty of the soil properties and earthquake motions, a simplified approach is often desirable.

### **6.3 Simplified Procedures**

Simplified approaches to the soil-structure interaction problem generally focus on two factors that are primarily responsible for the difference in response of a rigidly and flexibly supported structure. First, the base of the structure can translate or rotate changing the dynamic characteristics and displacements of the structure as compared with a rigidly supported structure (Fig. 6.1). The rocking motion may be particularly important for taller structures [Veletsos (1977)]. Second, a substantial amount of vibration energy of the structure can be dissipated in the soil medium by radiation and hysteretic (material) damping.

The simplified procedures discussed in the following subsections are based on linear elastic methods. The first procedure presents a method that simplifies the modeling of the soil, whereas the second procedure is recommended in ATC-3-06 (1978). Both methods

assume that the structure and the underlying soil remain bonded throughout the duration of motion and that there are no soil instabilities or large foundation settlements.

### **6.3.1 Elastic Half Space**

If the foundation of the building can be considered a rigid disk supported on a deep, relatively uniform soil medium an elastic halfspace model can be used [Clough and Penzien (1975)]. The three translational and three rotational degrees of freedom at the base of the structure are modeled using springs. Appropriate spring constants can be evaluated for the elastic halfspace by methods of continuum mechanics. In general, the stiffness, mass, and damping associated with the soil are frequency dependent. However, for most building systems, sufficient accuracy can be obtained by using frequency independent soil parameters [Newmark and Rosenblueth (1971)]. Clough and Penzien (1975) recommend values for frequency independent soil model parameters.

The response of the mathematical model to earthquake motions can be evaluated by the same procedures used for the complete discretized model. The equations of motion can be evaluated by transforming to normal coordinates and using numerical integration [Clough and Penzien (1975)]. Again, if damping properties of the building and of the soil are different, the generalized damping matrix is not diagonal, and the modal equations cannot be solved independently.

### **6.3.2 ATC-3-06 Procedure**

Two simplified approaches are often used to represent the effects of soil-structure interaction [Veletsos (1977)]. The first approach involves modifying the free-field motions and

evaluating the response of the fixed based structure to these motions. The second approach involves modifying the dynamic characteristics of the structure and evaluating its response to the free-field motions. Either approach can be used to yield satisfactory results [Veletsos (1977)].

The ATC-3-06 (1978) procedures for soil-structure interaction are based on methods that modify the dynamic characteristics of the structure [Veletsos (1977)]. It has been shown that the interaction effects may be expressed by an increase in the fundamental period of vibration of the structure, and by a change (usually an increase) in the effective damping [Veletsos (1977)]. The increase in the fundamental period is a result of the flexibility of the foundation soil, whereas the change in damping is mainly a result of the energy dissipation in the soil due to radiation and material damping.

The structure is assumed to be supported on a rigid circular mat foundation with negligible thickness at the surface of a homogeneous elastic halfspace. The weight of the structure and its foundation are assumed to be uniformly distributed over the foundation-soil contact area. The fundamental period of the structure supported on soft soil is given by

$$\tilde{T} = T \sqrt{1 + \frac{k}{K_x} \left(1 + \frac{K_x h^2}{K_\theta}\right)} \quad (6.6)$$

where  $T$  is the period of the fixed-base structure;  $K_x$  is the translational stiffness of the foundation;  $K_\theta$  is the rocking stiffness of the foundation;  $k$  is the lateral stiffness of the structure (for the mode of interest); and  $h$  is the height from the base of the structure to the centroid of the inertia forces (for the mode of interest).

The stiffness of the foundation material,  $K_x$  and  $K_\theta$ , depend on the geometry of the

foundation-soil contact area, the properties of the soil, and the intensity of the ground motion. For a rigid circular foundation mat, the translational and rotational stiffness are defined by [Veletsos (1977), Newmark and Rosenblueth (1971)]

$$K_x = \frac{8}{2 - \nu} Gr \quad (6.7.1)$$

$$K_\theta = \frac{8}{3(1 - \nu)} Gr^3 \quad (6.7.2)$$

where  $r$  is the radius of the foundation,  $G$  is the shear modulus of the soil, and  $\nu$  is Poisson's ratio. The shear modulus can be calculated using Eq. 4.3 or 4.5. Both can be modified for ground motion intensity [ATC-3-06 (1978)].

For mat foundations of arbitrary shape, the soil stiffness defined by Eq. 6.7.1-2 are modified. The radius,  $r$ , in Eq. 6.7.1 is specified by

$$r_a = \sqrt{\frac{A_0}{\pi}} \quad (6.8.1)$$

and the radius in equation 6.7.2 is specified by

$$r_m = \sqrt[3]{\frac{4I_0}{\pi}} \quad (6.8.2)$$

where  $A_0$  is the effective area of contact between the foundation and the soil, and  $I_0$  is the static moment of inertia of the area about the centroidal axis in the direction in which the response is being evaluated.

The effective damping for the combined soil-structure system may be expressed by

$$\tilde{\beta} = \beta_0 + \frac{\beta}{(\tilde{T}/T)^3} \quad (6.9)$$

where  $\beta$  represents the damping of the fixed base structure, and  $\beta_0$  represents the contribution of the foundation damping. The foundation damping factor,  $\beta_0$ , has been found to

depend primarily on three parameters [Veletsos (1977)]: (1) the ratio of the natural periods of the elastically supported and fixed base structures,  $\tilde{T}/T$ ; (2) the ratio of the height of the structure to the radius of the foundation,  $h/r$ ; and (3) the damping capacity of the soil material. The damping ratio of the soil is commonly expressed as a function of the hysteretic stress-strain relationship of the soil.

Because the stress-strain relationships for soils are nonlinear, the values for  $G$  and  $V_s$  are functions of the intensity of ground shaking. Table 6.1 lists recommended values for  $G$  and  $V_s$  as a function of effective peak ground acceleration [ATC-3-06, Table 6-A (1978)].

The effect of soil-structure interaction in the ATC-3-06 (1978) procedures always is a reduction in the lateral forces, base shear, and overturning moment [Veletsos (1977)]. Because of the rocking and translation of the foundation the displacements relative to the base may be larger than those for the fixed-base structure.

#### **6.4 Recorded Information on Soil-Structure Interaction**

Due to the likelihood of aftershocks, a group from the United States Geological Survey (USGS) went to Chile soon after the 3 March 1985 earthquake. Several significant aftershocks occurred, and instrumental recordings were obtained in several buildings to address the importance of site response and soil-structure interaction [Celebi, ed. (1986) and Bongiovanni et al. (1987)].

One of the buildings in which instrumental recordings were obtained was a triangular-shaped, 22-story, reinforced concrete condominium building called Torres de Miramar. It was one of two identical buildings along the beach in Viña del Mar that were undamaged in

the 1985 earthquakes. Figures (6.2.a-d) present plan and elevation views of the buildings. The lateral and vertical load resisting system is composed of three channel-shaped walls and perimeter columns coupled by a thin floor slab. Free vibration testing of the building conducted after the earthquake revealed a fundamental period of approximately 1.06 sec [Bongiovanni et al. (1987) and Calcagni (1987)]. Fourier amplitude spectra for the recorded roof displacements in aftershocks revealed a fundamental period of approximately 1.1 sec [Bongiovanni et al. (1987)].

## **6.5 Analysis of Torres del Miramar Building**

To ascertain the importance of the soil system on the dynamic response of the buildings along the beach in Viña del Mar the Torres de Miramar building was studied in detail. The computer program **CAL-86** [Wilson (1986)] was used initially to compute response characteristics of the mathematical model, because it was capable of solving the coupled modal equations of motion that resulted from the non-proportional damping matrix. Later studies showed the coupling to be insignificant; therefore, any standard structural analysis program could have been used. The **SAP80** [Wilson (1988)] program was used for all results reported in this Chapter, except where noted.

### **6.5.1 Building Model**

The building was modeled using both a complete 3D representation of the building and a simplified model consisting of a 3D-column element for each story. The simplified model, assuming the three channel-shaped walls composing the lateral load resisting system

(Fig. 6.2.a-b) were uncoupled above the second floor, and rigidly coupled in the first and second floors, was found to accurately represent the complete 3D model. The geometric properties of the walls were computed based on concrete gross sections, and are presented in Table 6.2 for the simplified model. The modulus of elasticity of the concrete was taken as  $240,000 \text{ t/m}^2$  (3,400 ksi) [Wood et al. (1986)]. The mass distribution for the building was taken as  $1.0 \text{ t/m}^2$  (205 psf), which is typical for most Chilean buildings. The computed fixed base fundamental period was approximately 0.92 sec for both the 3D and simplified models, compared with the measured free vibration period of 1.06 sec. Based on the good correlation between the simplified and 3D models, the simplified model will be used for all subsequent discussion.

### 6.5.2 Soil Model

The importance of soil-structure interaction for the Miramar building was investigated based on the assumption that the deep, relatively uniform soil in Viña del Mar could be represented as an elastic halfspace. The simplified model of the superstructure was used with the stiffness, mass, and damping values for the soil taken from Clough and Penzien (1975). The shear modulus for the soil was computed using the relation recommended by Seed et al. (1984), and is primarily a function of effective overburden pressure, soil density, and soil shear strain. The effective overburden pressure at the base of the building is equal to the weight of the building minus the pore water pressure. The water table along the beach varies from approximately 2 to 8.5 m [Wood et al. (1986)]. A depth of 6 m was assumed. The average relative density of the foundation material for depths of 6 m (building base) to one equivalent foundation diameter below (16 m) was computed [Peck, Hanson and

Thornburn (1974)] to be 60 to 70% based on standard penetration tests [Appendix A]. A maximum shear modulus of  $22,000 t/m^2$  was computed based on the above parameters.

A site response analysis for an equivalent linear horizontally layered soil system [Schnabel et al. (1972)] was used to calculate the effective soil strain for both low (0.05g) and high (0.18g) intensity ground motions (base rock). The motions recorded during the 3 March 1985 earthquake at Valparaíso were used to represent the base rock motion. Because the effective depth to bedrock is not known analyses for depths of 50, 75, and 100 m were considered. The calculated strain-dependent moduli did not vary significantly with depth, and averaged 90 and 45% of the maximum modulus for the low and high intensity motions, respectively. These percentages are close to the values of 81 and 42% suggested by ATC-3-06 (1978). The higher percentages calculated are due to the relatively high overburden pressure [Seed et al. (1984)].

### 6.5.3 Analysis Results

Table 6.3 presents the results of four analyses. The first assumes no flexibility of the soil. The second through fourth analyses consider the effect of soil flexibility as the ground motion intensity increases. The second analysis is representative of the very low intensity motions that would produce building response similar to that for free vibration testing. The third analysis is representative of low to moderate intensity ground motions similar to those recorded during the aftershocks from the 3 March 1985 earthquake. The fourth analysis is representative of severe intensity ground motions similar to those recorded in the 3 March 1985 earthquake.

For the fixed base model, the computed fundamental period of 0.92 sec is 15% lower than that recorded during free vibration tests. When the flexibility of the soil is included for very low soil strain conditions (second analysis) the period increases to 1.06 sec, which is equal to the recorded free vibration period. For low intensity motions, the reduction in soil shear modulus increases the calculated periods for the first and fourth modes to 1.12 and 0.22 sec, respectively. These periods agree with the periods observed from the recorded aftershock data. For severe ground motions, the first two sets of translational periods are computed to be equal to 1.32 and 0.26 sec. This change represents an increase of nearly 45% for the fundamental period compared with the fixed base model.

Figure 6.3 plots computed elastic roof displacement, base shear, and base overturning moment response for the fixed base (FB) and combined soil–building model (SB) using the CAL–86 program (non-proportional damping). Table 6.4 presents the response maxima. The Viña del Mar S20W record obtained in the 3 March 1985 earthquake was used as input. It was assumed that this motion is representative of the ground motions at the Miramar building, although it was shown in Chapter 4 that the motions along the beach may have been of lower frequency content. Roof displacements of 23 and 24 cm were computed for the FB and SB models, respectively, corresponding to roof drifts of 0.41 and 0.43% of the building height. The computed base shear and base overturning moment were  $0.40W$  and  $0.30Wh$ , and  $0.21W$  and  $0.17Wh$  for the FB and SB models, respectively. Apparently, consideration of base flexibility reduces the base shear and overturning demand for elastic response by 90% and 88%, respectively.

Figure 6.4 plots the same response parameters as Fig. 6.3 for the SB model using the SAP80 model (neglecting the soil damping) and the CAL–86 model (including the soil

damping). The computed displacement and base overturning response are nearly identical; however, the base shear response differs. Apparently, the soil damping has a significant influence on the contribution of higher modes to base shear.

Table 6.4 also presents the base shear and base overturning moments computed for a simplified version of the Viña del Mar S20W 5% damped response spectrum (Fig 6.5). The CQC modal combination method [Wilson, et al. (1981)] was used because the periods were not well separated ( $T_1 = T_2$ ,  $T_4 = T_5$ ). The results of the spectral analysis generally agree with the response history analysis results (neglecting the soil damping). For comparison, the modal responses combined using the SRSS method (Table 6.4). The results using the SRSS method are not reliable because the translational periods are identical and there mode shapes are coupled.

Figure 6.6 plots the elastic spectral displacement relation calculated from the Viña del Mar S20W record for 5% damping. Figure 6.7 plots the corresponding relation for spectral acceleration, and the simplified spectrum. The fundamental periods computed for the fixed base model and the combined soil–building model for high intensity motion are indicated on the figures. The peak roof displacements calculated are not significantly influenced by the soil flexibility because the spectral displacement curve is essentially constant over a broad range of periods. Because the attenuation of spectral acceleration at periods greater than 0.75 sec can be estimated as a function of  $1/T^2$ , the elongation of the fundamental period due to the soil flexibility has a pronounced effect on the base shear and base overturning moment (See Table 6.4).

## 6.6 Simplified Analysis Using ATC-3-06 Procedure

The ATC-03-06 (1978) procedures are based on the methods outlined by Veletsos (1977). The period of the structure supported on an elastic halfspace is calculated by Eq. (6.6), whereas the effective damping is calculated by Eq. (6.9). Higher modes do not effect the results appreciably [Newmark and Rosenblueth (1971)], and thus are neglected. The effective modal weight and height are taken as  $0.70W$  and  $0.70H$ , respectively [Veletsos (1977)]. The effective shear modulus for the soil is taken as 42% of the maximum value ( $22,000 \text{ t/m}^2$ ), based on the values suggested in [ATC-3-06 (1978), Table 6-A] for ground accelerations greater than  $0.30g$ .

A period of 1.26 sec is calculated, which is 37% higher than the fixed base result. This result is very close to the results obtained using the combined soil-building model of Section 6.5. An effective damping coefficient of 5.4% is calculated using Eq. (6.9), which is not significantly different from the 5% fixed base damping coefficient. Computed responses using the simplified model are presented in Table 6.4. The values compare well with those cited previously.

## 6.7 Summary

The effect of soil flexibility on the dynamic response of the buildings in Viña del Mar was investigated. The response of one of the Torres de Miramar buildings was studied for varying ground motion intensity. The analysis results were compared with available data from free vibration testing [Calcagni (1987), and Celebi, ed. (1986)], and aftershocks recorded by the USGS [Celebi, ed. (1986), and Bongiovanni et al. (1987)].

Based on a 3D-stick model of the building supported on frequency independent soil springs good agreement was obtained between the analytical and measured periods for both the free vibration and aftershock tests. For high intensity motions the soil medium was found to significantly influence the dynamic characteristics of the building. The elongation of the fundamental period due to the flexibility of the soil resulted in a reductions of base shear and base overturning moment of 33% and 90% of the fixed base values, respectively. Simplified procedures [ATC-3-06 (1978)] were also able to estimate the influence of the soil medium on the building response.

Based on the analysis results of this chapter the influence of the soil medium on the dynamic characteristics of the buildings in Viña del Mar can be estimated. Due to the rapid attenuation of spectral acceleration at periods greater than 0.75 sec the effect of the soil flexibility on computed base shear and base overturning moment may be pronounced for taller buildings.

# CHAPTER 7

## EVALUATION OF FOUR BUILDINGS IN VIÑA DEL MAR

Studies of design, analysis, and performance during the 3 March 1985 earthquake are presented for four buildings located in Viña del Mar, Chile. The study is organized into seven parts in this chapter. The first section describes the buildings studied and the damage observed after the earthquake. This is followed by sections on the materials used for construction and general design considerations. The fourth section presents and discusses the results of elastic code analysis of the buildings. Strength analysis and evaluation of deformation demands compose the fifth section. Response analysis for elastic and inelastic methods is presented in the sixth section, followed by a summary.

### 7.1 Description of Buildings Studied

The buildings selected for study were picked from the large number available for several reasons. Both damaged and undamaged buildings of similar construction were selected to determine the differences between the buildings, and to correlate the differences with observed damage. The proximity of the buildings, the availability of structural drawings, and materials information were also considered.

Four buildings were selected for study. All are located on or near the beach in Viña del Mar (Fig. 7.1). The buildings are referred to in this report by their names, Plaza del Mar (Fig. 7.2), Festival (Fig. 7.3), Acapulco (Fig. 7.4), and Torres de Miramar (Fig. 6.2). The buildings vary in height from about 40 m for the Festival and Acapulco buildings, to

56 and 69 m for the Miramar and Plaza del Mar buildings, respectively. The buildings were constructed between 1975 and 1982, except for the Acapulco building, which was constructed in 1964. No structural damage was observed in the Plaza del Mar and Miramar buildings. The Festival building was moderately damaged, whereas the Acapulco building suffered greater damage. Detailed building descriptions and reported damage from the 3 March 1985 earthquake are summarized in Appendix B.

## 7.2 Construction Materials

For the Plaza del Mar, Festival, and Torres de Miramar buildings the materials used for construction were Class E concrete and A-63-42H steel [Appendix C]. Concrete tests conducted during construction of the buildings gave cube strengths of approximately 260 kg/cm<sup>2</sup> and 300 kg/cm<sup>2</sup> for 7 and 28 day tests, respectively [Appendix C]. The cube strength corresponds to approximately 255 kg/cm<sup>2</sup> cylinder strength for the 28 day test [Wood et al. (1987)]. The material properties used for the analyses of all but the Acapulco are building are summarized below.

Concrete:	$f'_c =$	255 kg/cm <sup>2</sup>	[ 3.6 ksi]
	$E_c =$	240000 kg/cm <sup>2</sup>	[ 3400 ksi]
Steel :	$f_y =$	4200 kg/cm <sup>2</sup>	[ 60 ksi]
	$E_s =$	2040000 kg/cm <sup>2</sup>	[29000 ksi]

Class D concrete and two types of steel were used in the construction of Acapulco [Appendix C]. Concrete tests conducted during construction gave average cube strengths of 160 kg/cm<sup>2</sup> and 235 kg/cm<sup>2</sup> for 7 and 28 day tests, respectively. The cube strength corresponds

to 190 kg/cm<sup>2</sup> cylinder strength for the 28 day test. The steel consists of plain and twisted (deformed) bars. The plain bars have yield and ultimate strengths of approximately 2700 and 5300 kg/cm<sup>2</sup>, respectively. The twisted bars have yield and ultimate strengths of 5100 and 6800 kg/cm<sup>2</sup>, respectively. Damage to the building revealed that approximately equal amounts of twisted and plain steel were used at the wall boundaries [See Wood et al. (1987) Fig. 6.6, or Wyllie et al. (1986) Fig. 4.19]. The material properties used for the analyses of the Acapulco building are:

Concrete:		$f'_c =$	190 kg/cm <sup>2</sup>	[ 2.7 ksi]
		$E_c =$	210000 kg/cm <sup>2</sup>	[ 2950 ksi]
Steel:	(plain)	$f_y =$	2800 kg/cm <sup>2</sup>	[ 40 ksi]
	(twisted)	$f_y =$	5100 kg/cm <sup>2</sup>	[ 72 ksi]
		$E_s =$	2040000 kg/cm <sup>2</sup>	[29000 ksi]

### 7.3 General Design Considerations

Although detailed calculations are not available, all four of the buildings were designed according to the Chilean code, *Cálculo Antisísmico de Edificios*: NCh 433-Of.72 (1979). (Although designed earlier, the design for Acapulco was based on a preliminary draft of this code). According to NCh 433, the taller buildings (Plaza del Mar and Miramar) would be designed for a seismic coefficient of 0.06 (code minimum). The seismic coefficient for the Acapulco and Festival buildings would depend the estimate of the fundamental period of the building. Assuming that a soil coefficient ( $T_0$ ) of 0.3 was used, the minimum code seismic coefficient does not govern until the fundamental period is greater than 0.9 sec. Although the Chilean code does not suggest an approximation of the fundamental building period

some Chilean engineers use  $T = 0.012H$  m [Baeza (1963)]. Based on these assumptions a seismic coefficient of 0.088 is computed for the Acapulco and Festival buildings.

According to NCh 433, the lateral displacement for all buildings is limited to 1/500 of the height to limit secondary damage (code requirement for buildings in which the non-structural elements are not isolated from the structural elements). The slab is typically assumed to provide a rigid floor diaphragm, but not to flexurally couple the shear walls; therefore, it is common to design structural walls as cantilevers.

The Acapulco building was designed with hand calculation methods. The analysis model for Plaza del Mar consisted of three degrees of freedom at each floor level. Because of the wall layout, attempts were made to reduce torsion. The lintels over the doors in the hallway were precast and lightly connected to the walls. A water tank at the roof coupled the walls in the transverse direction, but was not considered in the design. Static code procedures were probably used for the Festival and Miramar buildings. In the Festival building, walls forming the water tanks at the roof level act as coupling beams in the transverse and longitudinal directions (See Appendix B), but were not likely to have been considered in the design.

Each of the buildings has one or two basement levels, or a mat (solid or cellular) foundation, that provide ample anchorage for the wall steel at the base of the walls. The boundary steel in the walls of the Plaza del Mar building was anchored through the massive basement levels into the 1-m thick foundation mat. The boundary steel in the walls of the Festival building (# 9 U.S. bar) is anchored from 100 to 250 cm (40 to 100 in.) into the 3.2 m cellular mat foundation. The wall boundary steel for the Acapulco building has anchorages of 2.5 to 6 m (with hooks). The basement levels in the Miramar building

provided substantial anchorage for the wall boundary steel. Lap splices typically occur at, or just above, the floor slab level. The splice lengths were 100 cm in the Festival building, approximately 100 to 150 cm in the Plaza del Mar building, and approximately 250 cm in the Acapulco building. Anchorage and splice failures were not reported.

Beam stirrups usually consist of 8 or 10-mm single closed hoops at 20 cm. Details of beam reinforcement on structural drawings are not common. Main reinforcement is typically called out in tables, but specifics are left up to the contractor. The contractor generally follows guidelines published by the reinforcing bar manufacturer, CAP [Barras para Hormigón Armado].

#### **7.4 Results of Elastic Building Analyses**

Elastic periods, mode shapes and response levels were calculated according to the procedures outlined in Section 5.1. The Acapulco, Plaza del Mar, and Miramar buildings were assumed to be fixed at the base of the first floor because wall areas significantly increased in the basement levels for these buildings. The model of the Festival building was assumed to be fixed at the base of the parking level. Computed periods were compared with measured data [Calcagni (1987)] using three-dimensional models of the buildings. The calculated periods were used to evaluate the static code base shear and compute code drift for both the UBC (1985) and Chilean code. The response characteristics were typically computed for the transverse direction only, as damage in the longitudinal direction was generally less severe. A 2D model for the transverse direction was also investigated for the Festival building to compare with the 3D results, and to facilitate the development of a 2D inelastic model.

#### 7.4.1 Periods and Mode Shapes

The **SAP80** structural analysis program [Wilson (1988)] was used to compute elastic periods and mode shapes for the fixed base building models. No attempts were made to adjust computed results to match measured periods (discussed in the next paragraph). Table 7.1 presents the first three computed periods for each of the four buildings assuming fixed bases. The mode shapes are plotted in Fig. 7.5–7.8. The computed fundamental periods vary between  $N/15$  (Acapulco) and  $N/25$  (Festival), where  $N$  is the number of stories. The first two mode shapes for the Festival and Miramar buildings are translation. Because of the layout of the structural walls in the Acapulco and Plaza del Mar buildings, the first two mode shapes are short axis translation coupled with torsion.

Table 7.1 also presents periods for the four buildings measured in small amplitude vibrations [Calcagni (1987)]. The measured periods are slightly greater than those computed for the Festival and Miramar buildings, and less for the Plaza del Mar and Acapulco buildings. The difference in the measured and computed period for the fundamental mode of the Plaza del Mar and Acapulco buildings may be due in part to the torsional movement of the building not measured in the small amplitude vibrations.

The difference between the computed and measured periods may be due to factors such as damage caused by the earthquake or flexibility of the foundation materials. Chapter 6 revealed that the foundation flexibility could have a pronounced effect on building response; therefore, the effect of base flexibility on the building periods is estimated. Because soil flexibility depends on intensity of ground motions, calculations were made for both small amplitude vibrations and severe ground shaking using ATC-3-06 (1978) procedures. Table

7.2 presents the computed flexible base periods. Computed damping ratios including soil-structure interaction are in Table 7.3.

Consideration of soil flexibility increases the fundamental periods from 5 to 17 percent for small amplitude vibrations (Table 7.2). Good agreement was obtained between the computed and measured periods for modes that were uncoupled (Festival and Miramar buildings, and for the longitudinal directions of the Plaza del Mar and Acapulco buildings). Where coupling occurred, the poorer agreement may result because of difficulties in identifying the modes in free vibration testing. The consideration of soil flexibility for strong ground motions increases the computed periods from 12 to 37%.

#### 7.4.2 Code Analysis

Seismic code requirements for the Uniform Building Code (1985) and the Chilean Code [Cálculo Antisísmico de Edificios (1979)] were compared so that code conformity could be ascertained. Both equivalent static and dynamic (response spectrum) methods were used following the specifications of each code. The procedures and code requirements are discussed in the following paragraphs.

The equations for the code seismic coefficient can be used directly to calculate the equivalent static lateral force, or to produce an equivalent code acceleration spectra for modal analysis. The spectra are plotted in Fig. 7.9 for both codes. Soil coefficients of 1.2 and 0.3 were used for the UBC and Chilean code, respectively. For the UBC, values for  $Z$ ,  $I$  and  $K$  were taken as unity. For the Chilean code, both  $K_1$  and  $K_2$  were taken as unity. Load factors of 1.4 and 1.70 were used for the UBC and Chilean code, respectively.

A higher value is used for the Chilean code because the allowable concrete stress is 49% of the cylinder strength compared with an equivalent value of 60% ( $=0.85/1.4$ ) for the UBC (A similar factor is obtained by comparing steel stresses). The factored code base shear for the equivalent static lateral load procedure for both the UBC and Chilean code are presented in Table 7.4 (for all four buildings). The differences in the required base shear are not significant.

Figures 7.10.a–7.13.a plot the story drift ratio over the height of the building for both static code elastic analyses. Load factors were taken as unity for both the UBC and the Chilean Code. Figures 7.10.b–7.13.b plot the interstory drift ratio over the height of the building. The code allowable drifts (0.005h for UBC, and 0.002h for NCh 433) are also plotted on the figures for reference. The plots indicate that the buildings are very stiff. Drift ratios calculated by the two codes are very similar. Calculated drift ratios are 10 to 20% of the UBC allowable, and 20 to 40% of the Chilean code allowable. Table 7.4 presents the maximum drift ratios computed. Because of water tanks that couple the walls at the roof levels in the Plaza del Mar and Festival buildings, maximum interstory drift ratios are computed in the middle to upper stories.

Local UBC strength requirements were checked for several walls in the three buildings. Calculations were based on rectangular wall sections. Both major and minor resisting walls were checked for the Festival and Acapulco buildings. Only minor walls were checked for Plaza del Mar building because of difficulties in defining design procedures for the major resisting elements. Table 7.5 presents results of the analysis. The strength ratios indicate that provided member strengths exceed those required by the UBC.

Although all the walls checked satisfied the strength requirements of the UBC, detailing

generally does not. The major differences in the Chilean and UBC design requirements are that the UBC typically requires boundary elements with special transverse reinforcement (because the extreme fiber stress exceeds  $0.2f'_c$ ). No boundary or special transverse steel requirements exists for the Chilean code. The UBC also requires web steel of 0.25 percent, whereas the Chilean code requires 0.2 percent. Therefore, walls designed for the same forces are markedly different. Figure 7.14 presents two walls designed and constructed in Chile. Figure 7.15 presents an example of a two walls designed for the same forces by each code.

## 7.5 Strength Analysis

If a building system does not provide sufficient strength for elastic response the ability of the structure to deform in the inelastic range is critical. In Section 3.2.3 displacement ductility spectra were presented (Fig. 3.7 and 3.8) that indicated significant elasto-plastic response demands for structures of moderate strength ( $0.40W$ ) for the Viña del Mar S20W ground motion. Given that conventional ductile detailing generally was not used, and that observed damage in the majority of the buildings was light, one might conclude that Chilean buildings must be relatively strong. Therefore, strength of the buildings was investigated to ascertain its importance to the performance of the Chilean buildings during the 3 March 1985 earthquake.

Base shear strengths for the transverse and longitudinal directions of the four buildings were computed for a triangular loading distribution over the building height. The controlling mechanism typically consisted of yielding at the base of the walls and in the coupling beams over the height of the building (Fig. 7.16). Uplifting of the walls due to rocking was neglected; therefore, the work required to uplift walls tributary gravity loads was not

considered. The distribution of strength over the height of the wall was checked to ensure that yielding did not occur in other stories. For all but the Acapulco building the longitudinal steel was decreased gradually so that wall yielding was computed to occur only at the base. Because of bar cutoffs in floors 3 through 7 in the Acapulco building, yield of the walls at levels other than the base was possible and is investigated fully in Section 7.5.3. Walls coupled with beams were checked to determine whether the controlling mechanism included yielding of the coupling beams (Fig. 7.16). The methods used to compute member strengths are described in Section 5.2. The flexural strength of the beams and walls were computed including the effects of steel strain hardening. Unconfined concrete was assumed because the detailing provided in the beams and walls would not significantly increase the flexural strength. The shear capacity was computed to compare with the flexural capacity. Equation (11-6) of ACI 318 (1983) was used to compute beam shear strength. Wall shear strength was computed by

$$V_n = A_{cv} \left[ 0.53\sqrt{f'_c} + \rho_n f_y \right] \quad (7.1)$$

where,  $A_{cv}$  is the shear area of the wall in square centimeters,  $\rho_n$  is the steel ratio for the wall web, and  $f_y$  is the yield stress for the web steel in  $\text{kg}/\text{cm}^2$ . Concrete strength is based on specified values, or tests results (Appendix C). Specified yield stress is used for the steel. For buildings where the walls are not aligned with the transverse or longitudinal axes of the building, wall shear area was computed as the product of the wall area times the cosine of the angle formed between the axis of the wall and the axis of the building.

Table 7.6 presents the computed base shear strengths of the four buildings. The following sections discuss the computed base shear strengths and investigate the interrelation of building strength, detailing, and damage.

### 7.5.1 Plaza del Mar Building

Figure 7.17 presents wall boundary steel and general geometry used to calculate the base shear strength of the Plaza del Mar building. Uniform wall steel consists of 10-mm (0.4 in.) bars at 25 cm. Slab steel is typically 8-mm (0.31 in.) bars at 20 cm. Table 7.7 presents the contribution of each axis of the building plan (Fig. 7.17) to the base shear strength. Base shear strengths of 0.18W and 0.13W were computed for the transverse and longitudinal directions of the building, respectively. The relatively low strengths are a result of the height of the building (23 stories), and the relatively light boundary steel used in the walls.

The wall shear area at the base of the building is approximately 30 m<sup>2</sup> in both the transverse and longitudinal directions. The computed shear strengths at the building base (for  $f'_c=255$  kg/cm<sup>2</sup>,  $f_y=4200$  kg/cm<sup>2</sup>, and  $\rho_n=0.002$ ) are 5060 tons (0.25W). The computed shear strengths are at least 40% greater than the computed flexural strengths; therefore, the base shear strength of the building is limited by the flexural strength of the walls at the bottom of the first story of the building.

The required displacement ductility for the 3 March 1985 earthquake can be estimated from Fig. 3.7 and 3.8 (Viña del Mar S20W). If the effect of the soil flexibility is neglected ( $T_1 = 1.39$  sec) the required displacement ductility is approximately two for both response models. For a fundamental period of 1.70 sec (period including soil flexibility, Table 7.2) the displacement ductility is slightly greater than unity for both the elasto-plastic and bilinear response models. Both are consistent with the low level of damage observed in the building.

### 7.5.2 Festival Building

Section geometry and steel quantities are presented in Fig. 7.18. Structural details for the beams were not available; therefore, 1% longitudinal steel was assumed to compute beam strength. Table 7.8 presents the contribution to base shear strength for the beams and walls in the building (by axis, Fig 7.18). Base shear strengths of  $0.34W$  and  $0.30W$  were computed for the transverse and longitudinal directions of the building, respectively. The considerable strength of the building can be attributed to the generous quantities of boundary steel used in the walls. The majority of the building strength is concentrated along axes C, F, I, and L (Table 7.8, Fig. 7.18). The walls at axes C and L have openings over the height. For axis C the openings are small enough so that they do not likely affect the strength of the wall. For axis L the opening is larger, and the controlling mechanism results when the coupling beam created by the opening yields in shear.

In Section 7.3 the design base shear coefficient was estimated to be 0.09. If a load factor of 1.70 is used, and a factor of 1.25 is also applied to account for steel strain hardening in the walls, a minimum strength of  $0.19W$  is estimated from the code requirements. An increase of 25% to account for the contribution of the beams results in a strength of  $0.24W$ . Computed building strengths ( $0.30W$  and  $0.34W$ ) are approximately 1.3 times greater than this estimate, suggesting that the building is stronger than the minimum strength resulting from code requirements.

The wall area at the base of the building is approximately  $27 \text{ m}^2$  in both directions. Using Eq. (7.1), the computed shear strengths are 4550 tons ( $0.34W$ ) in both directions. Thus, the computed shear strength is equal to the flexural in the transverse direction,

and only slightly greater than the flexural strength in the longitudinal direction. However, experimental data compiled by Wood (1988) suggests that the shear strength of lightly reinforced walls is  $1.60\sqrt{f'_c}$  kg/cm<sup>2</sup> ( $6\sqrt{f'_c}$  psi) (versus the value computed with Eq. 7.1); therefore, the strength of the building is probably controlled by flexural yielding, although significant shear deformations would also occur.

The required displacement ductility for the 3 March 1985 earthquake can be estimated from Fig. 3.7 (Viña del Mar S20W). For periods of 0.61 and 0.58 sec (fixed base) in the transverse and longitudinal directions, elasto-plastic displacement ductilities of 5 and 8 are required, respectively. Consideration of soil flexibility ( $T_1=0.79$  sec and  $T_2=0.66$  sec, Table 7.2) does not significantly reduce deformation demands. Such high deformation demands would cause significant cracking and the building would become more flexible. Assuming a cracked stiffness equal to half the gross section stiffness as being representative of the effective linear stiffness, the effective period increases by a factor of the square root of two. Based on this assumption, displacement ductility demands are between two and three for both directions.

For buildings constructed with structural walls, the structural walls force coupling beams yield to over the height of the structure resulting in a gradual loss of stiffness until the walls yield at the base of the building. Therefore, displacement ductilities computed with an elasto-plastic response model may not be representative because the true force-deformation relation of the building is not elasto-plastic. A more representative model may be a bi-linear response model with strain-hardening. Figure 3.8 presents required displacement ductility for a bi-linear system with a yielding stiffness of 20% of the initial stiffness. Based on Fig. 3.8, displacement ductilities of approximately two are required for

both directions of the Festival building for the gross section stiffness. The values are only slightly reduced if cracking effects are considered.

Structural damage in the building (Appendix B) consisted of flexural cracking in corridor slab over the entire length of the building (in the upper stories), shear cracking in the walls, and crushing at the boundaries of walls F and I. A displacement ductility demand of two or three is not inconsistent with the level of damage observed in the building.

### 7.5.3 Acapulco Building

Because of the complex layout of the building, the importance of torsional response (Fig. 7.7), and the bar cutoffs in stories 3 through 7, a two-dimensional collapse mechanism for the building was difficult to define. Therefore, the base shear strengths were estimated using a simplified procedure, as follows. The beams and slab elements (Fig. 7.19) were assumed to yield over the entire height of the building (this assumption is supported by inelastic analysis [Section 7.6]). Steel ratios were assumed for several beams (1%), because details of the reinforcement were not available. The moment distribution over the height of the walls was assumed to be that occurring for a cantilever wall subjected to a triangular loading (Fig. 7.20). The assumption is justified because beam coupling was minimal. The moment at the base of each wall was calculated by limiting the total load (under triangular loading) to that required to reach the strength at the weakest level (Fig. 7.20). Figure 7.21 presents the sections and steel quantities used to compute the strength of the wall elements. Equal amounts of plain and twisted bars were assumed at the wall boundaries. The distributed steel in the walls consists of plain bars. The base shear strength of the

building was estimated by assuming the mechanism shown in Fig. 7.16 for the base wall moments computed as specified above.

Base shear strengths of  $0.18W$  were estimated for both the transverse and longitudinal directions. Table 7.9 presents the contribution to base shear strength for the beams and walls in the building (by axis, Fig 7.19 and 7.21). The weak stories for the walls are also noted in Table 7.9. Although considerable steel was used in the building, the strength is relatively low compared with the Festival building (which has about the same overall dimensions). The primary reasons for this lower strength were the use of lower strength materials, and the bar cutoffs. If the bar cutoffs are neglected, the base shear strength estimate increases 22% to  $0.22W$ .

De la Llera and Riddell (1988) also computed the base shear strength of the Acapulco building. They assumed that all of the boundary steel in the walls consisted of the lower strength plain bars. They also neglected the strength of the beams because they were damaged in previous earthquakes (Appendix B). Based on these assumptions they computed strengths of  $0.071W$  and  $0.096W$  for the transverse and longitudinal directions, respectively, for mechanisms starting at an intermediate story and extending through the height (Fig. 7.20). They report almost equal base shear strengths for mechanisms forming at the third through seventh stories.

Because significant damage occurred at the fourth level of wall M (levels six and eight were also damaged), the strength distribution over the height for this wall was examined in detail. Figure 7.21.m indicates the location and quantity of steel used in wall M. Figure 7.22 plots the computed flexural resistance to loads in the transverse direction, and the story moments that would result for a triangular loading over the wall height. The plot

indicates that yield is more likely in levels 3–8 than at the base.

The wall shear area at the building base is approximately 28 m<sup>2</sup> in the transverse direction, and 35 m<sup>2</sup> in the longitudinal direction. The computed shear strengths at the building base (for  $f'_c=190$  kg/cm<sup>2</sup>,  $f_y=2800$  kg/cm<sup>2</sup>, and  $\rho_n=0.002$ ) are 3600 tons (0.33W) and 4515 tons (0.41W) for the transverse and longitudinal directions, respectively. The computed shear strengths are 1.83 to 2.28 times greater than the computed flexural strengths; therefore, the base shear strength of the building is limited by the flexural capacity of the walls.

The required displacement ductility for the 3 March 1985 earthquake can be estimated from Fig. 3.7 and 3.8. For a fundamental period of 1.13 sec (Table 7.2) and a base shear strength of 0.18W, displacement ductility demands of three to four are estimated for both the elasto-plastic and bi-linear response models. Consideration of cracking effects reduces the displacement ductility demand to approximately two. A strength of 0.10W for the building [based on the assumptions of De la Llera and Riddell (1988)] increases the displacement ductility demands to between 8 and 10 for the elasto-plastic response model (Fig. 3.7). Consideration of cracking effects for their strength reduces the displacement ductility to five or six. Local demands for curvature ductility are greater than displacement ductility [Paulay (1986)]; therefore, significant flexural damage would be expected in the building if the assumptions of De la Llera and Riddell (1988) are accepted.

The building was significantly damaged in the earthquake. The damage reported consisted of flexural and shear cracking concentrated in levels 3–7 throughout the building, and crushing at the boundaries of walls M (at the fourth story) and K (at the first story). The significant amount of damage in the building is more than can be attributed to displacement

ductilities of less than four (computed based on building strength of  $0.18W$ ). Two possible reasons for the building damage are (1) that assumptions made by De la Llera and Riddell more accurately represent the real building, and (2) that torsional response of the building contributed to the damageability of the building (as well as the distribution of the damage). This subject will be addressed further in the latter parts of this chapter.

#### 7.5.4 Torres de Miramar Building

Figure 7.23 presents wall steel at the base of the Miramar building used to compute the building flexural strength. The core wall and the six columns at axes one through six (Fig. 6.2.a) were assumed to act in unison. The contribution of the beams, slabs, and the six corner columns were neglected. A base shear strength of  $0.27W$  was computed based on these assumptions.

The design base shear for the building was estimated to be  $0.06W$  in Section 7.3. If a load factor of 1.70 is used, and a factor of 1.25 is also applied to account for steel strain hardening in the walls, a strength of  $0.13W$  is estimated from the code requirements. An increase of 20% to account for the contribution of the beams results in a strength of  $0.16W$ , which is significantly less than the computed strength ( $0.27W$ ). This suggests the building is stronger than the minimum strength resulting from code requirements.

The wall shear area at the base of the building is approximately  $19 \text{ m}^2$ . The computed shear strength at the building base (for  $f'_c=255 \text{ kg/cm}^2$ ,  $f_y=4200 \text{ kg/cm}^2$ , and  $\rho_n=0.002$ ) is 3200 tons ( $0.30W$ ). The computed shear strength is 12% greater than the computed flexural strength; therefore, the base shear strength of the building is limited by the flexural strength of the walls.

The required displacement ductility for the 3 March 1985 earthquake can be estimated from Fig. 3.7 and 3.8. For a fundamental period of 1.26 sec (Table 7.2) the displacement ductility is slightly greater than unity for both the elasto-plastic and bi-linear response models. This is consistent with the low level of damage observed in the building. No structural damage was observed, and non-structural damage was light.

## **7.6 Dynamic Response Analysis for 3 March 1985 Earthquake**

Elastic response spectrum and inelastic response history analyses were conducted to estimate the building responses to the ground motion recorded in Viña del Mar. Although the analysis of local soil conditions at the building sites revealed that slightly longer-period motions might have occurred compared with the ground motions recorded (Chapter 4), no attempts were made to modify the recorded motion. Response was calculated for a simplified representation of the calculated response spectrum for the Viña del Mar S20W component (Fig. 6.5).

### **7.6.1 Elastic Response Spectrum Analysis**

Elastic response spectrum analysis to compute drift ratios and elastic base shear and base overturning moment were conducted using the **SAP80** computer program [Wilson (1988)]. A simplified spectrum for the Viña del Mar S20W ground motion (Fig. 6.5) was assumed to act in the transverse direction of the buildings. Analysis of the complete 3D structural systems was done for concrete gross sections for fixed base models. The CQC procedure [Wilson et al. (1981)] was used to combine modal responses because building

periods were not well separated. The elastic base shear is compared with the computed strength of the building to determine if the building was overstressed. In addition to the complete 3D analyses, a simplified analysis procedure was used to incorporate soil-structure interaction effects. The simplified analysis procedure assumes that 65% of the building mass participates in first mode response, and that the base overturning moment can be approximated by assuming the resulting base shear acts at 70% of the building height. The roof drift of the buildings was approximated by multiplying the spectrum drift (Fig 6.6) by 1.4.

Figures 7.24–7.27 plot the computed story drifts over the height of the building for the response spectrum analyses. Figures 7.24–7.27 also plot the interstory drift ratios over the height of the building. Maximum drift ratios are presented in Table 7.10. For the Acapulco and Plaza del Mar buildings, curves are plotted for both the centers of mass and corners of the building. The plots indicate that the drift ratios for the center of mass of the buildings are less than the UBC allowable (0.5%). (It is noted that the values are not directly comparable because the UBC limits are intended to apply to the code loadings, which are significantly reduced from the elastic spectrum values.) For the Plaza del Mar and Acapulco buildings maximum roof and interstory drift ratios for the building corners are approximately 0.7% and 0.85%, respectively.

Table 7.11 presents the elastic base shear for response spectrum analysis of the fixed base building models. The elastic base shear for the Festival building is the highest (0.82W), whereas that for the Plaza del Mar building is the lowest (0.21W). The elastic base shears for the Acapulco and Miramar buildings are approximately 0.40W. Elastic base shear exceeds computed base shear strength for all four buildings.

Table 7.12 presents the results of the simplified analysis for both fixed and flexible base analyses. The table reveals that the fixed base SDOF model gives a good approximation for base shear, base overturning moment, and roof drift compared with the values computed with the complete 3D models (Tables 7.10 and 7.11). Consideration of soil flexibility reduces the base shear and base overturning moment for all buildings. The largest reductions (approximately 50%) occur for the Plaza del Mar and Miramar buildings (Detailed studies of the Miramar building in Chapter 6 indicated reductions of base overturning moment of 90%). Computed base shear strength for both buildings exceeds the elastic base shear when soil-structure interaction is considered. Reductions for the Festival and Acapulco buildings are modest (from 10 to 25%), and elastic base shear exceeds the computed base shear strength by approximately two for both buildings.

Roof drifts for all but the Festival building were unaffected by the consideration of soil flexibility because the displacement spectrum (Fig. 6.6) is relatively constant for periods greater than 0.75 sec.

### **7.6.2 Inelastic Response History Analysis**

To evaluate the global effects of nonlinear response and to compare with the elastic results, inelastic response history analyses were conducted. The elastic analyses indicated that inelastic response should occur for the Acapulco and Festival buildings. The Festival building was selected for study because the structural layout was relatively simple, and the modes of the building are uncoupled (Fig. 7.6). Response was computed for the transverse direction of the building using the motion recorded in Viña del Mar (S20W component) as base input. Element modeling techniques for the analysis are described in Chapter 5. The

building model consisted of 6 frames, representing axes A, C, D & K, E & J, F & I, and L. The resistance of axes N was neglected.

Figure 7.28 plots the computed roof displacements and base shears. Figure 7.29 plots the envelop of the computed floor displacements and interstory drifts. The results for the elastic spectrum analysis are also plotted for reference in Fig. 7.29. Maximum roof displacement and maximum interstory drift of 17 cm (0.41%) and 0.65% were computed, respectively. The values are close to those computed for the elastic spectrum analysis. The maximum computed inelastic base shear was  $0.35W$ , compared with a computed strength of  $0.35W$ . Thus, the computations indicate the building was near its flexural strength. The computed nominal shear stresses for axes C and L are approximately  $1.33\sqrt{f'_c}$  kg/cm<sup>2</sup> ( $5\sqrt{f'_c}$  psi), suggesting the possibility of some shear distress in these walls. Plastic hinges “formed” in many of the coupling beams and slabs over the building height (Fig. 7.30). No hinges formed at the base of the walls, although maximum moments were close to yield.

## 7.7 Summary Evaluation

The following subsections summarize the analysis results for the four buildings in Viña del Mar, and attempts to correlate the results with observed damage. It is reiterated that all four buildings satisfied the UBC requirements for strength and drift. Requirements for ductile detailing generally were not satisfied.

### 7.7.1 Plaza del Mar Building

An eigenvalue analysis of the building revealed that the first two modes of the building were translation coupled with torsion (Fig. 7.5). Based on a collapse mechanism analysis, a

base shear strength of  $0.18W$  was computed for the transverse direction of the building. The relatively low base shear coefficient of the building results from moderate building height, and walls that are lightly reinforced. For the Viña del Mar S20W spectrum, elastic base shear for the transverse direction was computed to be  $0.21W$  for a fixed base model of the building; however, consideration of soil flexibility reduced the elastic base shear to  $0.15W$ . Computed roof and interstory drift ratios were 0.64 and 0.83%, respectively.

The analysis results indicate that extensive structural damage would not be expected in the building; however, the drift ratios suggest non-structural damage [Algan (1982), Freeman (1985)]. The torsional response also suggests that damage would occur at the building ends. No reconnaissance reports of building damage were available, although building designers reported that light non-structural damage occurred at several locations (Appendix B).

### 7.7.2 Festival Building

An eigenvalue analysis of the building revealed that the mode shapes of the building were essentially uncoupled (Fig. 7.6). For a collapse mechanism analyses, base shear strengths of  $0.35W$  and  $0.30W$  were computed for the transverse and longitudinal directions, respectively. Elastic spectral analysis for both fixed and flexible base models indicated relatively high demands for base shear (approximately  $0.70W$  for the transverse direction).

Computed roof drifts for the elastic and inelastic analyses were approximately equal. This suggests [Newmark and Hall (1982)] a displacement ductility of two based on the ratio of the elastic base shear to the computed base shear strength. Local demand for curvature

ductility is greater than displacement ductility. Paulay and Uzumeri (1975) suggest a relation that computes required wall curvature ductility for a given displacement ductility. Based on this relationship, a curvature ductility of four is estimated (for ratio of wall height to length equal to 5:1). The walls are likely to possess moderate curvature ductility because of low axial stress and light reinforcement. (This subject is discussed further in Chapter 8.) Therefore, severe flexural damage is not likely for the walls.

The inelastic analysis for the transverse direction of the building revealed flexural yielding of the beams and slabs in the middle and upper stories. Although, flexural strength of the walls was not exceeded for the inelastic analysis, high shear stresses were computed for some walls. The resistance of the building is concentrated along axes C and L (Fig. 7.3). Shear stresses of  $1.33\sqrt{f'_c}$  kg/cm<sup>2</sup> ( $5\sqrt{f'_c}$  psi) were computed for the walls along these axes. A wall shear strength of  $1.1\sqrt{f'_c}$  kg/cm<sup>2</sup> ( $4.10\sqrt{f'_c}$  psi) is computed for the walls using Eq. 7.1 (for  $f'_c = 255$  kg/cm<sup>2</sup>, a steel ratio of 0.00209, and a steel yield stress of 4200 kg/cm<sup>2</sup>). Therefore, the computed strength is 20% less than the computed shear stresses. The analysis suggests that significant shear cracking and possible even shear failure may occur; however, a greater strength is likely due to actual material properties. Experimental data compiled by Wood (1988) suggest a minimum shear strength of  $1.60\sqrt{f'_c}$  kg/cm<sup>2</sup> ( $6\sqrt{f'_c}$  psi) for walls with low transverse steel ratios. Shear failure appears unlikely based on these data.

The analysis results are consistent with the moderate damage reported following the earthquake. Demands on the building from the earthquake were high; however, the building possessed considerable strength. Evaluation of code strength requirements (Section 7.5.2) could not explain the overstrength.

### 7.7.3 Acapulco Building

Eigenvalue analysis of the building revealed that the first two modes of the building were translation coupled with torsion (Fig. 7.7). Base shear strengths of  $0.18W$  were estimated for both directions of the building. For the Viña del Mar S20W spectrum, the fixed base elastic analysis indicated relatively high demands ( $0.38W$ ) relative to the building strength. Consideration of soil flexibility (Table 7.2) increased the fundamental period to 1.13 sec, resulting in a reduction in base shear demand to  $0.31W$ . If the elastic and inelastic displacements are assumed to be equal, displacement ductilities of approximately two are calculated. This result is consistent with the results obtained from the inelastic displacement ductility spectra in Section 7.5.3. However, the result is inconsistent with the severe damage sustained in the building.

The discrepancy between the damage and ductilities quoted above can be explained in terms of torsion. The layout of the walls in the Acapulco building create considerable torsion (Fig 7.7). The torsion results in a concentration of drift and force at the ends of the building. Table 7.13 presents the results of two analyses for walls A and M (Fig. 7.21.m). The walls are at opposite ends of the building. Wall M was badly damaged. The first analysis restricts the torsional movement of the building, whereas the second allows torsion. The table presents the computed wall moments and shears for each analysis. The ratios of the forces, for the two analyses, indicate that torsion increases moments by a factor 2.0 and 1.5 for Wall A and Wall M, respectively. Shear forces are increased by approximately the same ratio. Concentration of the building damage in stories 3 through 7 resulted from bar cutoffs. Elastic drifts of approximately 1% were computed for the building corners.

#### 7.7.4 Miramar Building

Detailed analyses of the Miramar building (presented in Chapter 6) revealed that soil-structure interaction was an important consideration in evaluating the behavior of the building. An elastic base shear of  $0.43W$  was computed for a fixed base model. Consideration of soil flexibility reduced the elastic base shear to  $0.21W$ . A base shear strength of  $0.27W$  was computed; therefore, extensive structural damage is not expected. Light non-structural damage that was observed in the building is consistent with the computed interstory drift ratios (0.64%).

## CHAPTER 8

### IMPLICATIONS FOR DESIGN OF BEARING WALL BUILDINGS

To transfer information obtained from post earthquake evaluations to other geographic areas, variations in code requirements, construction practices, and earthquake ground motions must be considered. This chapter addresses these issues and investigates the implications of the 3 March 1985 earthquake on seismic design practices for structural wall buildings in the United States.

The first section investigates U.S. code requirements [ACI (1983) and UBC (1985)] to evaluate the effects of detailing requirements on building strength, and compares the U.S. requirements with Chilean code requirements [*Cálculo Antisísmico de Edificios - NCh 433-Of.72 (1979)*]. The second section compares spectra for earthquake motions in the U.S. with those for the 3 March 1985 earthquake. The next section investigates response parameters, for the buildings studied in Chapter 7, for spectra representing U.S. ground motions. Results of building studies from the University of Illinois [Stark (1988)] and the University of Michigan [Wight (1988)] are also incorporated in the evaluation. Based on these analyses, the final section investigates detailing requirements for bearing wall buildings.

## 8.1 Code Strength Requirements for Structural Wall Buildings

Because code requirements for structural walls in the U.S. differ from the common practice in Chile (See Section 2.3), the following sections investigate minimum building base shear strength resulting from the different code requirements. The strength values are compared with the computed base shear strengths for the Chilean buildings [Chapter 7, Stark (1988), and Wight (1988)]. Table 8.1 summarizes important characteristics of these buildings.

### 8.1.1 Minimum Base Shear Strength for Code Requirements

The base shear strength of a building is keyed to the design base shear, but depends also on detailing provisions specified in the codes [UBC (1985), ACI (1983)] and construction practices. Due to these latter two considerations, the actual base shear strength may be considerably greater than the design base shear. In U.S. buildings with structural walls, flexural overstrength arises from the requirements for (1) 0.25% minimum uniform steel, and (2) boundary elements that must carry the full design moment when the extreme fiber stress exceeds  $0.2f'_c$ . The Chilean code [*Cálculo Antisísmico de Edificios - NCh 433-Of.72* (1979)] does not required boundary elements, and the minimum required uniform steel is 0.20%. Additional factors that contribute to overstrength are (1) capacity reduction factors, (2) strain hardening of reinforcement, (3) slab contribution to beam flexural strength, (4) material overstrengths, and (5) redundancy of the structural system.

### 8.1.2 Comparison of Code Strength Requirements

A direct comparison of the minimum base shear strength for the U.S. and Chilean codes is possible by making several assumptions. First, a fundamental period of  $N/20$  is assumed. This assumption gives a good estimate for Chilean construction (Fig. 2.2), and is also representative of U.S. buildings having numerous shear walls. Second, the code base shear is assumed to act at 70% of the building height to compute overturning moment. This assumption is based on the code required static force distribution that results in a equivalent location at 67% of the building height for buildings with fundamental periods less than 0.7 sec, and slightly higher for more flexible buildings. In Chapter 7 (Tables 7.11 and 7.12), this approximation was shown to be reasonably accurate for spectral analysis of the Chilean buildings. Third, the contribution of the uniform steel in the wall is computed in non-dimensional form [Park and Paulay (1975)] assuming a compression force of  $0.1A_g f'_c$ . Fourth, the structural walls are assumed to extend over the full height of the building without abrupt changes in cross section. Lastly, the contribution of beams are neglected. Based on these assumptions the minimum code strength ( $C_y$ ) for wall buildings can be plotted versus number of floors ( $N$ ), and wall height to length ratio ( $h_w/l_w$ ), given a ratio of wall area to floor area. Load factors of 1.4 and 1.7 were applied to the code design base shear for the UBC-85 and NCh-433 code, respectively (See Section 2.2). A factor of 1.25 is also applied to account for the effects of steel overstrength and strain hardening.

Figure 8.1 plots minimum code base shear flexural strength for the UBC-85, for a wall area to floor area ratio ( $A_w/A_b$ ) of 0.5% in one direction. This wall to floor area ratio is representative of the current U.S. practice of relying on relatively few walls with boundary elements to resist the total lateral load. It is noted that web steel in addition to the assumed

0.25% would typically be required to resist shear stresses, increasing the strength for lower  $h_w/l_w$  ratios slightly relative to the contours plotted. For  $h_w/l_w$  of 5 to 7, flexural strengths of approximately 0.20W, 0.16W, and 0.14W are computed for buildings of 10, 15, and 20 stories, respectively (W is the weight of the building).

Figure 8.2 plots minimum code base shear flexural strength for the Chilean code, for a wall area to floor area ratio of 2.5% in one direction (typical of most Chilean buildings, Fig. 2.1). For  $h_w/l_w$  of 5 to 7, flexural strengths of approximately 0.19W, 0.15W, and 0.13W are required for buildings of 10, 15, and 20 stories, respectively. This is slightly less than that required by the UBC-85 (Fig. 8.1) because of the boundary element requirement for U.S. walls. At lower  $h_w/l_w$  ratios the Chilean strength becomes greater relative to the UBC-85 values due to minimum steel requirements acting in conjunction with the higher wall to floor area ratio. Also plotted in Fig. 8.2 are the computed base shear strengths for the buildings summarized in Table 8.1. The computed building strengths are consistently greater than the minimum required code strength, especially for the Torres del Sol, Festival, and Torres de Miramar buildings. This is primarily due to boundary steel used in excess of that required by code (Table 7.5).

Figure 8.3 plots the minimum code base shear flexural strength for U.S. buildings with wall area to floor area of 2.5% (comparable to Chilean buildings). The minimum strengths are considerably greater than those in Fig. 8.1 (for  $A_w/A_b = 0.005$ ), because of the significant contribution of the uniform steel in the wall web. For  $h_w/l_w$  of 5 to 7, flexural strengths of approximately 0.30W, 0.24W, and 0.20W are computed for buildings of 10, 15, and 20 stories, respectively. Computed base shear strengths for the Chilean buildings (Table 8.1) are also plotted in Fig. 8.3. Again the computed building strengths are greater than,

or approximately equal to, the minimum code base shear strength.

Figure 8.4 plots available shear strength for three ratios of wall to floor area. A shear strength of  $1.60\sqrt{f'_c}$  kg/cm<sup>2</sup> ( $6\sqrt{f'_c}$  psi) was assumed for the walls [Wood (1988)]. The plot indicates that design for shear is an important consideration when low ratios of wall area to floor area are used; however, for ratios typical of Chilean practice, shear strength is not likely to be a concern.

The observation that the base shear flexural strengths of the Chilean buildings are similar to minimum strengths that would be obtained for U.S. buildings with similar layouts is significant. If ground motion characteristics from the 3 March 1985 Chile earthquake are similar to those anticipated for U.S. design earthquakes, it may be possible to transfer the experiences of the Chilean practice directly to U.S. practice. Ground motion characteristics are studied in the next section.

## 8.2 Comparison of Spectra for U.S. and Chilean Ground Motions

In Chile, the eastward subduction of the Nazca plate under the continental margin produces the frequent earthquakes in the region. In contrast, most major faults in the western United States are strike-slip (San Andreas); therefore, it is important to compare the engineering characteristics of the ground motions before general conclusions can be drawn from the 3 March 1985 Chile earthquake. In the following paragraphs, the simplified acceleration and displacement spectra for the Viña del Mar S20W record (Fig. 8.5) are compared with spectra for previously recorded U.S. motions.

Table 8.2 presents characteristics for twelve ground motions recorded in the western U.S. for 5% damping. The records were selected to represent major earthquakes recorded

in the United States. The spectral displacements and accelerations are plotted in Fig. 8.6. Simplified representations of the spectral shapes are also plotted. The simplified acceleration spectrum has a peak acceleration of 0.80g for periods up to 0.50 sec, and decreases as a function of  $1/T$  at greater periods. The simplified displacement spectrum increases linearly (except at low periods) to 30 cm at a period of three seconds.

Figure 8.7 plots the simplified spectra for the recorded U.S. earthquake motions and for the Viña del Mar S20W record. The comparison reveals that the spectra for the Chilean record is more intense than that for the U.S. records for periods less than 1.5 sec, but less intense for greater periods.

In 1978, the Applied Technology Council published ATC-3-06 which recommended three spectral shapes to represent U.S. earthquakes. The three spectral shapes define ground motion characteristics for local geological conditions represented by (1) rock or stiff soils, (2) deep cohesionless soils or stiff clays, and (3) soft-to-medium stiff clays and sands. These three soil types are designated S1, S2, and S3, respectively. The spectral acceleration relations for regions of high seismicity (5% damped) are defined by

$$S_a = \frac{0.48Sg}{T^{2/3}} \quad (8.1)$$

where S equals 1.0, 1.2, and 1.5 for soil types S1, S2, and S3, respectively. The value of  $S_a$  need not exceed 1.00g for soil types S1 and S2. For soil type S3,  $S_a$  need not exceed 0.80g.

Figure 8.8 plots the spectral accelerations and displacements for the three ATC soil types, and the simplified spectra for the Viña S20W record. (It is noted that the Viña del Mar record was obtained on approximately 35 m of cohesionless soils, Chapter 4.) The plots reveal (1) that the ordinates of spectral acceleration for the Viña S20W record exceed those

for the ATC spectra for periods less than one second, but are lower for greater periods (Fig. 8.8.a), and (2) that ordinates of spectral displacement are similar for periods less than 1.00 sec, but the ATC ordinates are significantly higher for greater periods (Fig. 8.8.b).

Newmark and Hall (1982) have also recommended procedures to obtain response spectra for strong ground motions. According to the recommendations, building response spectra are calculated using frequency dependent amplification of a ground spectrum. The ground spectrum is defined by the maximum ground acceleration (0.5g), velocity (24 in./sec), and displacement (18 in.). Newmark and Hall (1982) also present procedures for computing inelastic spectra to read acceleration and displacement.

Figure 8.9 plots the spectral accelerations and displacements for the Newmark-Hall procedure (for 5% damping), and the corresponding simplified spectra for the Viña del Mar S20W record. The plots reveal (1) that the ordinates of spectral acceleration for the Newmark-Hall spectrum exceed those for the Viña del Mar S20W record for all periods (Fig. 8.9.a), and (2) that the ordinates of spectral displacement for the Newmark-Hall spectrum are similar to those for the Viña del Mar S20W record below 0.75 sec (Fig. 8.9.b), but increase at greater periods, whereas those for the Viña S20W spectrum remain relatively constant.

In summary, spectra representing U.S. ground motions were compared with the spectra for the Viña del Mar S20W record. The comparison of the acceleration spectra revealed that the Chilean spectrum is more intense as those for recorded U.S. ground motions and for ATC-3-06 for periods less than one second, but less intense for greater periods. The Newmark-Hall acceleration spectrum was more intense for all periods. The comparison of the displacement spectra revealed that similar drift is expected for all spectra for periods less

than one second, but ordinates for Chilean spectrum remain constant for greater periods, whereas those for the U.S. spectra increase significantly.

### **8.3 Building Response Characteristics**

Building responses for the Chilean and U.S. ground motions described in Section 8.2 are investigated in the following sections. The study incorporates the buildings studied in Chapter 7 of this report, and also buildings studied by Stark (1988) at the University of Illinois, and Wight (1988) at the University of Michigan. Table 8.1 summarizes important characteristics of the buildings.

Results for the buildings are generalized by assuming a fundamental period of  $N/20$  [Wood et al. (1987)]. Where comparisons are made between wall and frame buildings, a period of  $N/10$  [UBC (1985)] was assumed for frame buildings.

#### **8.3.1 Roof Drift**

The U.S. and Chilean displacement spectra described in Section 8.2 were used to compute elastic drift for both wall and frame buildings. The roof drift of the buildings was approximated by multiplying the spectrum drift by 1.4, and by assuming a story height of 2.75 m (9 ft).

Figure 8.10 plots roof drift ratio versus number of stories for the ATC and Viña del Mar spectra (for wall buildings). Figure 8.11 plots the same comparison for the Newmark-Hall and Viña del Mar spectra. Both plots reveal that the drift ratios for the U.S. and Viña del Mar motions are similar for buildings less than 15 stories. For taller buildings, the drift ratio

for the U.S. spectra remains constant, whereas that for the Viña spectrum diminishes. The maximum drift ratio computed (approximately 0.5% for both U.S and Chile spectra) would be expected to cause non-structural damage, but not extensive structural damage [Freeman (1985), Algan (1982)]. A greater range of U.S. buildings (represented by the Newmark-Hall spectrum) would be susceptible to damage because drifts are at the maximum over a larger range of building heights.

Figure 8.12 plots roof drift ratio versus number of stories for frame buildings, for the Newmark-Hall and Viña spectrum. The drift ratios for both spectra increase approximately linearly until a drift value of slightly greater than 1% is reached (for buildings of 6 to 8 stories). As for wall buildings, drift ratio for the Newmark-Hall spectrum remains constant at 1.2%, whereas that for the Chilean spectrum diminishes rapidly. Because very few frame buildings existed in Viña del Mar at the time of the 3 March 1985 earthquake, the vulnerability of low-rise frame buildings was not tested.

The comparison of Fig. 8.10-8.12 reveals (1) drifts are similar for U.S. and Chilean wall buildings up to 15 stories, (2) drift for all heights of U.S. buildings are approximately equal to the drift estimated for the Chilean buildings studied, and (3) frames up to 15 stories in Chile might be susceptible to greater damage than wall buildings. For taller buildings, the roof drift ratio for the 3 March 1985 earthquake is independent of building system used. This suggests no advantages in using wall buildings versus frame buildings (for taller buildings). However, it is important to note that construction of frame buildings in Chile may require changes in practice to include increased quality control and inspection, as well as detailing practices similar to those used in the high seismic regions in the United States. Wall buildings similar to those used in Chile apparently prove adequate without

the detailing and inspection practices required for frames.

### **8.3.2 Displacement Ductility Requirements**

For cases where insufficient building strength exists for elastic response, global inelastic responses can be estimated using inelastic response spectra. To study inelastic responses of typical Chilean buildings, inelastic spectra were constructed from the elastic spectra using the procedure recommended by Newmark and Hall (1982). The elastic spectra considered include the Viña del Mar simplified spectrum, the ATC spectra, and the Newmark–Hall spectrum. Inelastic responses of several Chilean buildings (Table 8.1) were then estimated from the inelastic spectra. For this purpose the elastic base shear is generalized by approximating the elastic base shear for wall buildings using a SDOF model, and by assuming 65% of the mass participates in first mode response. This approximation was shown in Chapter 7 (Table 7.10 through 7.12) to give a reasonable estimate of the computed 3D elastic base shear and base overturning moment.

#### **8.3.2.1 Viña del Mar S20W Spectrum**

Figure 8.13 plots the approximation for elastic and inelastic base shear versus measured ambient fundamental building period. Displacement ductility demands range from one and one-half to three, with most values being approximately two. For this degree of global inelastic action, some local damage would be expected for all the buildings. However, four of the buildings for which data are plotted in Fig. 8.13 sustained little or no apparent damage. This disparity may be attributed partially to the observation that the ambient periods would not be representative of periods obtained during strong ground shaking. Also

plotted on Fig. 8.13 are building strength versus computed period including base flexibility (Table 8.1). Three of the four “undamaged” buildings fall on or above the elastic curve. The only exception is the Torres del Almendral building. This building is located in Valparaíso where slightly less intense motions were recorded. The buildings which were moderately damaged, Villa Real and Festival, indicate displacement ductilities between two and three, which is consistent with the level of damage observed in the buildings. It is also consistent with the analysis results for the Festival building presented in Chapter 7. Two of the badly damaged buildings, El Faro and Acapulco, indicate displacement ductility demands of approximately two. The apparent discrepancy between observed damage and ductility demand is explicable in that both buildings had unsymmetric layout of structural walls that resulted in increased distress due torsional response, and strength deficiencies (bar cutoffs, excessively light boundary reinforcement [Stark (1988)]).

In summary, assuming a fundamental period of  $N/20$ , Fig. 8.13 indicates that the ductility demands for the 3 March 1985 earthquake were between two and three for buildings less than 15 stories, and between one and two for buildings of 20 or more stories.

#### **8.3.2.2 ATC Spectra**

Figures 8.14–8.16 plot the approximations for elastic and inelastic base shear versus computed fundamental building period for the ATC spectra. For soil type S1, building periods measured in Chile are inappropriate because soil type S1 corresponds to rock or stiff soils. Instead, periods were computed for fixed bases and (a) gross section stiffness, and (b) an effective cracked section stiffness equal to half the gross section stiffness. For soil types S2 and S3, the gross section period is presented for both computed fixed and flexible

base assumptions.

Displacement ductility requirements for the ATC spectra are between one and three for all soil types for the fixed base periods. Consideration of cracking or soil flexibility reduces displacement ductility to two or less, for most buildings. Three of the buildings require displacement ductility between two and three for soil type S3. However, the flexible base period was computed for the soils in Viña del Mar, whereas soil type S3 corresponds to more flexible soils. Therefore, deformation demands for the ATC spectra are similar to those for the Viña del Mar spectra. Consequently, similar damage to that observed after the 3 March 1985 earthquake is expected for U.S. buildings with numerous structural walls.

#### 8.3.2.3 Newmark–Hall Spectrum

Figure 8.17 plots the Newmark–Hall inelastic spectra along with period and strength estimates for several Chilean buildings. Building periods were estimated assuming gross sections and fixed bases, and for cracked sections and fixed bases. Therefore, the computed inelastic demands are for buildings founded on rock or stiff soils. Displacement ductility demands range between two and four for the gross section period, and two and three for a cracked section period. Figure 8.18 plots the same relation, but for building periods computed considering effects of base flexibility. The displacement ductility demands are approximately three or less for all buildings. In general, deformation demands for the Newmark–Hall spectra are greater than those for the Viña del Mar spectra. Therefore, slightly increased damage compared with the Viña del Mar spectra is expected for U.S. buildings with numerous shear walls.

#### 8.3.2.4 Summary

The analyses indicate that base shear and deformation demands for the Viña S20W spectra are consistent with the observed damage for the undamaged and moderately damaged buildings in Viña del Mar. For the badly damaged buildings, more detailed analyses [Chapter 7, Stark (1988)] indicated causes of damage could be traced to torsion and strength deficiencies (bar cutoffs, excessively light boundary reinforcement). Lower strength materials and cumulative damage due to previous earthquakes for Acapulco building, and poor construction for the El Faro building [Bonelli (1986)] may also have contributed to poor behavior.

Analysis for spectra representing U.S. ground motions indicated that the displacement ductility demands for gross section, fixed base assumptions varied between one and four. Consideration of cracking or base flexibility results in a reduction of demands to between one and three. Thus, damage similar to, or slightly more severe than that observed after the 3 March 1985 in Chile, is expected in the U.S. for similar construction. The relationship between displacement ductility demands and expected damage is the focus of the next section.

### 8.4 Detailing Requirements for Bearing Wall Buildings

The relationship between global displacement ductility and local curvature ductility determines the level of detailing required for the plastic hinge regions of structural members. Based on the displacement ductility demands estimated in Section 8.3, the following sections

estimate required curvature ductility. The required curvature is compared with available section curvature capacity to evaluate detailing requirements for bearing wall buildings.

#### 8.4.1 Required Curvature Ductility

The relationship between displacement and curvature ductility was studied by Paulay and Uzumeri (1975) for a cantilever wall subjected to a point load at the roof. Yielding was restricted to the base of the wall and shear distortions were assumed to be negligible, resulting in the relationship for curvature ductility

$$\mu_\phi = 1 + \frac{\mu_\Delta - 1}{\frac{3l_p}{h_w} \left[ 1 - \frac{l_p}{2h_w} \right]} \quad (8.2)$$

where  $\mu_\Delta$  is the displacement ductility,  $h_w$  is the height of the wall,  $l_w$  is the length of the wall, and  $l_p$  is the plastic hinge length at the base of the wall. Park and Paulay (1975) present several estimates for plastic hinge length. Two estimates that are convenient for use in Eq. (8.2) are:

$$l_p = 0.4l_w + 0.050h_w \quad (8.3.a)$$

$$l_p = 0.2l_w + 0.075h_w \quad (8.3.b)$$

The two estimates are used to represent a range of plastic hinge lengths in Eq. (8.2). The computed curvature ductility for displacement ductilities of 2, 3, 4, and 5 are presented in Fig. 8.19. (Displacement ductility demands ranging from one to three were estimated in Section 8.3). The two curves for each displacement ductility ratio result from the two estimates of the plastic hinge length (Eq. 8.3). The figure reveals that curvature ductility is greater than displacement ductility, and increases with wall height to length ratio.

Several factors in addition to those represented in Eq. (8.2) affect the relationship between displacement and curvature ductility. Among them are the effects of section crack-

ing, anchorage slip, and soil–structure interaction. The effects of cracking and soil–structure interaction were accounted for in the estimate of the displacement ductility (Section 8.3). (Local foundation rocking beneath individual walls is neglected here.) The effect of anchorage slip is investigated in the following paragraphs.

Anchorage slip at the base of a wall affects the stiffness, yield displacement, and ultimate displacement of a cantilever wall. To include these effects, the equations presented by Paulay and Uzumeri (1975) are modified. The yield displacement and plastic rotation are defined by

$$\Delta_y = \frac{Ph_w^3}{3EI} + \frac{\delta_y h_w}{l_w} \quad (8.4)$$

$$\Theta_p = \phi_p l_p + \frac{\delta_u - \delta_y}{l_w} \quad (8.5)$$

where  $P$  is the applied load,  $\phi_p$  is the plastic curvature, and  $\delta_y$  and  $\delta_u$  represent the anchorage slip at yield and ultimate, respectively. Combining the definition of displacement ductility

$$\mu_\delta = 1 + \frac{\Delta_p}{\Delta_y} \quad (8.6)$$

and Eq. (8.4), and dividing by the height to the center of rotation produces:

$$\Theta_p = (\mu_\Delta - 1) \left[ \frac{\phi_y h_w^2}{3 \left( h - \frac{l_p}{2} \right)} + \frac{\delta_y}{l_w} \right] \quad (8.7)$$

Equating Eq. (8.5) and (8.7) results in the following relation to compute the required curvature ductility:

$$\mu_\phi = 1 + \frac{\mu_\Delta - 1}{\frac{3l_p}{h_w} \left[ 1 - \frac{l_p}{2h_w} \right]} + \frac{\mu_\Delta \delta_y - \delta_u}{l_w \phi_y l_p} \quad (8.8)$$

The slip at yield and ultimate can be computed using Eq. (5.1), and depends on the bar diameter and steel stress to be developed, the concrete bond stress, and the steel modulus.

For a given wall length, bar diameter, and bond stress, an iterative procedure can be used to solve Eq. (8.8) if the following assumptions are made: (1) The ultimate steel stress is  $1.25f_y$ , (2) the ultimate curvature of the section is limited by crushing of the compression zone at a strain of 0.004, and (3) the yield curvature is estimated as

$$\phi_y = \frac{(\epsilon_y + \epsilon_c/2)}{l_w} \quad (8.9)$$

where,  $\epsilon_y$  is the yield strain of the steel,  $\epsilon_{cy}$  is the compressive strain of the concrete (0.003). The estimate of yield curvature was varied, and did not affect the results appreciably. Figure 8.20 plots Eq. (8.8) for wall lengths of 10 and 20 ft. Number 9 bars and a bond stress of 500 psi were assumed. The effect of anchorage slip is appreciable, especially for higher displacement ductility ratios for the 8 ft wall. The effect of anchorage slip is less pronounced as wall length increases, and at low ductility ratios.

#### 8.4.2 Available Curvature Ductility

The available curvature ductility of a member depends primarily on the stress-strain characteristics of the concrete and steel, the amount of tension reinforcement, the level of axial load, and the degree of confinement of the compression zone. The following paragraphs discuss the computation of the available curvature ductility for typical material properties for unconfined and confined concrete.

Available curvature ductility for walls typical of Chilean construction are evaluated using the wall section shown in Fig. 8.21. ACI code requirements are used for the wall web steel (0.25%). For greater steel ratios, the steel in excess of 0.25% is lumped equally at the wall boundaries. Grade 60 steel and 4000 psi concrete are assumed. The modified Kent-Park

model is used to describe the concrete stress-strain curve. Steel strain hardening effects are included. Moment-curvature relations were computed for both unconfined concrete, and the confinement provided by minimum code requirements.

Figure 8.22 plots the moment curvature relation for wall lengths of 10 and 20 ft, with and without confined concrete at the boundaries. A thickness of 10 inches and a gravity load of  $0.1A_g f'_c$  are assumed for all walls. Available curvature ductility decreases slightly with increasing steel ratio. Curvature ductility for lightly reinforced walls (0.25 and 0.5%) are approximately ten to twelve. For higher steel ratios, curvature ductilities are approximately six to eight.

Required curvature ductility for the 10 ft wall (Fig. 8.20.a) is approximately three and six for displacement ductilities of two and three, respectively (for wall height to length ratios between five and eight). Available section capacity (Fig. 8.22.a) is approximately six to twelve; therefore, member deformation capacity is equal to, or exceeds, that required.

Required curvature ductility for the 20 ft wall (Fig. 8.20.b) is approximately four and seven for displacement ductilities of two and three, respectively (for wall height to length ratios between five and eight). Available section capacity (Fig. 8.22.b) is approximately six to twelve; therefore, member deformation capacity is approximately equal to, or exceeds that required.

Although the available curvature ductility is equal to, or exceeds the required curvature ductility, the proximity of the numbers requires a closer look. Figures 8.14–8.18 were used to evaluate displacement ductility for the Chilean buildings for spectra representing U.S. ground motions. A close examination of these figures leads to the following observations:

- (1) That of the four buildings that consistently require the highest displacement ductilities (Villa Real, El Faro, Acapulco, and Torres del Almendral), all except El Faro have strengths 30% lower than the minimum code strength (Fig. 8.3). Significant damage was reported in three of the buildings (with Torres del Almendral being the exception; however, this building is located in Valparaíso). If strength values for these buildings are increased to the code minimum, displacement ductilities are approximately two for all buildings.
- (2) That higher values of displacement ductility are required from plots where the effect of base flexibility is a parameter. The consideration of base flexibility apparently was an important factor in explaining why some buildings were not damaged; however, when displacement ductility demands between two and three are required after the effects of base flexibility have been incorporated, cracking of the walls is likely, and the building becomes more flexible. If a cracked stiffness of one-half the gross section stiffness is assumed, a displacement ductility of approximately two results for all buildings (except Torres del Almendral).
- (3) That damaged buildings revealed beam and slab yielding occurred over the height of the building due to the use of structural walls. The use of elasto-plastic spectra (the basis of the Newmark-Hall procedure used to calculate inelastic demand for base shear) for such buildings may not be appropriate due to the gradual loss of stiffness that results as beams and slabs yield. A comparison of Fig. 3.7 and 3.8 reveals that moderate strain hardening (20%) results in significant reductions in required ductility.
- (4) That due to framing continuity, building strengths are likely to be larger than the minimum code strength used to estimate deformation demands. For buildings with

numerous walls, continuity (or redistribution capacity) is likely to increase strength appreciable.

Based on these observations, a displacement ductility of two is representative of the demands expected for bearing wall buildings of construction similar to that used in Chile (for the ATC and Newmark–Hall spectra). Therefore, required curvature ductility (Fig. 8.20) is approximately four (for wall height to length ratios between four and eight). Without confinement, available curvature ductility exceeds that required by 50 to 250%. For motions more intense than those represented by the ATC and Newmark–Hall spectra, more significant damage would result.

Based in these analyses, the current code requirements for bearing wall buildings [UBC (1988)] may be too restrictive. For buildings where numerous structural walls are used (similar to Chilean construction with approximately 2.5% wall area to floor area in each direction) design forces and detailing requirements appear stringent.

## 8.5 Summary

The design implications for bearing wall buildings was investigated using data obtained in the 3 March 1985 earthquake. Variations in U.S. and Chilean code for minimum strength revealed that the Chilean buildings typically have strengths greater than that required by the Chilean code, and are approximately equal to that required by the U.S. code. Therefore, the data obtained from the evaluation of Chilean buildings was used to investigate requirements for bearing wall buildings in the United States. A comparison acceleration response spectra for the Viña del Mar S20W and U.S. ground motions revealed that the

U.S. motions are of similar, or slightly higher, intensity. Evaluation of deformation demands for the spectra representing U.S. ground motions revealed maximum displacement ductility of approximately two, and required curvature ductilities between three and four. For minimum code requirements, available wall curvatures exceed those required by 50 to 250% (without confinement). Therefore, for earthquake ground motions represented by the ATC-3-06 (1978) recommendations and the Newmark-Hall procedure (1982), damage in buildings constructed in the U.S. with numerous shear walls would be similar to that observed in Chile after the 3 March 1985 earthquake. Based on these analyses, current code requirements [UBC (1988)] appear too restrictive.

# CHAPTER 9

## SUMMARY AND CONCLUSIONS

On 3 March 1985, a major earthquake occurred off the coast of Chile. The epicenter of the earthquake was located approximately 80 km from the city of Viña del Mar. At the time of the earthquake more than 400 buildings of modern reinforced concrete construction existed in Viña del Mar. A strong-motion instrument recorded the ground motions in the vicinity of several of the buildings. Following the earthquake an investigation was undertaken to study the implications of the earthquake on seismic performance of reinforced concrete construction. This report documents the study.

### 9.1 Summary

The first part of the study focused on the evaluation of the 3 March 1985 Chile earthquake. Chilean design philosophy, and the historical development of earthquake engineering in Chile, are presented in Chapter 2. Typical structural details and construction practices are also discussed.

Engineering characteristics of the ground motions recorded at four locations in Chile are presented and discussed in Chapter 3. Both subjective and analytical measures of intensity and inelastic deformation demands are investigated. Soil properties for the cohesionless sands and gravel in Viña del Mar are presented in Chapter 4, along with a study of variations in ground motions due to local soil conditions.

Four buildings located in Viña del Mar were selected for detailed study. Analytical modeling techniques for the elastic and inelastic analyses are presented in Chapter 5. A

detailed investigation of soil-structure interaction for one of the buildings is presented in Chapter 6. Computed periods for the soil-structure interaction analyses are compared with periods measured in free vibration tests [Calcagni (1987)], and earthquake aftershocks [Bongiovanni et al. (1987)]. The effects of soil-structure interaction on building responses (roof drift, base shear, and base overturning moment) are studied, and compared with simplified procedures recommended by ATC-3-06 (1978).

Detailed investigations for the four selected buildings are presented in Chapter 7. The buildings, observed damage, and measured material properties are described. Computed 3D Periods for the buildings are compared with measured periods [Calcagni (1987)]. ATC-3-06 (1978) procedures are used to evaluate the effect of soil flexibility on building period. Building strength, stiffness, and detail are compared with requirements of UBC (1985) and the Chilean seismic code. Building base shear strengths and global deformation demands are estimated. Deformation demands are compared with observed damage.

Results of elastic response spectrum analyses to compute drift ratios, base shear, and base overturning moment for each of the buildings during the 3 March 1985 earthquake are presented. A simplified procedure is used to incorporate the effects of soil-structure interaction. Elastic spectral demands are compared with computed base shear strength to correlate computed responses with observed damage. An inelastic analysis was conducted for one of the buildings to gauge the effects of inelastic responses on building behavior.

The results from the study of the Chile earthquake are used to evaluate structural requirements for bearing wall buildings in the United States. Variations between Chilean and U.S. code requirements are investigated to determine the effect of the detailing and proportioning on building flexural and shear strength. Minimum required code flexural

strength and probable shear strength are compared with computed strengths for the Chilean buildings. Differences between the Viña del Mar and U.S. ground motions are studied for three representations of U.S. ground motions (simplified spectra for recorded U.S. ground motions, ATC-3-06 spectra (1978), and Newmark-Hall spectra (1982)). Roof drift, base shear, and displacement ductility demands for the Chilean buildings are computed for the spectra representing U.S. ground motions, and compared with responses for the Viña del Mar ground motion. Global and local demands for ductility are estimated to evaluate structural requirements for bearing wall buildings. Conclusions are drawn as to the seismic performance of bearing wall buildings in the United States.

## 9.2 Conclusions

Based on the studies summarized above the following conclusions are made:

- (1) The ground motions recorded in Viña de Mar during 3 March 1985 had spectral acceleration, in the period range of interest, equivalent to those expected during strong U.S. earthquakes. Furthermore, the long duration of ground shaking ensured that the buildings subjected to the motion underwent numerous cycles of response. Thus, it is concluded that the earthquake provided a good test for the Chilean buildings.
- (2) The good performance of the majority of the moderately tall bearing wall buildings in Chile is explicable in that this type of construction tends inherently to have low shear stress, high stiffness, and moderate strength and ductility. The poor performance of some buildings could be attributed to poor layout and strength distribution. Therefore, it is concluded that for buildings with a relatively symmetric and continuous distribu-

tion of lateral force resisting elements, this form of construction performs well in the apparent absence of conventional ductile detailing and inspection.

- (3) Buildings similar to those constructed in Chile would be successful in the United States. For such buildings, detailing and inspection requirements less stringent than those currently implemented in the U.S. codes are appropriate.

Date	Epicentral Region	Magnitude
1570 February 8	Concepción	8 - 8½
1575 March 17	Santiago	7 - 7½
1757 December 16	Valdivia	8½
1604 November 24	Arica	8½ - 8½
1615 September 16	Arica	7½
1647 May 13	Santiago	8½
1657 March 15	Concepción	8
1681 March 10	Arica	7 - 7½
1687 July 12	San Felipe	7 - 7½
1715 August 22	Arica	7½
1730 July 8	Valparaíso	8¾
1737 December 24	Valdivia	7½ - 8
1751 May 25	Concepción	8 - 8½
1796 March 30	Copiapó	8½ - 8
1819 April 3,4,11	Copiapó	8½ - 8½
1822 November 19	Valparaíso	8½
1809 September 26	Valparaíso	7
1835 February 20	Concepción	8 - 8½
1837 November 7	Valdivia	8+
1847 October 8	Illapel	7 - 7½
1849 November 17	Coquimbo	7½
1850 December 6	Valle de Maipo	7 - 7½
1851 April 2	Casablanca	7 - 7½
1859 October 5	Copiapó	7½ - 7¾
1868 August 13	Arica	8½
1869 August 24	Pisagua	7 - 7¾
1871 October 5	Iquique	7 - 7½
1877 May 9	Pisagua	8 - 8½
1879 February 2	Estrecho de Magallanes	7 - 7½
1880 August 15	Illapel	7½ - 8
1906 August 16	Valparaíso	8.6
1918 December 4	Copiapó	7½+
1922 November 10	Huasco	8.4
1928 December 1	Talca	8.4
1939 January 24	Chillán	8.3
1943 April 6	Illapel	8.3
1949 December 17	Punta Arenas	7½
1950 December 9	Chillán	8.3
1953 May 6	Chillán	7½
1960 May 21	Concepción	7.5
1960 May 22	Valdivia	8.5
1965 March 28	Santiago	7.3
1971 July 8	Valparaíso	7.5
1975 May 10	Lebu	7.8
1985 March 3	San Antonio	7.8

Table 2.1 Summary of Strong Earthquakes in Chile  
[Lomnitz (1969)]

Station	Coordinates		Peak Ground Acceleration (g)			Site Geology	Instrument Location	Instrument Model
	S	W	L	T	V			
Viña del Mar	33°02'	71°35'	0.36	0.22	0.19	Sand	10-story Blg Basement	SMA-1
Valparaíso	33°01'	71°38'	0.17	0.19	0.12	Sand	1-story Blg Ground Level	SMA-1
El Almendral	33°01'	71°38'	0.29	0.16	---	Fill	Church	SMA-1
Llolleo	33°41'	71°36'	0.67	0.43	0.86	Sand	1-story Blg Basement	SMA-1
Melipilla	33°41'	71°13'	0.67	0.60	0.59	Rock	1-story Blg Ground Level	SMA-1

**Table 3.1: Strong Motion Instrument Data [Wyllie et al. (1986)]**

Record	Housner SI (m)	Arias Intensity (g-sec)
Llolleo N10E	1.96	1.64
Llolleo S80E	1.07	0.75
Viña del Mar S20W	1.46	0.58
Viña del Mar N70W	0.98	0.34
Valparaíso S20E	0.26	0.08
Valparaíso N70E	0.71	0.12
El Almendral S40E	0.77	0.24
El Almendral n50E	1.33	0.35
El Centro NS	1.34	0.18

**Table 3.2: Housner and Arias Intensities**

---

<b>Maicillos:</b>	
Classification	SM with some SC
Liquid Limit	20%
Plastic Limit	7%
Natural moisture content	7%
% fines passing a #200 sieve	12%
Internal angle of friction	33° - 54°
Effective cohesion	0.07 - 0.35 kg/cm <sup>2</sup>
<b>Uncemented Sands:</b>	
Classification	SP
% fines passing a #200 sieve	1%
Relative density	70%
Internal angle of friction	38° - 41°
Effective cohesion	0
<b>Cemented Sands:</b>	
Classification	SP
% fines passing a #200 sieve	2%
Natural moisture content	7%
Internal angle of friction	39° - 43°
Effective cohesion	0.04 - 0.57 kg/cm <sup>2</sup>

---

**Table 4.1 Typical Engineering Properties of  
Foundation Materials in Viña del Mar**

[Aquirre, Petersen, and Eduardo (1986)]

Boring # 1		Boring #8	
Depth (m)	$V_s$ (m/sec)	Depth (m)	$V_s$ (m/sec)
0-1	75	0-1	75
1-3	240	1-3	255
3-6	265	3-4.8	320
6-7	280	4.8-8	300
7-11	295	8-12	325
11-20	305	12-16	345
—	—	16-21	270
—	—	21-28	300
—	—	28-30	320

Table 4.2 Computed Shear Wave Velocity from SPT Tests

Layer (m)	Depth (m)	$\gamma'$ ( $t/m^3$ )	$\sigma'_m$ ( $t/m^2$ )	$K_2$	G ( $t/m^2$ )	$V_s$ (m/sec)
0-05	2.5	1.75	2.75	40	4660	160
5-10	7.5	1.20	7.45	55	10500	215
10-15	12.5	1.20	11.25	60	14100	250
15-20	17.5	1.20	15.05	60	16300	270
20-25	22.5	1.20	18.85	60	18230	285
25-30	27.5	1.20	22.65	60	19980	300

Table 4.3 Computed Shear Wave Velocity for Eq. 4.5.2

Layer No.	Depth (ft)	$V_{S1}$ (fps)	$V_{S2}$ (fps)	$V_{S3}$ (fps)
1	0- 3	250	250	250
2	3- 8	780	780	625
3	8- 21	790	790	630
4	21- 23	870	870	695
5	23- 35	910	910	710
6	35- 47	960	960	755
7	47- 60	1000	1000	805
8	60- 80	1080	1080	865
9	80-100	1130	1130	910
10	100-120	1200	1200	1200
11	120-140	1200	1200	1200
12	140-160	1200	1200	1200
13	160-180	1200	1200	1200
14	180-200	1200	2000	1200
15	200-220	1200	2100	1500
16	220-240	1200	2200	1500
17	240-260	1500	2300	1500
18	260-280	1500	2400	1500
19	280-300	1500	2500	1500
Period		0.93 sec	0.74 sec	0.94 sec

**Table 4.4 Shear Wave Velocity for Site Response Analyses**  
 Estimated by H. B. Seed and J. Sun

Value of A (g)	$\leq 0.10$	0.15	0.20	$\geq 0.30$
Value of $G/G_0$	0.81	0.64	0.49	0.42
Value of $V_s/V_{s0}$	0.90	0.80	0.70	0.65

**Table 6.1 Soil Stiffness Modification [ATC-3-06 (1978)]**

Stories	A ( $m^2$ )	$I_{xx} = I_{yy}$ ( $m^4$ )
0 - 2	34.0	775.0
3 - 5	28.0	270.0
6 - 10	25.0	250.0
11 - 15	21.0	210.0
16 - 22	18.0	175.0

**Table 6.2 Building Model Properties**

	Fixed Base	Very Low Intensity	Low Intensity	High Intensity
$G(t/m^2)$	-	22,000	20,000	9,250
$T_1 = T_2$	0.92	1.06	1.12	1.32
$T_4 = T_5$	0.16	0.21	0.22	0.26

**Table 6.3 Soil Properties and Computed Periods**

Analysis Model	Analysis Type	Damping	$\delta_{roof}/H$	$V_{base}$	$M_{base}$
(1) Fixed Base (SAP-80)	Response History	Proportional	0.41%	0.40W	0.30WH
(2) Flexible Base (CAL-86)	Response History	Non-Proportional	0.41%	0.21W	0.17WH
(3) Flexible Base (SAP-80)	Response History	Proportional	0.43%	0.30W	0.18WH
(4) Flexible Base (SAP-80)	Response Spectrum (CQC)	Proportional	0.41%	0.30W	0.18WH
(5) Flexible Base (SAP-80)	Response Spectrum (SRSS)	Proportional	0.30%	0.22W	0.13WH
(6) Flexible Base (ATC-3-06)	Response Spectrum	Proportional	0.41%	0.23W	0.16WH

Table 6.4 Response Characteristics

Building	Computed Periods			Measured Periods	
	$T_1$ (sec)	$T_2$ (sec)	$T_3$ (sec)	$T_X$ (sec)	$T_Y$ (sec)
Plaza del Mar	1.39	1.17	1.02	1.29	1.13
Festival	0.61	0.58	0.32	0.72	0.61
Acapulco	1.00	0.61	0.60	0.83	0.67
Torres de Miramar	0.92	0.92	0.75	1.06	1.06

Table 7.1 Computed and Measured Building Periods

Building	Direction	$A_0$ ( $m^2$ )	$r_a$ (m)	$r_m$ (m)	W (Tons)	$\bar{T}$ (sec)	
						Low Intensity	High Intensity
Plaza	Tran.	1125	18.9	14.8	20000	1.52	1.70
		1125	18.9	14.8	20000	1.32	1.51
	Long.	1125	18.9	23.4	20000	1.08	1.15
Festival	Tran.	1080	18.6	15.6	13500	0.69	0.79
	Long.	1080	18.6	23.6	13500	0.62	0.66
Acapulco	Tran.	920	17.1	14.1	10950	1.05	1.13
		920	17.1	14.1	10950	0.69	0.80
	Long.	920	17.1	21.4	10950	0.65	0.69
Miramar	Both	365	10.8	11.3	11130	1.08	1.26

Table 7.2 Computed Periods Including Soil-Structure Interaction

Building	Direction	$\bar{h}$	$L_0$	$r$	$\tilde{T}/T$	$\beta_0$	$\tilde{\beta}$
		(m)	(m)	(m)			
Plaza	Tran.	44.6	22.5	14.8	1.21	0.025	0.053
	Long.	44.6	50.0	22.4	1.12	0.020	0.056
Festival	Tran.	28.7	22.5	15.6	1.29	0.060	0.083
	Long.	28.7	48.7	19.5	1.14	0.037	0.071
Acapulco	Tran.	28.9	20.0	14.1	1.13	0.025	0.060
	Long.	28.9	46.0	18.2	1.13	0.030	0.065
Miramar	Both	39.1	25.0	10.8	1.37	0.035	0.054

Table 7.3 Computed Damping Ratios Including Soil-Structure Interaction

Building	Factored Base Shear		Drift Ratios (%)			
	UBC-85	NCh-433	UBC-85		NCh-433	
	% Weight	% Weight	Roof	Interstory	Roof	Interstory
Plaza del Mar	9.5	10.2	0.093	0.119	0.080	0.103
Festival	14.3	13.4	0.043	0.054	0.034	0.042
Acapulco	11.2	10.2	0.063	0.078	0.058	0.073
Torres de Miramar	11.6	10.2	0.071	0.109	0.051	0.081

Table 7.4 Code Design Requirements

Building	Axis	Length x Width (cm x cm)	Strength Ratio		
			$\phi P_n/P_u$	$\phi V_n/V_u$	$\phi M_n/M_u$
Plaza del Mar	3a	210 x 20	1.3	6.7	2.3
	2	245 x 30	3.3	8.0	1.9
Festival	A	245 x 30	3.5	3.4	5.1
	C	1010 x 30	5.0	2.0	1.8
Acapulco	A	540 x 25	4.0	1.6	2.2
	J	530 x 25	2.0	4.4	1.8

**Table 7.5 Strength Ratios for Several Chilean Walls**

Building	Base Shear Strength	
	Transverse	Longitudinal
Plaza del Mar	0.18W	0.13W
Festival	0.35W	0.30W
Acapulco	0.18W	0.18W
Torres de Miramar	0.27W	0.27W

**Table 7.6 Computed Base Shear Strengths**

TRANSVERSE				LONGITUDINAL			
Axis	Walls (tons)	Beams (tons)	Total (tons)	Axis	Walls (tons)	Beams (tons)	Total (tons)
1	5	55	60	1	15	20	35
2	5	85	90	2	20	145	165
3a	7	—	7	3a	—	80	80
3	555	245	800	3	415	80	495
4	—	85	85	4	—	145	145
5	400	200	600	5	245	—	245
6	220	45	265	6	140	70	210
7	—	85	85	7	—	145	145
8	550	245	795	8	415	80	495
9	—	85	85	9	—	145	145
10	400	260	660	10	245	—	245
SLAB	—	125	125	Slab	—	90	90
Totals	2150	1500	3650	Totals	1495	1000	2415
	0.11W	0.07W	0.18W		0.075W	0.050W	0.13W

**Table 7.7 Plaza del Mar Building Strength Calculations**

TRANSVERSE				LONGITUDINAL			
Axis	Walls (tons)	Beams (tons)	Total (tons)	Axis	Walls (tons)	Beams (tons)	Total (tons)
A	130	115	245	1&16	100	90	190
B	70	—	70	2&15	85	190	275
C	1390	60	1450	3&14	135	60	195
D&K	365	255	620	4&13	15	450	465
E&J	365	135	500	5&12	2400	—	2400
F&I	555	20	575	7&11	35	50	85
L	545	490	1035	8&10	60	75	135
N	—	145	145	9	285	40	325
Totals	3420	1355	4775	Totals	3115	955	4070
	0.25W	0.10W	0.35W		0.23W	0.07W	0.30W

**Table 7.8 Festival Building Strength Calculations**

Axis	TRANSVERSE				LONGITUDINAL	
	Walls (tons)	Beams (tons)	Total (tons)	Weak Point (Story)	Walls (tons)	Weak Point (Story)
A	190	25	215	6,7	110	6
B	15	5	20	1	10	1
C	290	25	315	1	165	1
D	100	90	190	1,3,7	20	3,7
E	170	115	285	3,4	85	3,4
F	250	20	270	1,7	100	1,5
G	15	10	25	1	8	1
H	15	45	60	2	8	2
I	15	10	25	1	8	1
J	75	45	120	1	45	1
K	100	45	145	1	85	6
L	100	130	230	1,4,8	50	1
M	100	—	100	5,6,7	130	4,7
Y	—	—	—		215	5-8
Wall P	—	—	—		160	1
Wall R	—	—	—		615	4,6
Wall S	—	—	—		130	1
Totals	1435	565	2000		1944	
	0.13W	0.05W	0.18W		0.18W	

\* If more than one value is shown the stories indicated have approximately equal strengths

**Table 7.9 Acapulco Building Strength Calculations**

BUILDING	ROOF DRIFT (%)		INTERSTORY DRIFT (%)	
	Center of Mass	Building Corner	Center of Mass	Building Corner
Plaza del Mar	0.28	0.64	0.36	0.83
Festival	0.35	0.35	0.42	0.42
Acapulco	0.37	0.75	0.46	0.93
Torres de Miramar	0.41	0.41	0.64	0.64

**Table 7.10 Computed Response Spectrum Drift Ratios**

Building	Base Shear (tons)	Base Shear (% Weight)	Base Moment (tons-m)	$\bar{H}^*$
Plaza del Mar	4150	0.21W	193000	0.73H
Festival	11100	0.82W	319000	0.71H
Acapulco	4200	0.38W	127000	0.76H
Torres de Miramar	4700	0.40W	200000	0.73H

\* Effective height of lateral force

**Table 7.11 Computed 3D Model Response Characteristics**

Building	Model*	Period (sec)	Base Shear (tons)	Base Shear (% Weight)	Base Moment (tons-m)	Roof Drift (%)
Plaza del Mar	F. B.	1.51	4400	0.22W	196000	0.33
	SSI	1.70	2930	0.15W	130500	0.33
Festival	F. B.	0.61	11000	0.75W	292000	0.35
	SSI	0.79	9150	0.68W	262600	0.50
Acapulco	F. B.	1.00	4625	0.42W	134000	0.50
	SSI	1.13	3630	0.33W	105000	0.50
Torres de Miramar	F. B.	0.92	5500	0.50W	218000	0.38
	SSI	1.26	2975	0.27W	116400	0.38

\* F. B.= Fixed Base Model; SSI = Soil-Structure Interaction Model

**Table 7.12 Computed SDOF Model Response Characteristics**

Floor	Wall A1		Wall M1	
	$V_{3D}/V_{2D}$	$M_{3D}/M_{2D}$	$V_{3D}/V_{2D}$	$M_{3D}/M_{2D}$
5	2.0	2.0	1.25	1.45
4	2.0	2.0	1.30	1.50
3	1.9	2.0	1.30	1.55
2	2.0	2.0	1.30	1.65
1	2.0	2.0	1.60	1.80

**Table 7.13 Effect of Torsion on Wall Forces**

Building	Base Shear Strength	Computed Period		Measured Period
		Fixed Base	Flexible Base	
Plaza del Mar	0.18W	1.39	1.70	1.29
Festival	0.35W	0.61	0.79	0.73
Acapulco	0.18W	1.00	1.13	0.83
Torres de Miramar	0.27W	0.92	1.37	1.06
Torres del Sol	0.22W <sup>1</sup>	0.92 <sup>1</sup>	1.27	1.08
El Faro	0.38W <sup>1</sup>	0.47 <sup>1</sup>	—	—
Torres de Almendral	0.13W <sup>2</sup>	0.98	1.25	1.20
Villa Real	0.25W <sup>1</sup>	—	—	0.70

<sup>1</sup> Stark (1988)      <sup>2</sup> Wight (1988)

**Table 8.1 Building Characteristics**

Record	Year	Component	Peak Ground
			Accel. (g)
El Centro	1940	S00E	0.348
		S90W	0.214
Olympia	1949	N04W	0.165
		N85E	0.280
Taft	1952	N21E	0.156
		S69E	0.179
Parkfield	1966	N05W	0.355
		N85E	0.434
Castaic	1971	N21E	0.315
		N69E	0.271
Holiday Inn	1971	N21W	0.255
		N69W	0.134

**Table 8.2 Recorded U.S. Ground Motions**

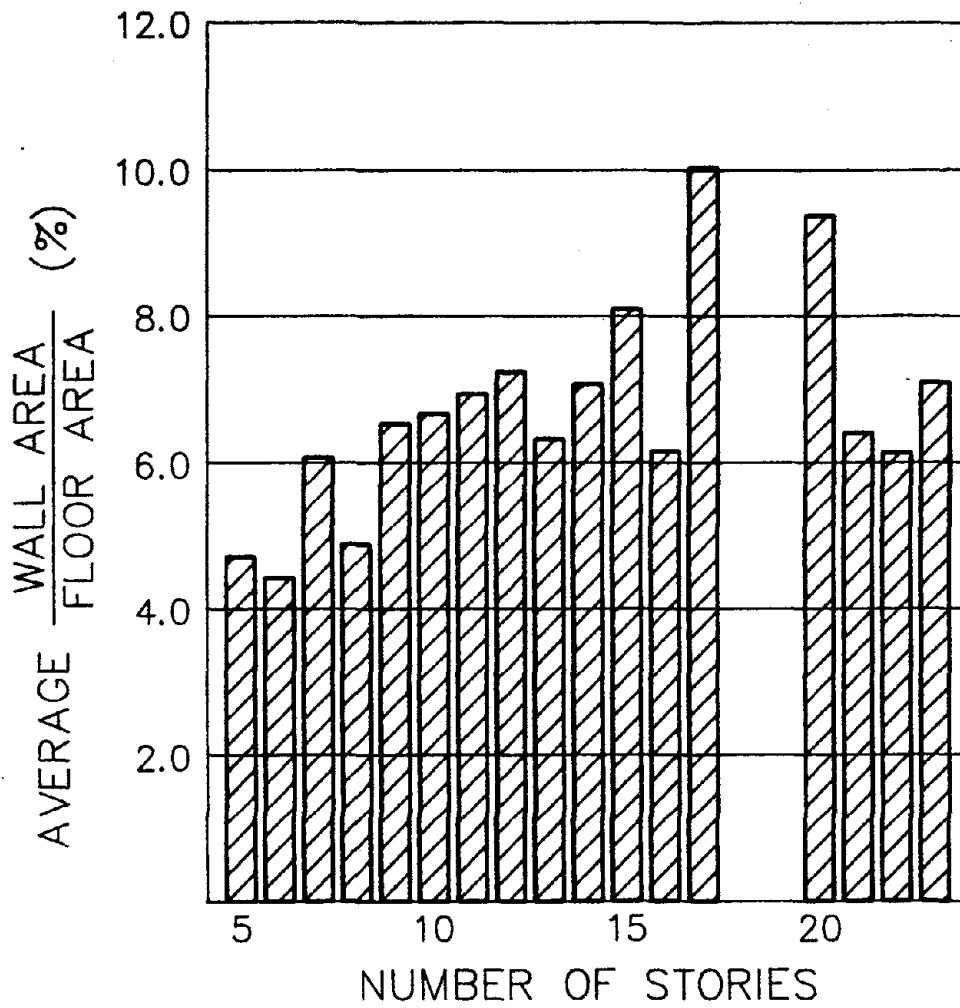


Fig. 2.1 Average Percent Wall Area versus Building Height  
[Riddell et al. (1987)]

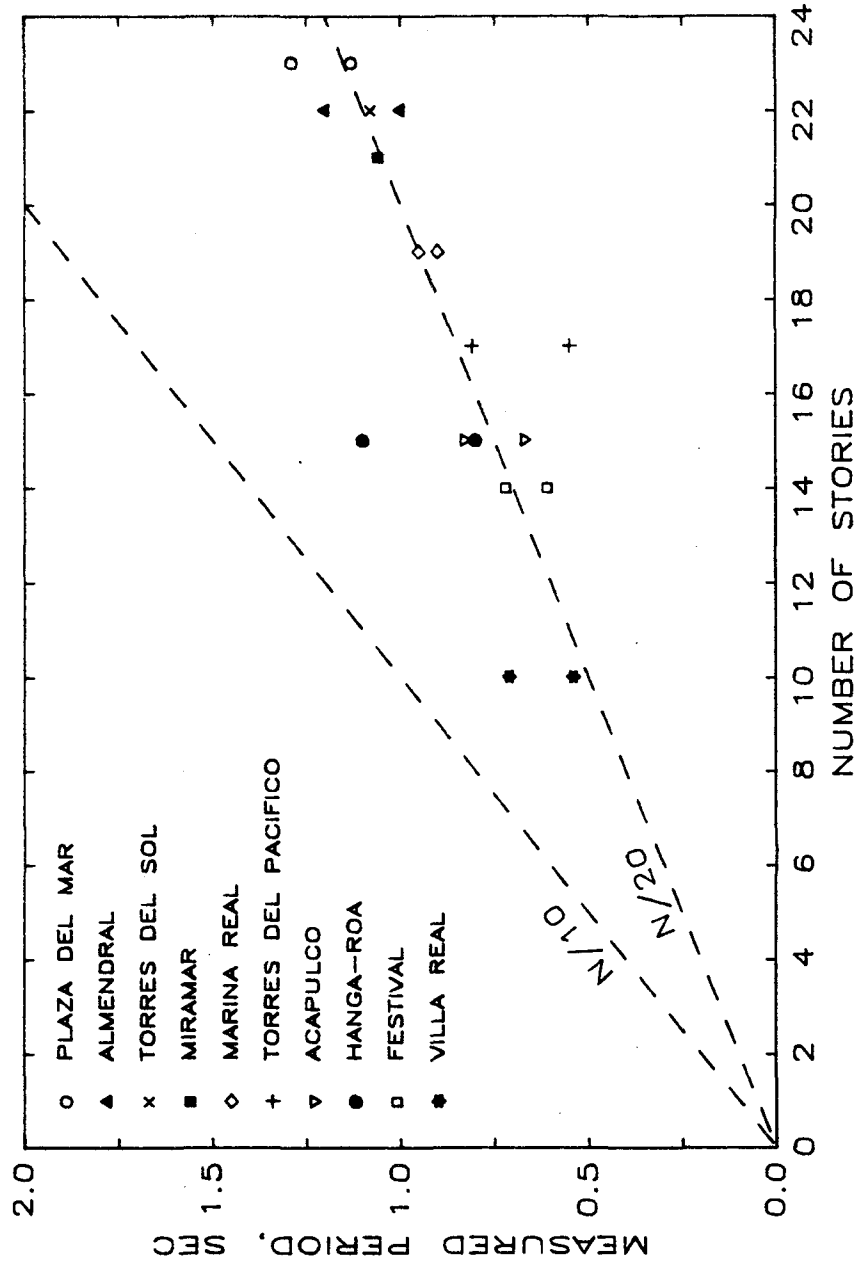


Fig. 2.2 Measured Periods for Chilean Buildings  
 [Calcagni (1987)]

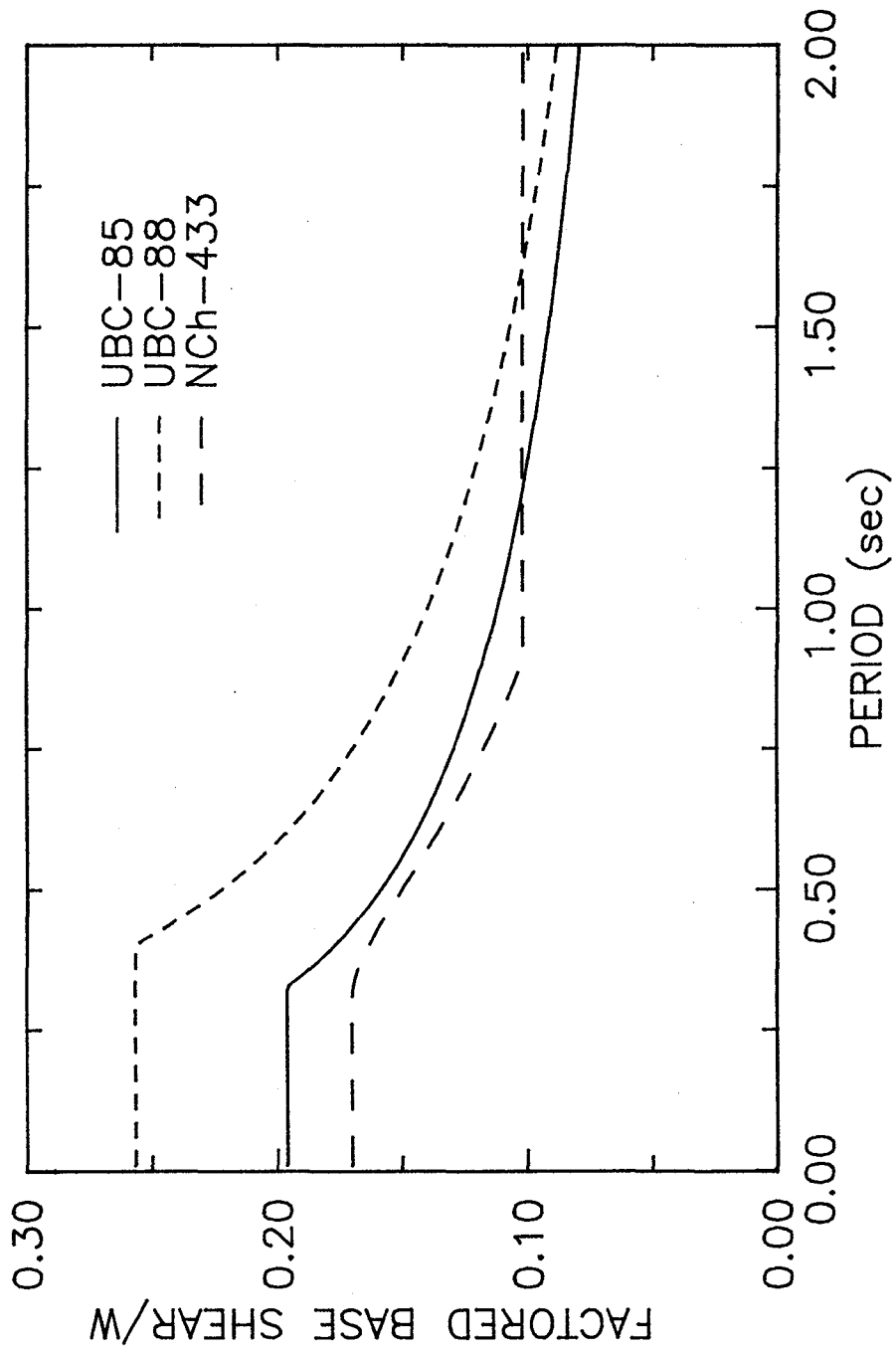


Fig. 2.3 Comparison of Code Spectra

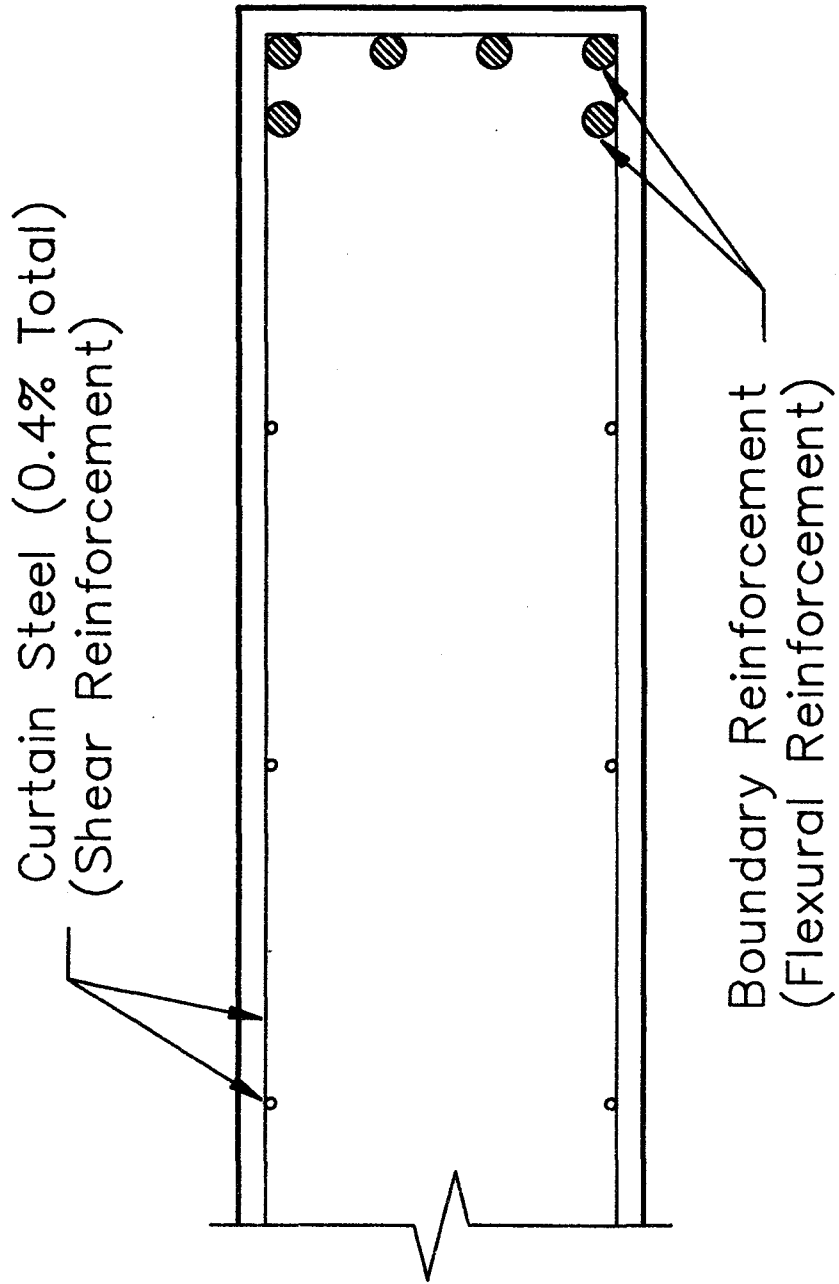
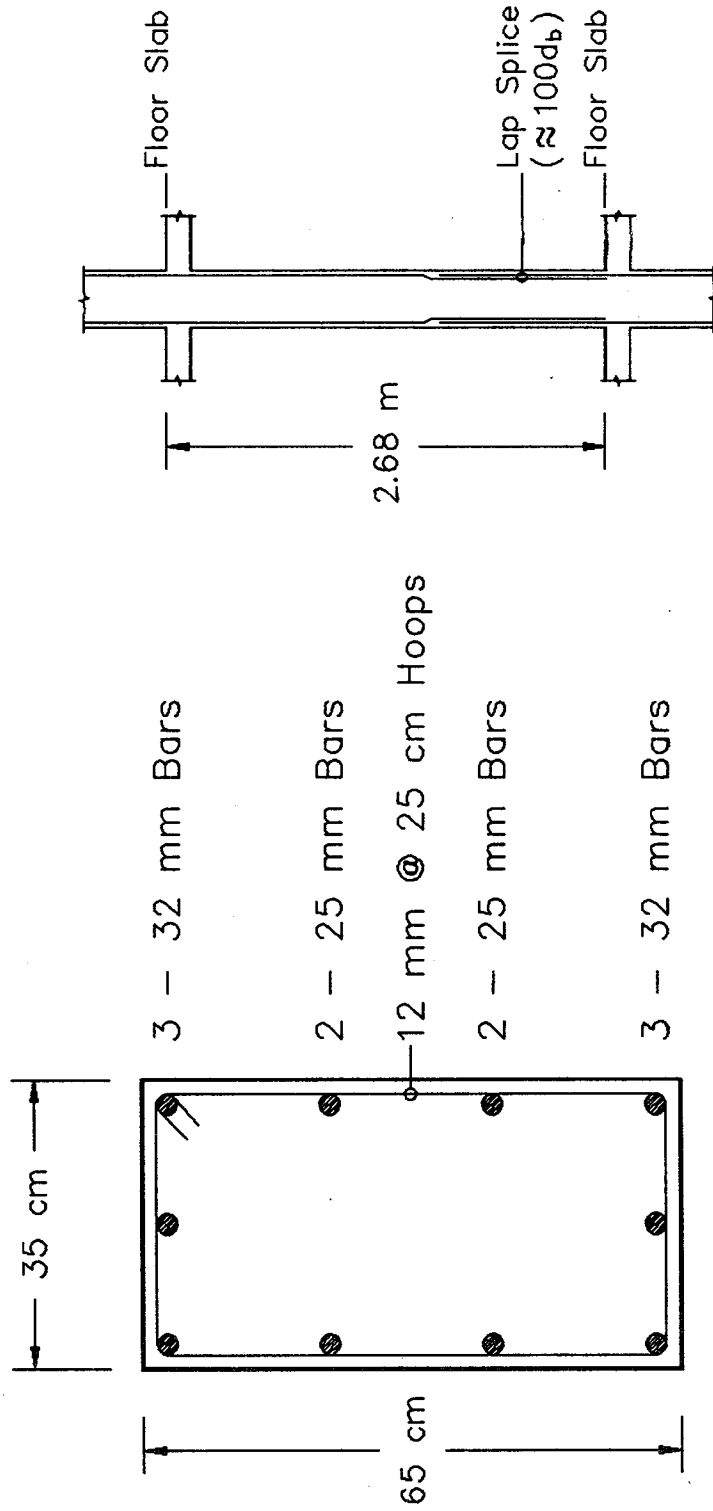


Fig. 2.4 Typical Wall Reinforcement



Column Splice

Column Reinforcement

Fig. 2.5 Typical Column Reinforcement - Plaza del Mar Building

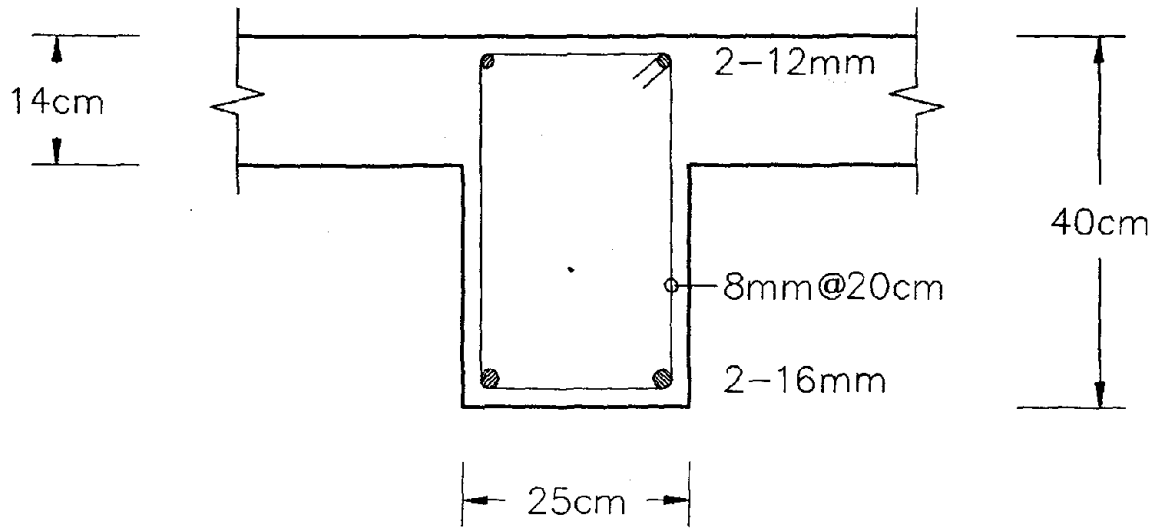
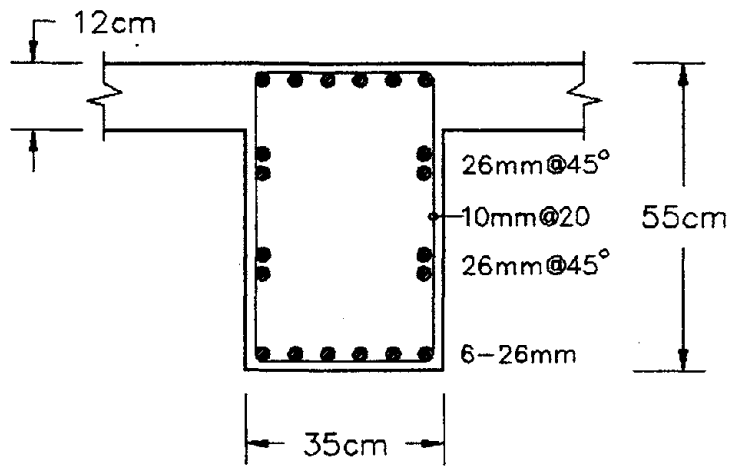
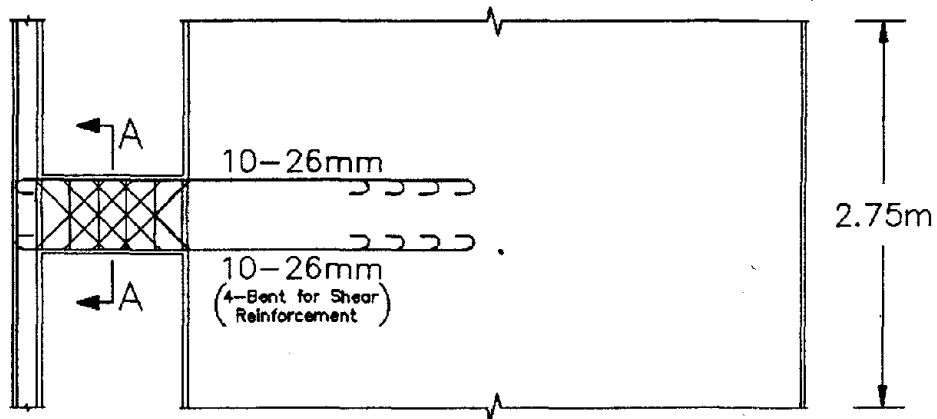


Fig. 2.6 Typical Beam Reinforcement – Plaza del Mar Building



Section A-A



Coupling Beam - Axis (D) (8<sup>th</sup> Floor)

Fig. 2.7 Coupling Girder Reinforcement - Acapulco Building

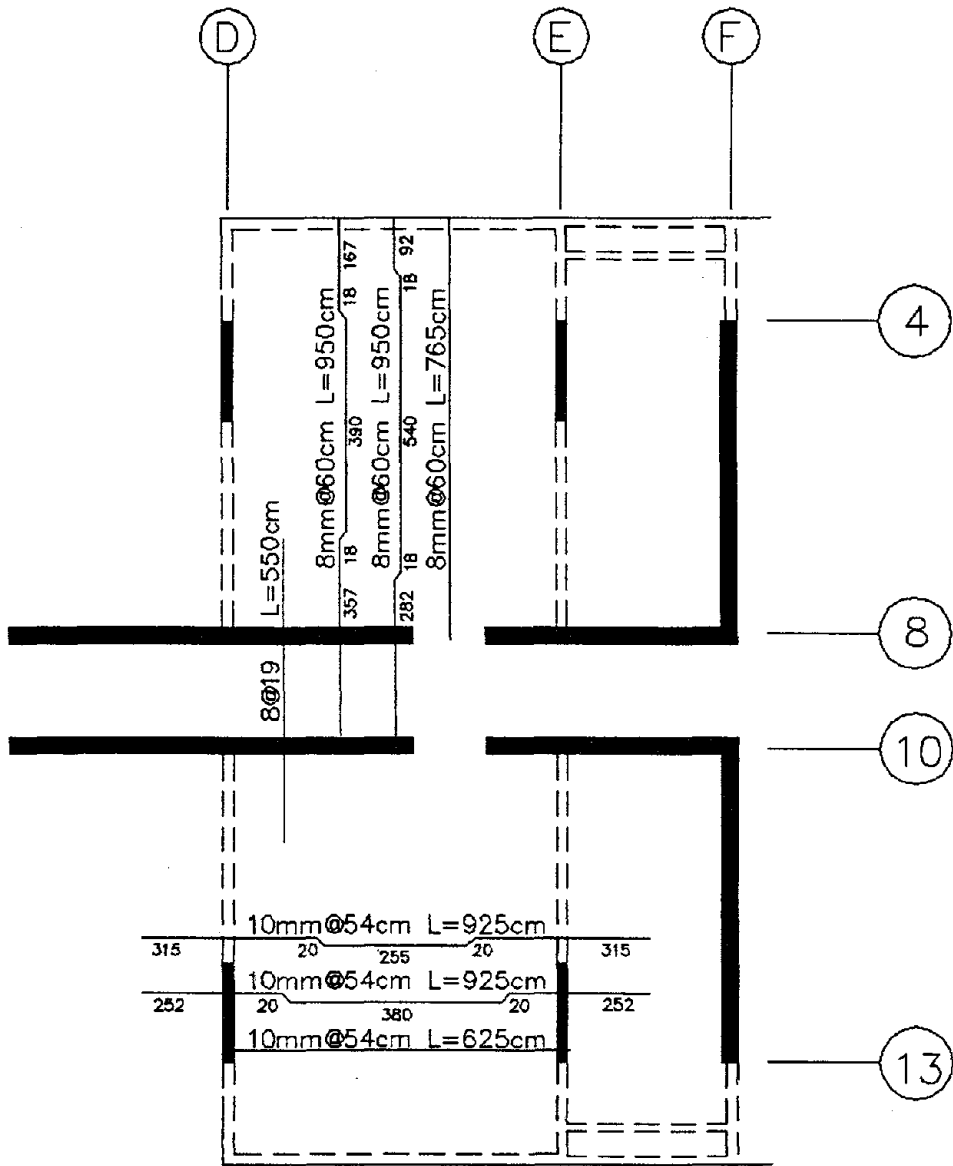


Fig. 2.8 Typical Slab Reinforcement – Festival Building

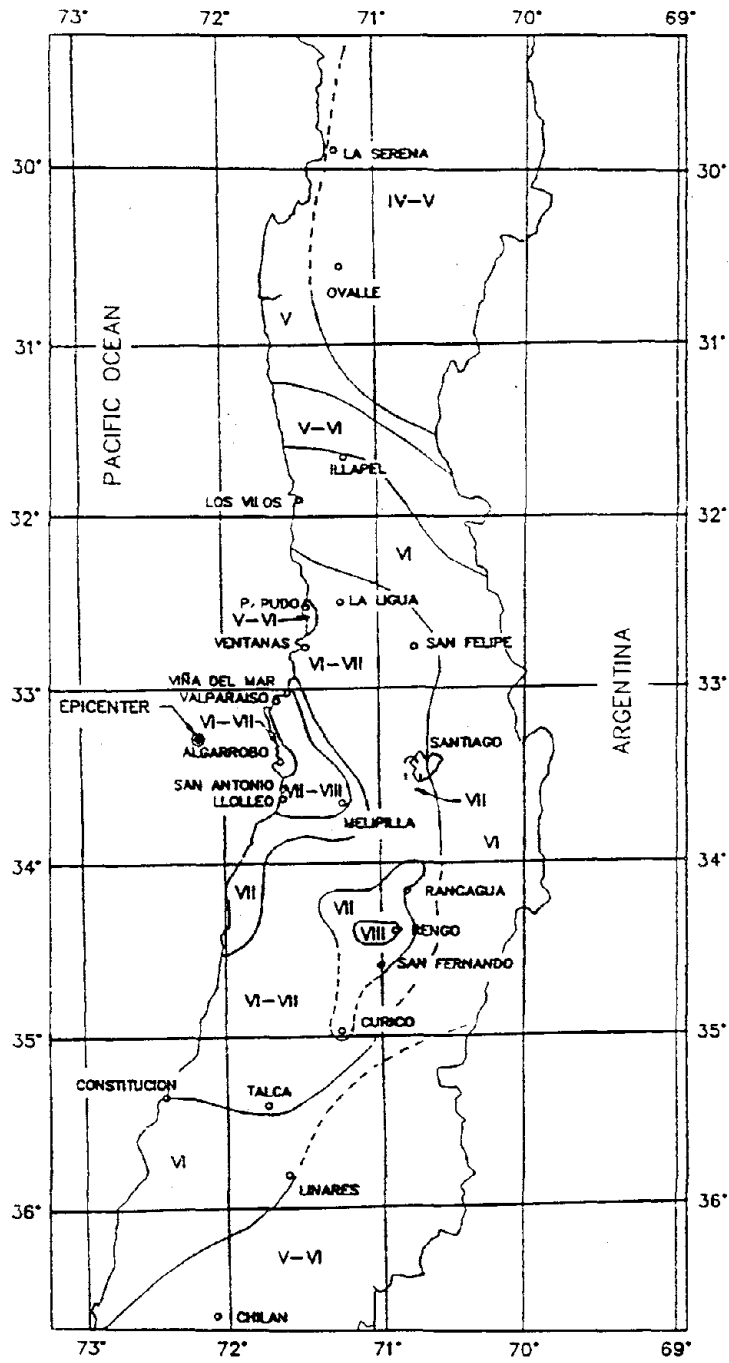


Fig. 3.1 Epicenter and Intensity Map for 3 March 1985 Earthquake  
 [Saragoni et al. (1985)]

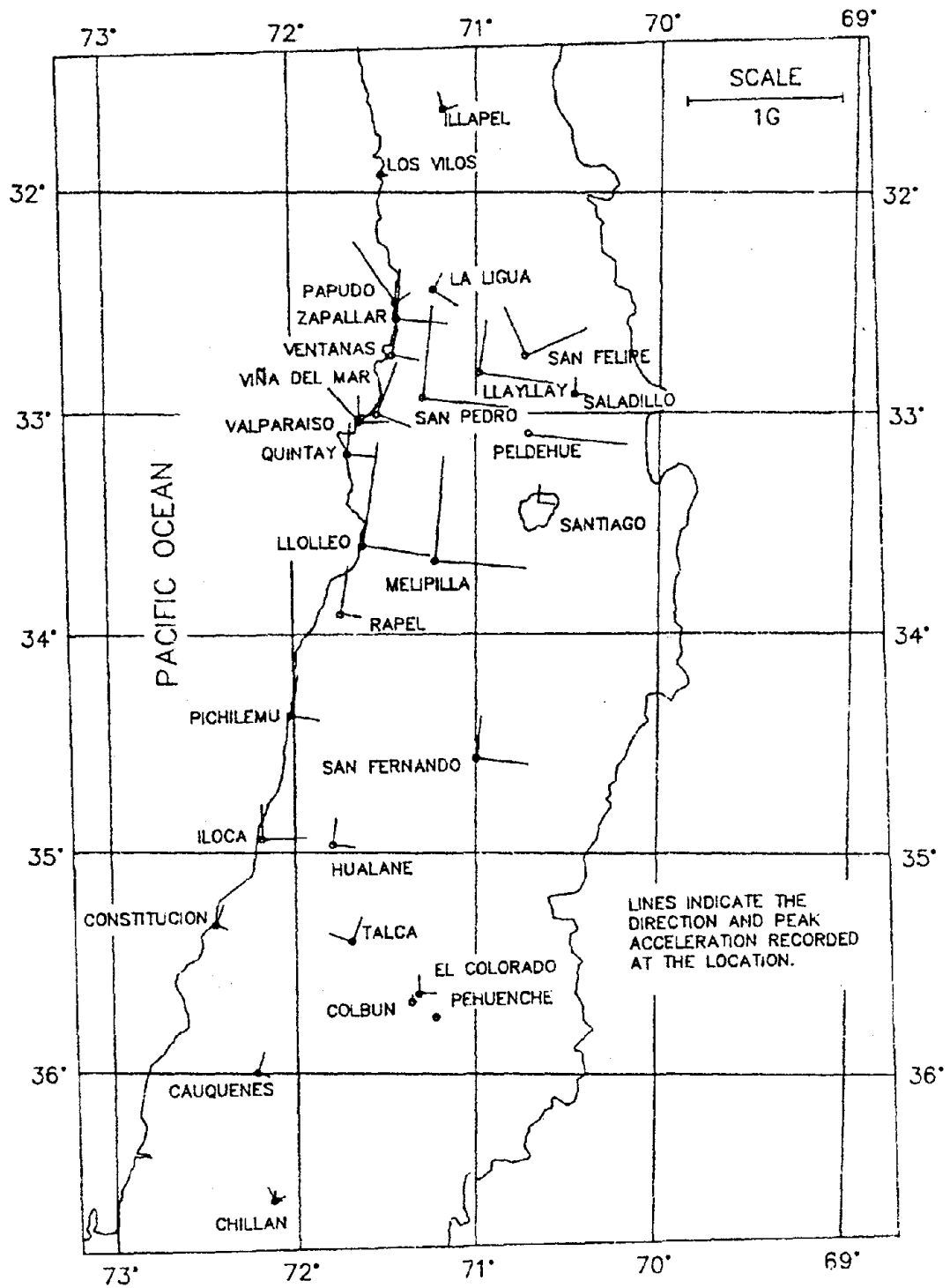


Fig. 3.2 Location of Strong-Motion Instruments in Epicentral Region of March 3, 1985 Earthquake [Saragoni et al. (1985)]

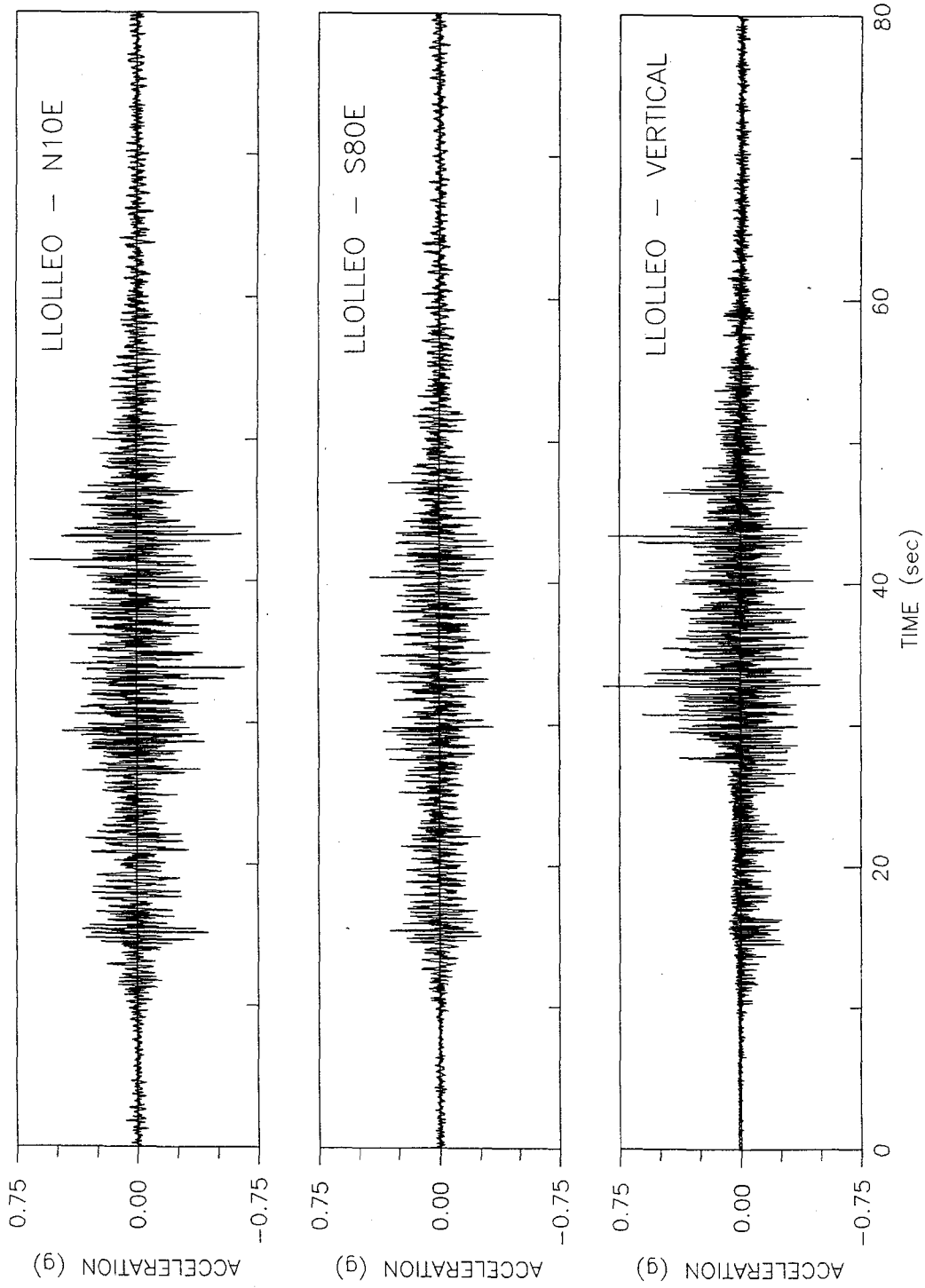


Fig. 3.3.a Strong-Motion Record - Llolleo

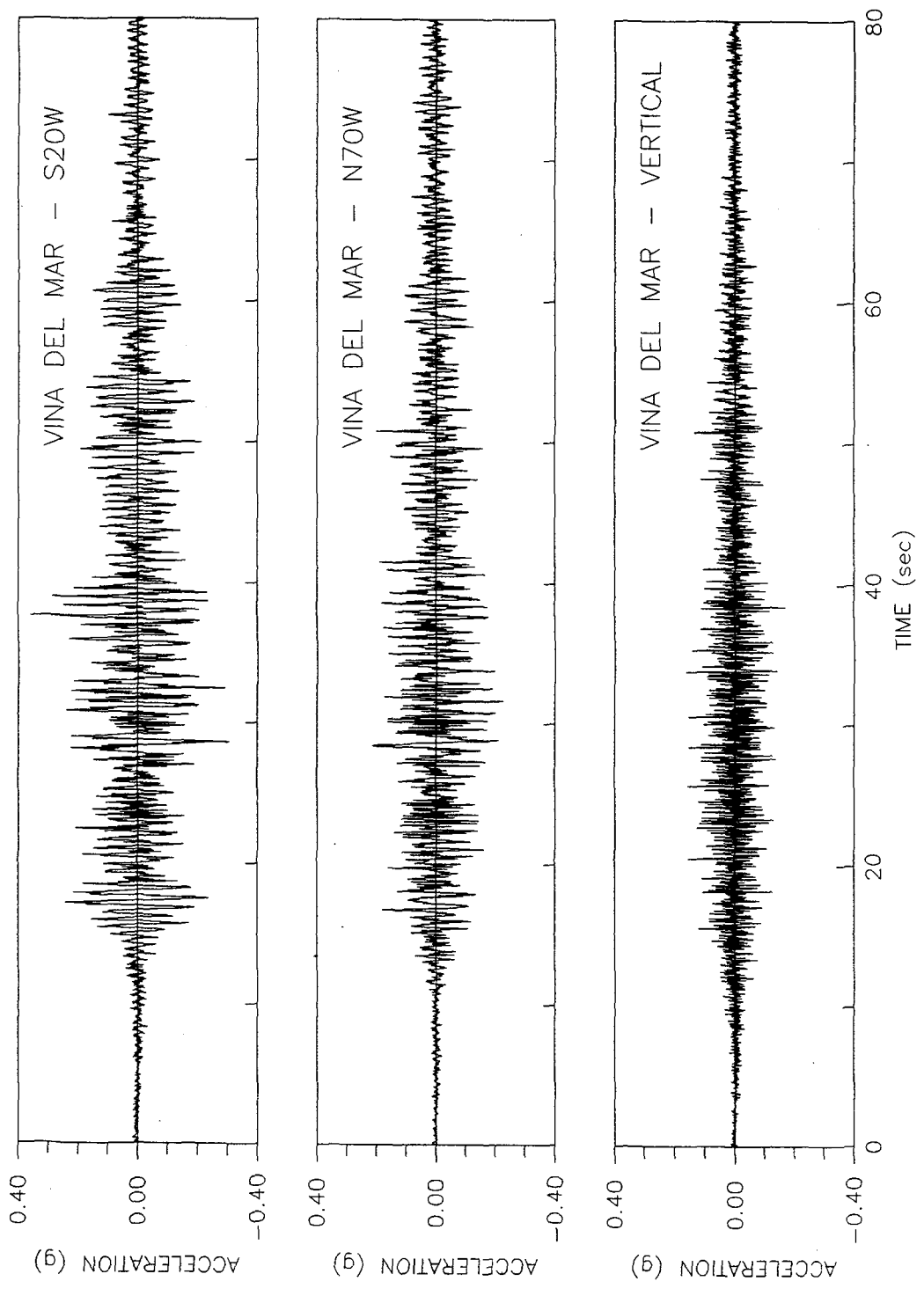


Fig. 3.3.b Strong-Motion Record - Viña del Mar

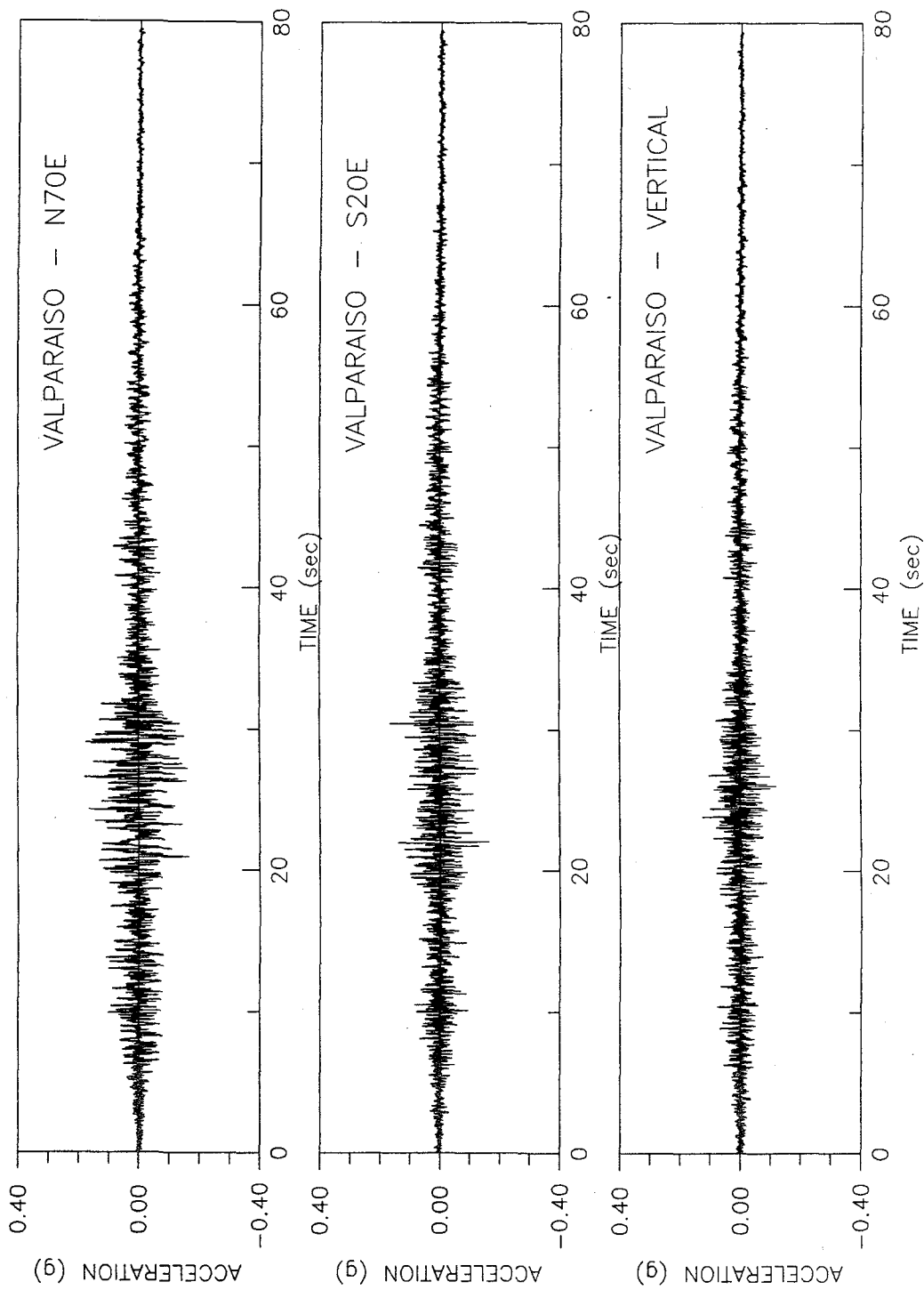


Fig. 3.3.c Strong-Motion Record - Valparaiso

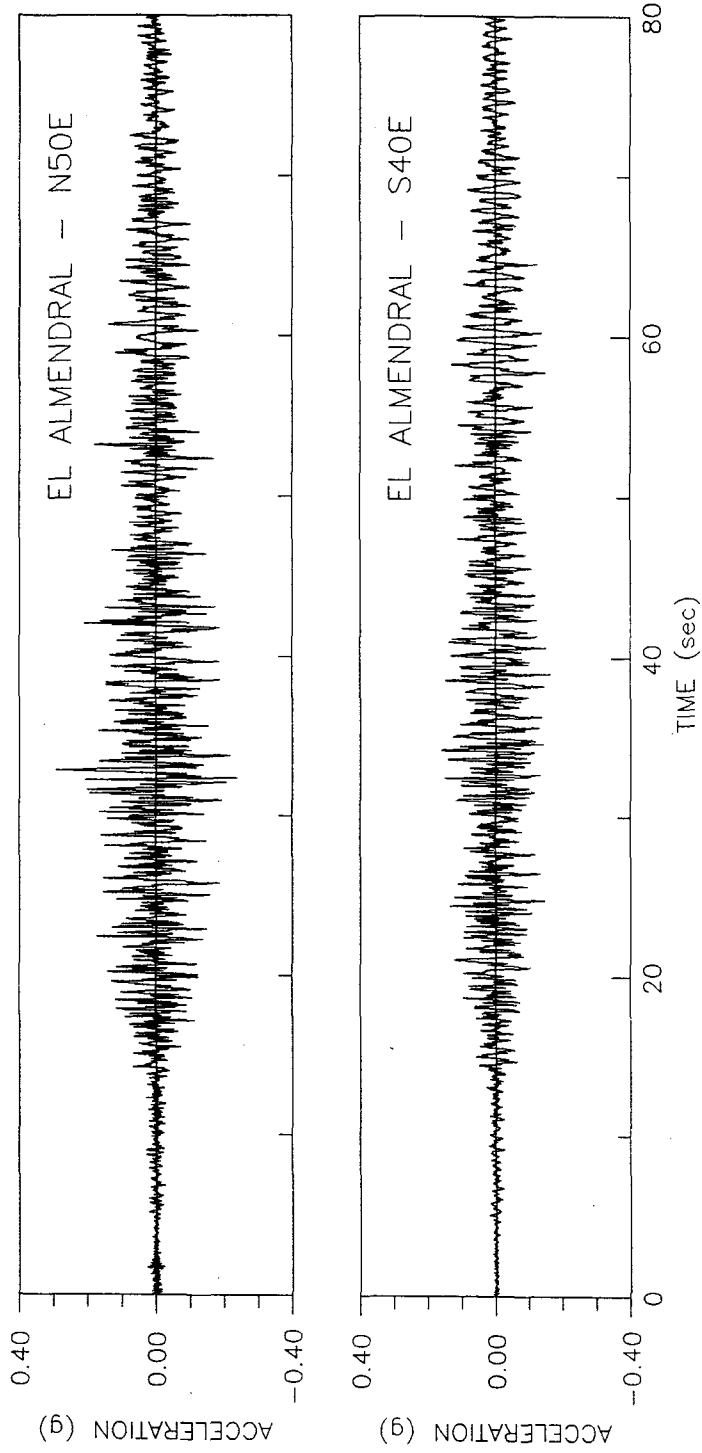


Fig. 3.3.d Strong-Motion Record - El Almendral

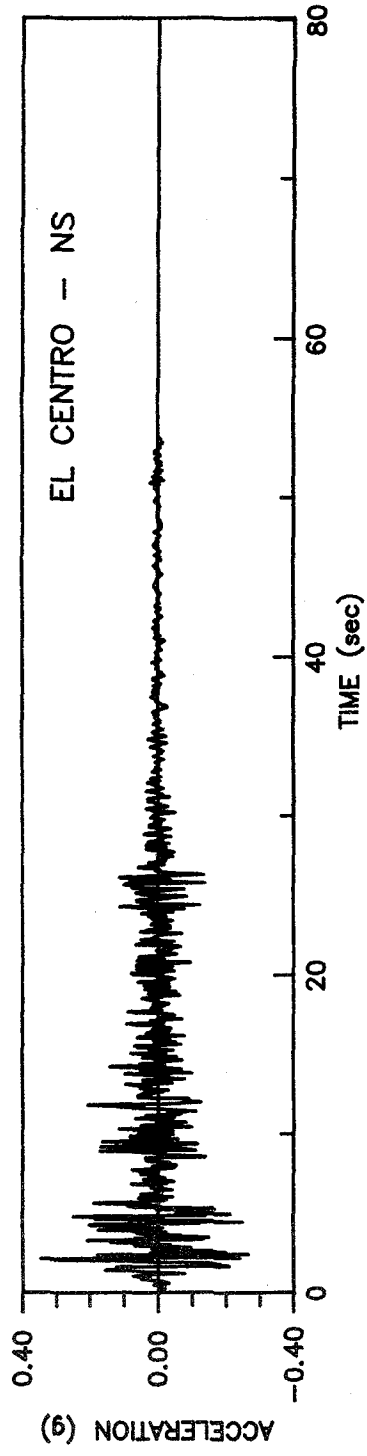


Fig. 3.4 Strong-Motion Record - El Centro 1940 NS

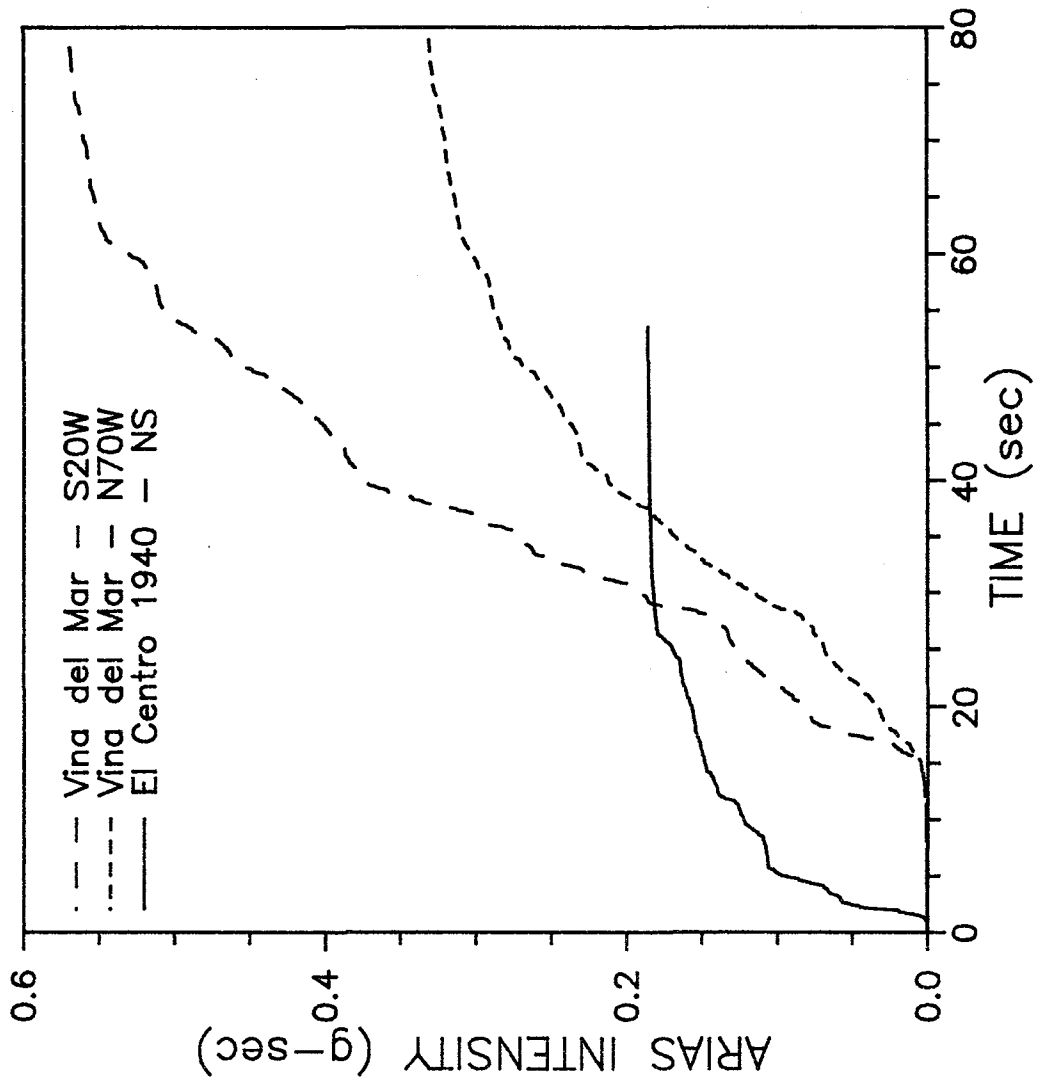


Fig. 3.5 Evolutionary Arias Intensity

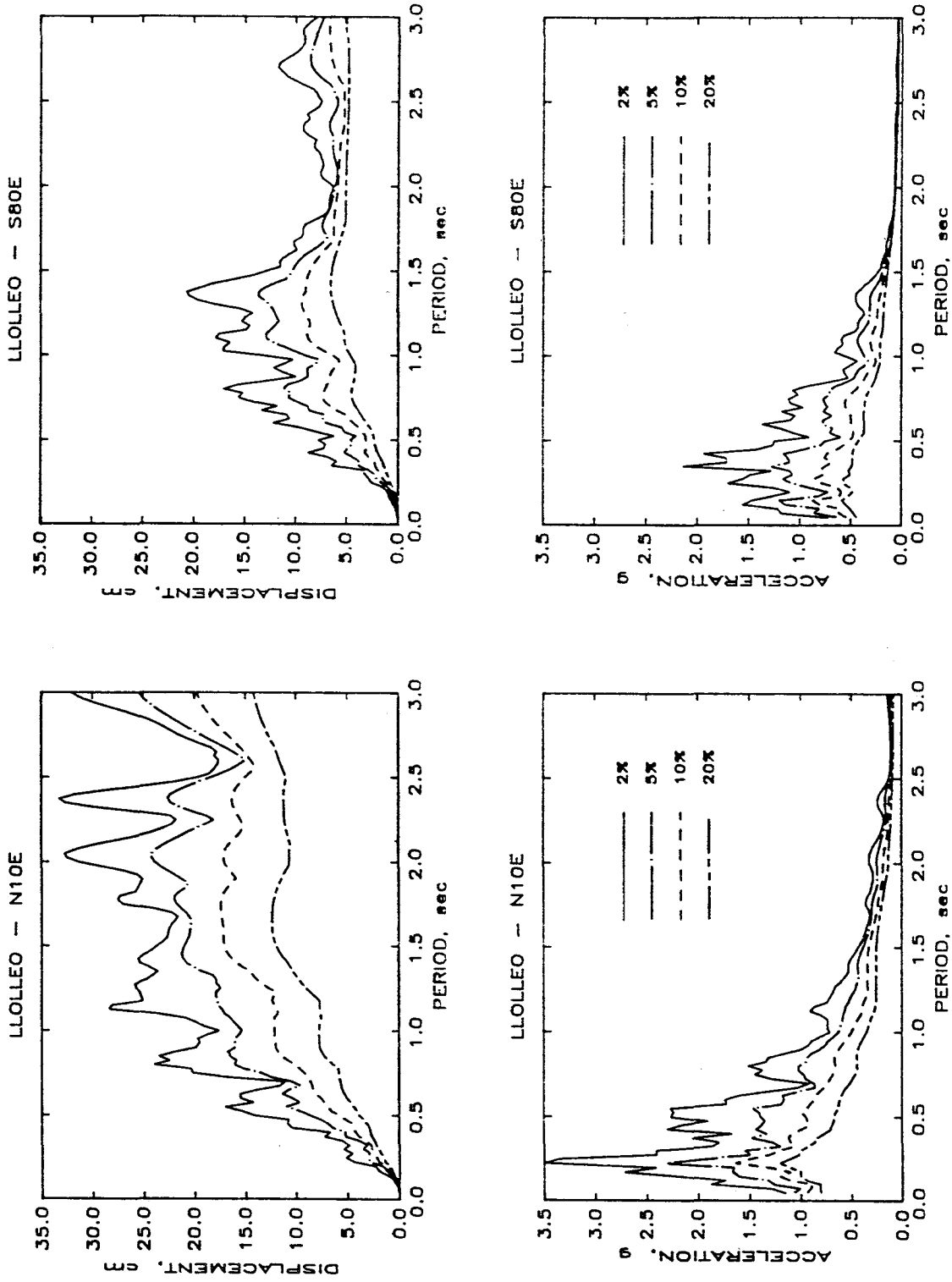


Fig. 3.6.a Elastic Response Spectra - Lolloo

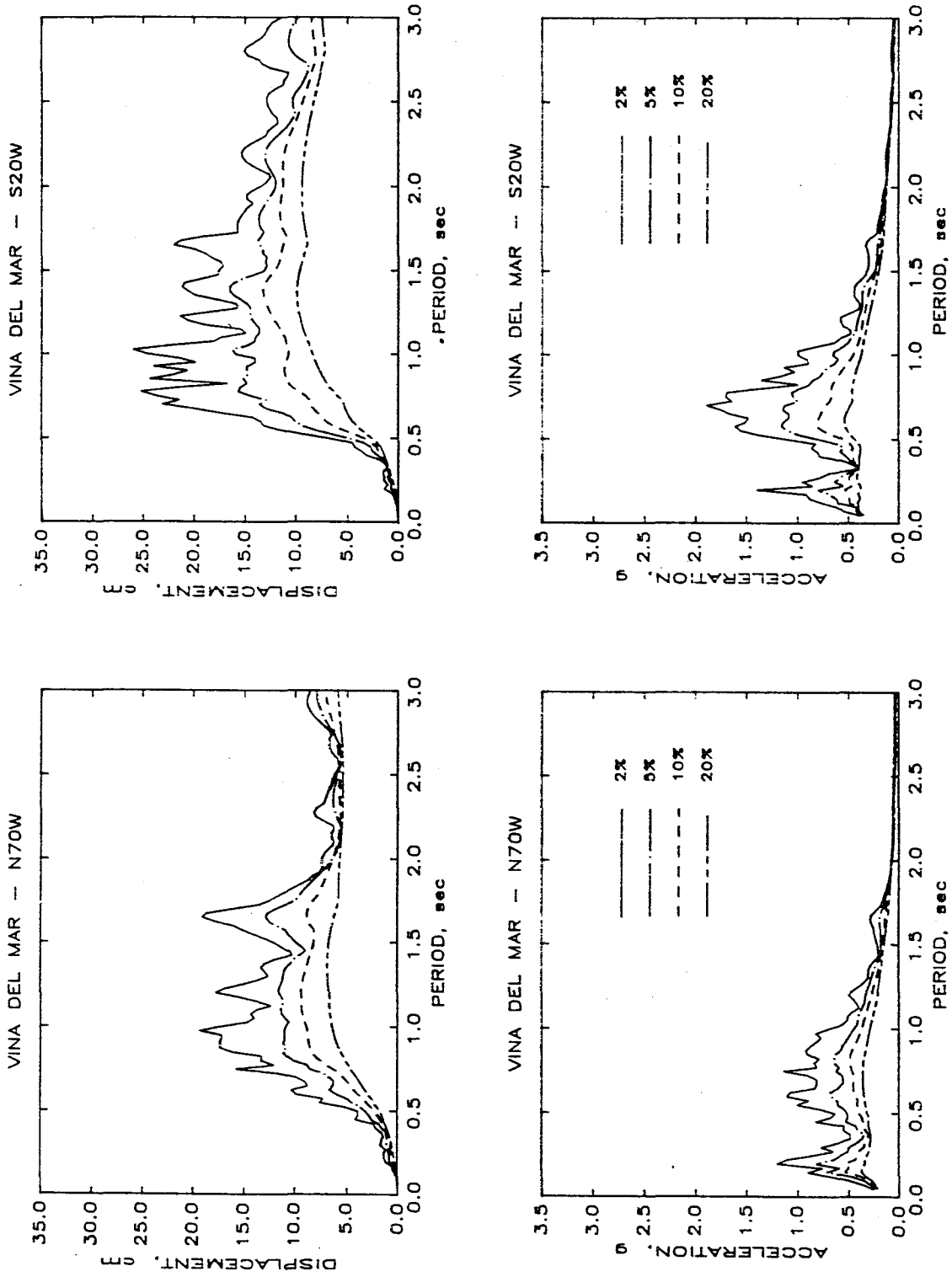


Fig. 3.6.b Elastic Response Spectra - Viña del Mar

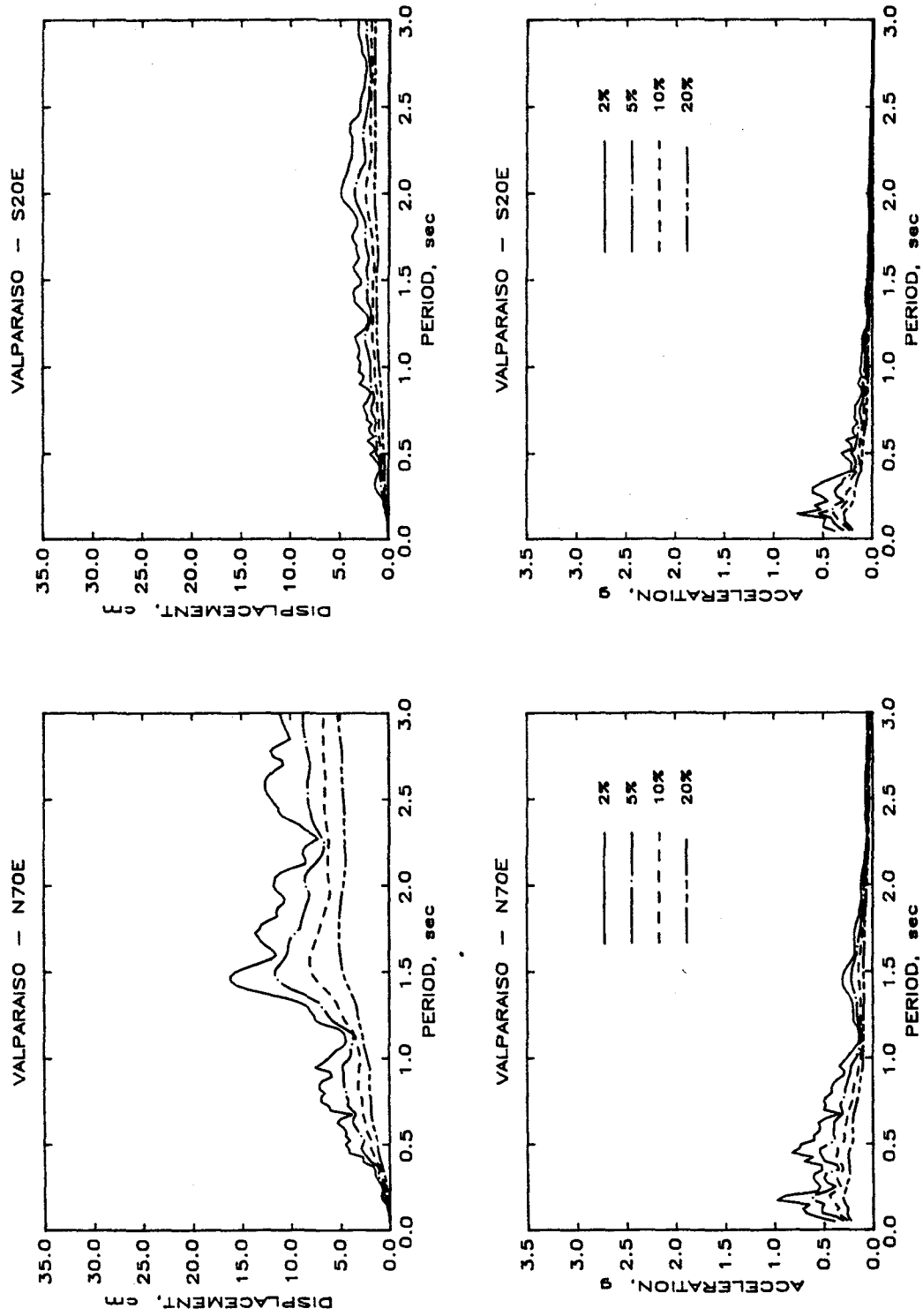


Fig. 3.6.c Elastic Response Spectra - Valparaiso

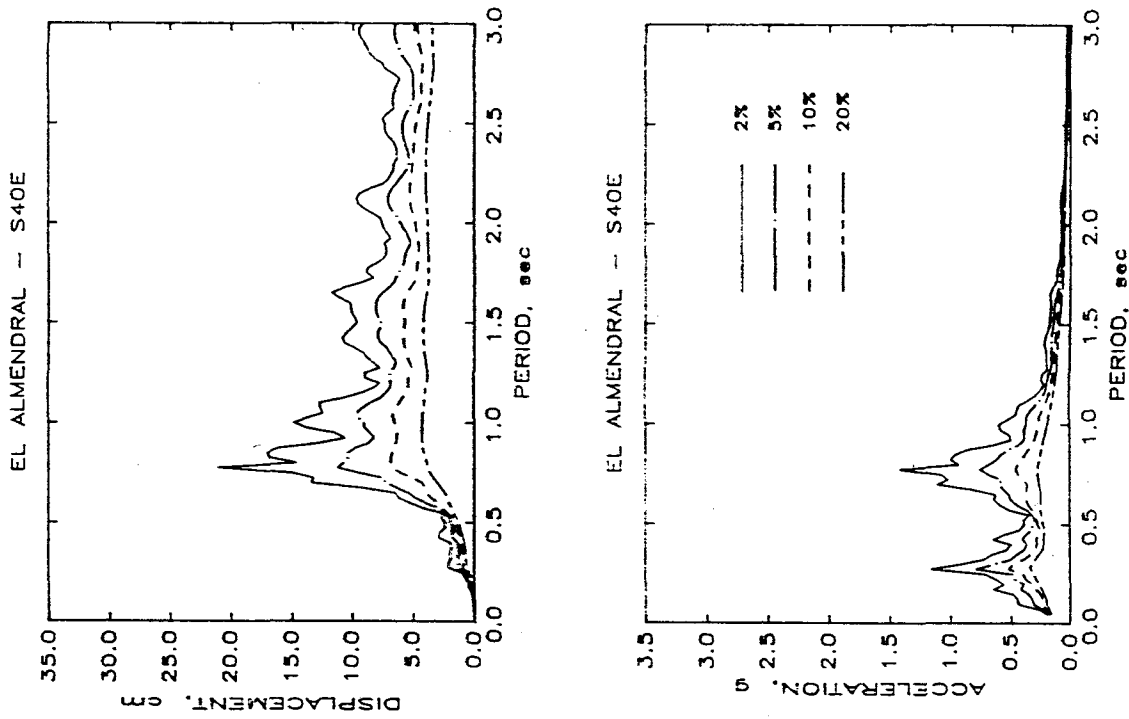


Fig. 3.6.d Elastic Response Spectra - El Almendral

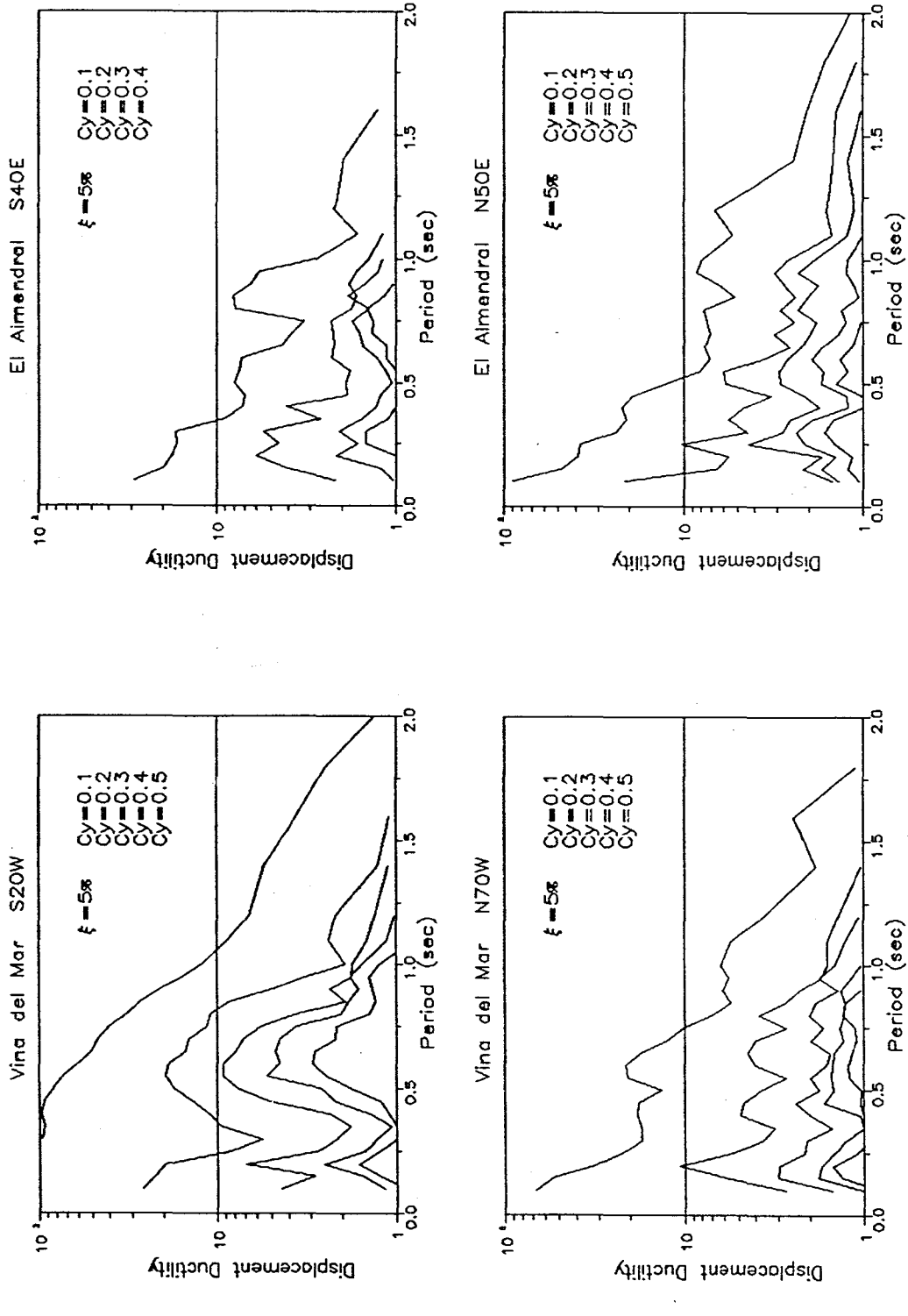


Fig. 3.7 Elasto-Plastic Response Spectra

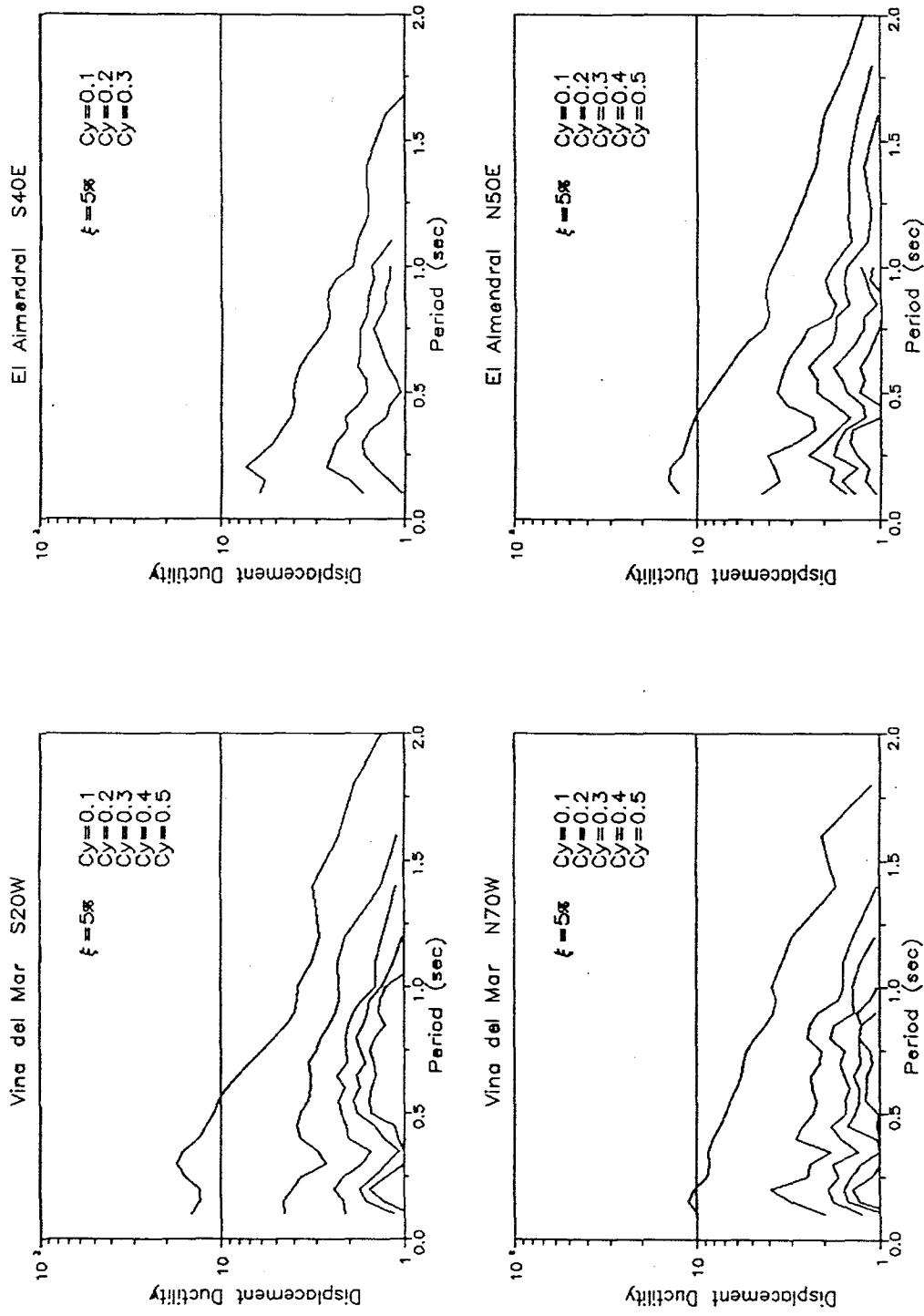


Fig. 3.8 Bilinear Response Spectra

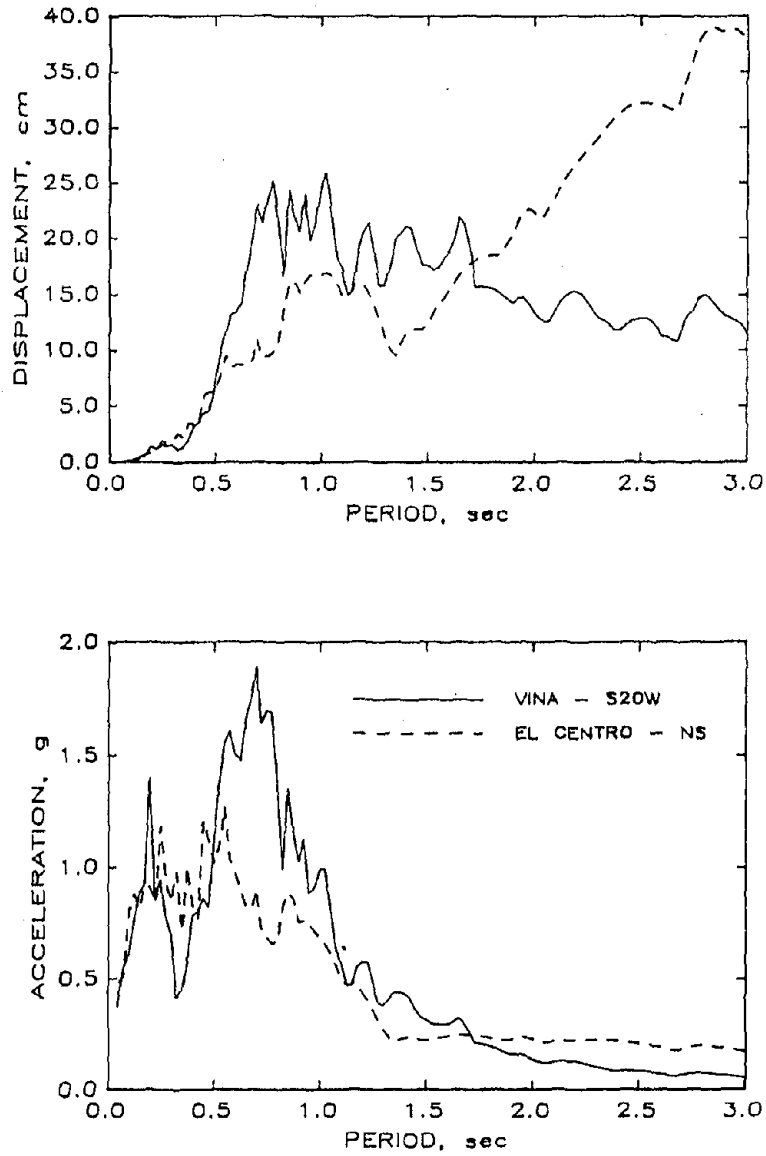


Fig. 3.9 Comparison of Elastic Response Spectra from the 1940 El Centro and 1985 Viña del Mar Records (2% Damping)

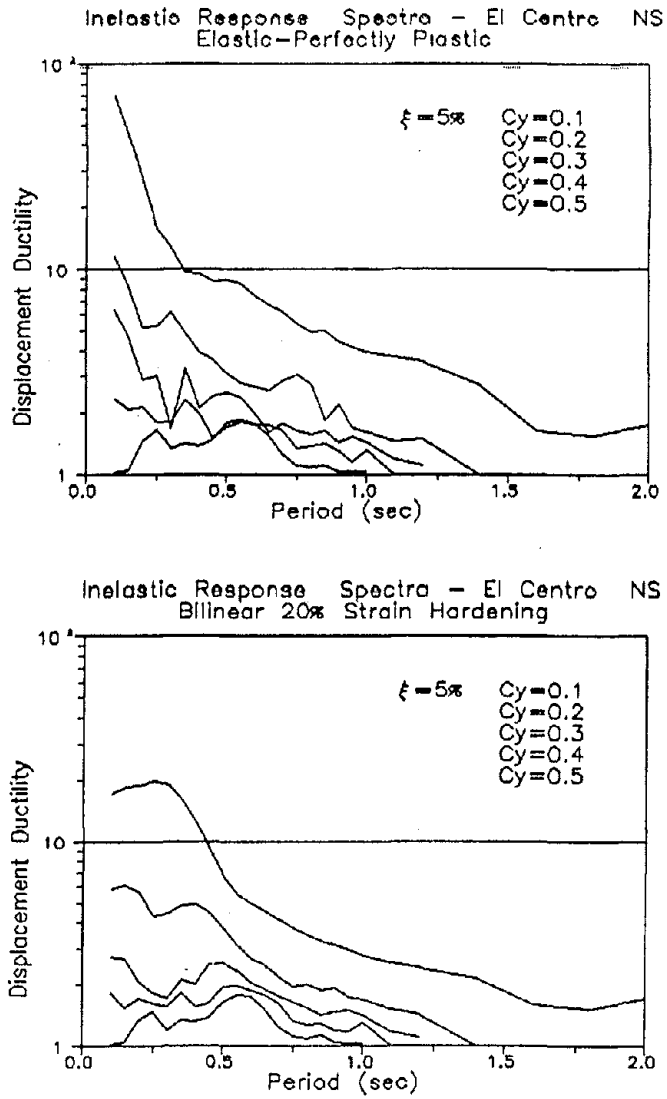


Fig. 3.10 Inelastic Response Spectra for the 1940 El Centro Record

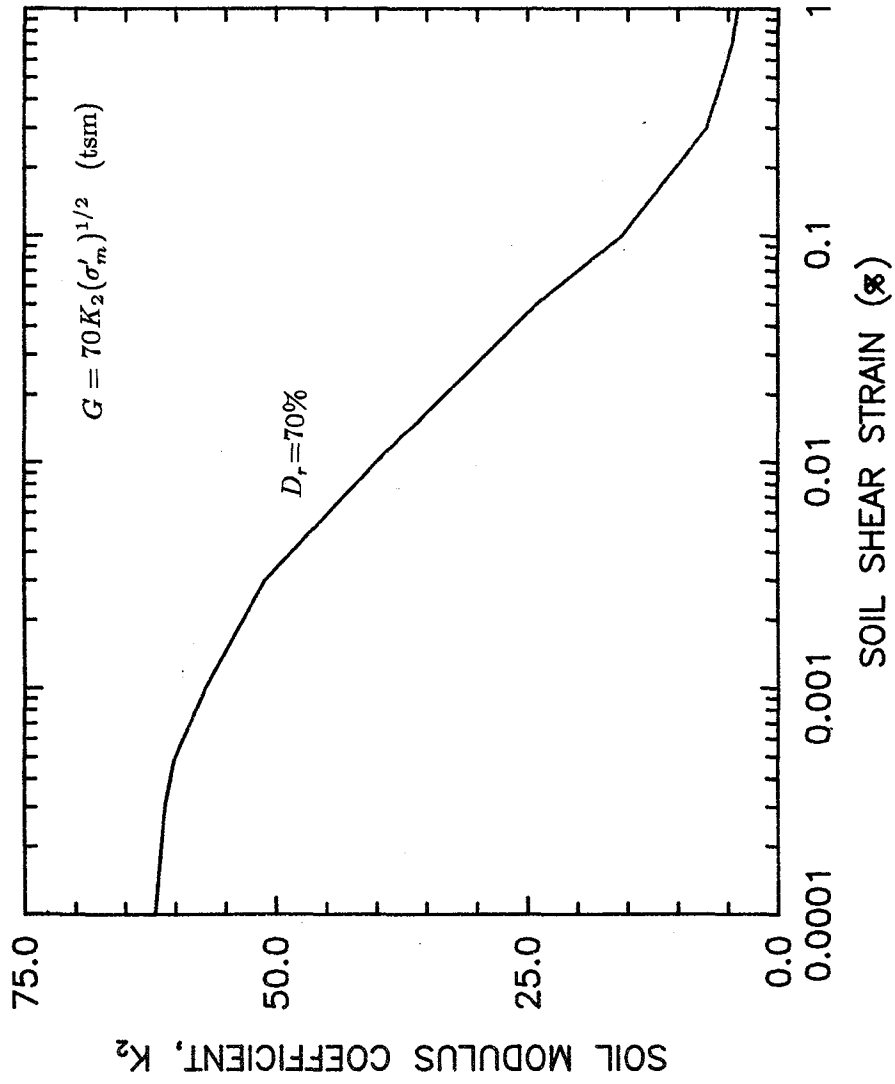


Fig. 4.1 Shear Modulus of Sand as a Function of Shear Strain

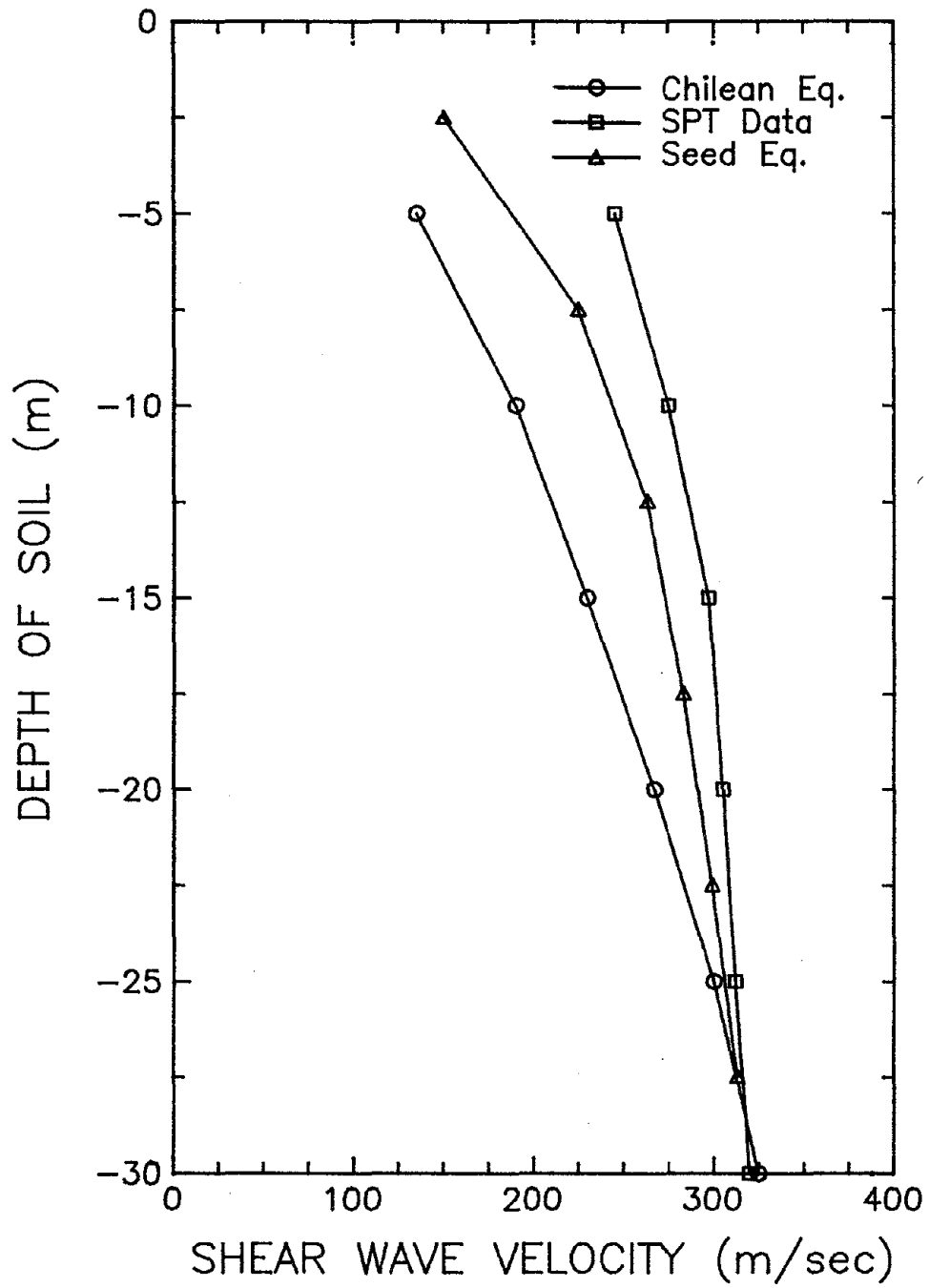


Fig. 4.2 Three Estimates for Shear Wave Velocity

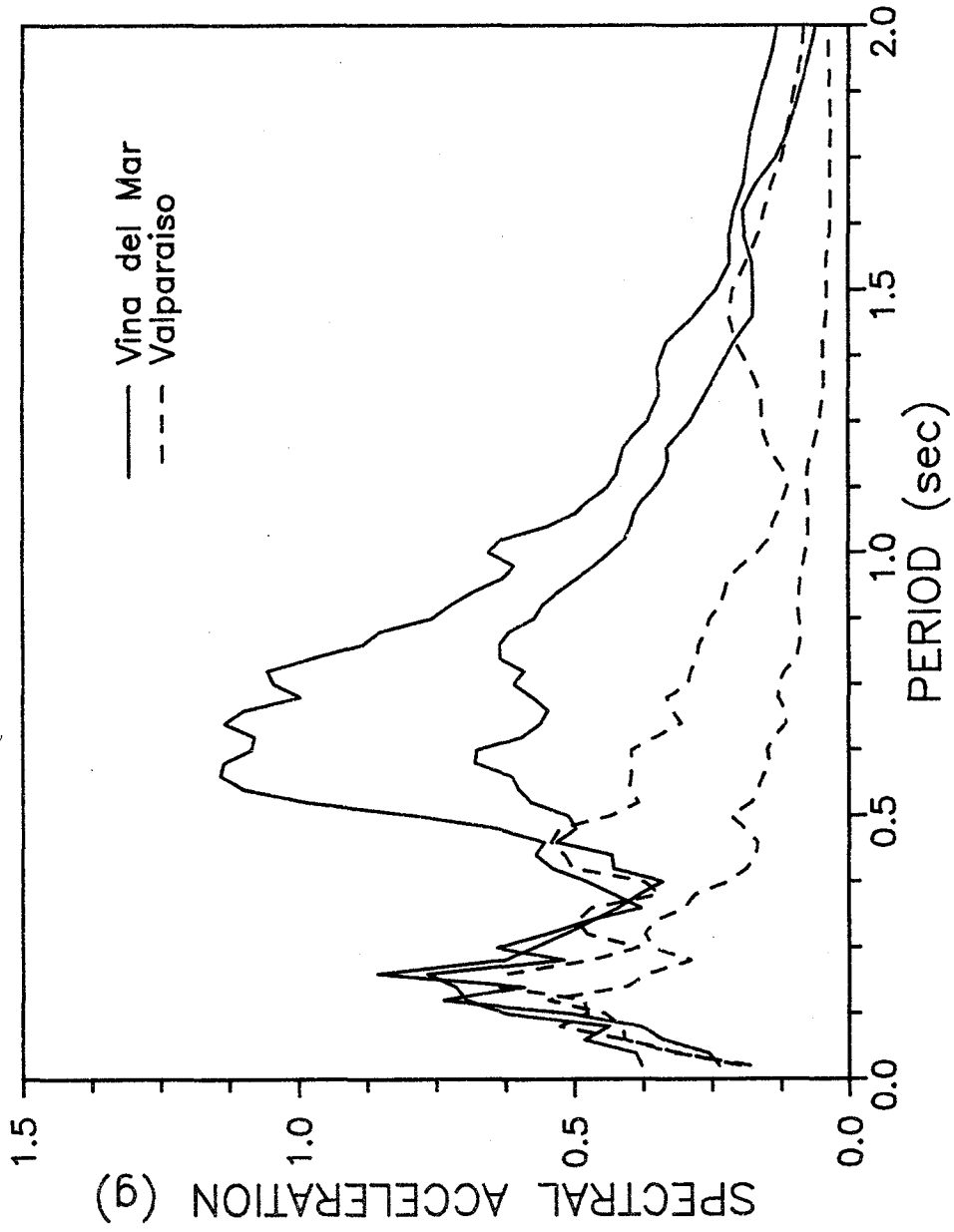


Fig. 4.3.a Comparison of Response Spectra for Rock and Soil Sites Valparaiso and Viña del Mar

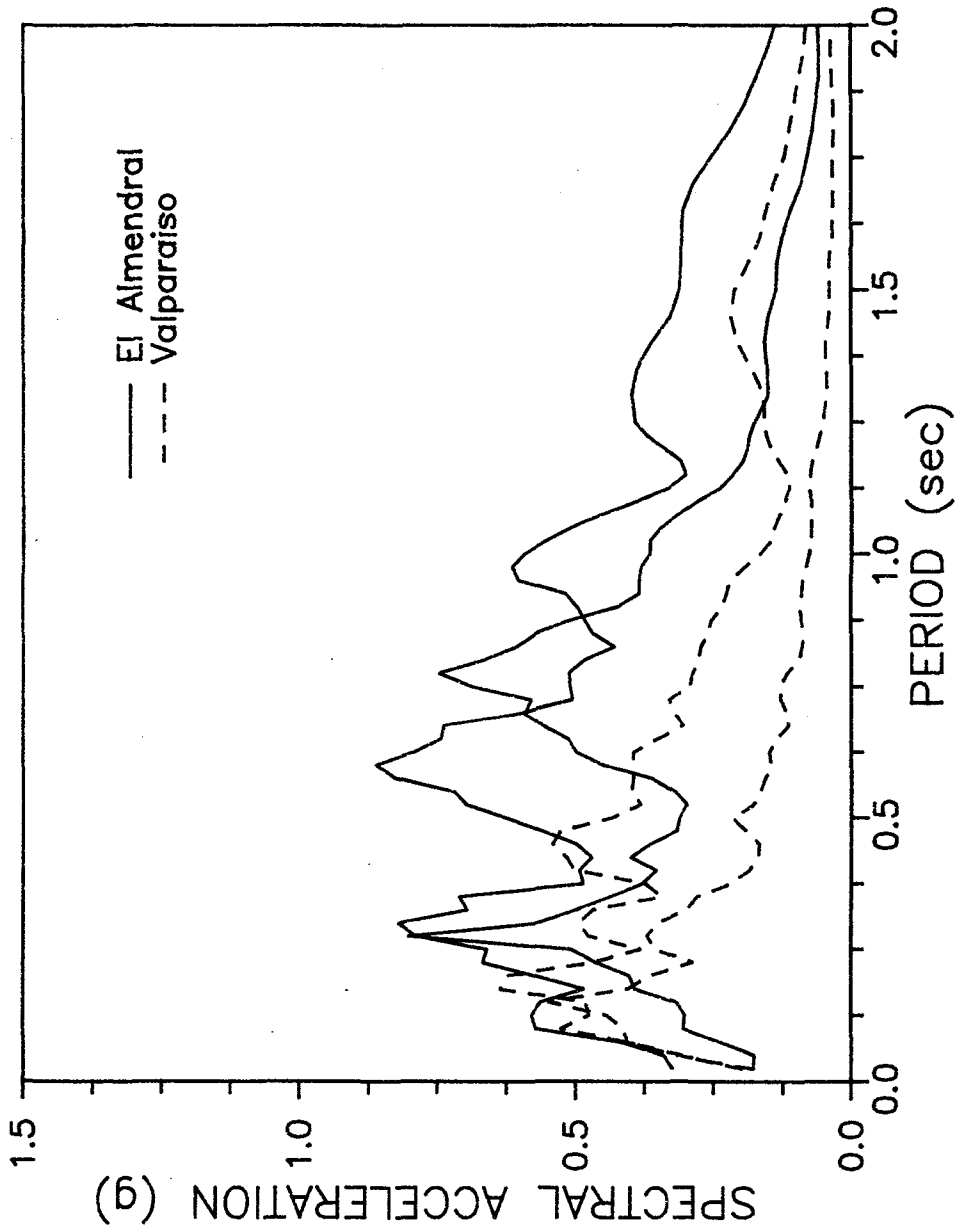


Fig. 4.3.b Comparison of Response Spectra for Rock and Soil Sites Valparaíso and El Almendral

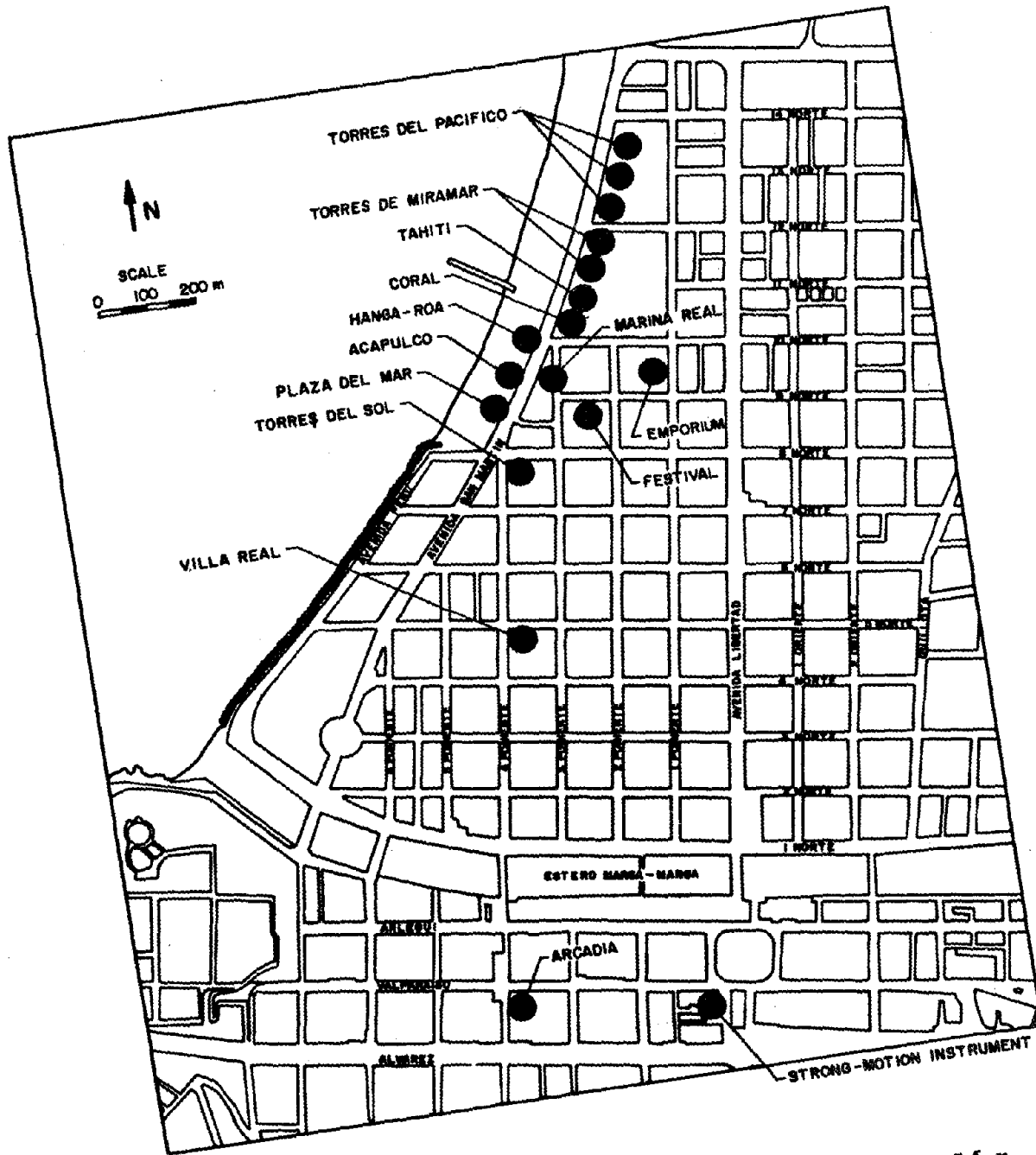


Fig. 4.4 Building and Instrument Locations in Viña del Mar  
[Wood et al. (1987)]

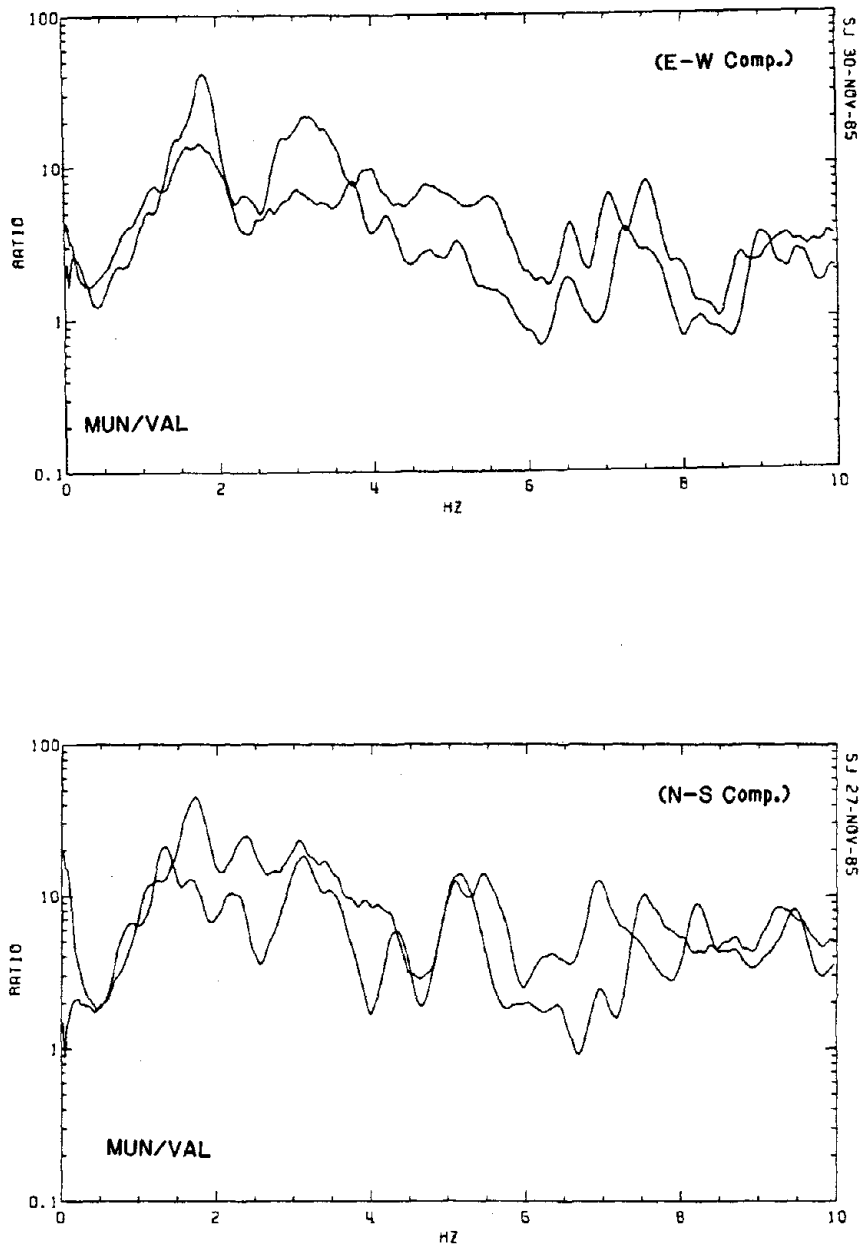
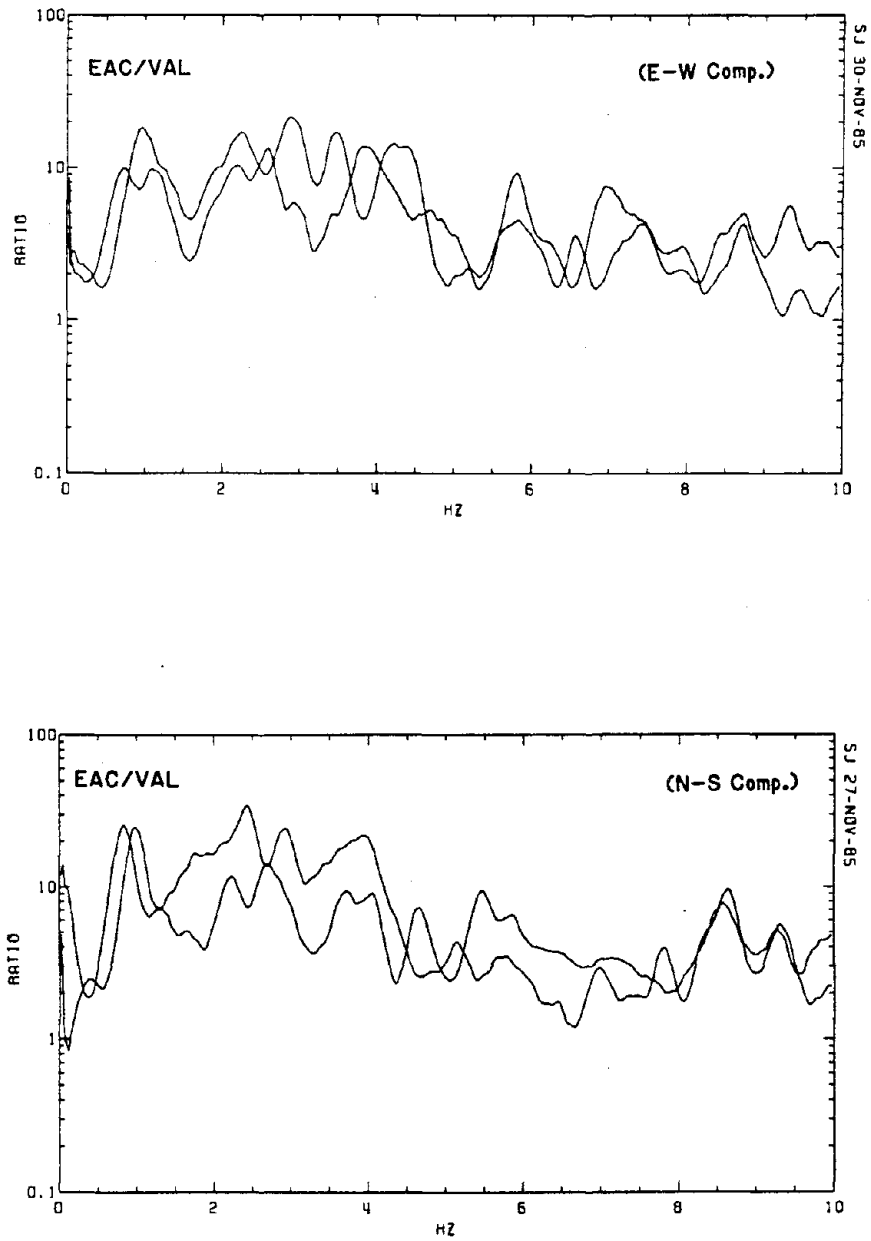
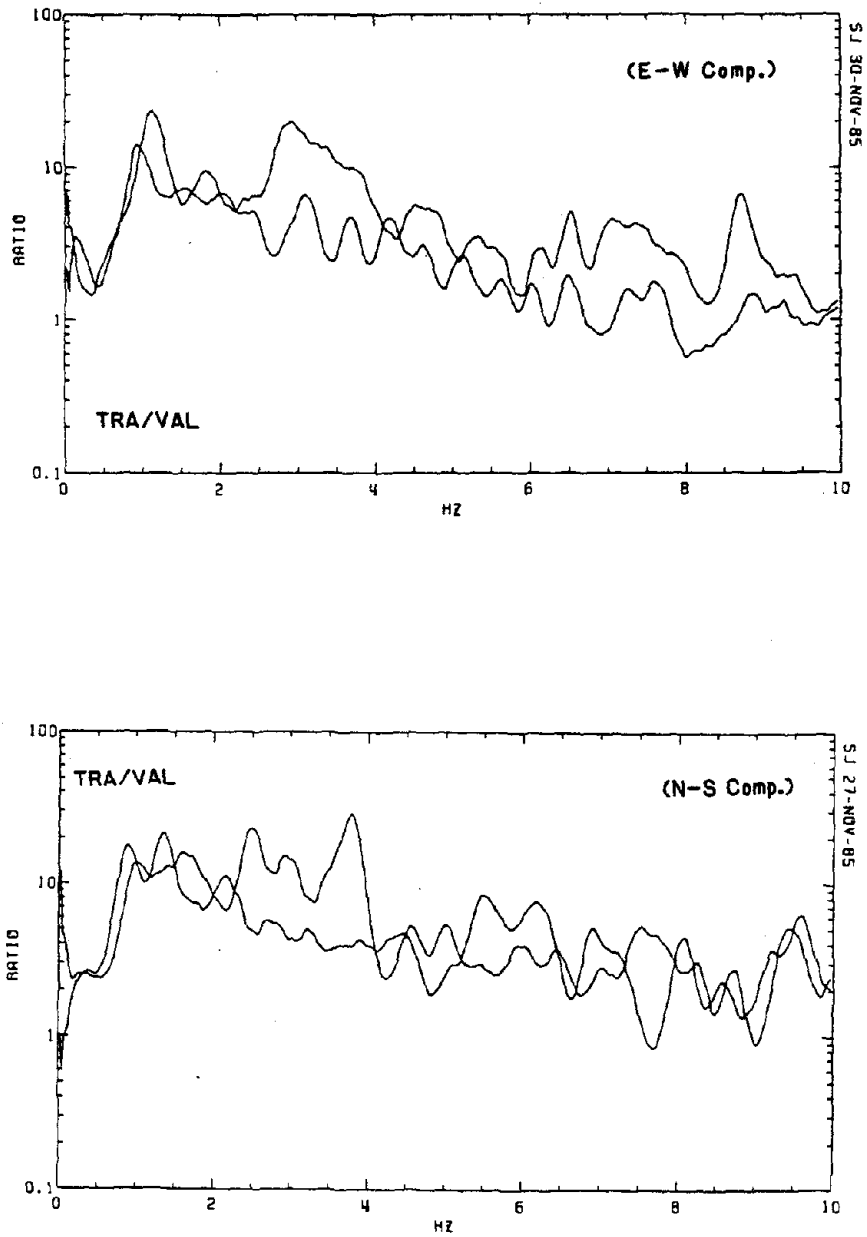


Fig. 4.5.a Ratios of Fourier Spectral Velocity for Two Events  
Municipal Building (Viña del Mar) over Valparaíso  
[Celebi, Editor (1986)]



**Fig. 4.5.b Ratios of Fourier Spectral Velocity for Two Events  
Edificio Acapulco (Viña del Mar) over Valparaíso  
[Celebi, Editor (1986)]**



**Fig. 4.5.c Ratios of Fourier Spectral Velocity for Two Events  
Torres de Miramar (Viña del Mar) over Valparaíso  
[Celebi, Editor (1986)]**

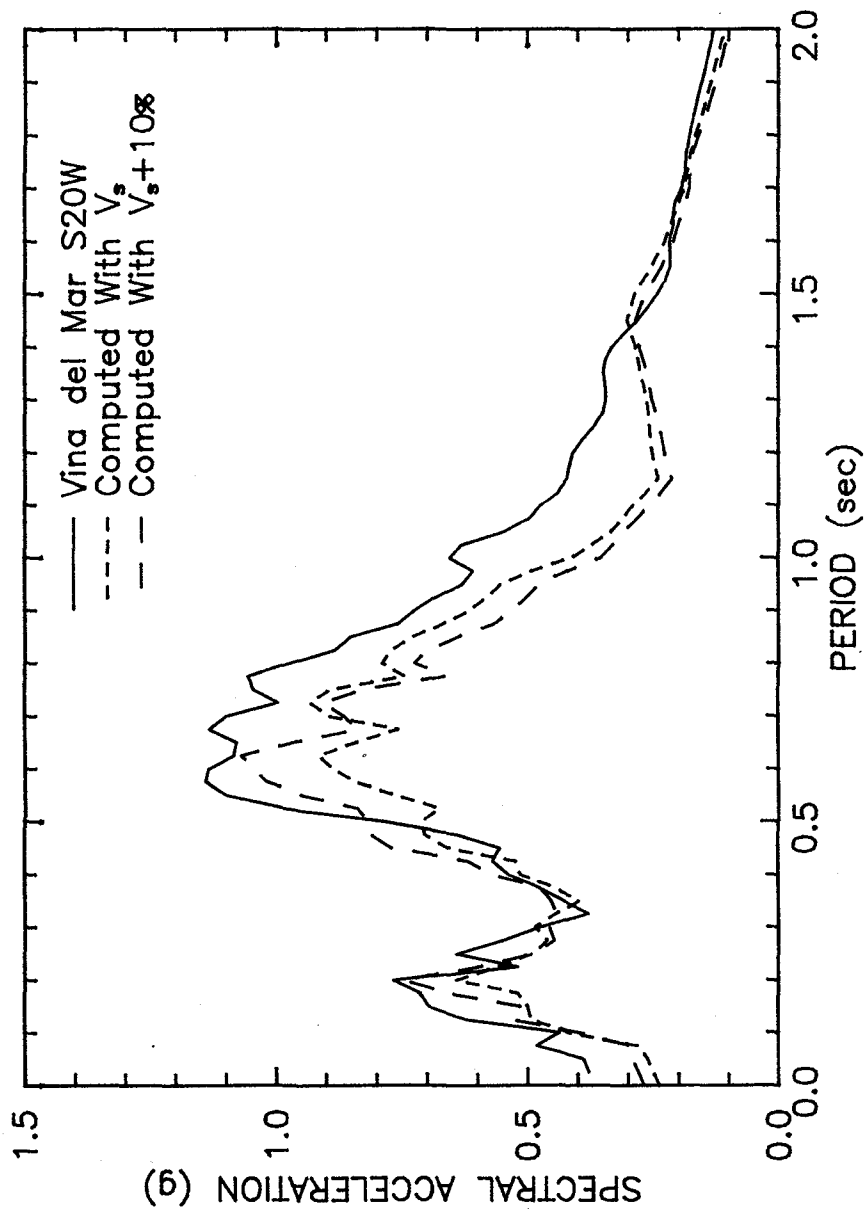


Fig. 4.6 Spectra for Site Response Analyses - Municipal Building

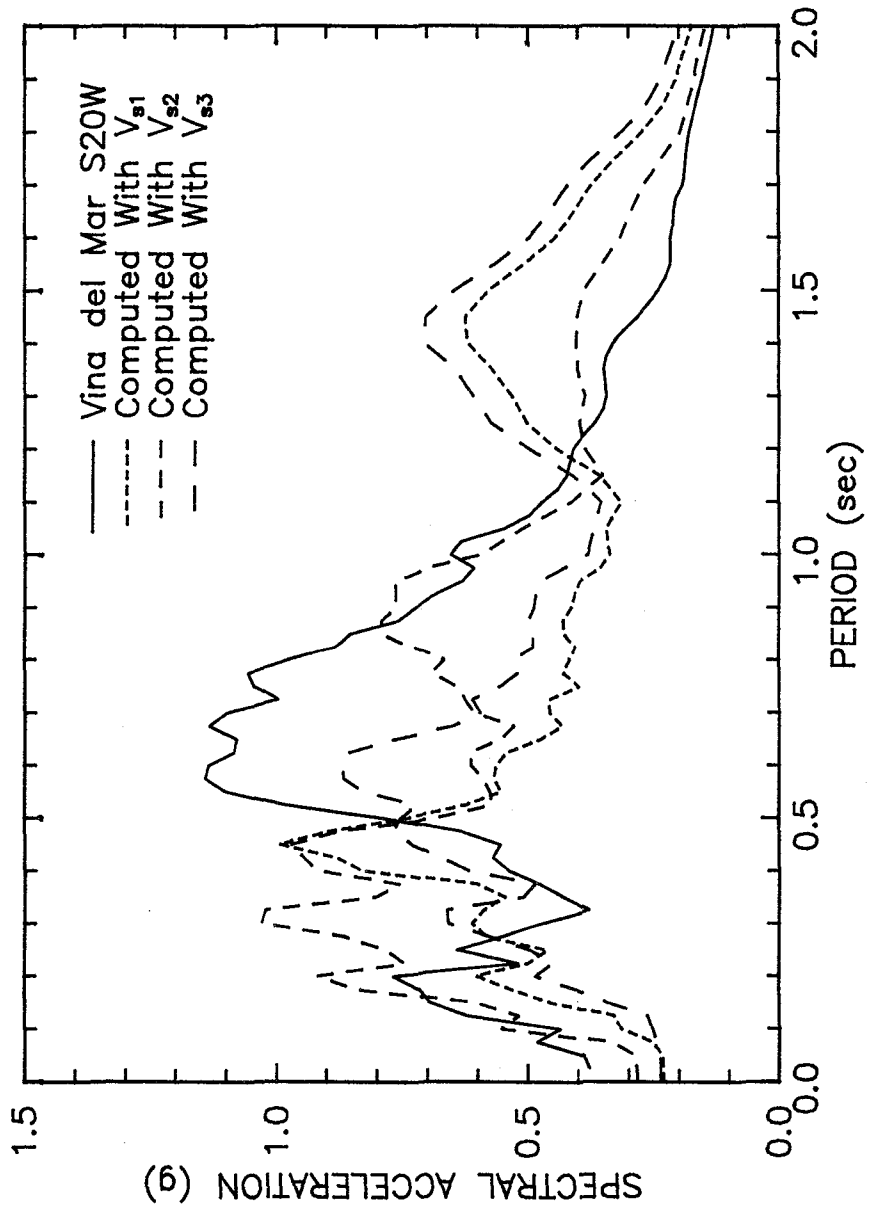


Fig. 4.7 Spectra for Site Response Analyses - Beach Locations

$$\text{Effective Flange Width} = \left\{ \begin{array}{l} \text{One-Fourth Unsupported Beam Span} \\ \text{Beam Width plus 16 Slab Thicknesses} \\ \text{Centerline to Centerline Beam Spacing} \end{array} \right\}$$

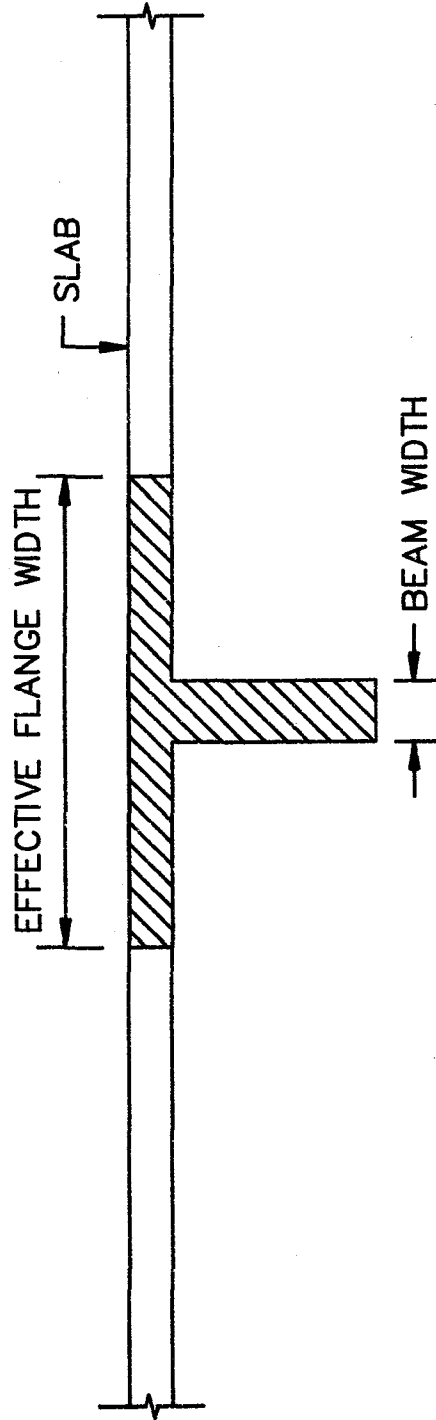


Fig. 5.1 Beam Effective Slab Width

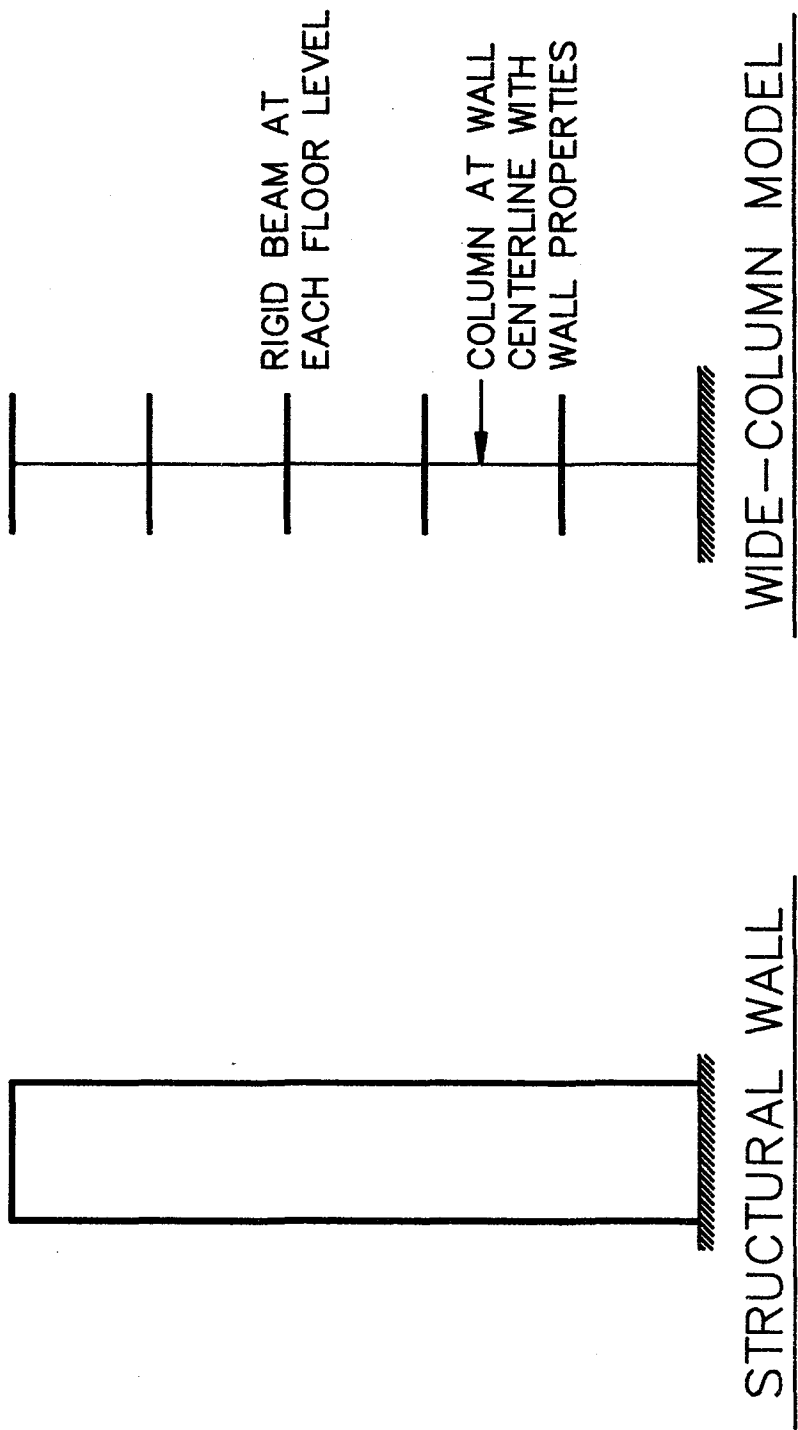


Fig. 5.2 Wide-Column Analogy for Slender Structural Walls

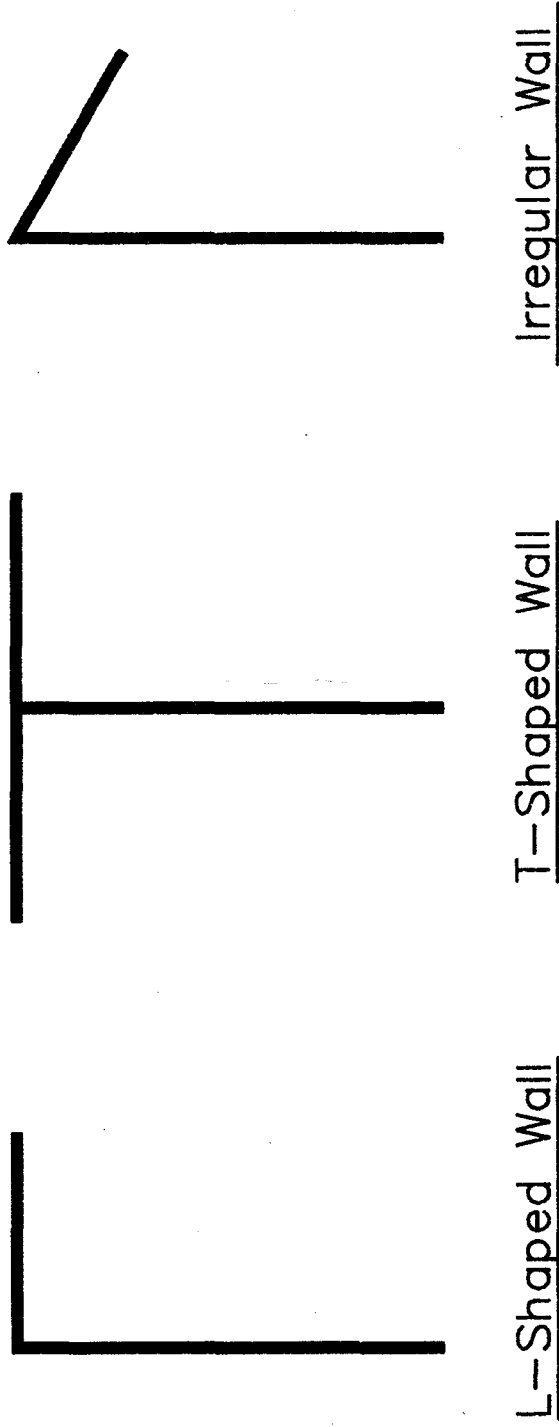
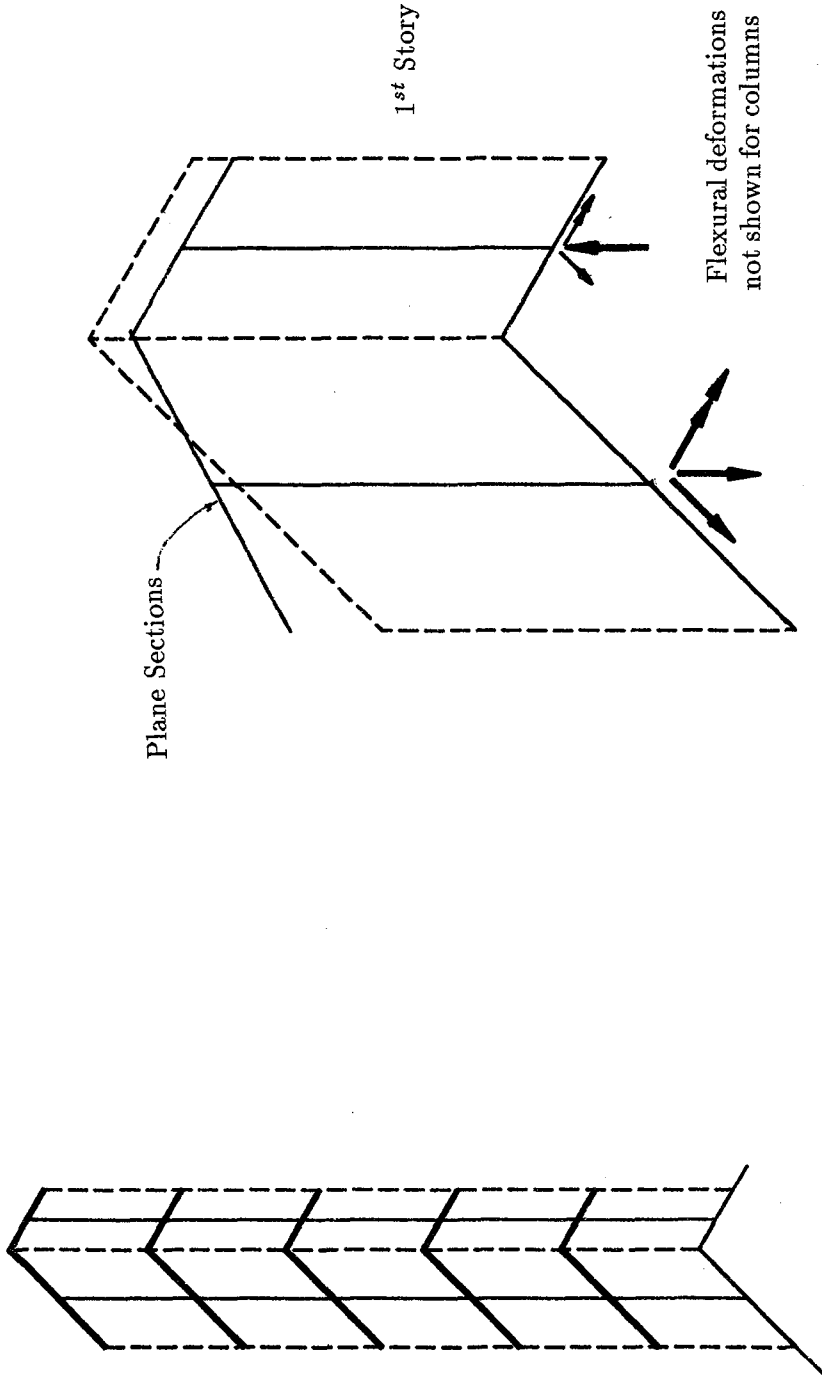


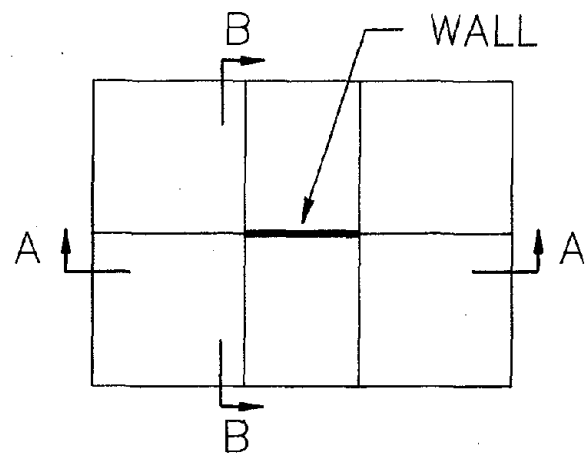
Fig. 5.3 Structural Walls with Flange Sections



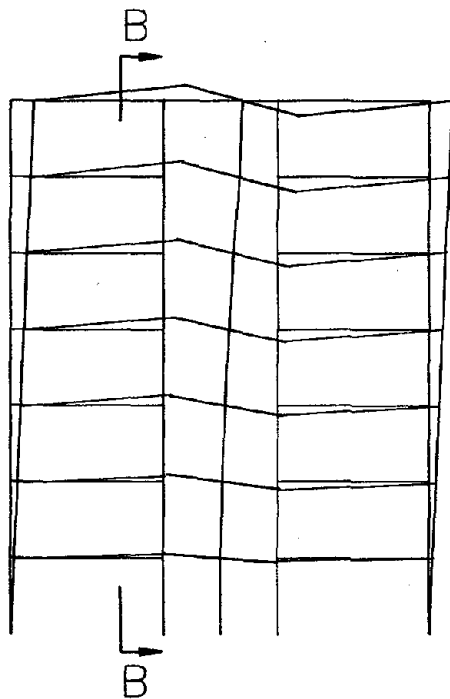
Connected Wide-Column

Plane Section Deformation  
(No Torsion)

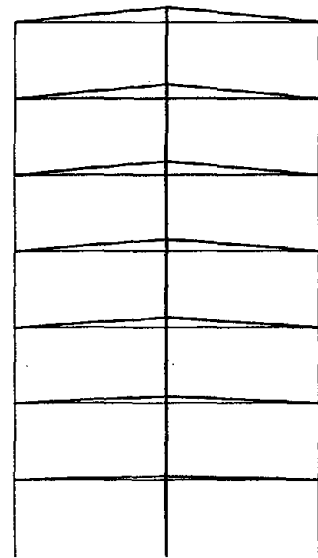
Fig. 5.4 Connected Wide-Column Model for Slender Structural Walls



BUILDING — PLAN VIEW

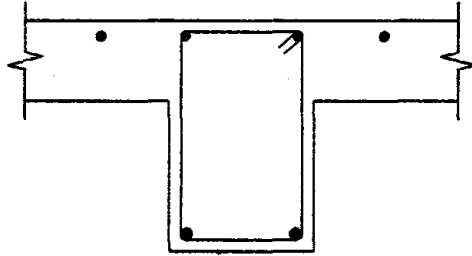


SECTION (A) — (A)

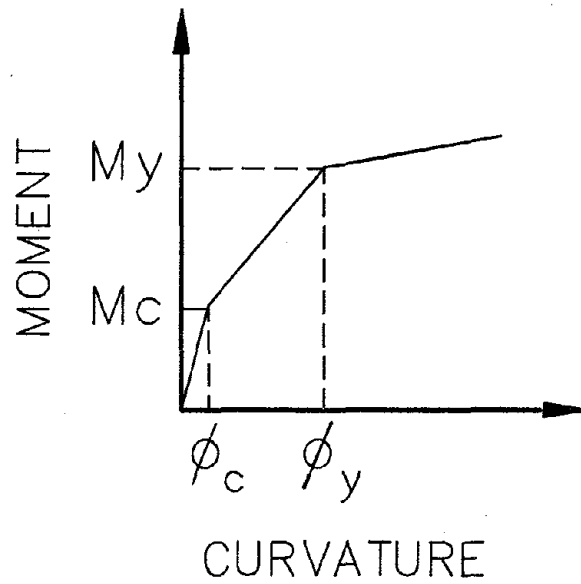


SECTION (B) — (B)

**Fig. 5.5 Three-Dimensional Frame-Wall Interaction**

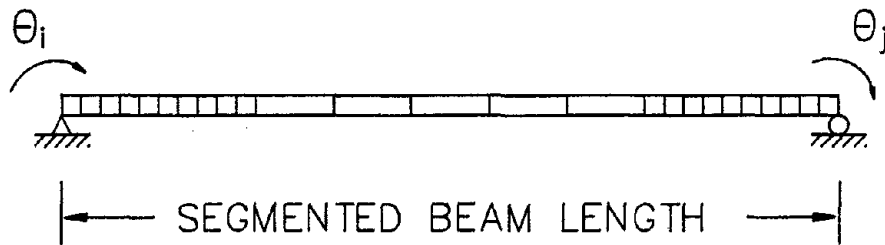


(a) SECTION DESCRIPTION

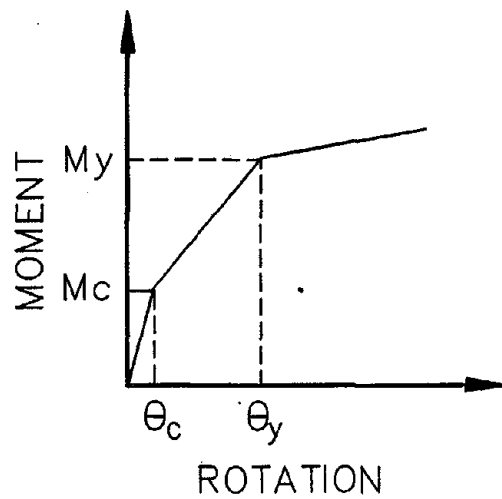


(b) SECTION  $M - \phi$ .

Fig. 5.6 Definition of Section Properties for Inelastic Modeling



(a) BEAM SEGMENTS WITH SECTION M -  $\phi$



(b) TRILINEAR M- $\theta$

Fig. 5.7 Procedure to Compute Properties of Trilinear Member End Springs

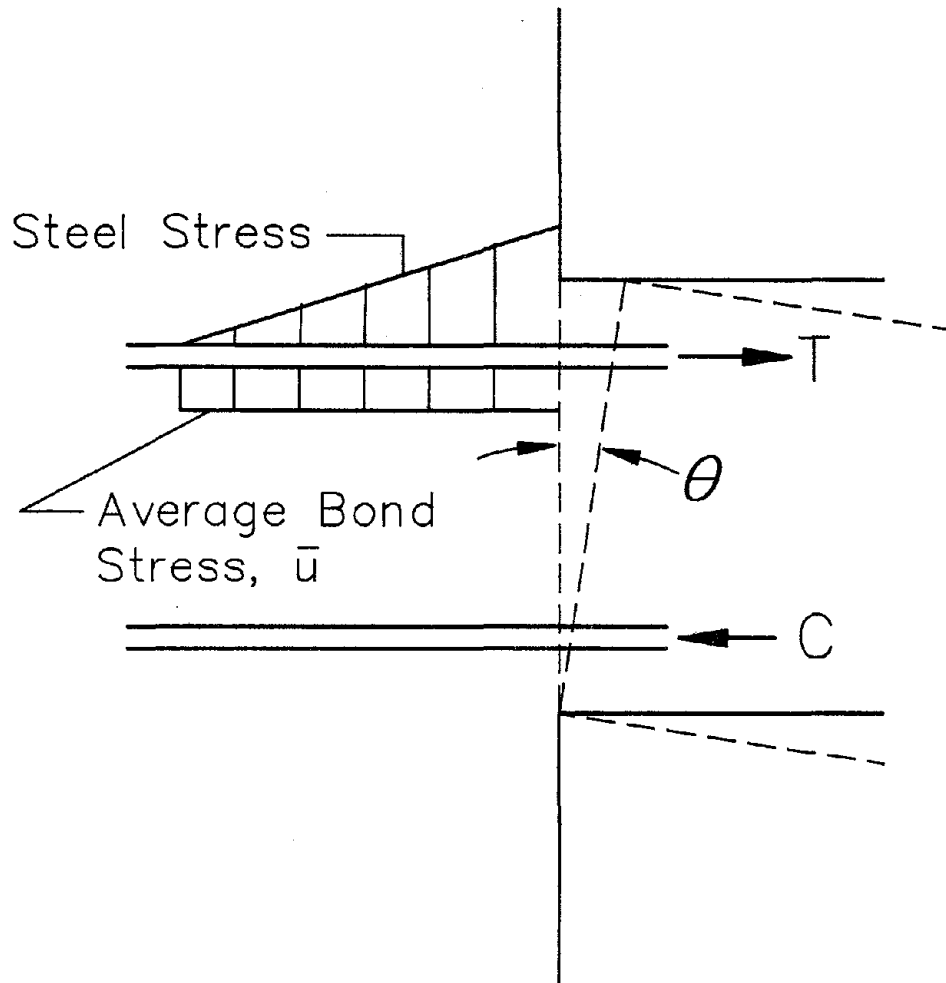
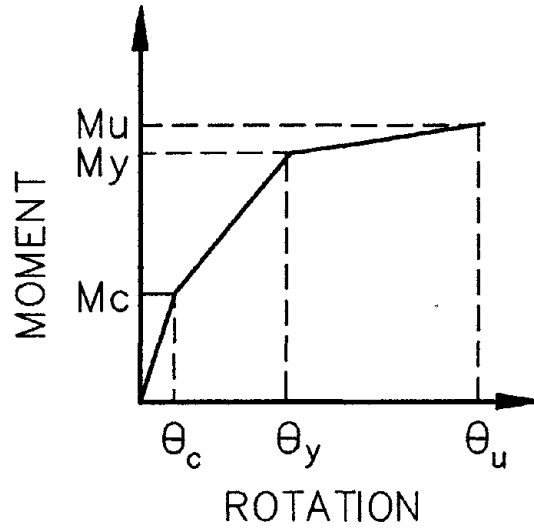
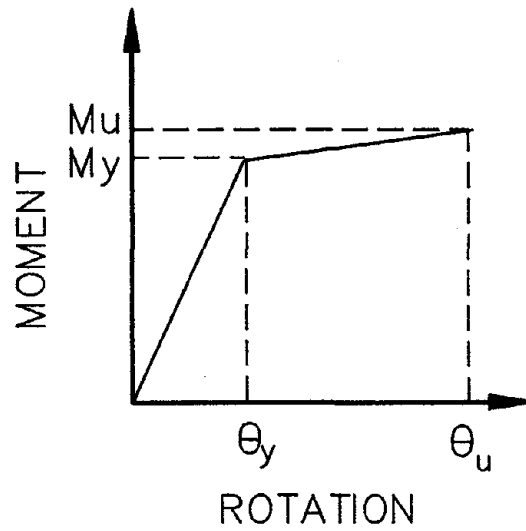


Fig. 5.8 Model to Compute Fixed End Rotation due to Reinforcement Slip



(a) TRILINEAR  $M-\theta$



(b) DRAIN-2D  $M-\theta$

Fig. 5.9 Bilinear Member End Springs for DRAIN-2D Program Modeling

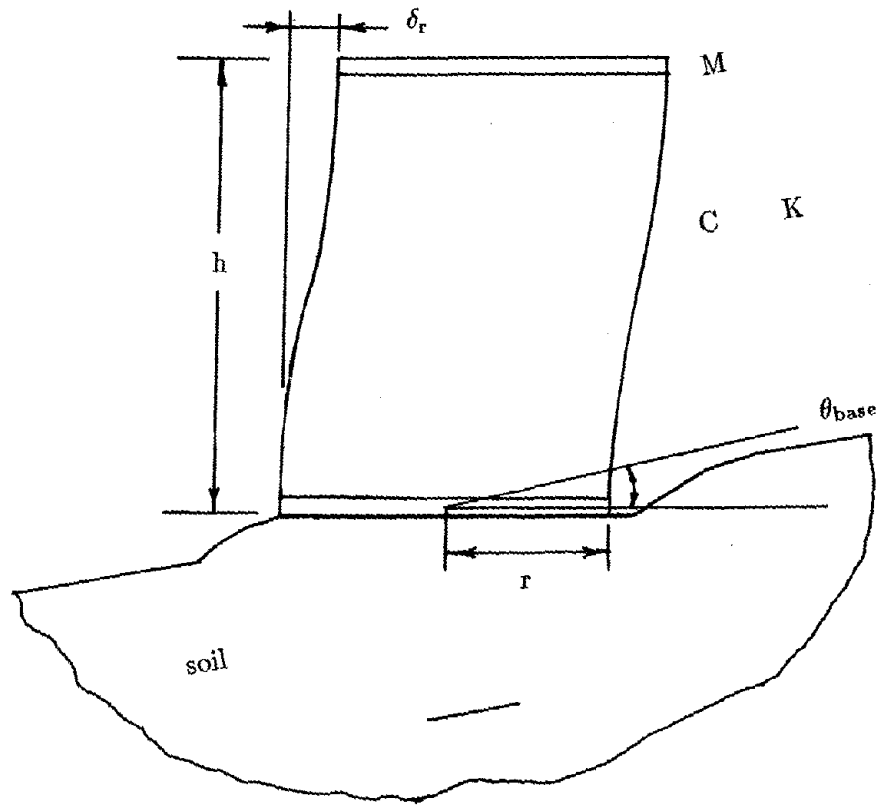


Fig. 6.1 Effect of Soil Flexibility on Building Response

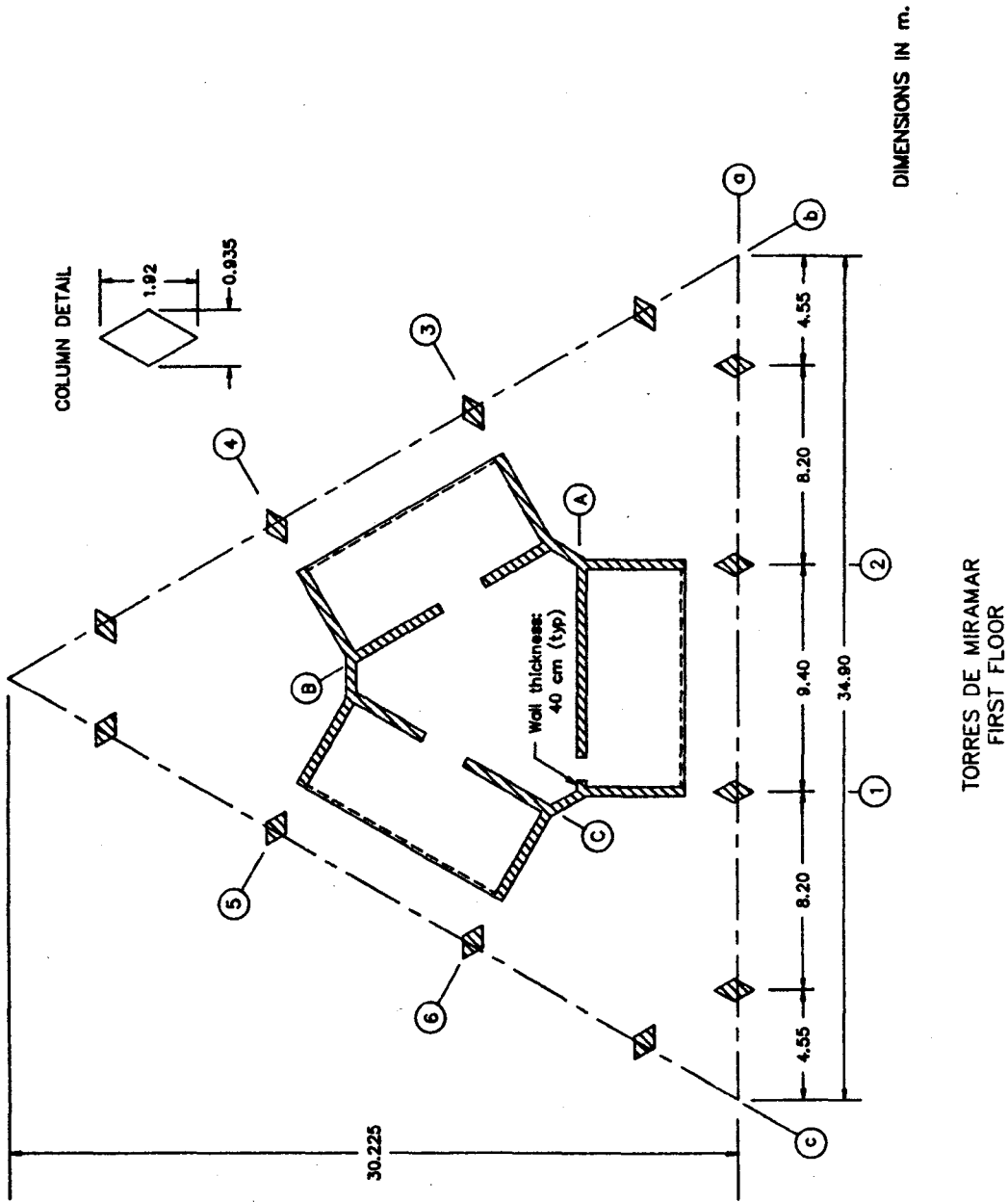


Fig. 6.2.a Floor Plan of Torres de Miramar - Level 1

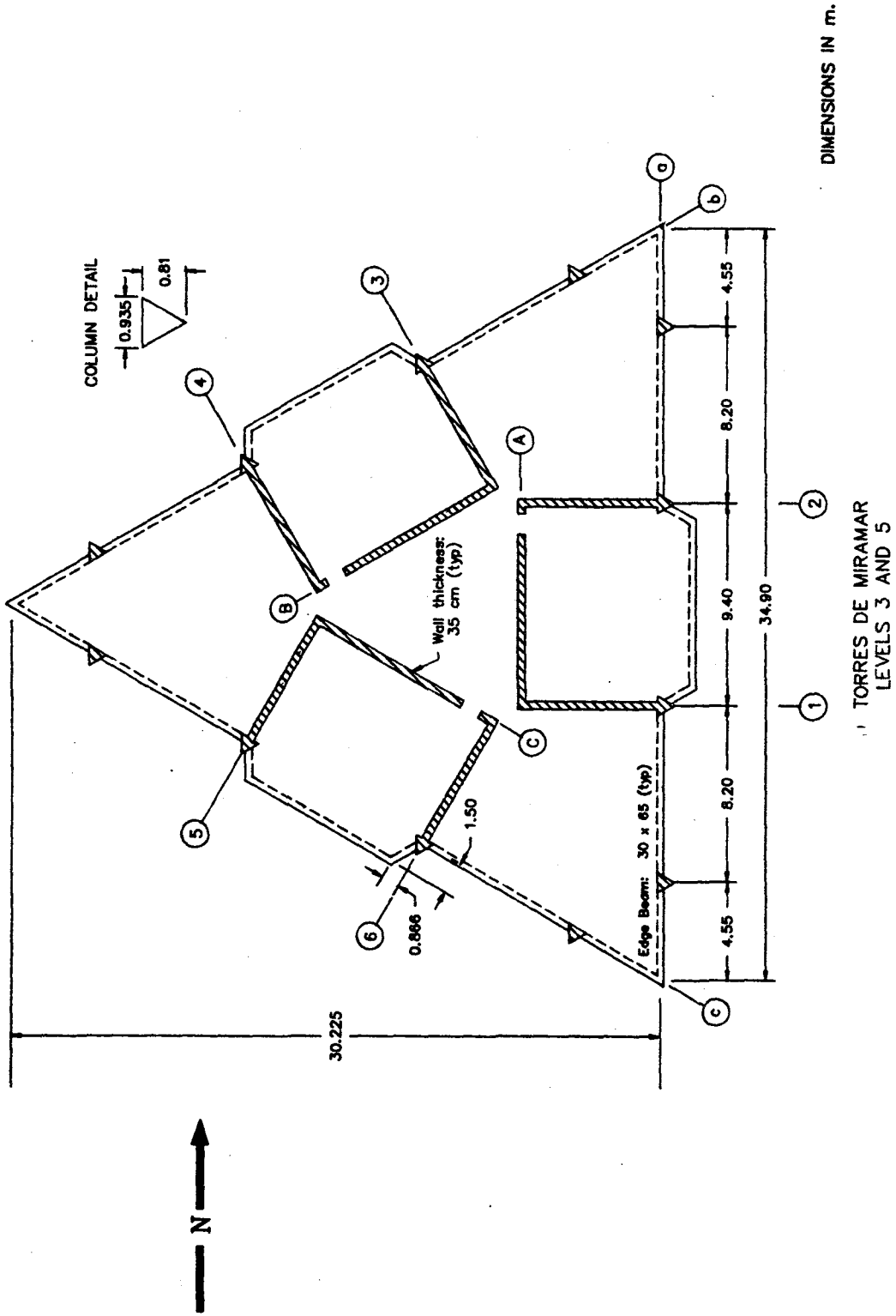


Fig. 6.2.b Floor Plan of Torres de Miramar – Levels 3 and 5

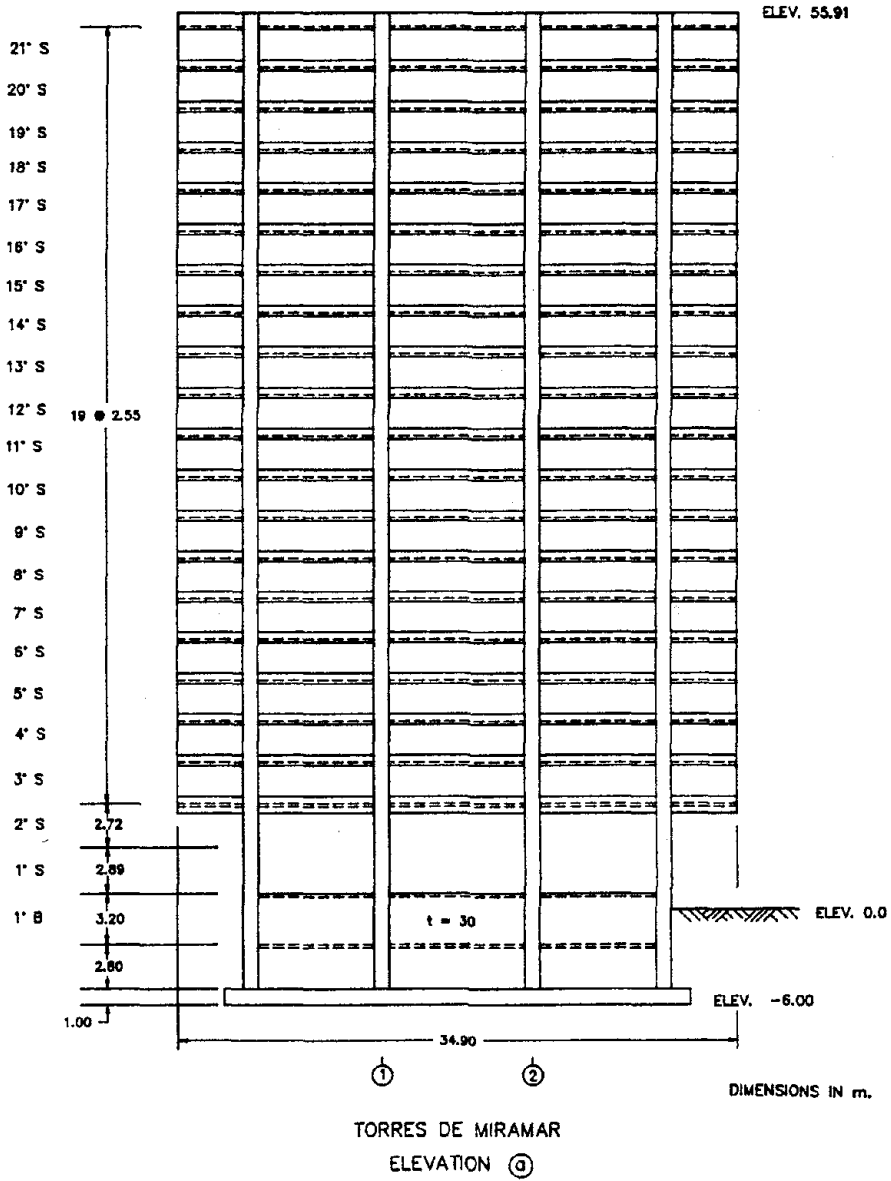


Fig. 6.2.c Elevation of Torres de Miramar – Axis a

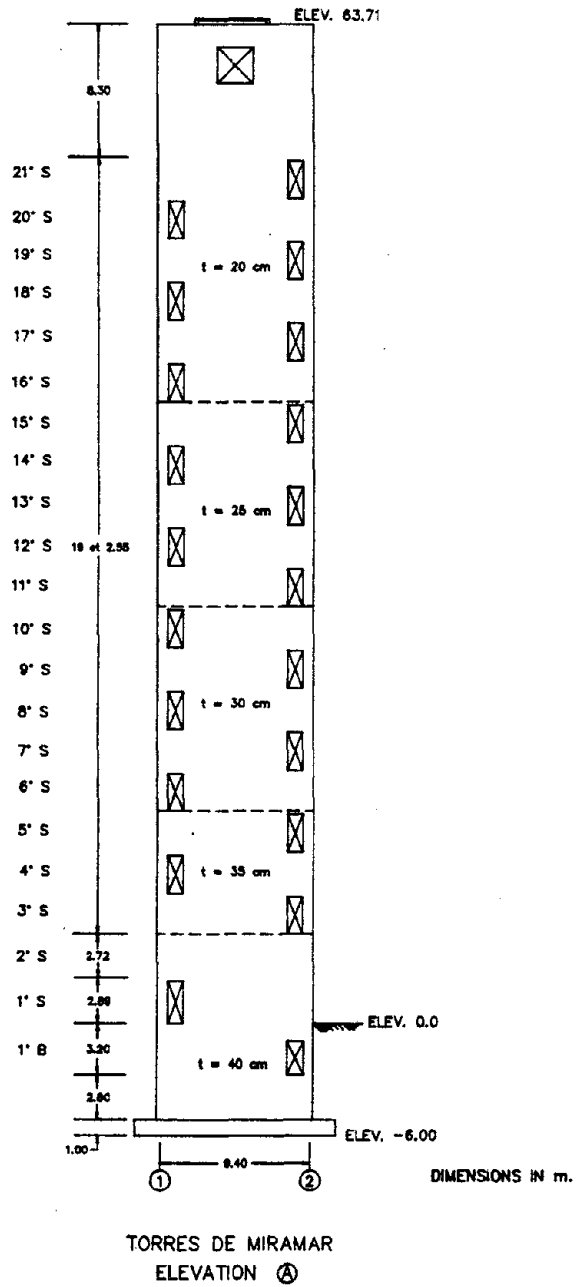
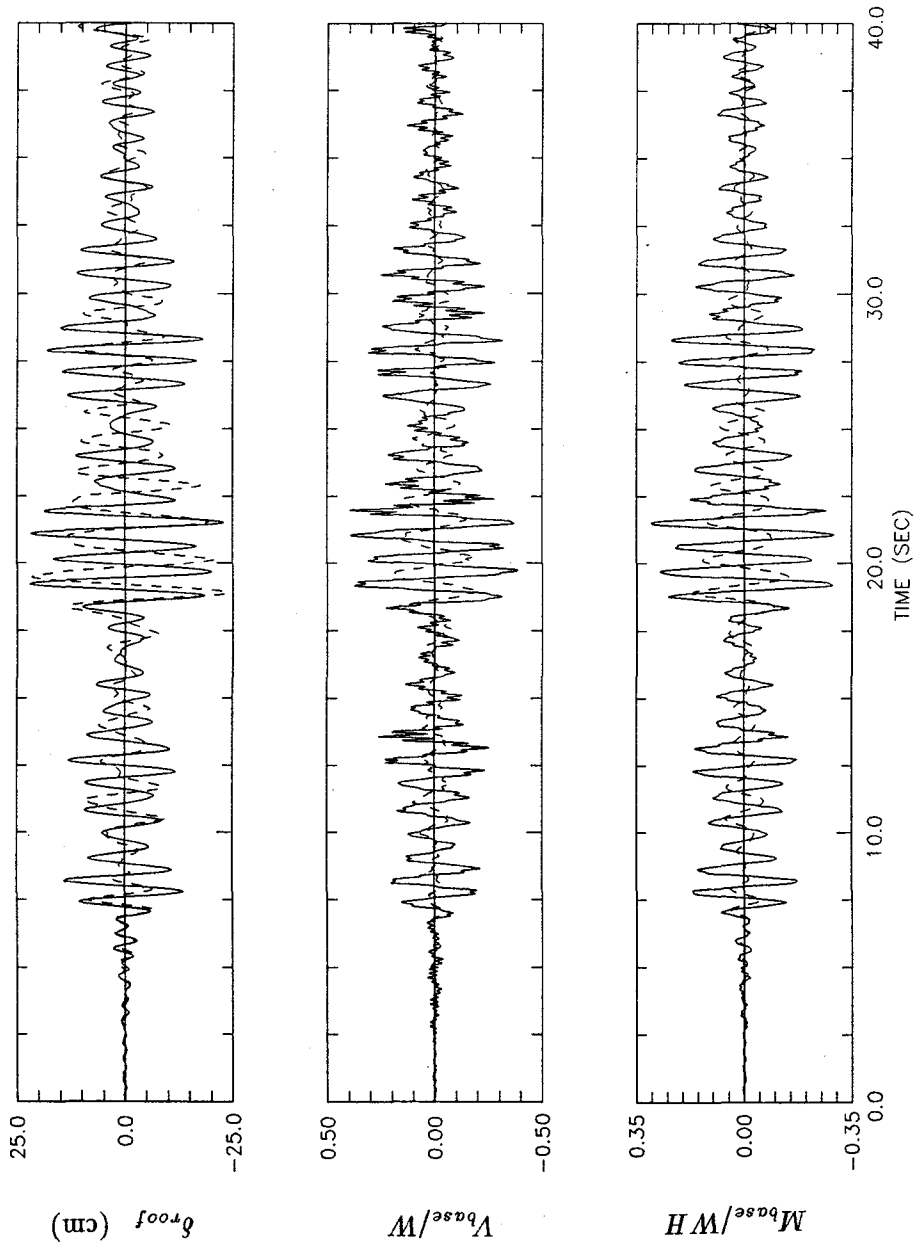
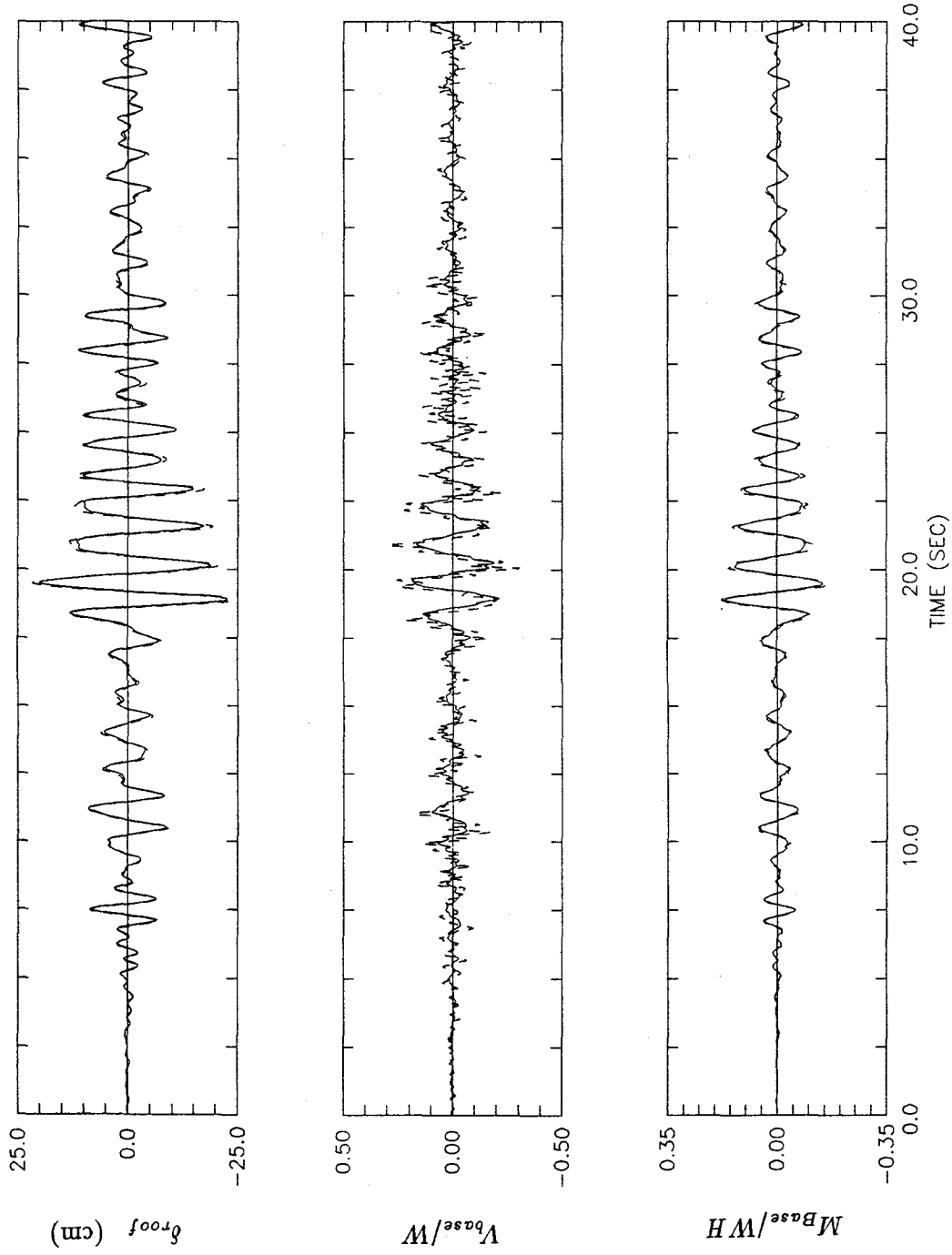


Fig. 6.2.d Elevation of Torres de Miramar – Axis A



**Fig. 6.3** Torres de Miramar - Response History Characteristics  
 — Fixed Base    - - - Flexible Base



**Fig. 6.4 Torres de Miramar - Response History Characteristics**  
 — Non-Proportional Damping (Building and Soil)  
 - - - Proportional Damping (Building Only)

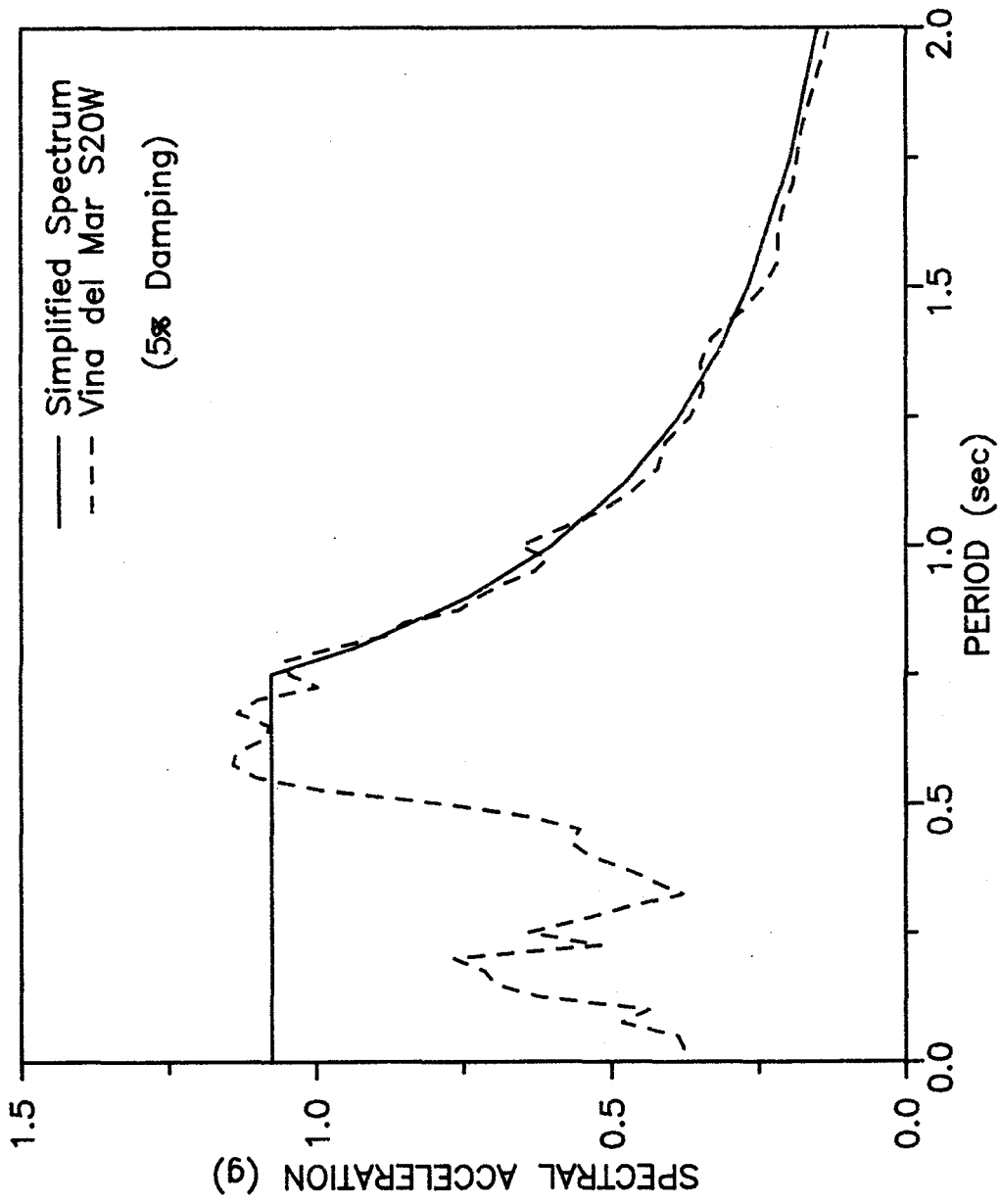


Fig. 6.5 Response Spectra - Viña del Mar S20W

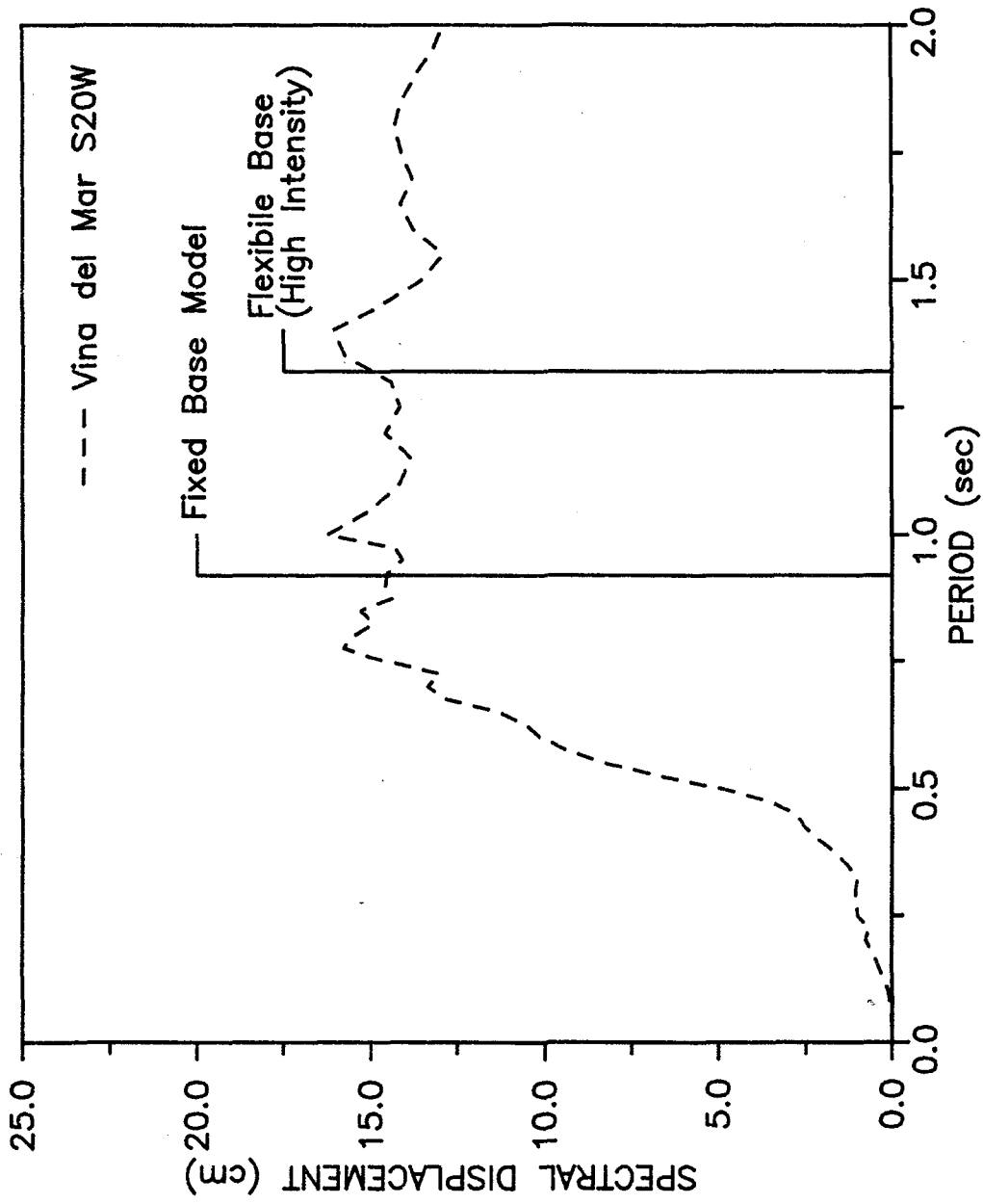


Fig. 6.6 Effect of Base Flexibility on Displacement

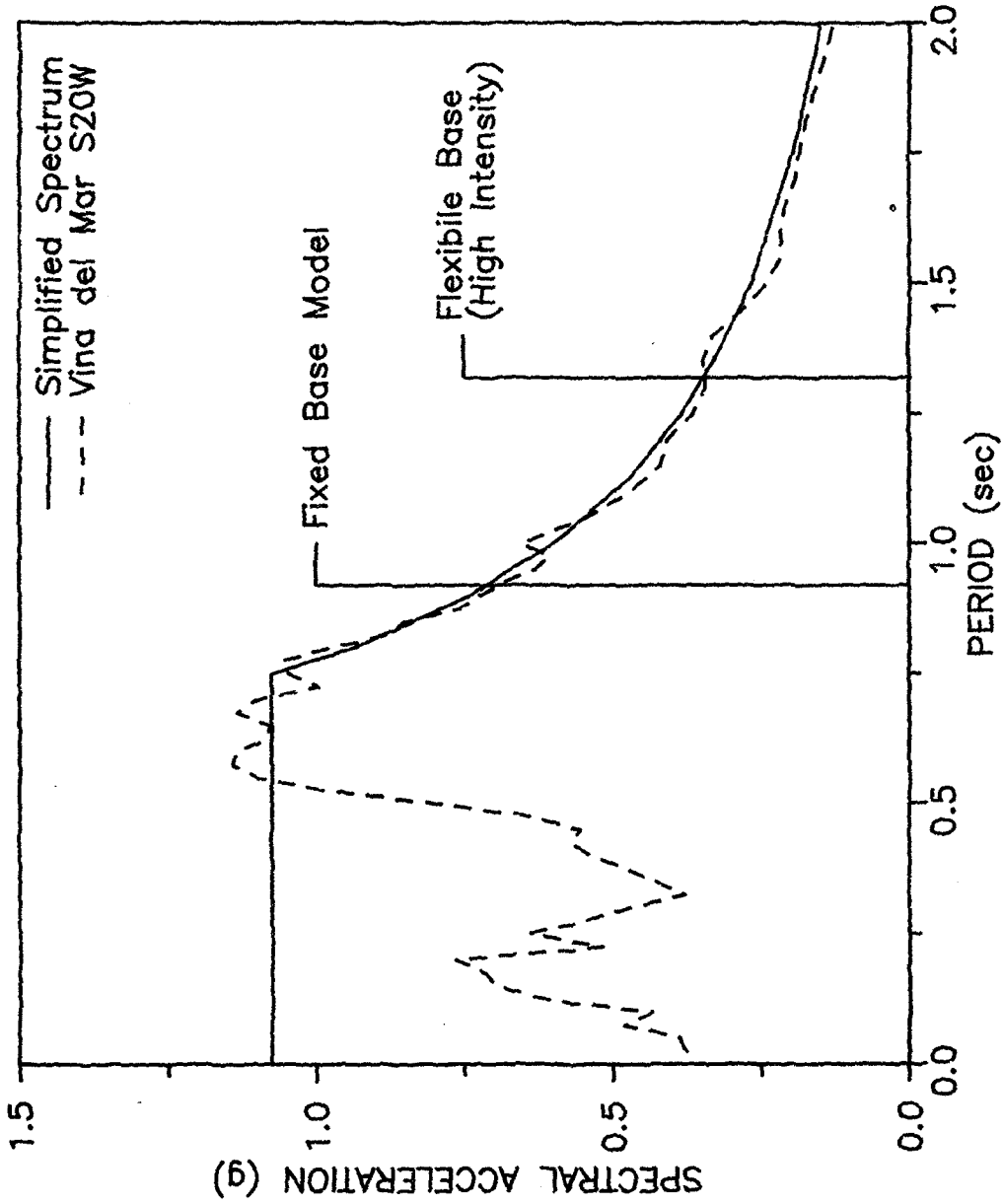


Fig. 6.7 Effect of Base Flexibility on Base Shear

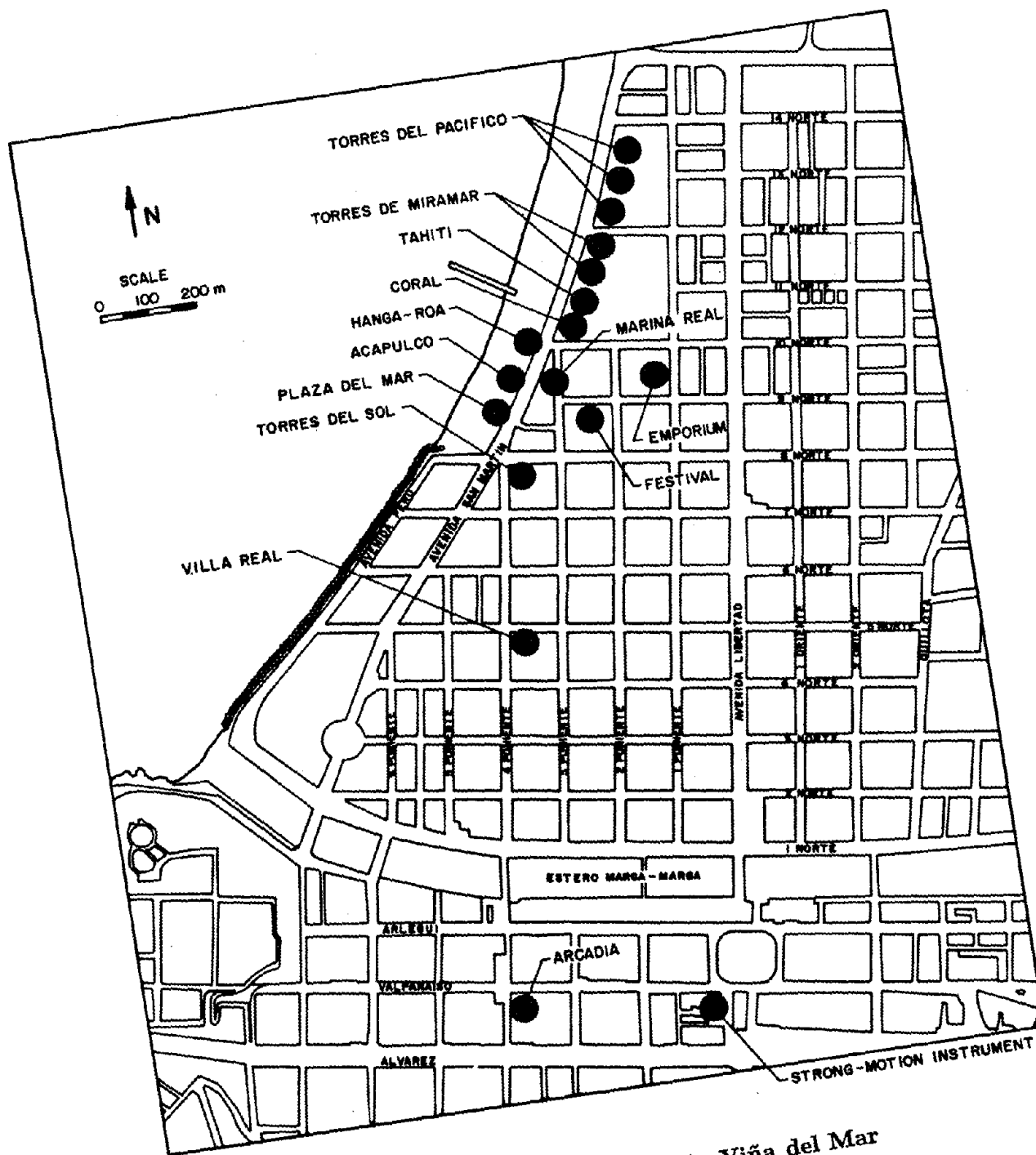
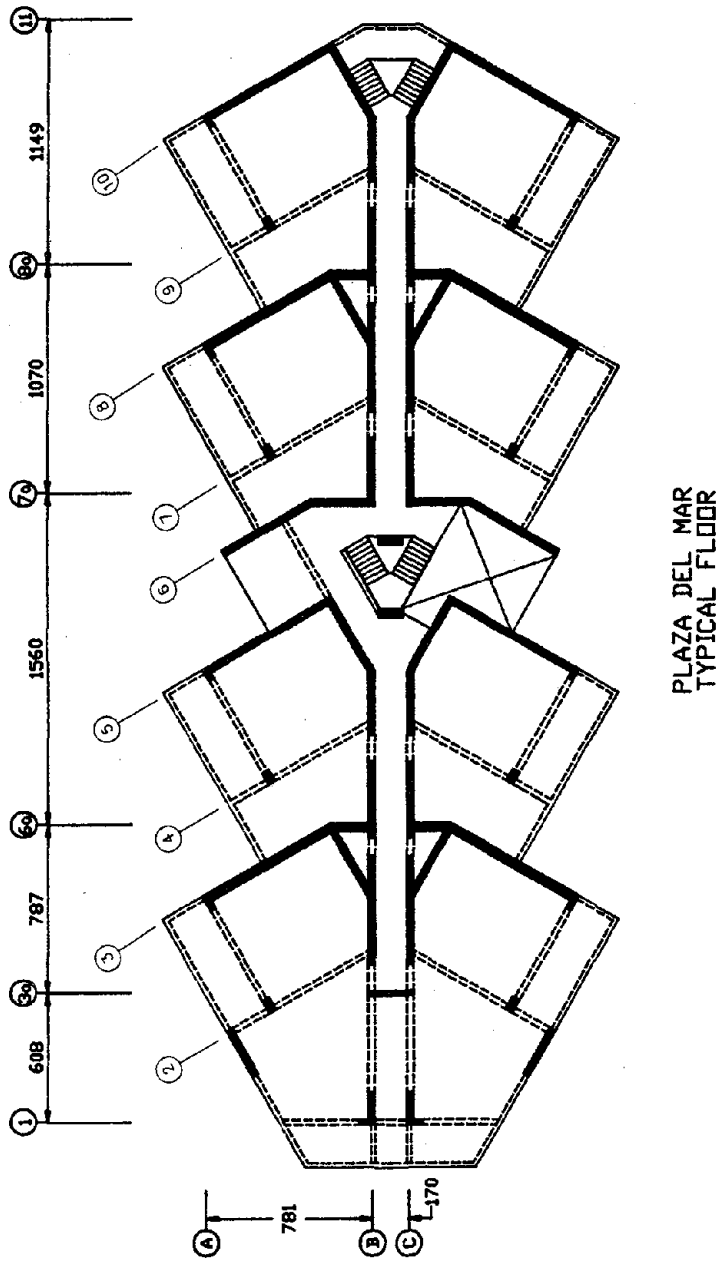


Fig. 7.1 Locations of Buildings in Viña del Mar



PLAZA DEL MAR  
TYPICAL FLOOR

Fig. 7.2.a Floor Plan of Plaza del Mar Building

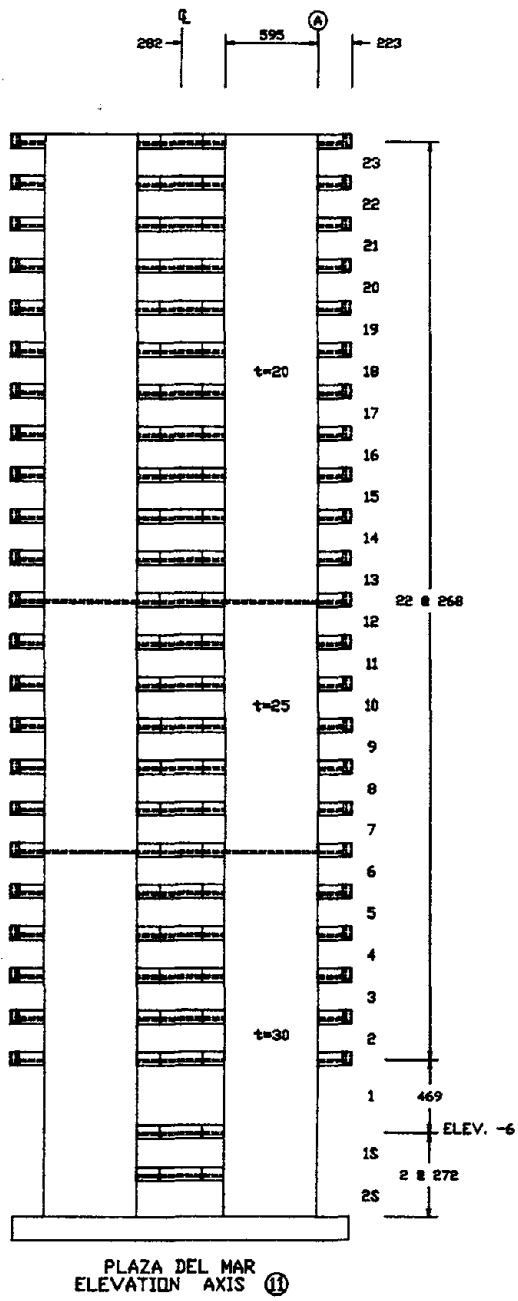


Fig. 7.2.b Elevation of Plaza del Mar Building

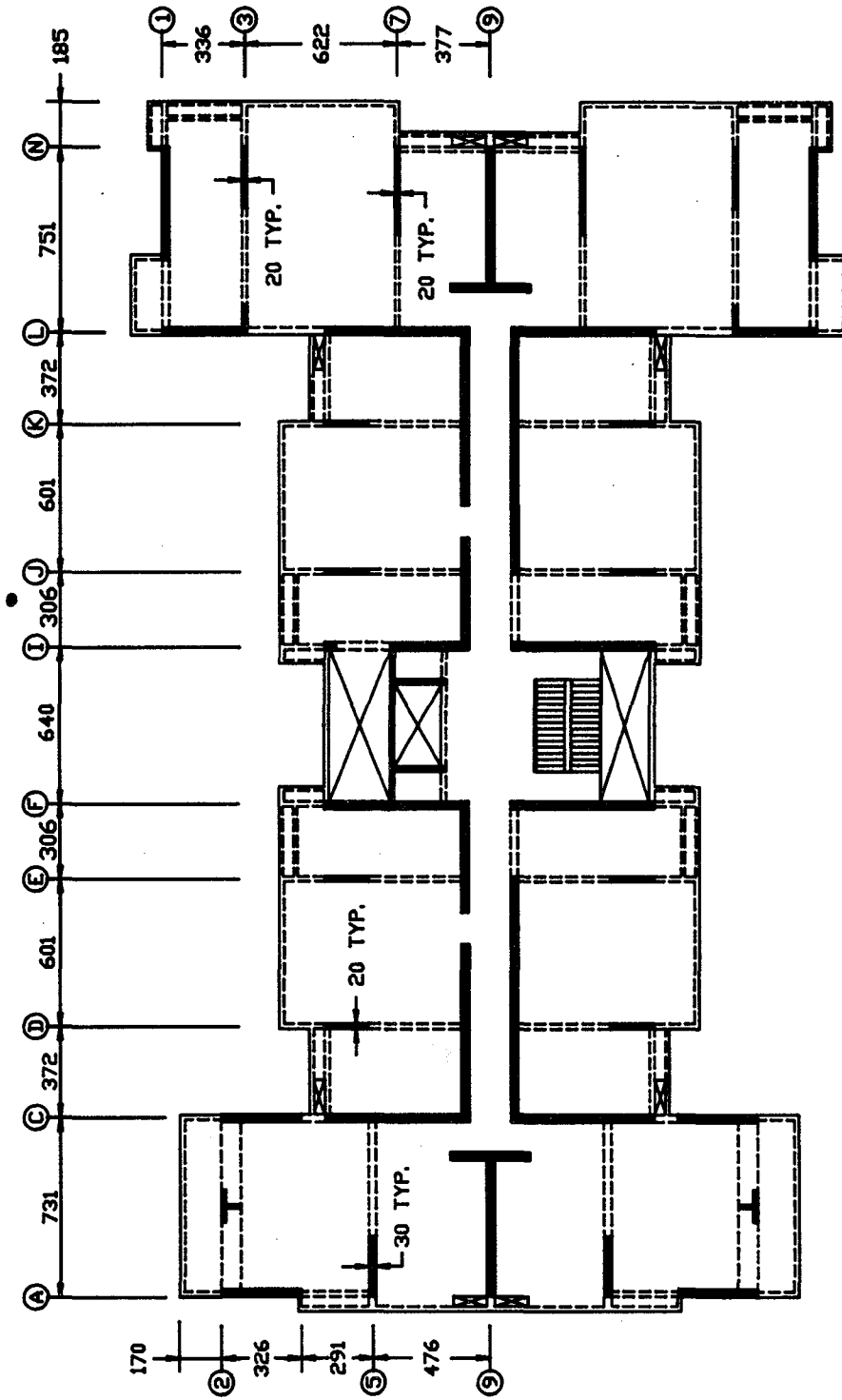


Fig. 7.3.a First Floor Plan of Festival Building

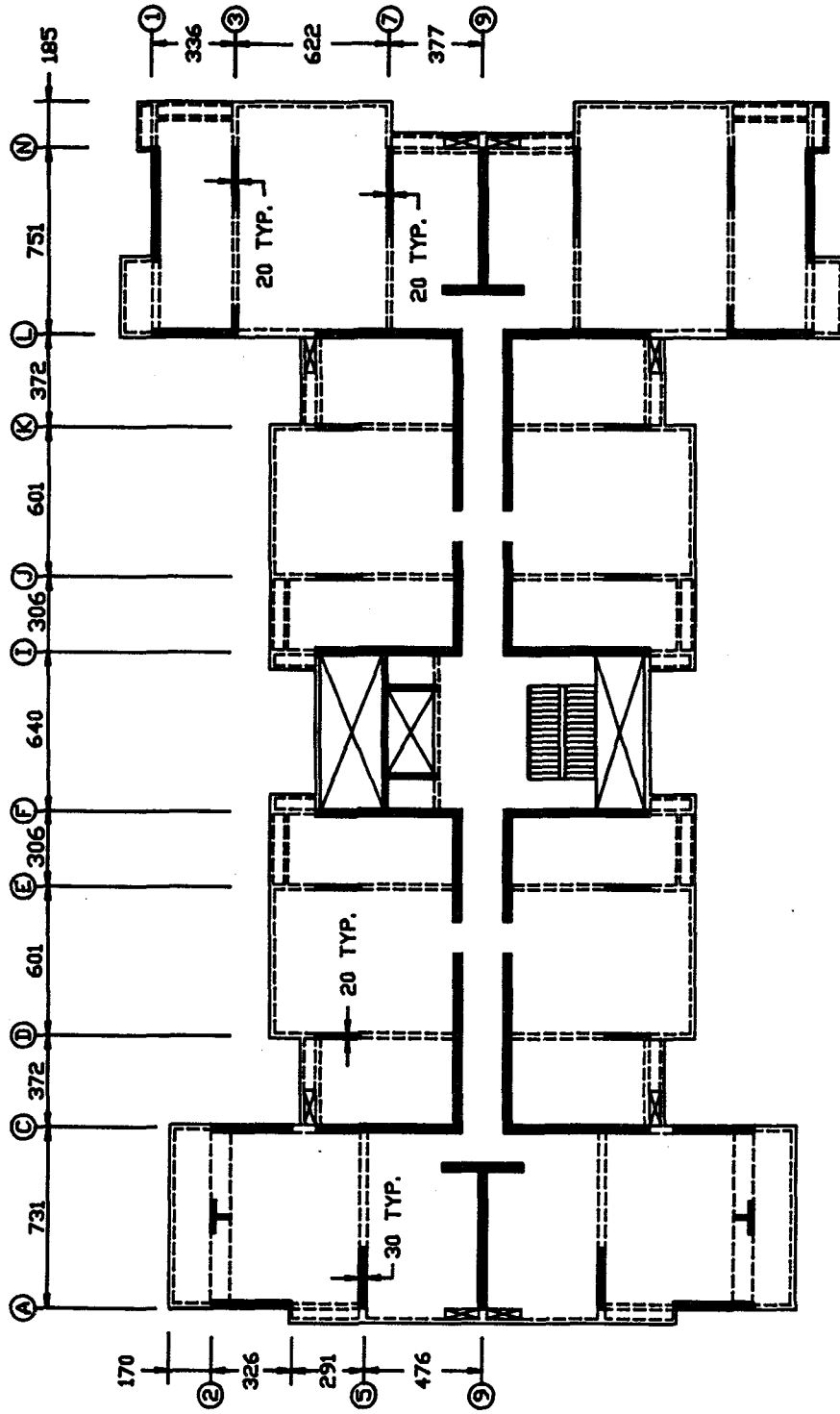


Fig. 7.3.b Typical Floor Plan of Festival Building

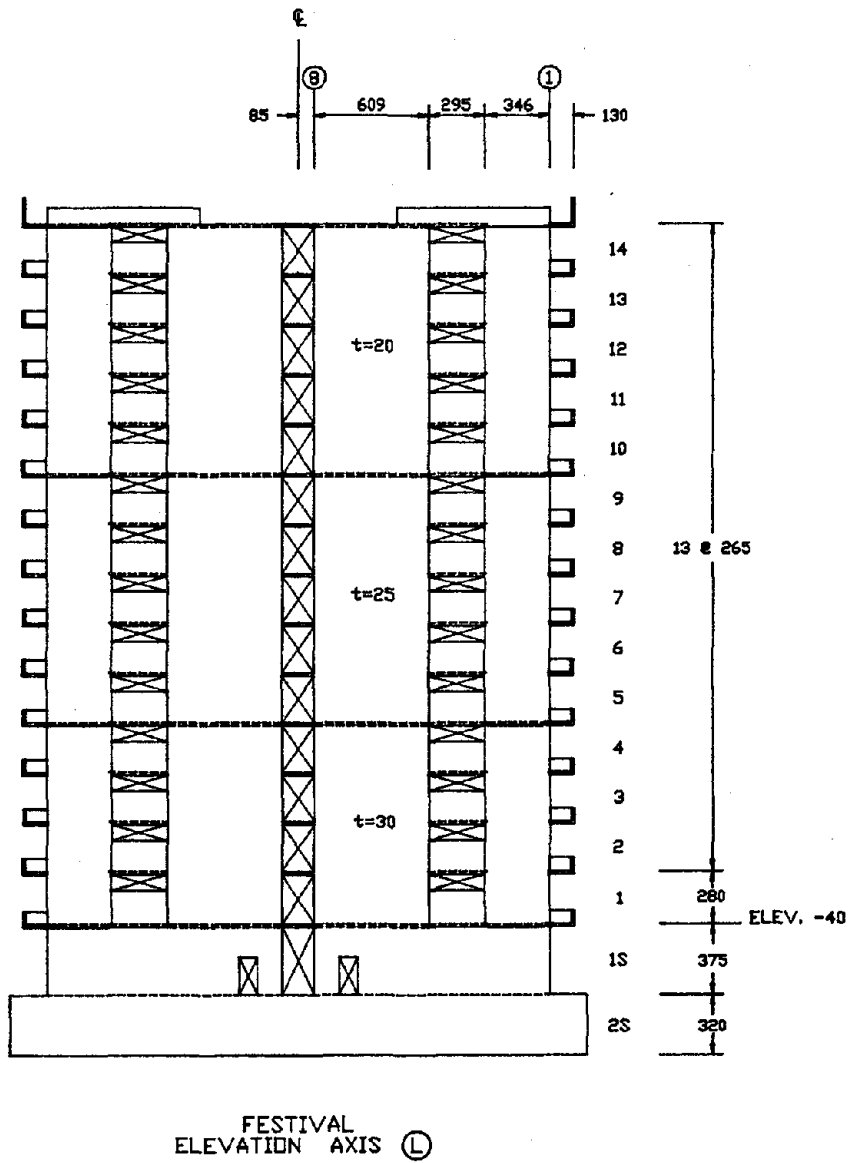


Fig. 7.3.c Elevation of Festival Building

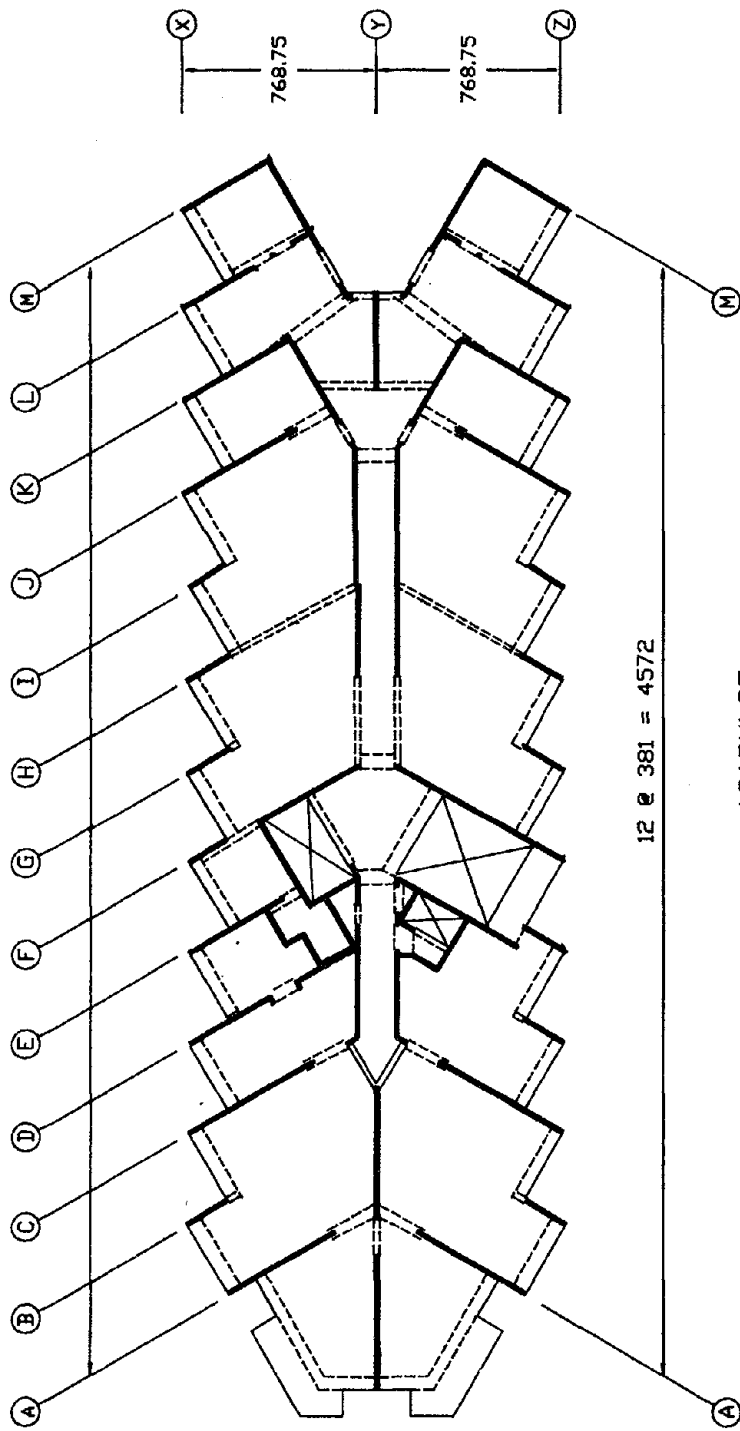


Fig. 7.4.a Typical Floor Plan of Acapulco Building

ACAPULCO  
FLOORS 3 - 15

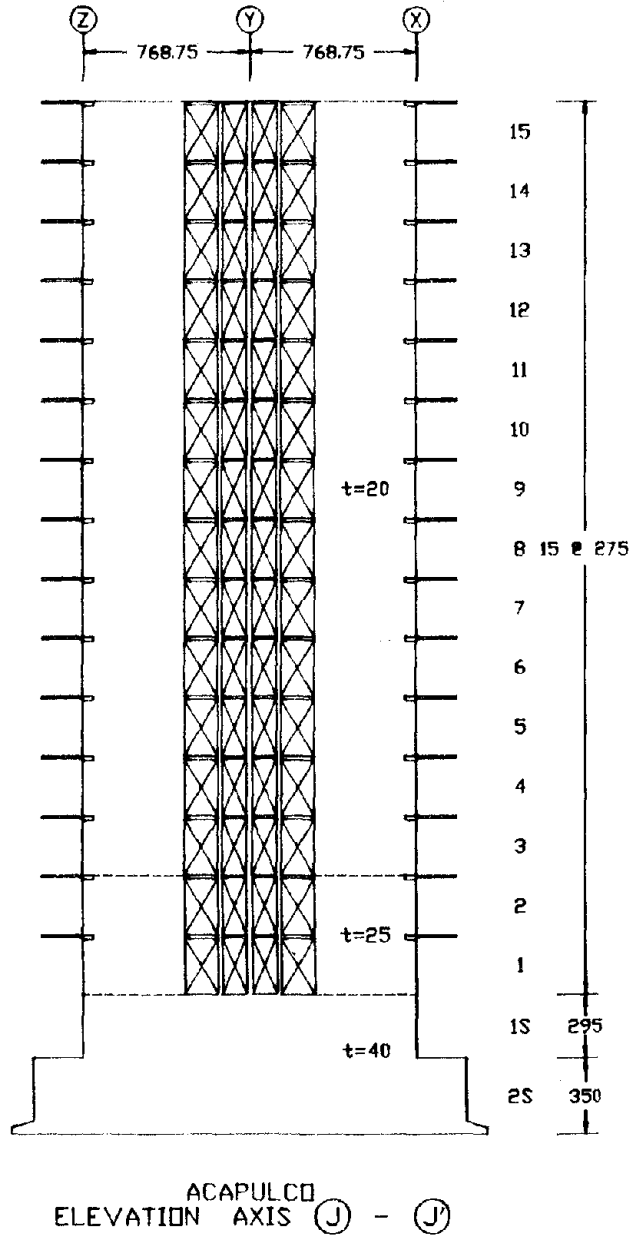


Fig. 7.4.b Elevation of Acapulco Building

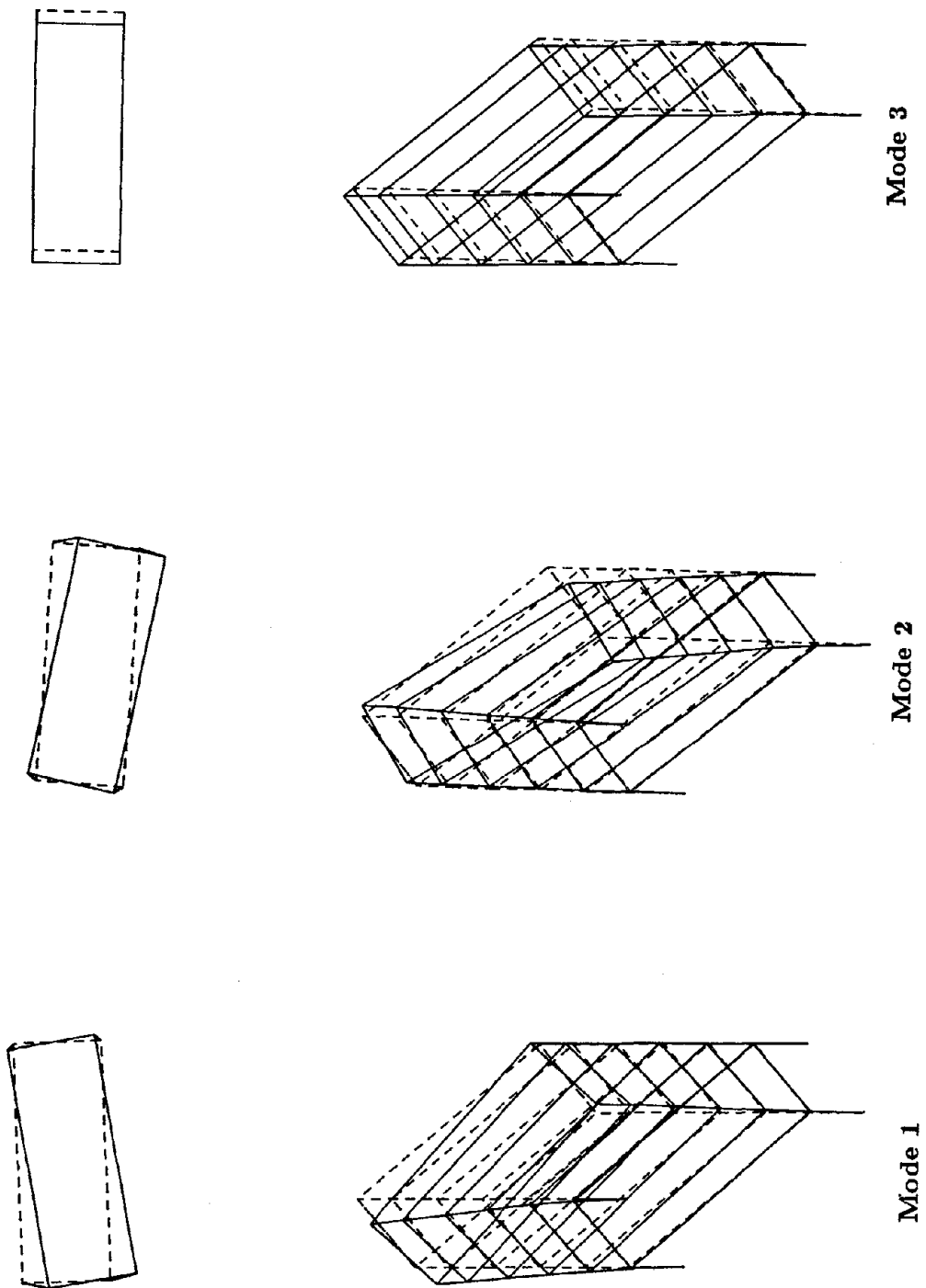
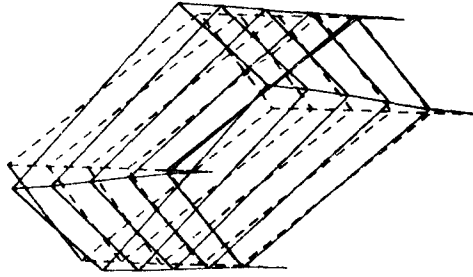
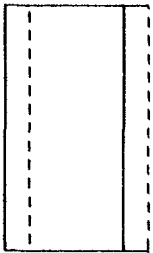
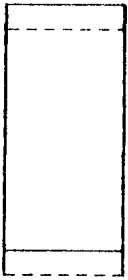
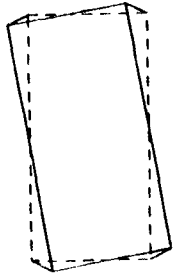
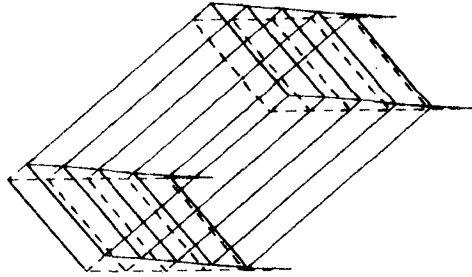


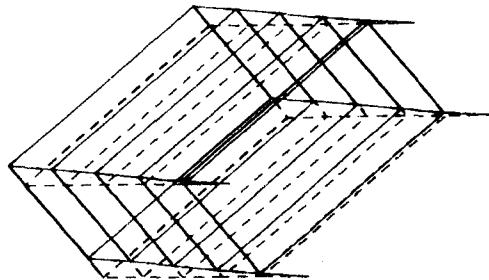
Fig. 7.5 Mode Shapes — Plaza del Mar Building



Mode 3



Mode 2



Mode 1

Fig. 7.6 Mode Shapes — Festival Building

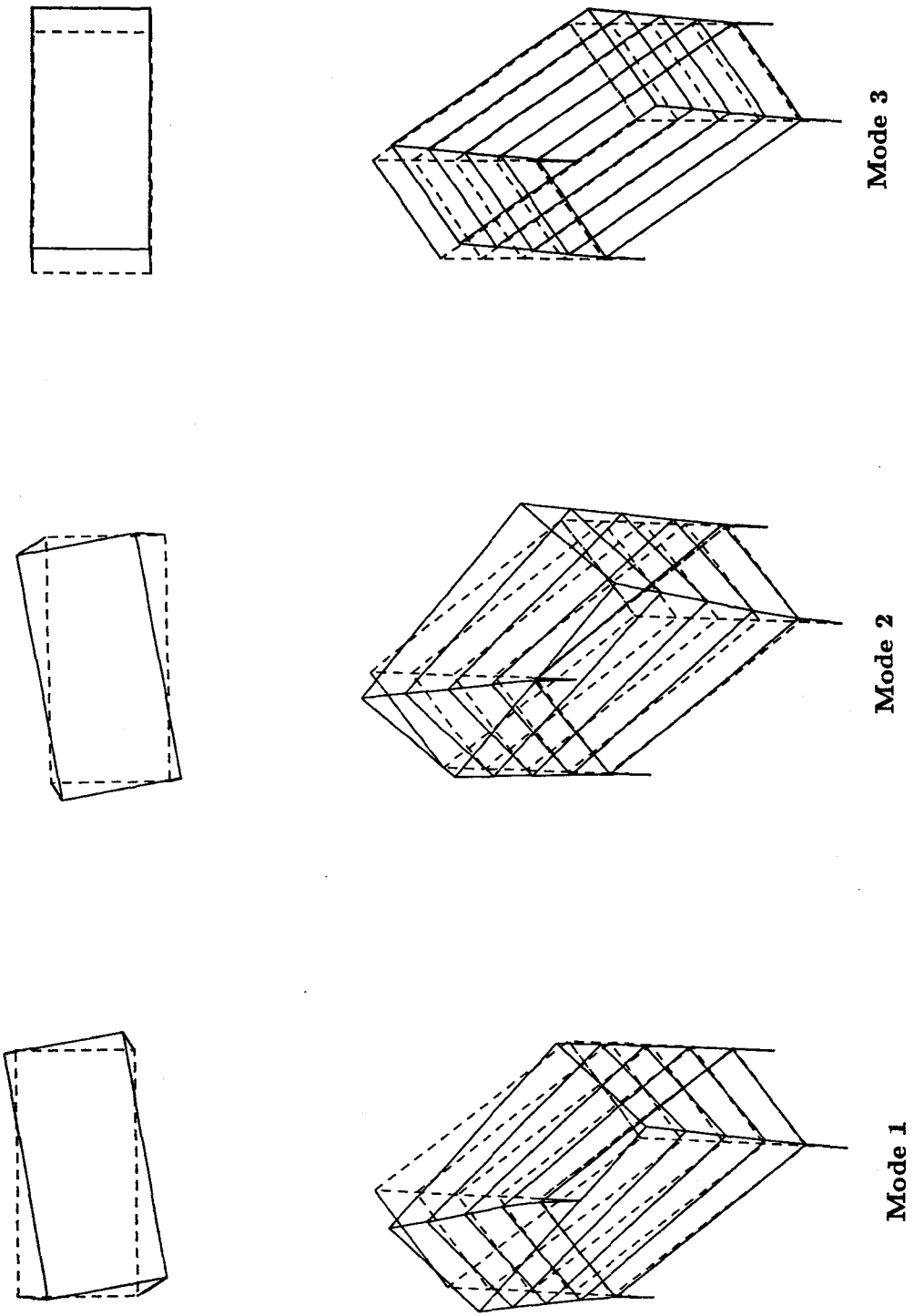


Fig. 7.7 Mode Shapes — Acapulco Building

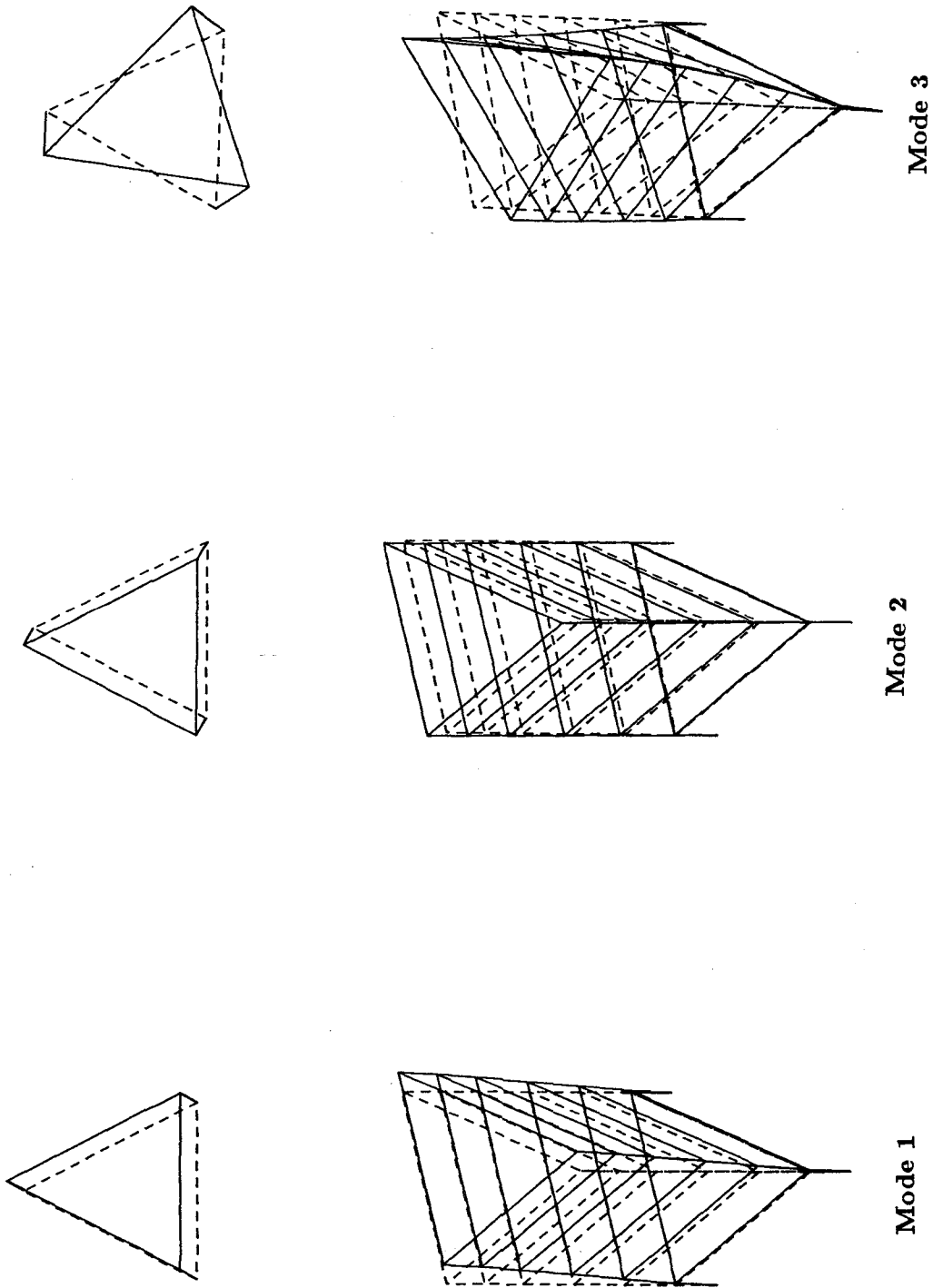


Fig. 7.8 Mode Shapes — Torres de Miramar Building

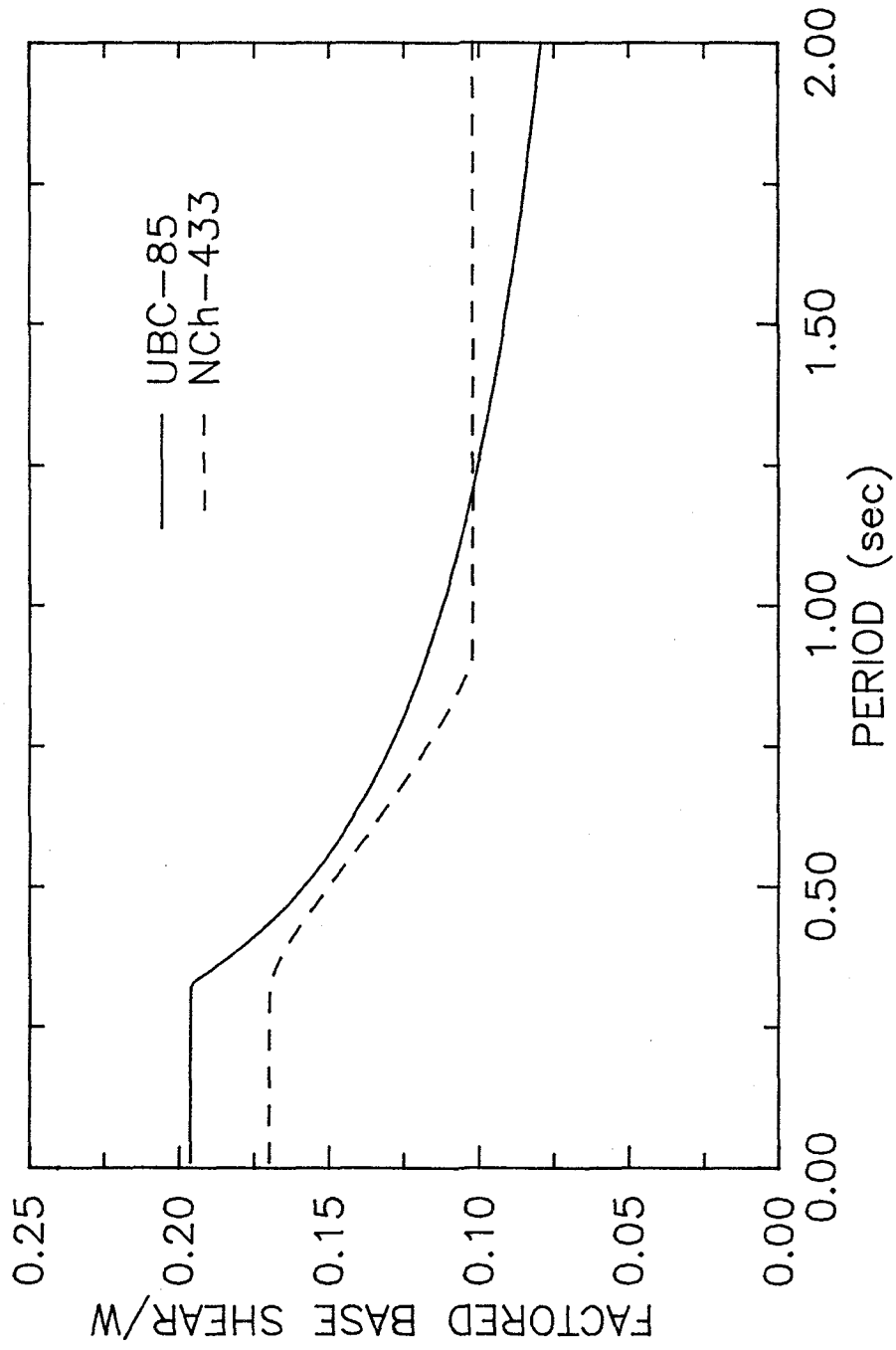


Fig. 7.9 Factored Code Spectra

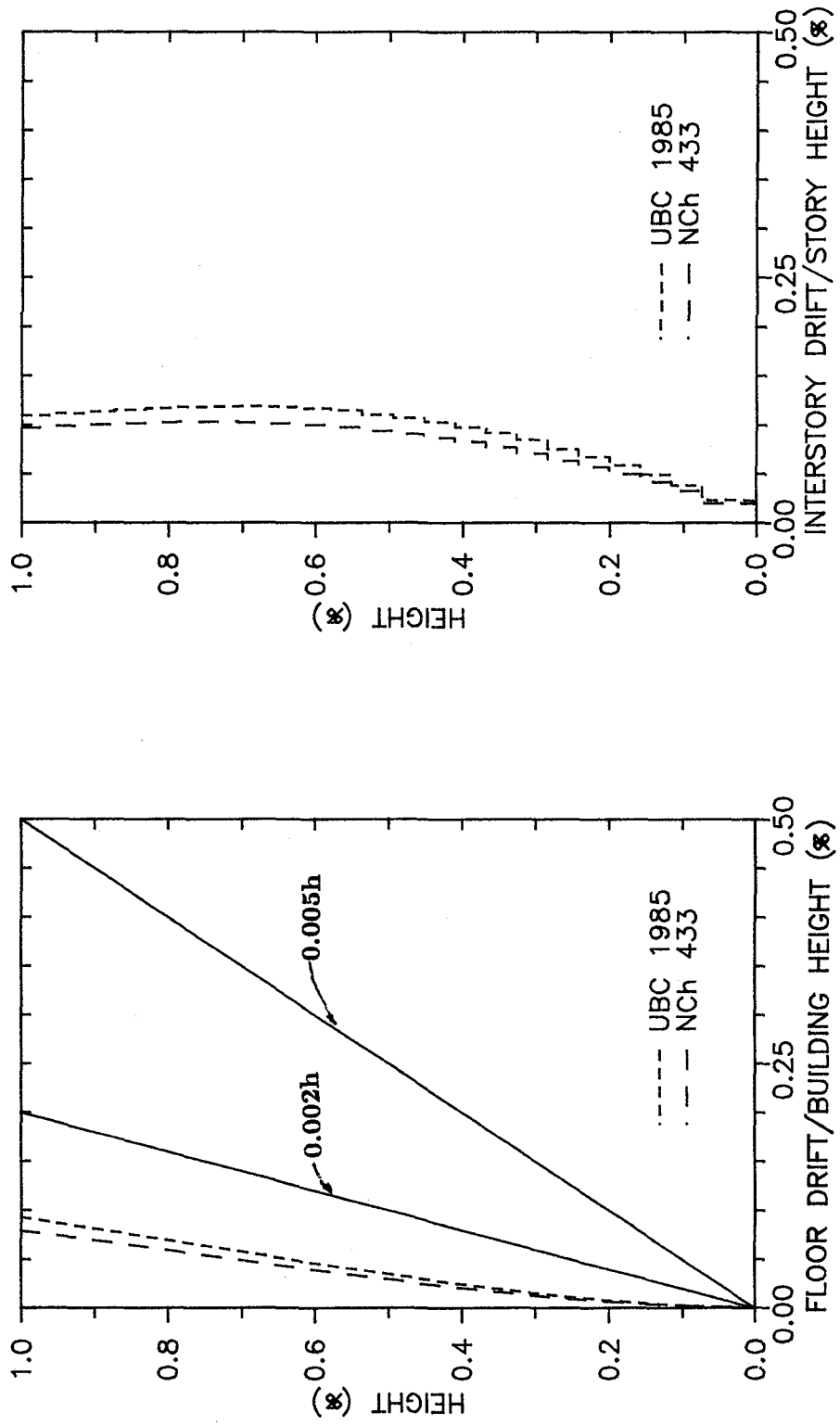


Fig. 7.10 Drift Ratios for Code Loads — Plaza del Mar Building

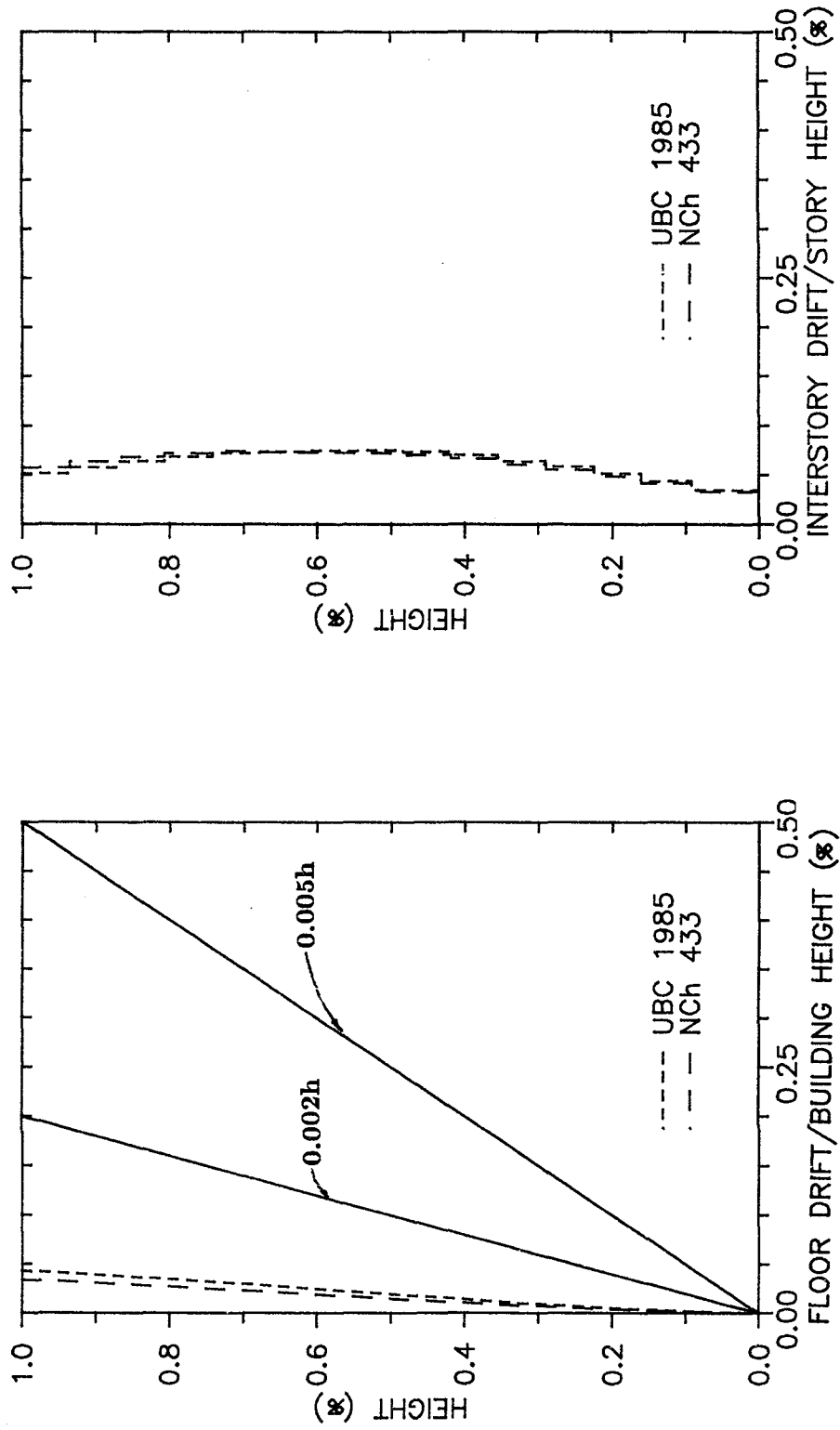


Fig. 7.11 Drift Ratios for Code Loads — Festival Building

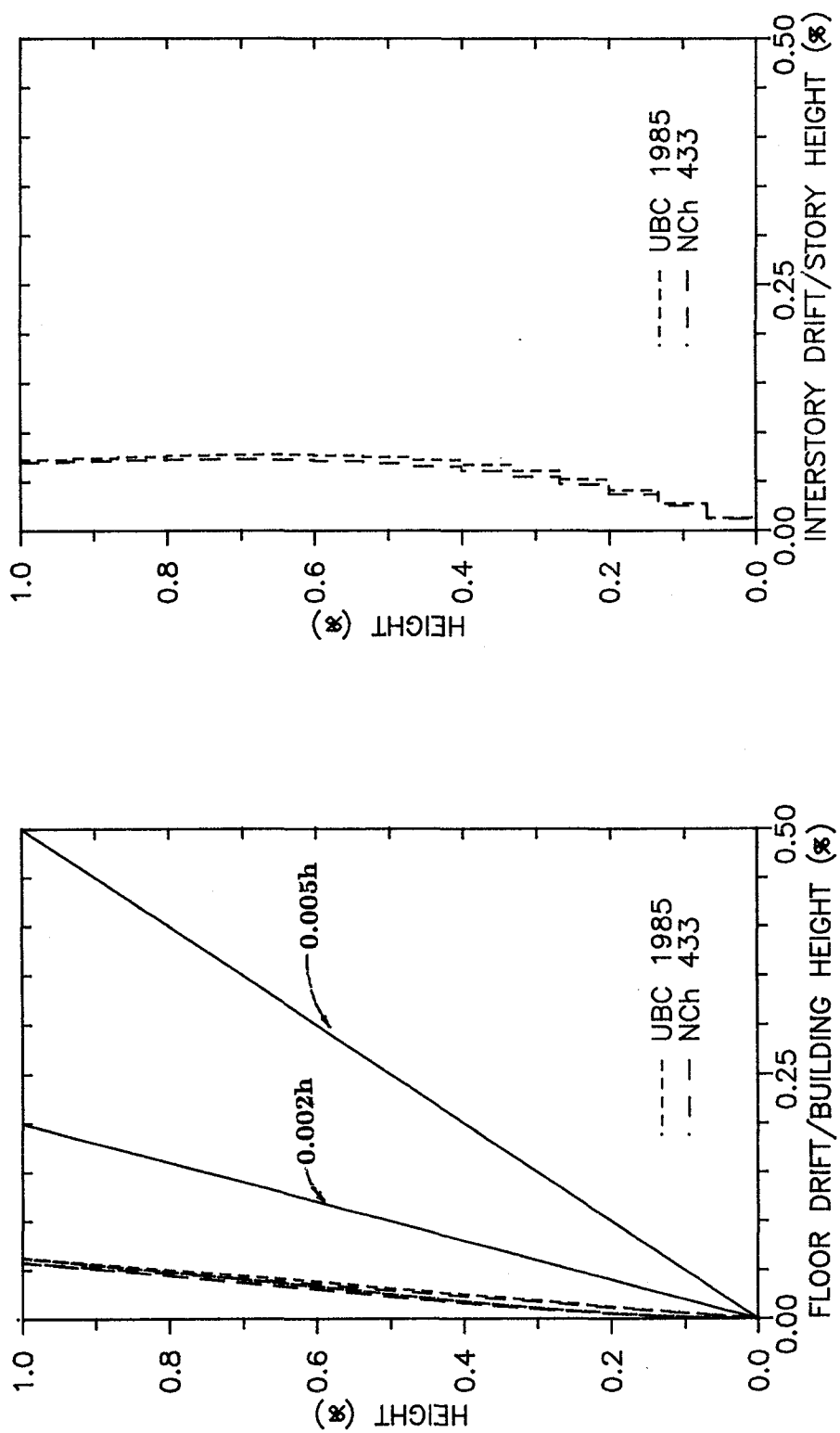


Fig. 7.12 Drift Ratios for Code Loads — Acapulco Building

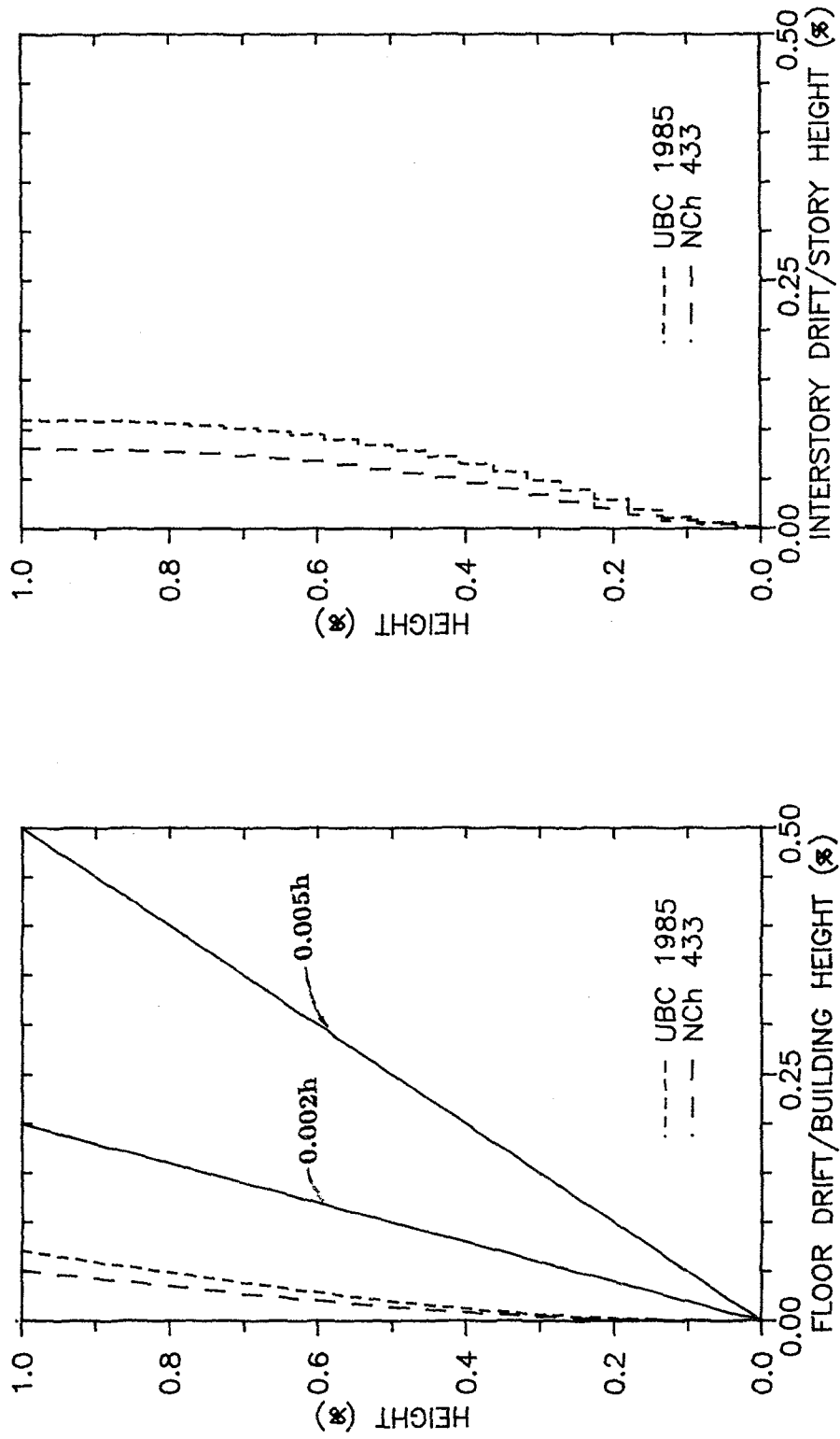
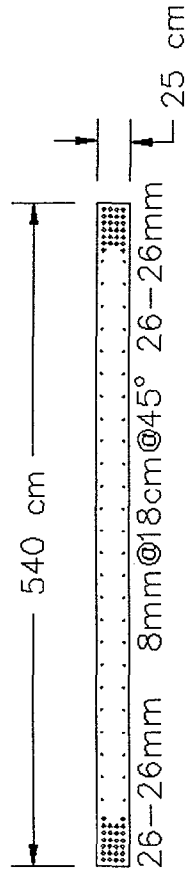
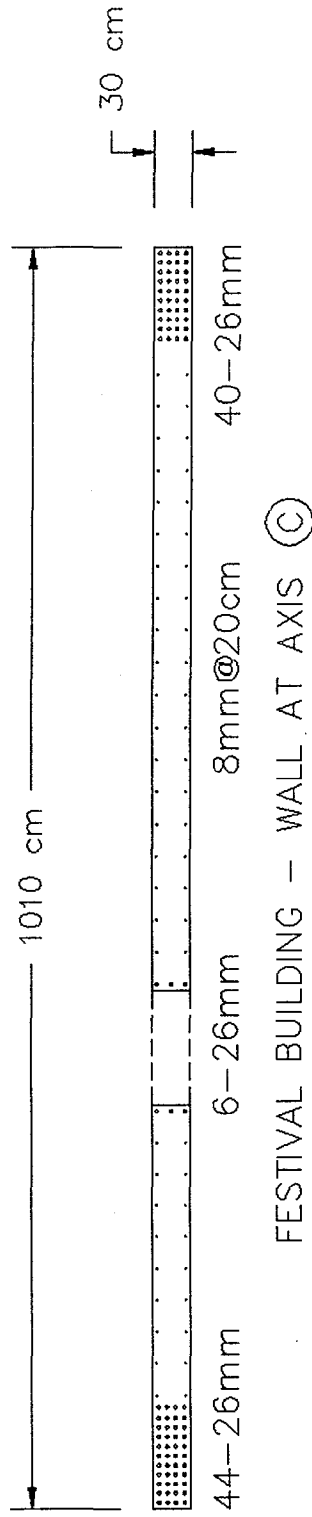


Fig. 7.13 Drift Ratios for Code Loads — Torres de Miramar Building

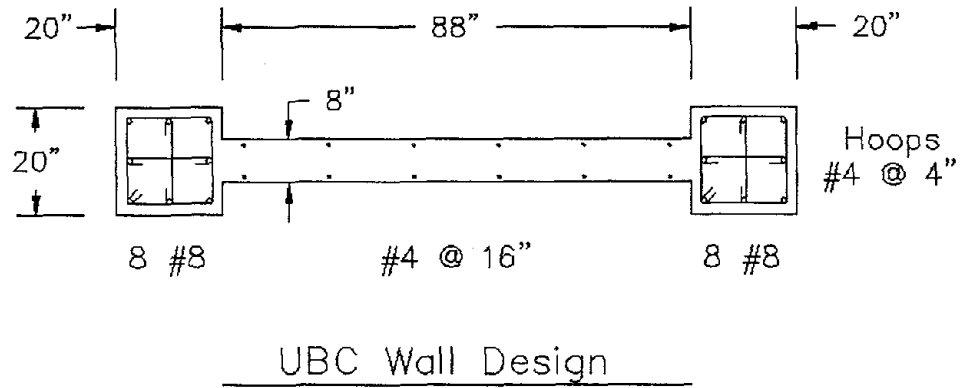


ACAPULCO BUILDING - WALL AT AXIS (A)



FESTIVAL BUILDING - WALL AT AXIS (C)

Fig. 7.14 Structural Walls Constructed in Chile



$M_u = 30000^{\text{in-kips}}$ $V_u = 150^{\text{kips}}$ $P_u = 1000^{\text{kips}}$
---

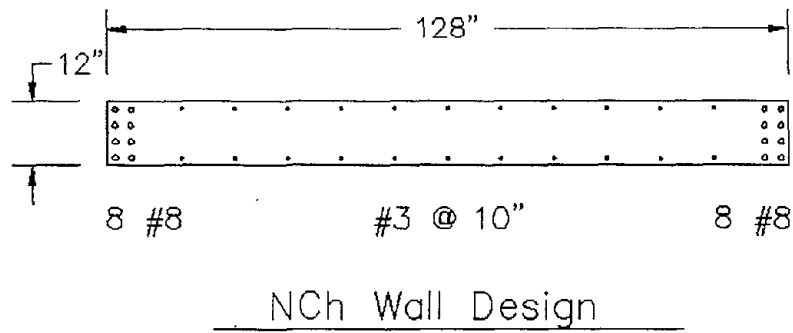


Fig. 7.15 Code Comparison of Design Requirements for Structural Walls

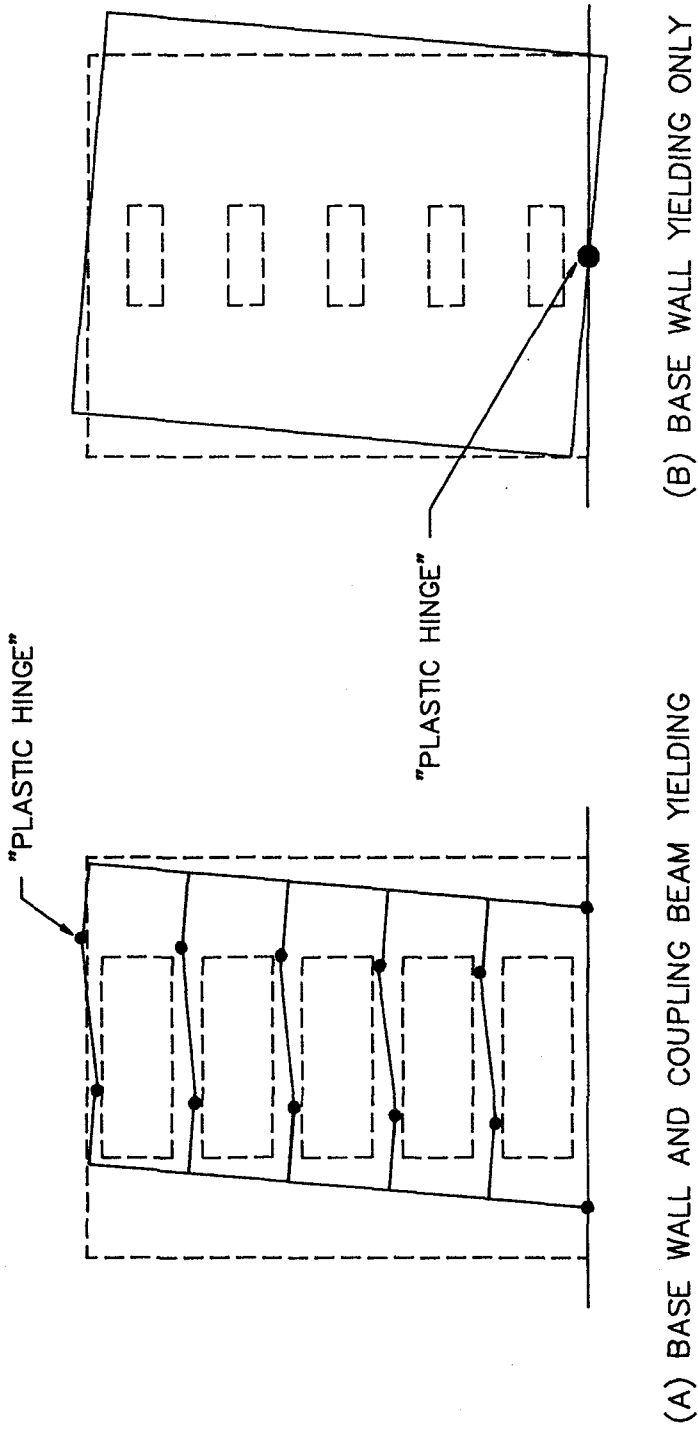


Fig. 7.16 Collapse Mechanisms



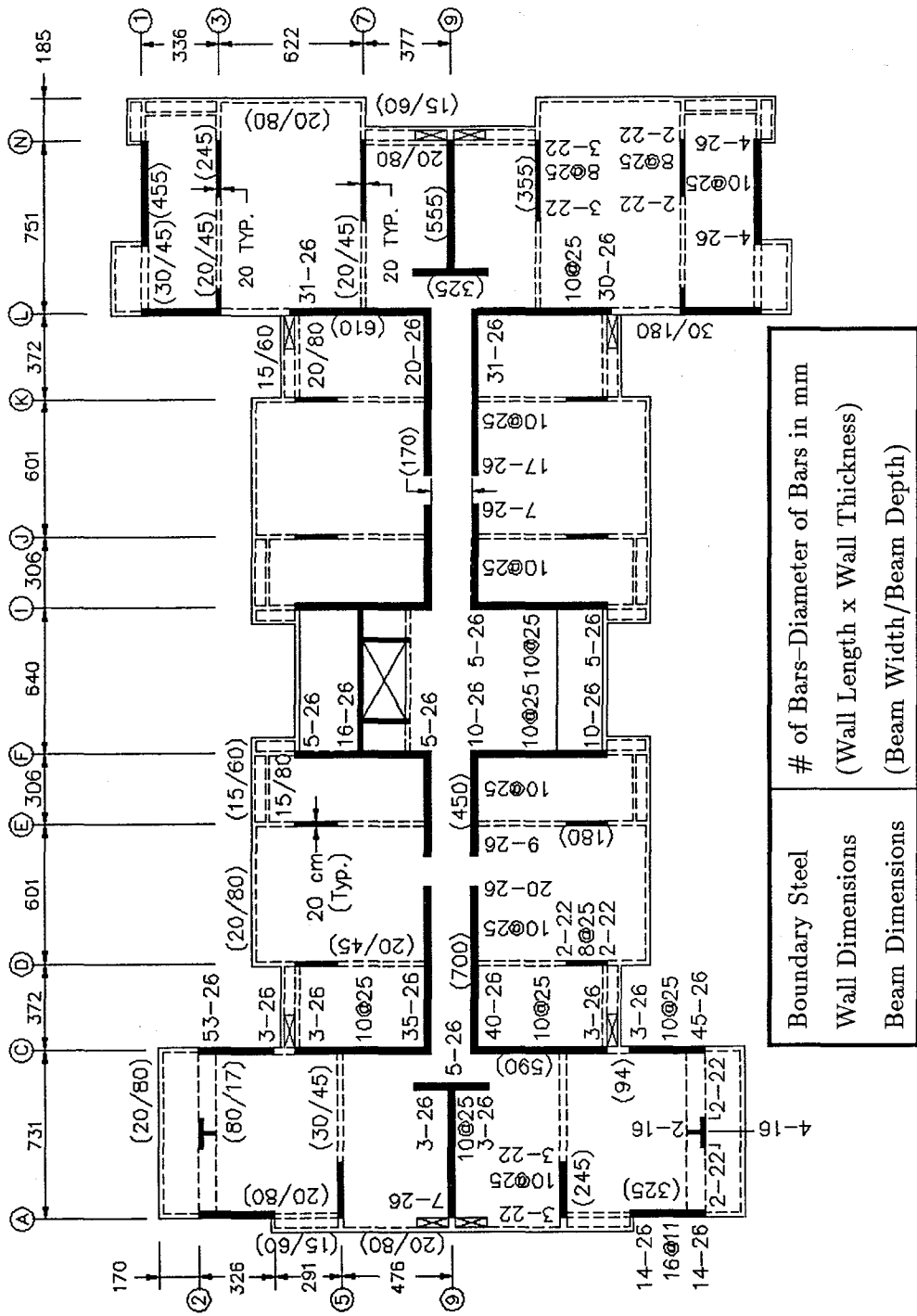


Fig. 7.18 Festival Building - Geometry and Steel Quantities

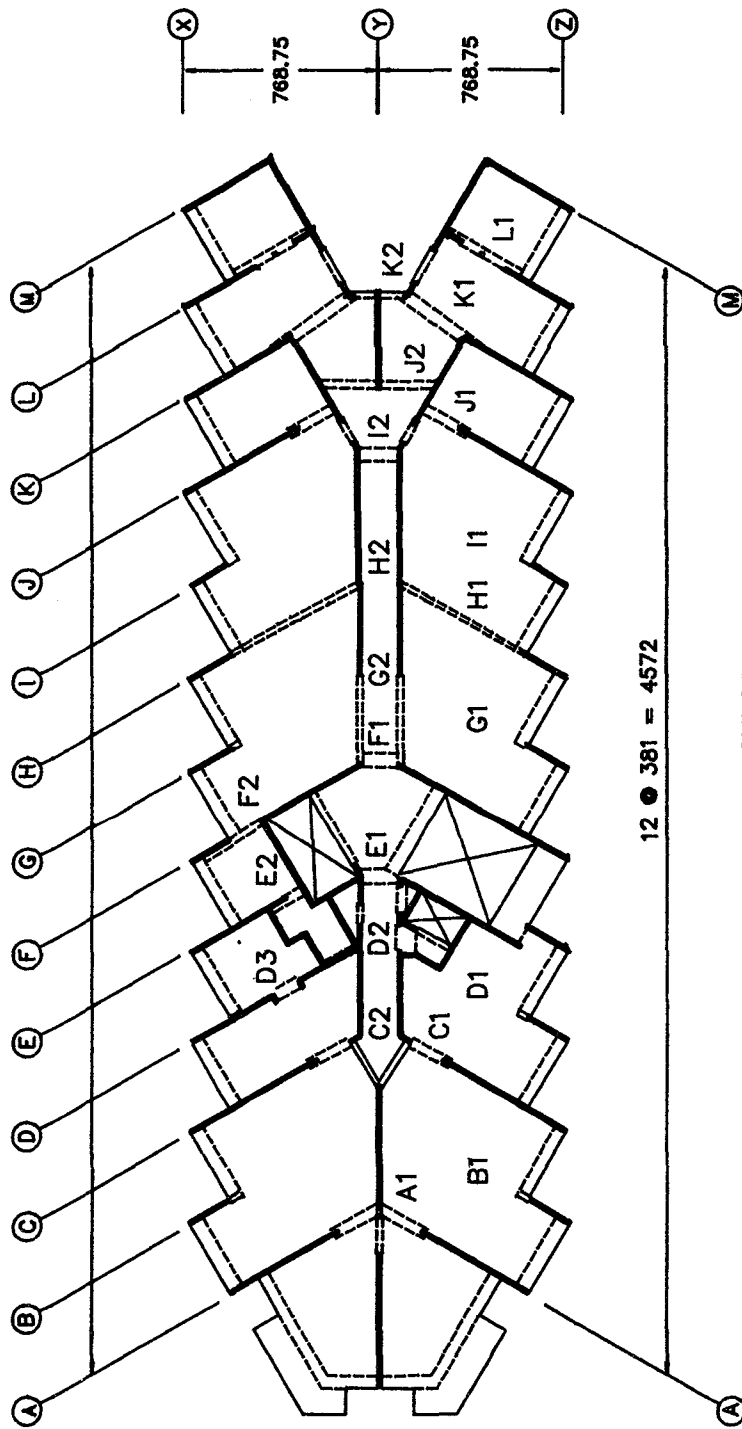


Fig. 7.19.a Acapulco Building – Beam Designations for Strength Calculations

TRANSVERSE BEAMS							
Axis	Beam	Story	Size (bxh)	Length (cm)	$\rho$	$\rho'$	$\rho_t$
A	A1	1-15	40/15	155	0.010	0.010	—
B	B1	1-15	200/12	640	0.006	0.006	—
C	C1	1-15	40/15	145	0.010	0.010	—
	C2	1-15	200/12	150	0.001	0.001	—
D	D1	1-15	200/12	365	0.006	0.006	—
	D2	1-15	380/12	150	0.001	0.001	—
	D3	1-8	50/55	90	0.017	0.017	10@12
		9-11	35/55	90	0.016	0.016	10@15
		12-15	20/55	90	0.005	0.005	10@25
E	E1	1-15	60/15	150	0.010	0.010	—
	E2	1-6	40/55	95	0.017	0.017	10@15
		7-11	30/55	95	0.016	0.016	10@15
		12-15	20/55	95	0.010	0.010	10@15
F	F1	1-15	60/15	150	0.010	0.010	—
G	G1	1-15	200/12	550	0.006	0.006	—
	G2	1-15	380/12	150	0.002	0.002	—
H	H1	1-15	45/55	550	0.015	0.015	10@15
	H2	1-15	380/12	150	0.006	0.006	—
I	I1	1-15	200/12	550	0.006	0.006	—
	I2	1-15	380/12	150	0.006	0.006	—
J	J1	1-15	40/15	155	0.010	0.010	10@15
	J2	1-15	30/30	200	0.010	0.010	10@15
K	K1	1-15	50/15	250	0.010	0.010	10@15
	K2	1-15	20/100	110	—	—	—
L	L1	1-6	40/55	90	0.017	0.017	10@15
		7-11	30/55	90	0.016	0.016	10@15
		12-15	20/55	90	0.010	0.010	10@15

Fig. 7.19.b Acapulco Building – Beam Geometry and Steel Ratios

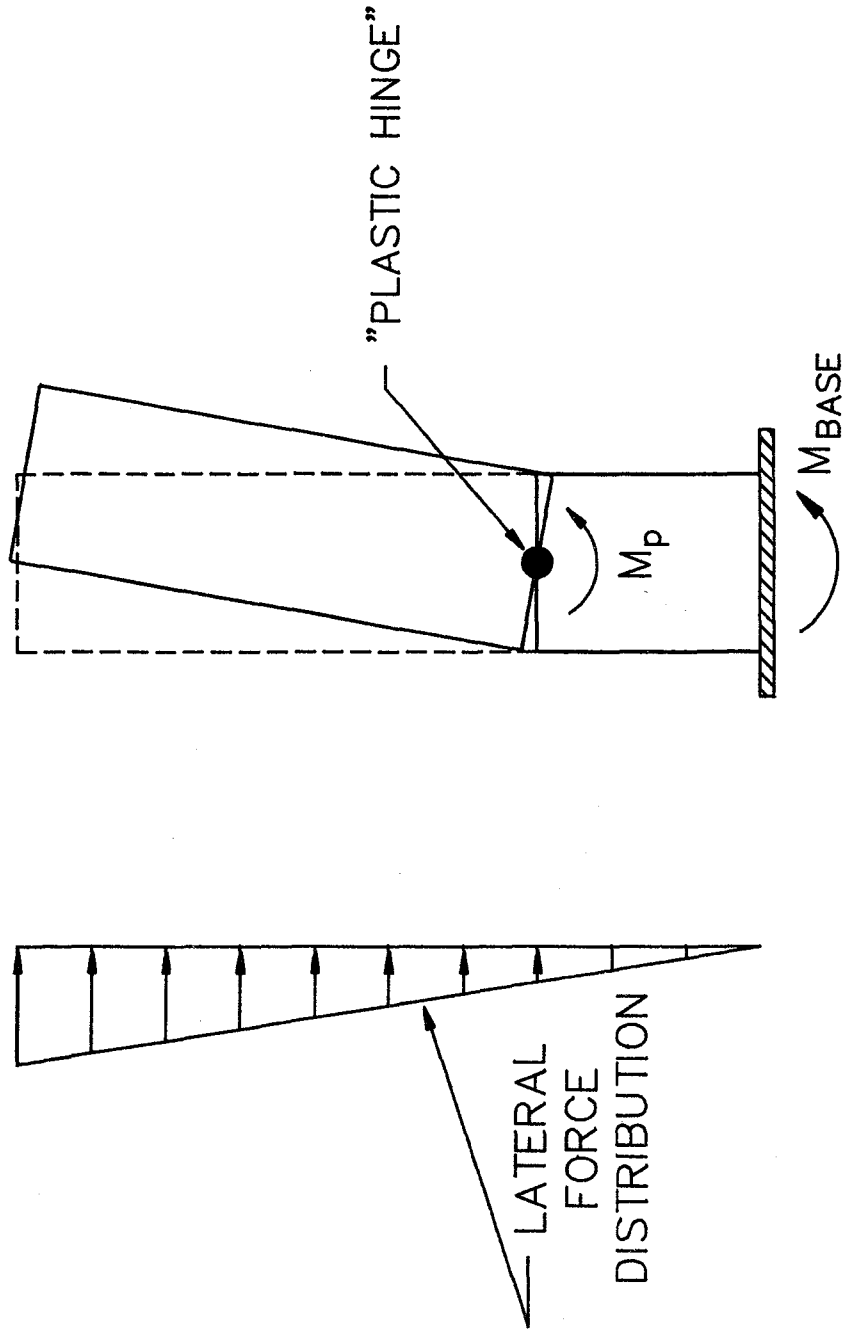


Fig. 7.20 Collapse Mechanism for Wall Yielding

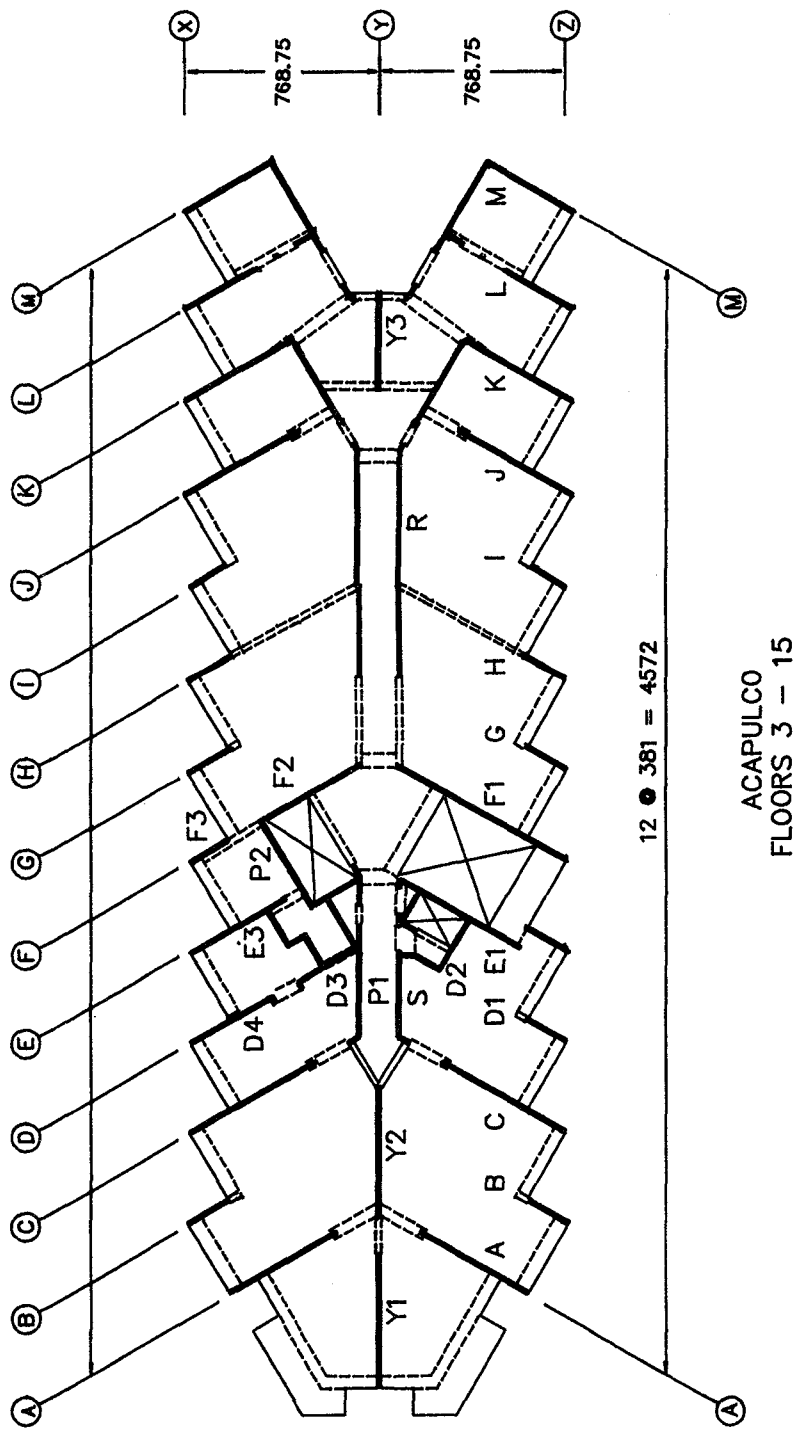
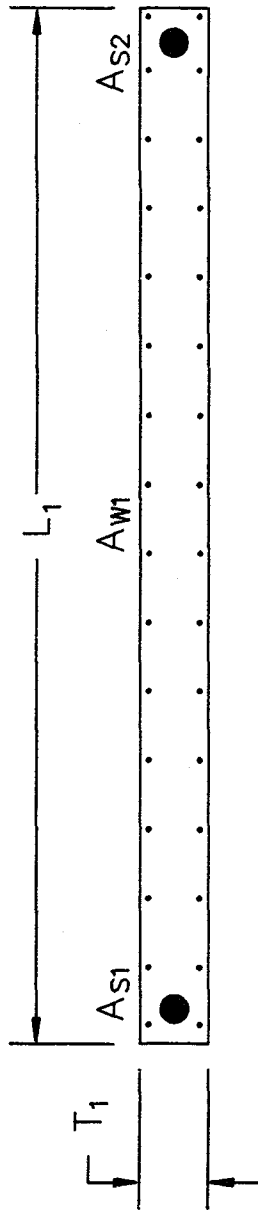
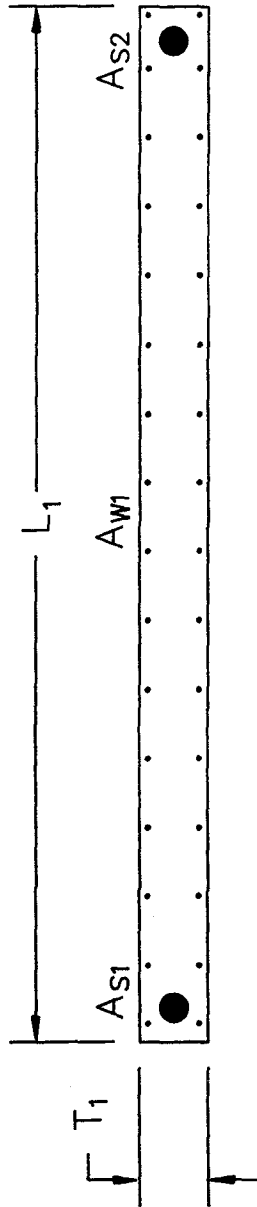


Fig. 7.21.a Acapulco Building - Wall Designations for Strength Calculations



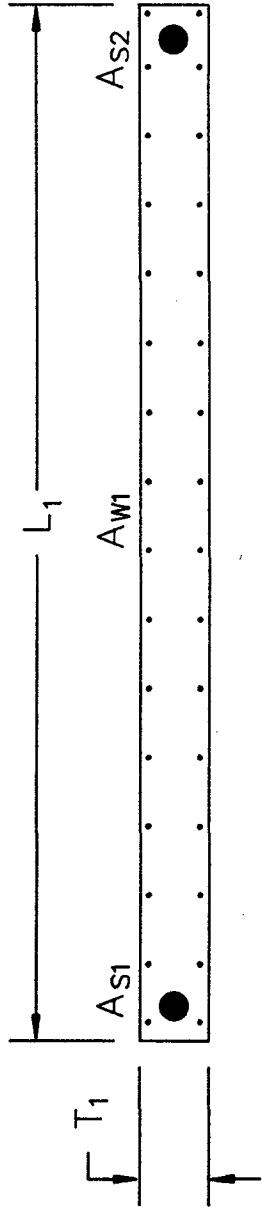
Story	$L_1$ (cm)	$T_1$ (cm)	$A_{S1}$ (#- $d_b$ )	$A_{S2}$ (#- $d_b$ )	$A_{W1}$ ( $d_b$ @cm)
7	540	20	6-26	6-26	6@18
6	540	20	7-26	7-26	6@18
3	540	20	21-26	21-26	8@20
2	540	25	26-26	26-26	8@18
1	540	25	26-26	26-26	8@18

Fig. 7.21.b Acapulco Building – Wall Geometry and Steel Quantities  
Wall A



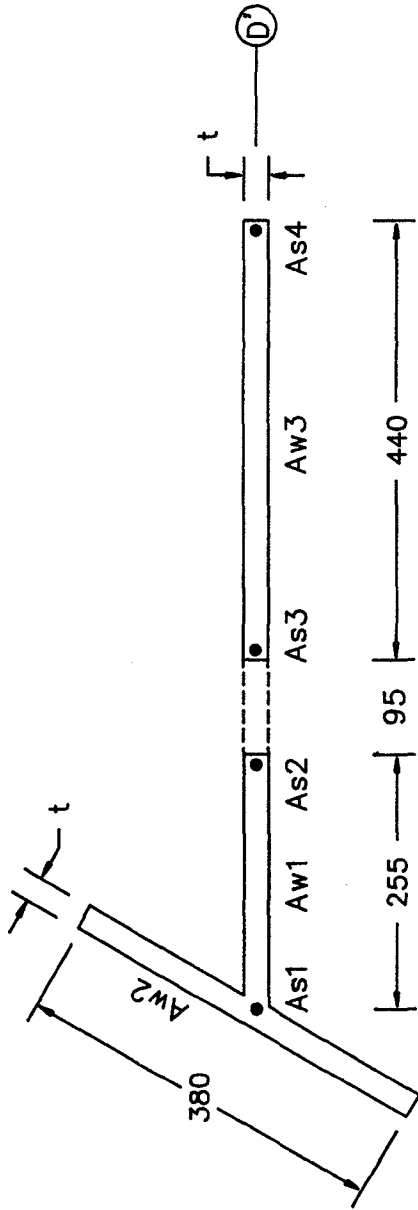
Story	$L_1$ (cm)	$T_1$ (cm)	$AS_1$ (#- $d_b$ )	$AS_2$ (#- $d_b$ )	$AW_1$ ( $d_b$ @cm)
7	240	20	2-22	2-22	10@20
6	240	20	2-22	2-22	10@20
5	240	20	2-22	2-22	10@20
4	240	20	2-26	2-26	10@20
3	240	20	2-26	2-26	10@20
1	240	20	2-26	2-26	10@20

Fig. 7.21.c Acapulco Building – Wall Geometry and Steel Quantities  
Walls B, D1, G, H, and I (assumed for D2)



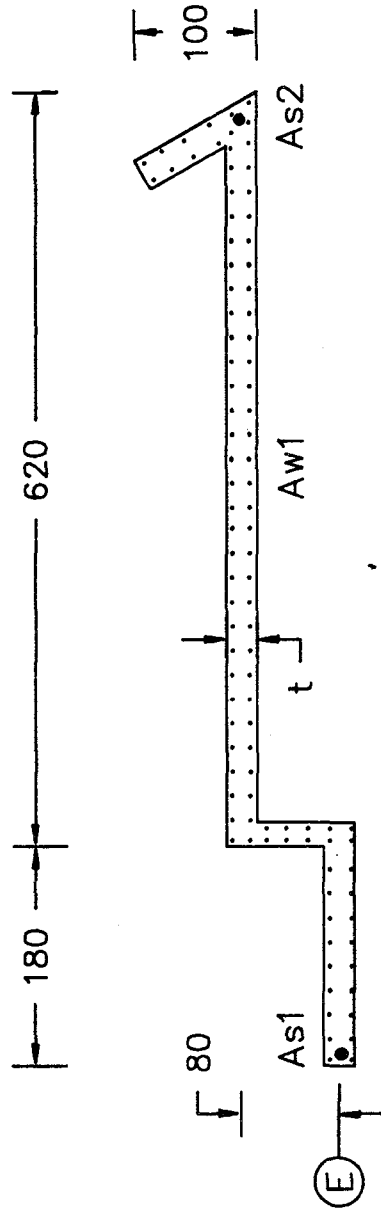
Story	$L_1$ (cm)	$T_1$ (cm)	$A_{S1}$ (#- $d_b$ )	$A_{S2}$ (#- $d_b$ )	$A_{W1}$ ( $d_b$ @cm)
7	590	20	8-26	8-26	6@18
6	590	20	12-26	12-26	8@22
3	590	20	25-26	25-26	8@18
2	590	25	28-26	28-26	8@16
1	590	25	28-26	28-26	8@16

Fig. 7.21.d Acapulco Building – Wall Geometry and Steel Quantities  
Wall C



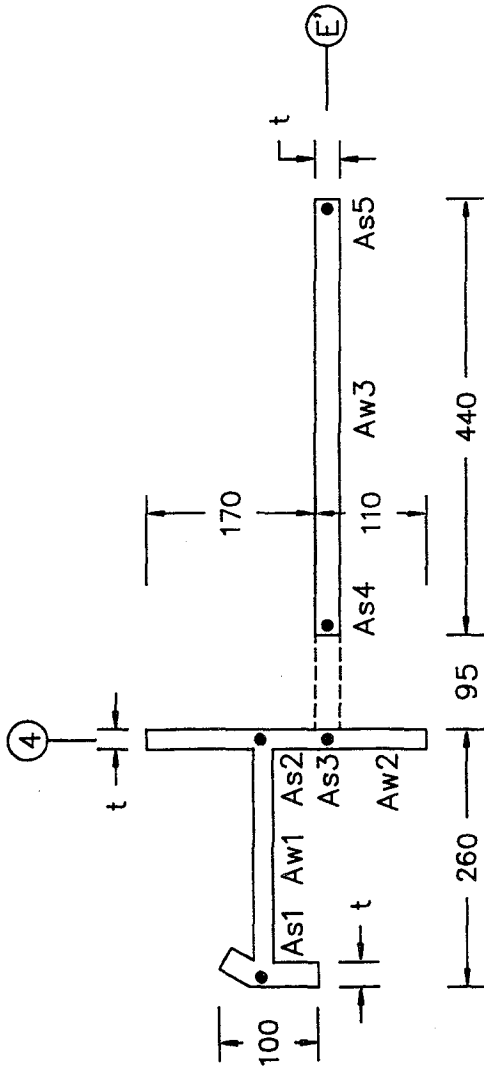
Story	t (cm)	As1 (#-d <sub>b</sub> )	As2 (#-d <sub>b</sub> )	Aw1 (d <sub>b</sub> @cm)	Aw2 (d <sub>b</sub> @cm)	As3 (#-d <sub>b</sub> )	As4 (#-d <sub>b</sub> )	Aw3 (d <sub>b</sub> @cm)
7	20	2-26	2-22	6@18	6@18	2-22	2-26	6@18
6	20	6-26	2-22	6@18	6@18	2-22	6-26	6@18
3	20	12-26	2-26	6@18	8@15	2-26	12-26	6@18
2	25	16-26	2-26	8@22	8@15	2-26	16-26	8@22
1	25	16-26	2-26	8@22	8@15	2-26	16-26	8@22

Fig. 7.21.e Acapulco Building – Wall Geometry and Steel Quantities  
Walls D3 and D4



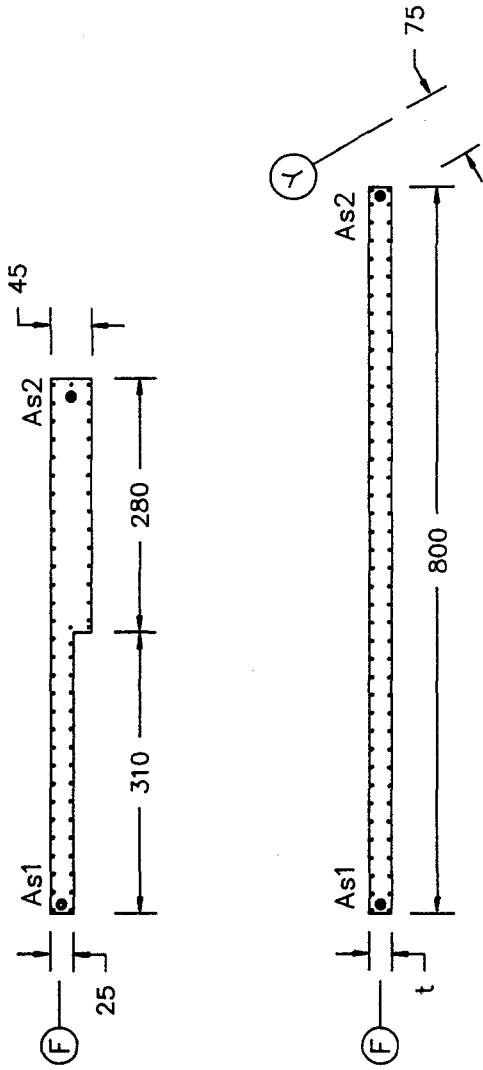
Story	t (cm)	$A_{s1}$ (#- $d_b$ )	$A_{s2}$ (#- $d_b$ )	$A_{w1}$ ( $d_b$ @cm)
7	20	2-22	2-22	6@18
6	20	4-26	4-26	6@18
4	20	6-26	6-26	6@18
3	25	12-26	12-26	8@20
1	25	20-26	20-26	8@20

Fig. 7.21.f Acapulco Building – Wall Geometry and Steel Quantities  
Wall E1



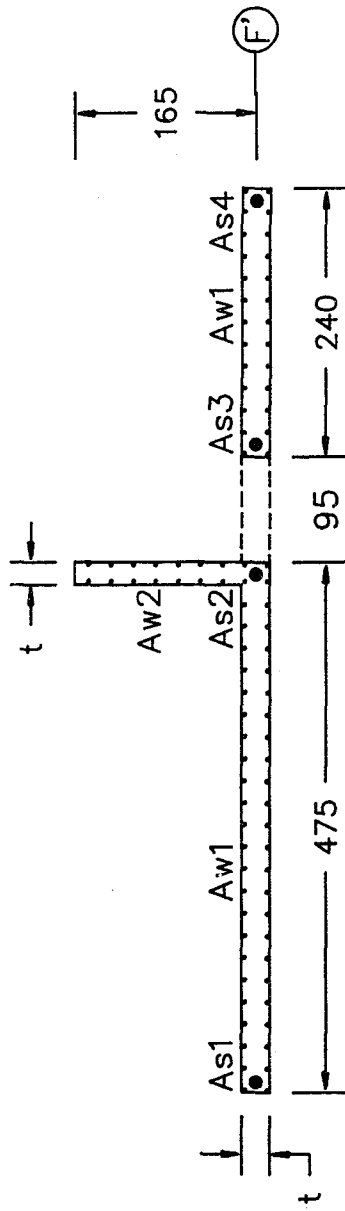
Story	t (cm)	AS1 (#-db)	AS2 (#-db)	AS3 (#-db)	AW1 (db@cm)	AS4 (#-db)	AW2 (db@cm)	AS5 (#-db)	AW3 (db@cm)
7	20	2-26	2-22	2-26	6@18	2-22	6@18	2-26	6@18
6	20	2-26	3-22	3-26	6@18	2-22	6@18	3-26	6@18
3	25	7-26	2-26	7-26	8@22	2-26	8@15	7-26	8@22
1	25	12-26	2-26	12-26	8@22	2-26	10@20	12-26	8@22

Fig. 7.21.g Acapulco Building – Wall Geometry and Steel Quantities  
Walls E2 and E3



Story	t (cm)	As1 (#-d <sub>b</sub> )	As2 (#-d <sub>b</sub> )	Aw1 (d <sub>b</sub> @cm)
8	20	4-22	4-22	6@18
7	20	4-22	4-22	6@18
6	20	6-26	6-26	8@22
5	20	8-26	8-26	6@18
2	25	10-26	10-26	8@20
1	—	19-26	19-26	8@20

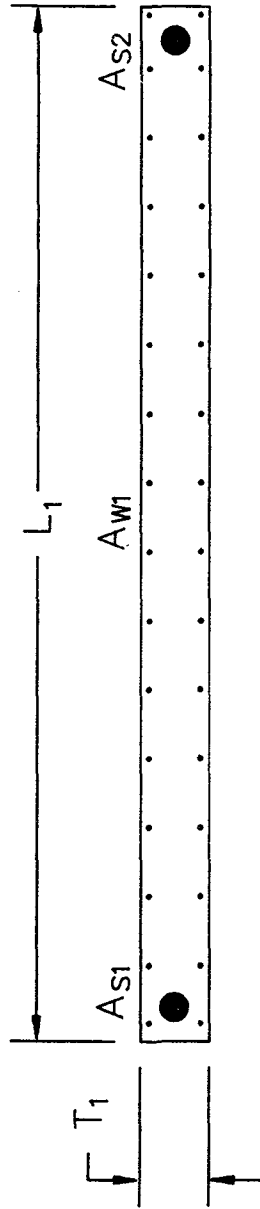
Fig. 7.21.h Acapulco Building – Wall Geometry and Steel Quantities  
Wall F1



Story	t (cm)	$A_{S3}$ (#- $d_b$ )	$A_{S4}$ (#- $d_b$ )	$A_{W1}$ ( $d_b$ @cm)
8	20	2-22	2-22	6@18
7	20	2-26	2-26	6@18
6	20	2-26	4-26	8@22
5	20	2-26	6-26	6@18
2	25	5-26	19-26	8@20
1	25	5-26	19-26	8@20

Story	t (cm)	$A_{S1}$ (#- $d_b$ )	$A_{S2}$ (#- $d_b$ )	$A_{W1}$ ( $d_b$ @cm)	$A_{W2}$ ( $d_b$ @cm)
8	20	4-22	2-26	6@18	6@18
7	20	5-26	2-26	6@18	6@18
6	20	6-26	4-26	6@18	6@18
5	20	10-26	6-26	6@18	8@25
2	25	10-26	16-22	8@20	8@15
1	45	19-26	12-26	8@20	10@20

Fig. 7.21.i Acapulco Building – Wall Geometry and Steel Quantities  
Walls F2 and F3



Story	$L_1$ (cm)	$T_1$ (cm)	$A_{S1}$ (#- $d_b$ )	$A_{S2}$ (#- $d_b$ )	$A_{W1}$ ( $d_b$ @cm)
7	530	20	2-22	2-22	6@18
6	530	20	2-22	2-22	6@18
3	530	20	2-26	2-26	6@18
2	530	25	2-26	2-26	8@20
1	530	25	2-26	2-26	8@20

Fig. 7.21.j Acapulco Building – Wall Geometry and Steel Quantities  
Wall J

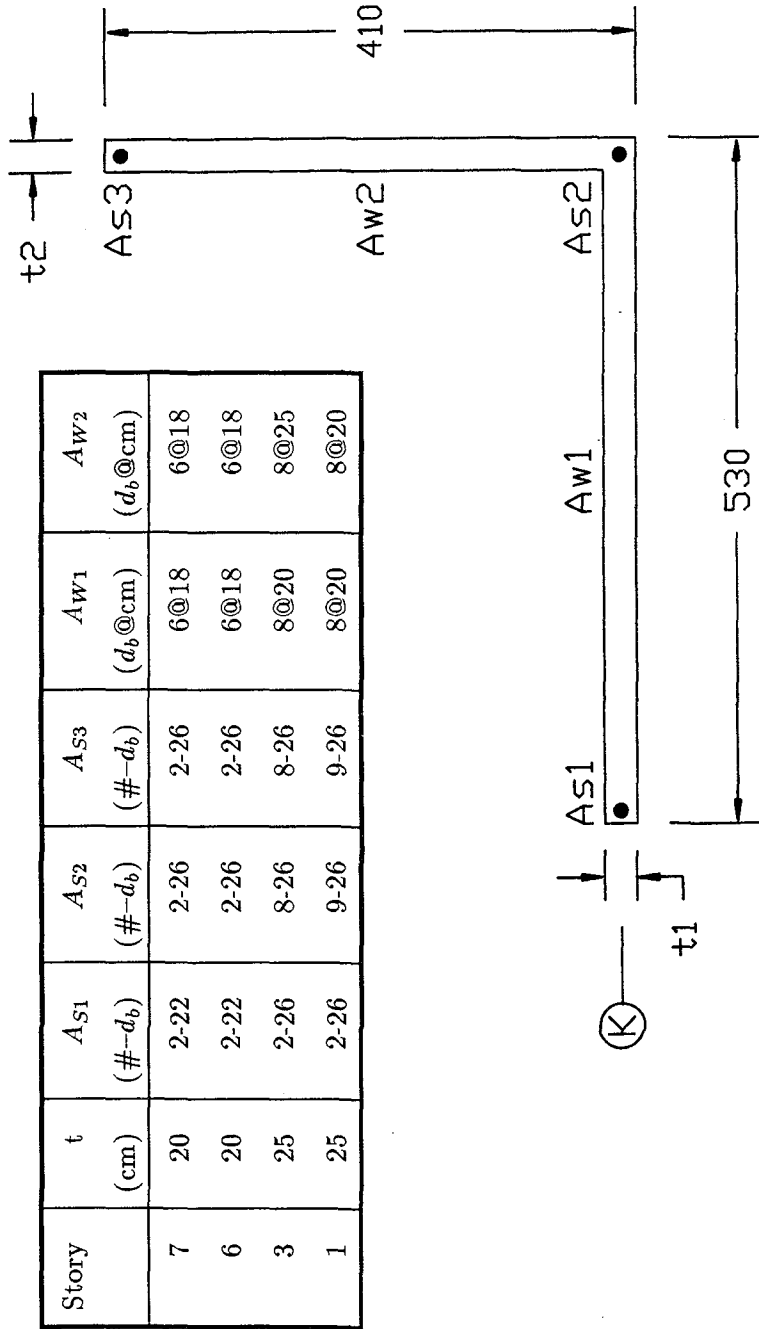
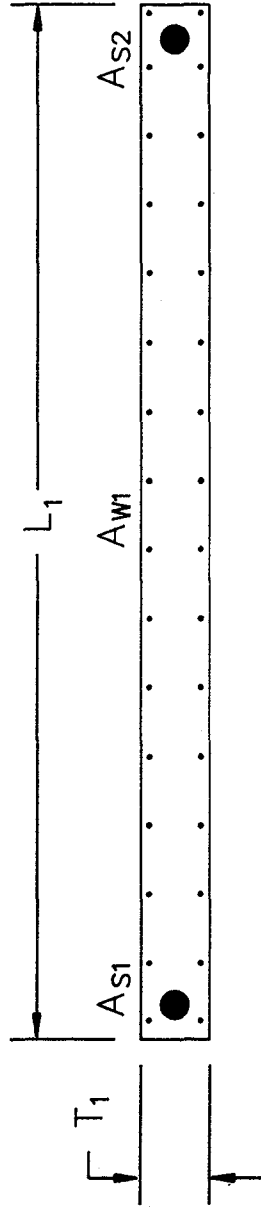


Fig. 7.21.k Acapulco Building – Wall Geometry and Steel Quantities  
Wall K



Story	$L_1$ (cm)	$T_1$ (cm)	$A_{S1}$ (#- $d_b$ )	$A_{S2}$ (#- $d_b$ )	$A_{W1}$ ( $d_b$ @cm)
8	335	20	2-26	2-26	10@13
7	335	20	6-26	2-26	10@12
6	335	20	10-26	2-26	10@10
5	335	20	15-26	2-26	10@10
4	335	20	18-26	2-26	10@10
3	335	20	22-26	3-26	10@10
2	335	25	26-26	3-26	10@20
1	335	25	26-26	3-26	10@20

Fig. 7.21.1 Acapulco Building – Wall Geometry and Steel Quantities  
Wall L

Story	$t_1$ (cm)	$A_{S1}$ (#- $d_b$ )	$A_{S2}$ (#- $d_b$ )	$A_{W1}$ ( $d_b$ @cm)	$t_2$ (cm)	$A_{S3}$ (#- $d_b$ )	$A_{S4}$ (#- $d_b$ )	$A_{W2}$ ( $d_b$ @cm)
7	20	4-26	2-26	6@18	20	6-26	2-26	8@20
6	20	4-26	3-26	6@18	20	10-26	3-26	10@20
5	20	9-26	4-26	6@18	20	15-26	4-26	10@18
4	20	10-26	6-26	6@18	25	18-26	6-26	10@17
3	25	12-26	8-26	6@18	25	22-26	8-26	10@16
1	25	16-26	15-26	8@20	30	26-26	15-26	10@12

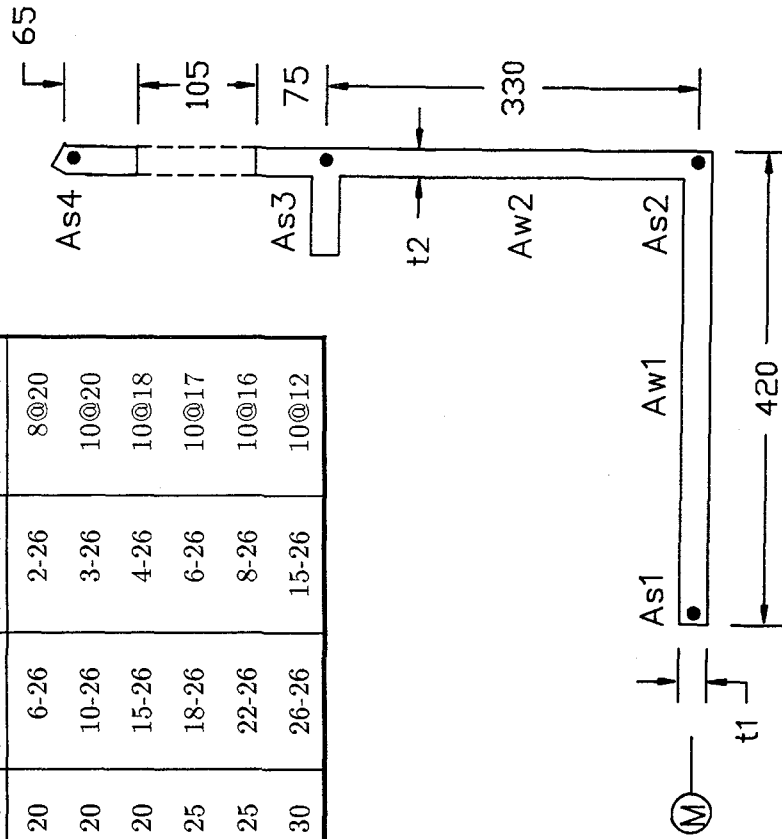
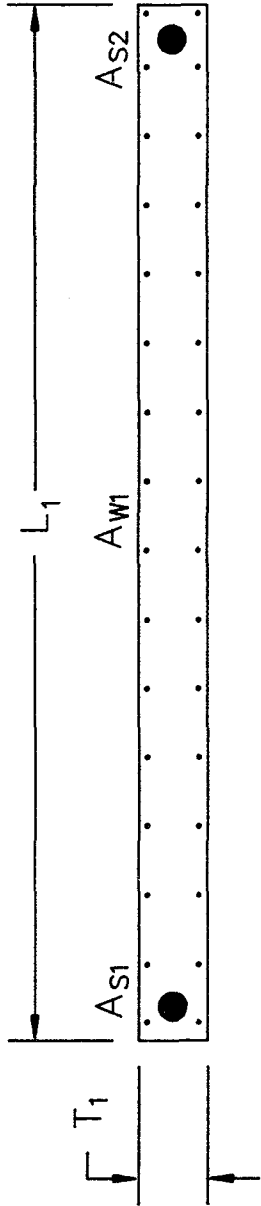
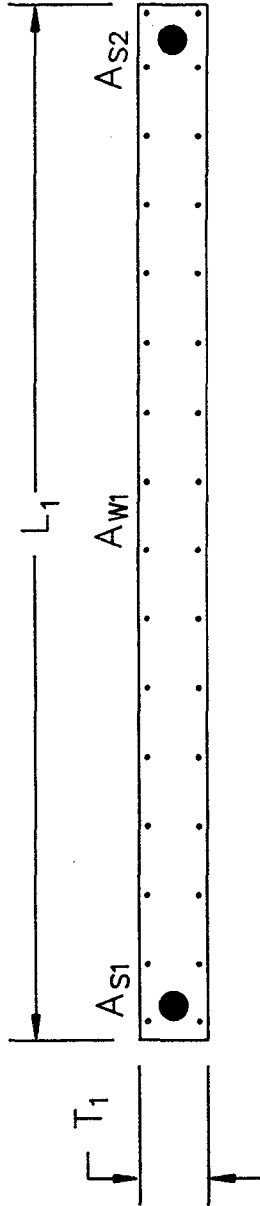


Fig. 7.21.m Acapulco Building - Wall Geometry and Steel Quantities  
Wall M



Story	$L_1$ (cm)	$T_1$ (cm)	$A_{s1}$ (#- $d_b$ )	$A_{s2}$ (#- $d_b$ )	$A_{w1}$ ( $d_b$ @cm)
8	580	20	2-26	3-26	6@18
6	580	20	6-26	6-26	6@18
5	580	20	9-26	7-26	8@25
4	580	20	12-26	10-26	8@19
3	580	25	16-26	13-26	10@20
2	580	25	18-26	18-26	10@17

Fig. 7.21.n Acapulco Building – Wall Geometry and Steel Quantities  
Wall Y1



Story	$L_1$ (cm)	$T_1$ (cm)	$AS_1$ (#- $d_b$ )	$AS_2$ (#- $d_b$ )	$AW_1$ ( $d_b$ @cm)
8	530	20	2-26	3-26	6@18
6	530	20	6-26	6-26	6@18
5	530	20	9-26	7-26	8@25
4	530	20	12-26	10-26	8@19
3	530	25	16-26	13-26	10@20
2	530	25	18-26	18-26	10@17

Fig. 7.21.0 Acapulco Building – Wall Geometry and Steel Quantities  
Wall Y2

Story	t (cm)	As1 (#-db)	As2 (#-db)	Aw1 (db@cm)
7	20	7-26	7-26	6@18
6	20	9-26	9-26	6@18
5	20	11-26	11-26	6@18
4	20	12-26	12-26	8@15
3	25	18-26	18-26	8@15
1	25	12-26	12-26	10@18

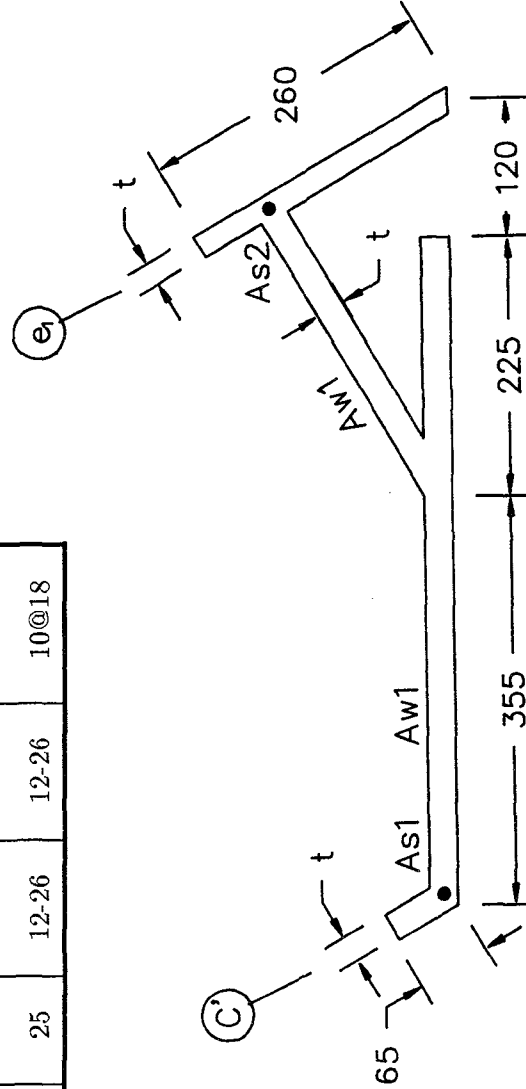
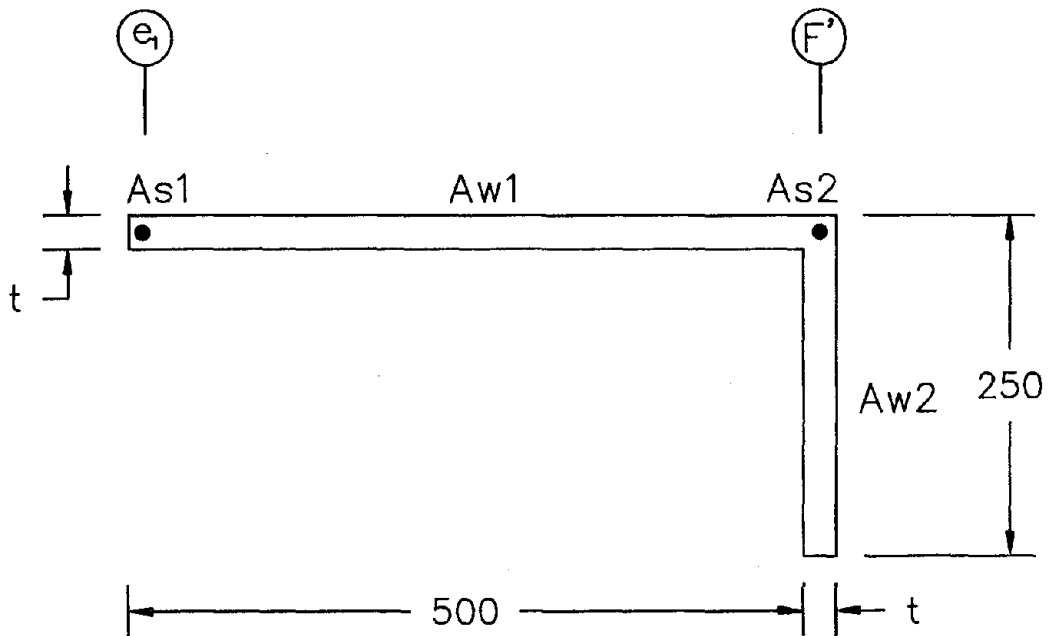


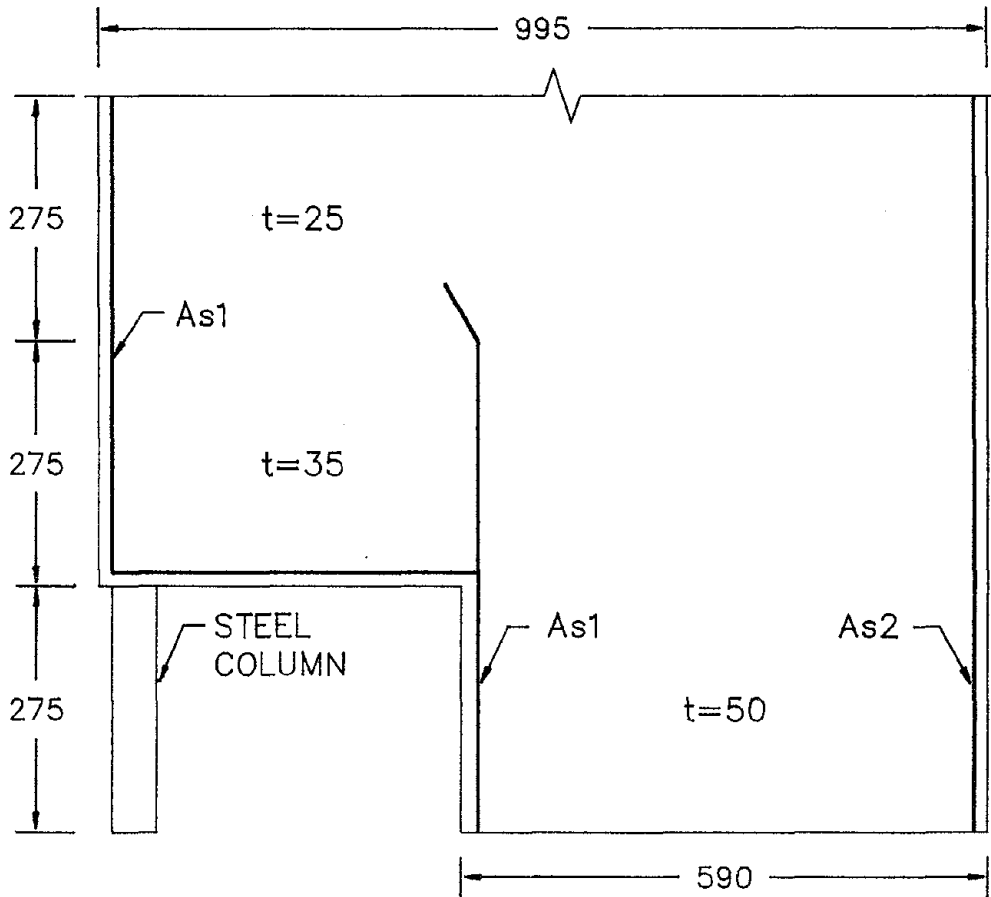
Fig. 7.21-p Acapulco Building – Wall Geometry and Steel Quantities  
Wall P1



Story	t (cm)	$A_{s1}$ (#- $d_b$ )	$A_{s2}$ (#- $d_b$ )	$A_{w1}$ ( $d_b$ @cm)	$A_{w2}$ ( $d_b$ @cm)
7	20	2-26	2-26	6@18	6@18
6	20	4-26	4-26	6@18	6@18
5	20	6-26	6-26	8@25	6@18
4	20	10-26	10-26	8@17	6@18
3	25	14-26	14-26	8@15	8@20
1	25	12-26	12-26	10@18	8@20

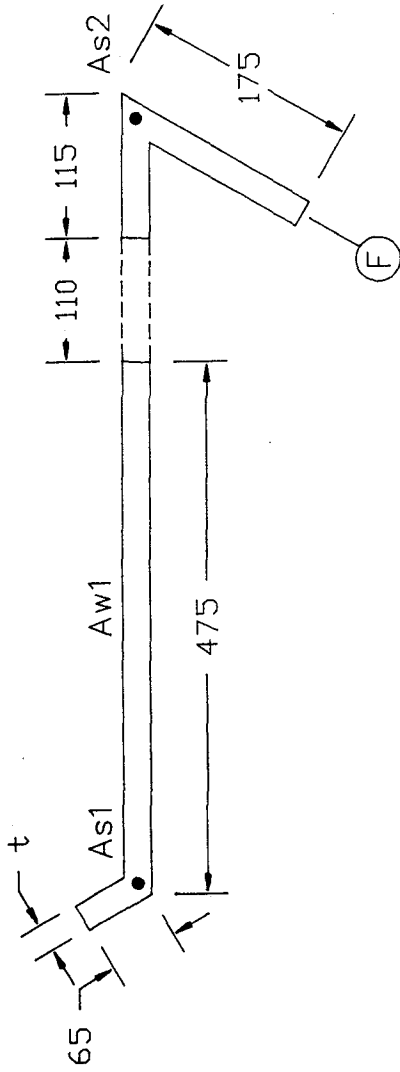
Fig. 7.21.q Acapulco Building – Wall Geometry and Steel Quantities  
Wall P2

Story	$L_1$ (cm)	$T_1$ (cm)	$A_{S1}$ (#- $d_b$ )	$A_{S2}$ (#- $d_b$ )	$A_{W1}$ ( $d_b$ @cm)
4	995	20	15-26	24-26	8@15
3	995	25	25-26	27-26	8@15
2	995	35	28-26	39-26	8@15
1	590	50	45-26	55-26	10@17



ELEVATION – WALL R

Fig. 7.21.r Acapulco Building – Wall Geometry and Steel Quantities  
Wall R



Story	t (cm)	$A_{s1}$ (#- $d_b$ )	$A_{s2}$ (#- $d_b$ )	$A_{w1}$ ( $d_b$ @cm)
7	20	7-26	2-26	6@18
6	20	9-26	4-26	6@18
5	20	11-26	6-26	6@18
4	20	12-26	10-26	8@15
3	25	18-26	16-26	8@15
1	25	12-26	19-26	10@18

Fig. 7.21.s Acapulco Building – Wall Geometry and Steel Quantities  
Wall S

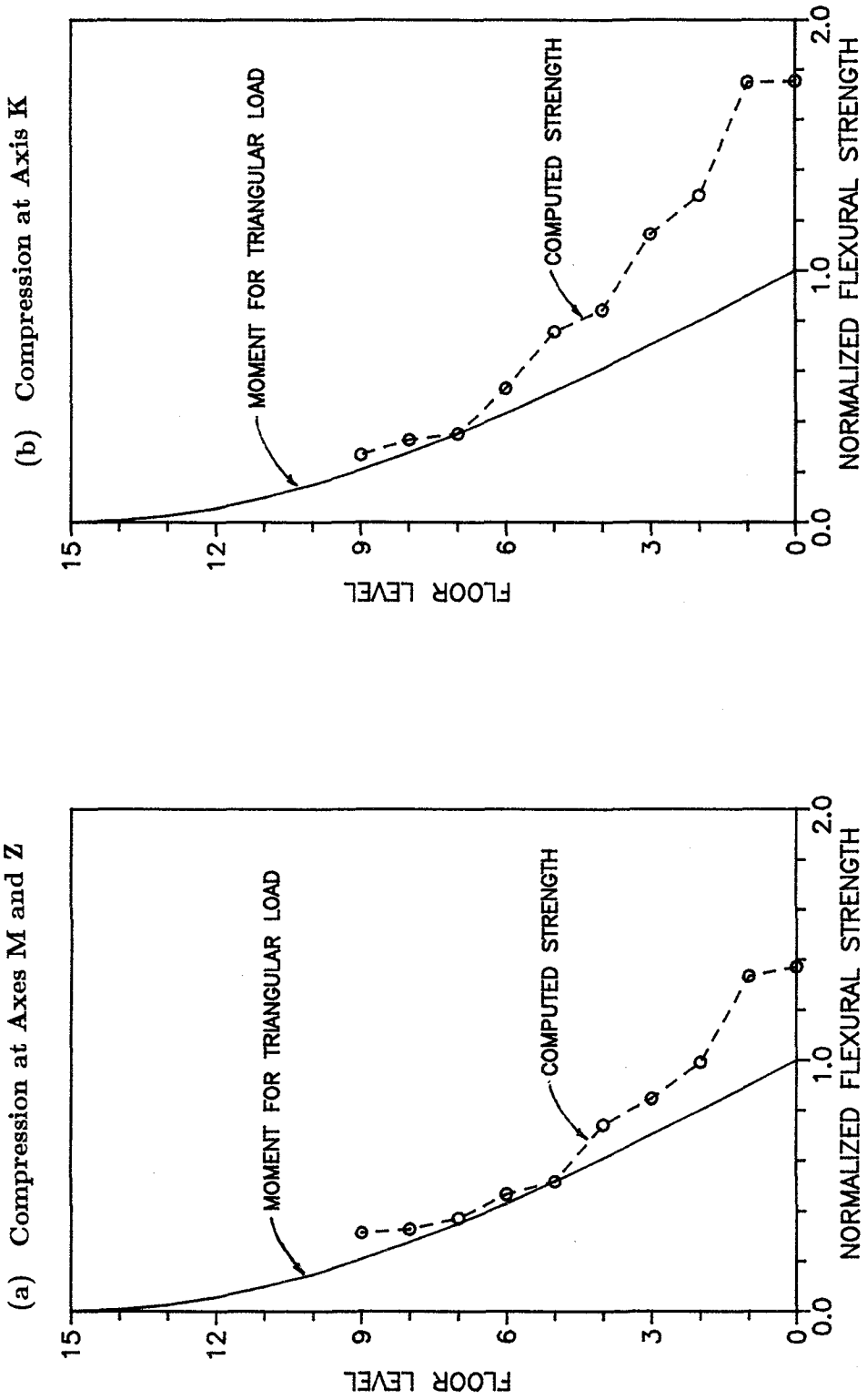


Fig. 7.22 Acapulco Building - Strength Distribution versus Height  
Wall M

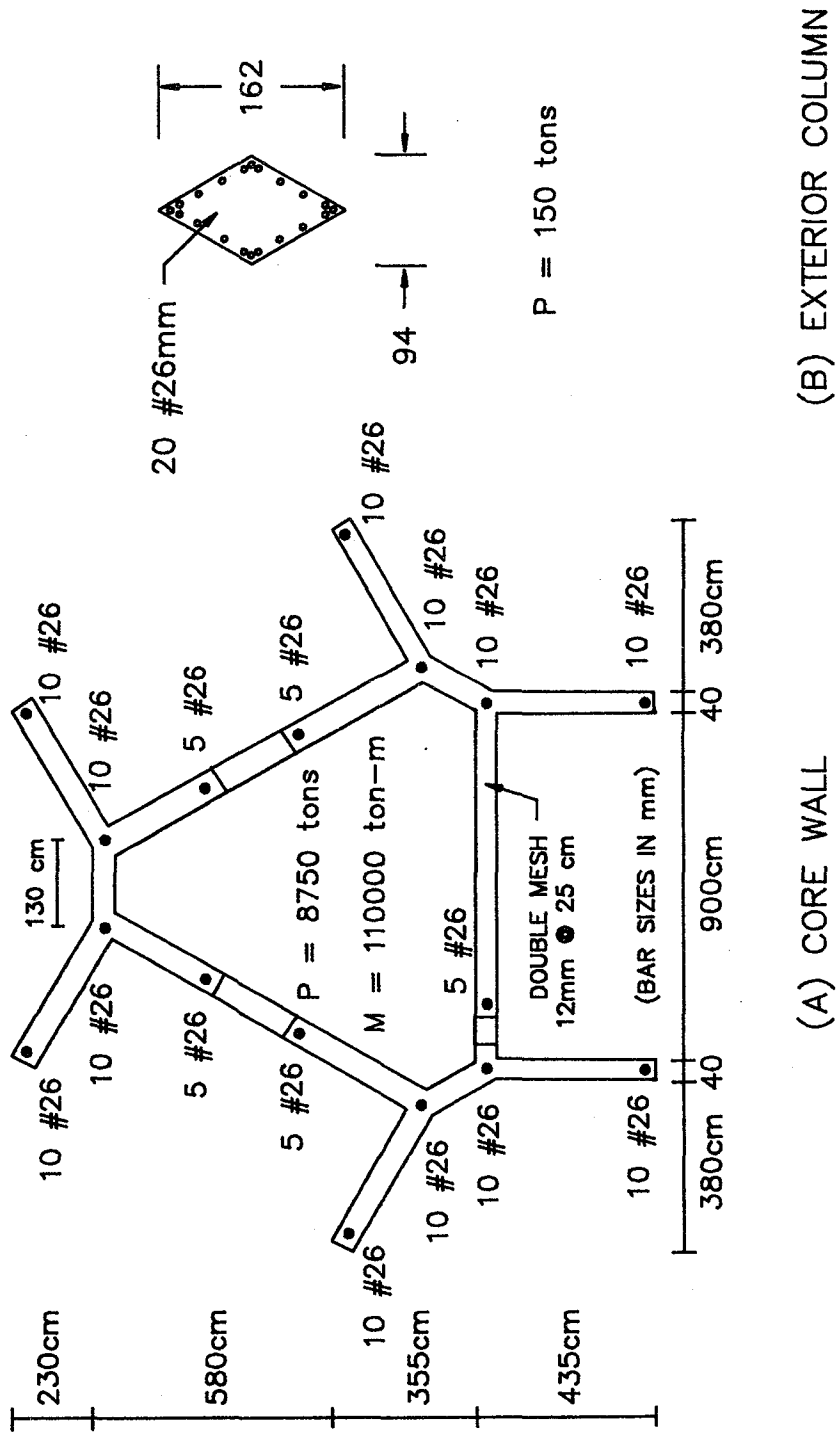


Fig. 7.23 Torres de Miramar – Core Wall Geometry and Steel Quantities

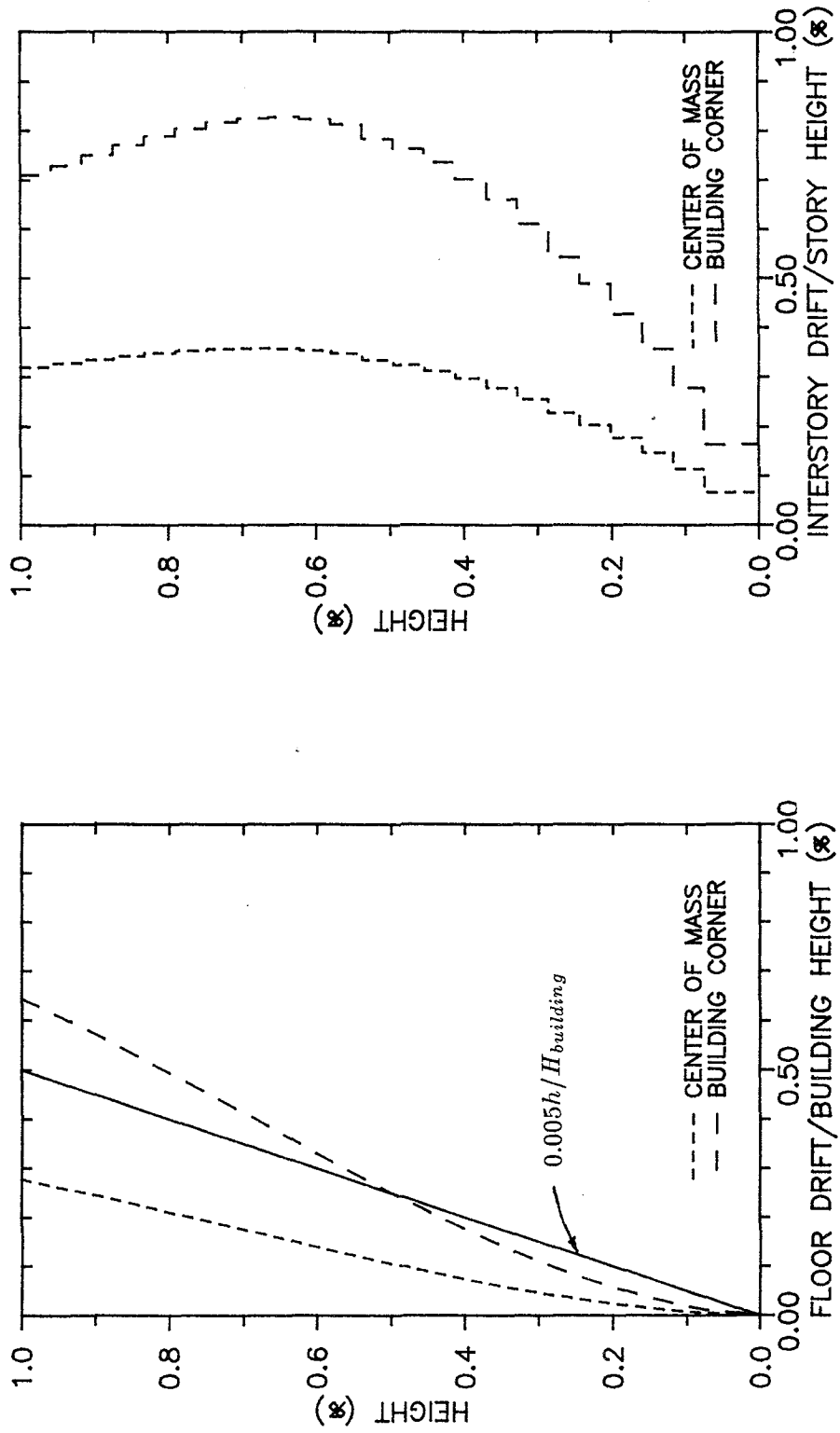


Fig. 7.24 Drift Ratios for Response Spectrum Analysis — Plaza del Mar Building

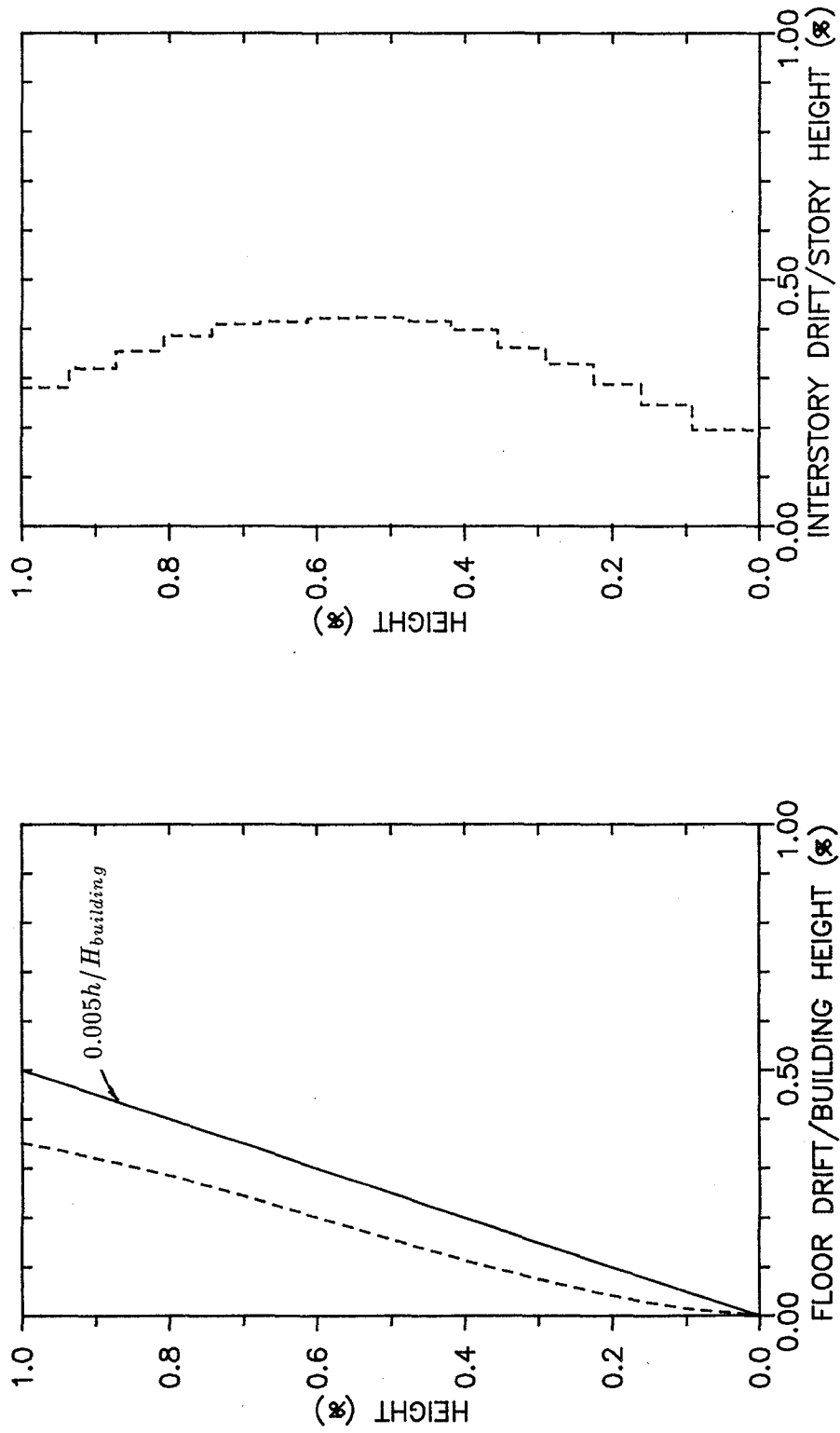


Fig. 7.25 Drift Ratios for Response Spectrum Analysis — Festival Building

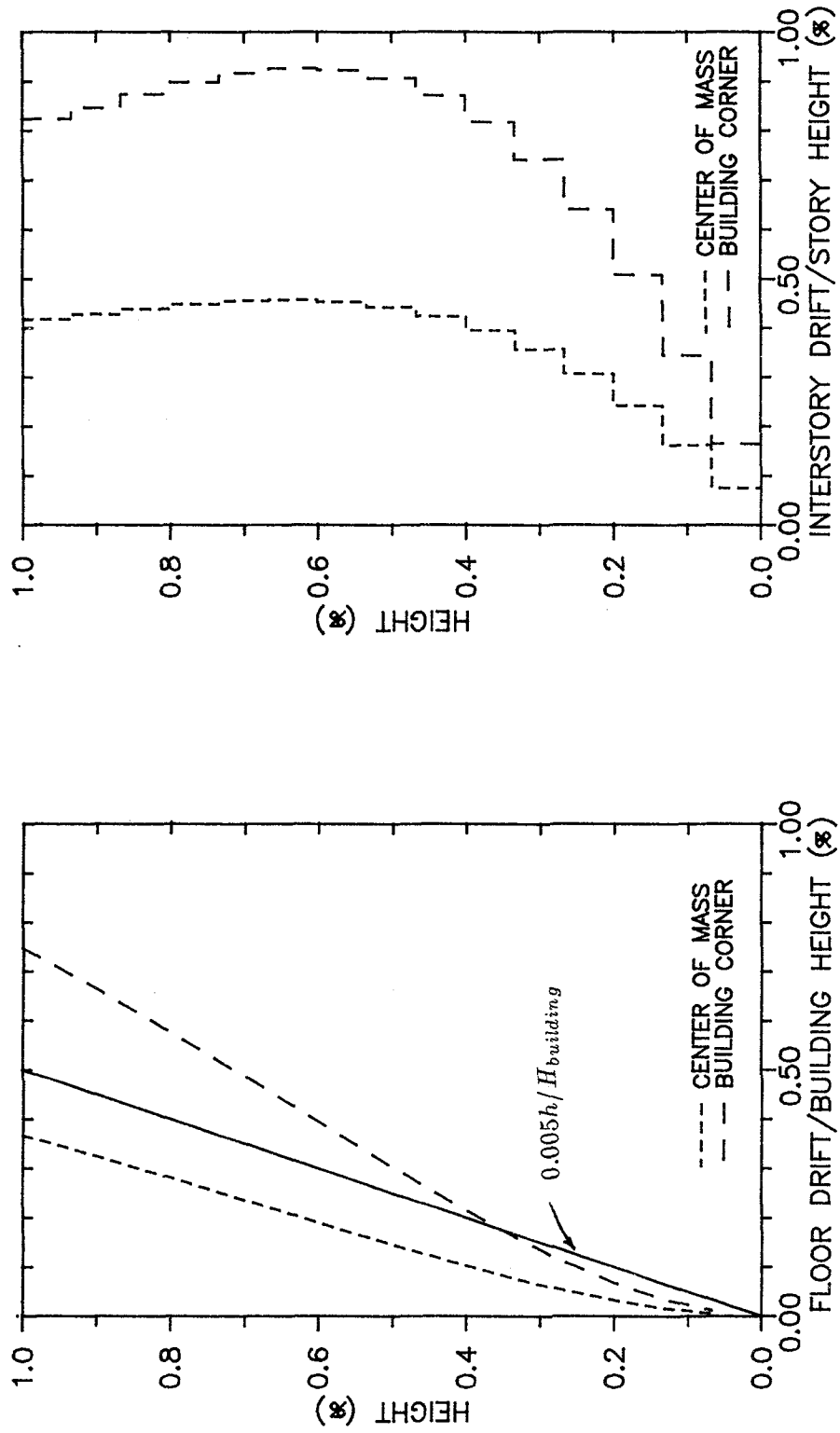


Fig. 7.26 Drift Ratios for Response Spectrum Analysis — Acapulco Building

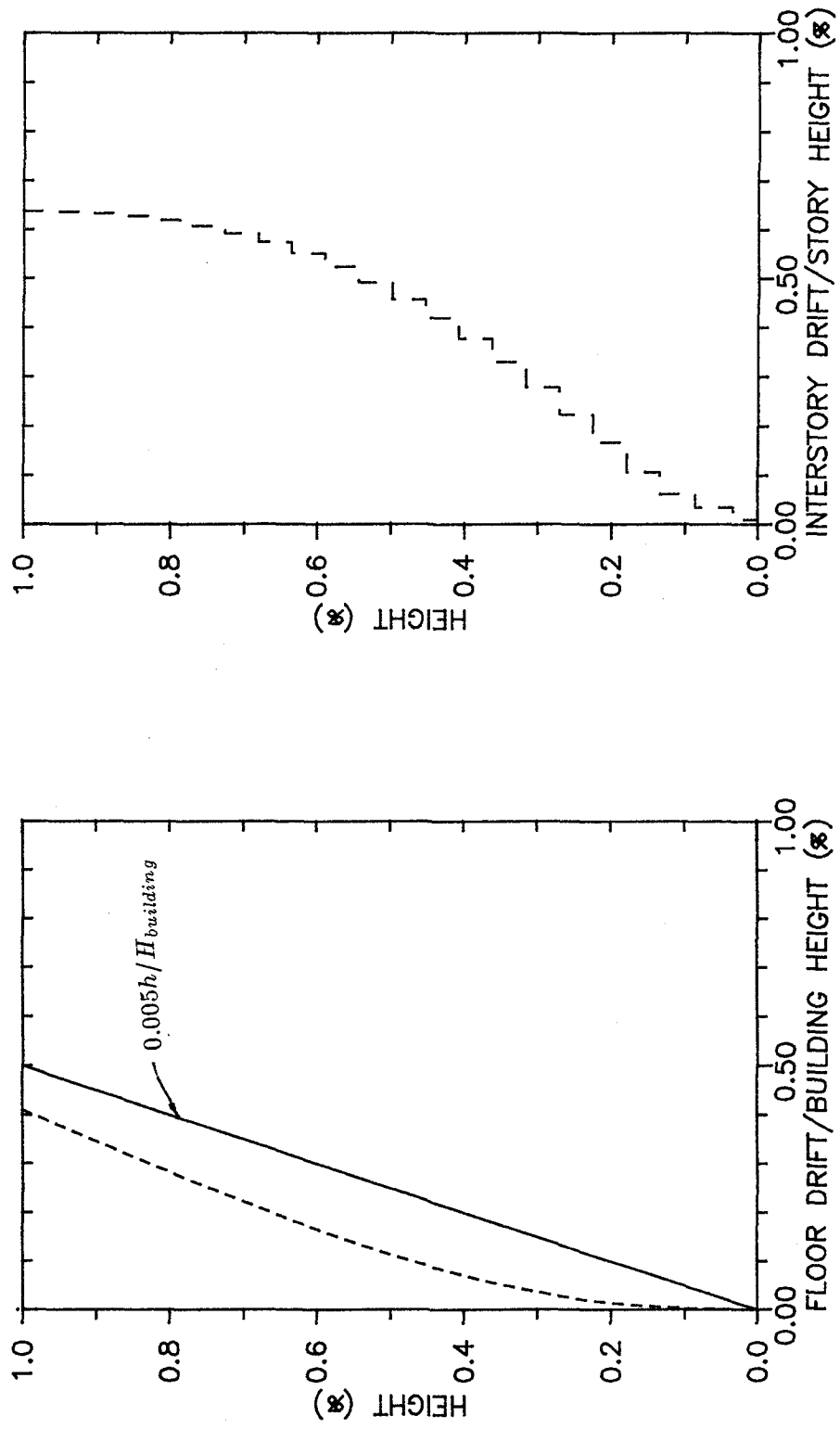


Fig. 7.27 Drift Ratios for response Spectrum Analysis — Torres de Miramar Building

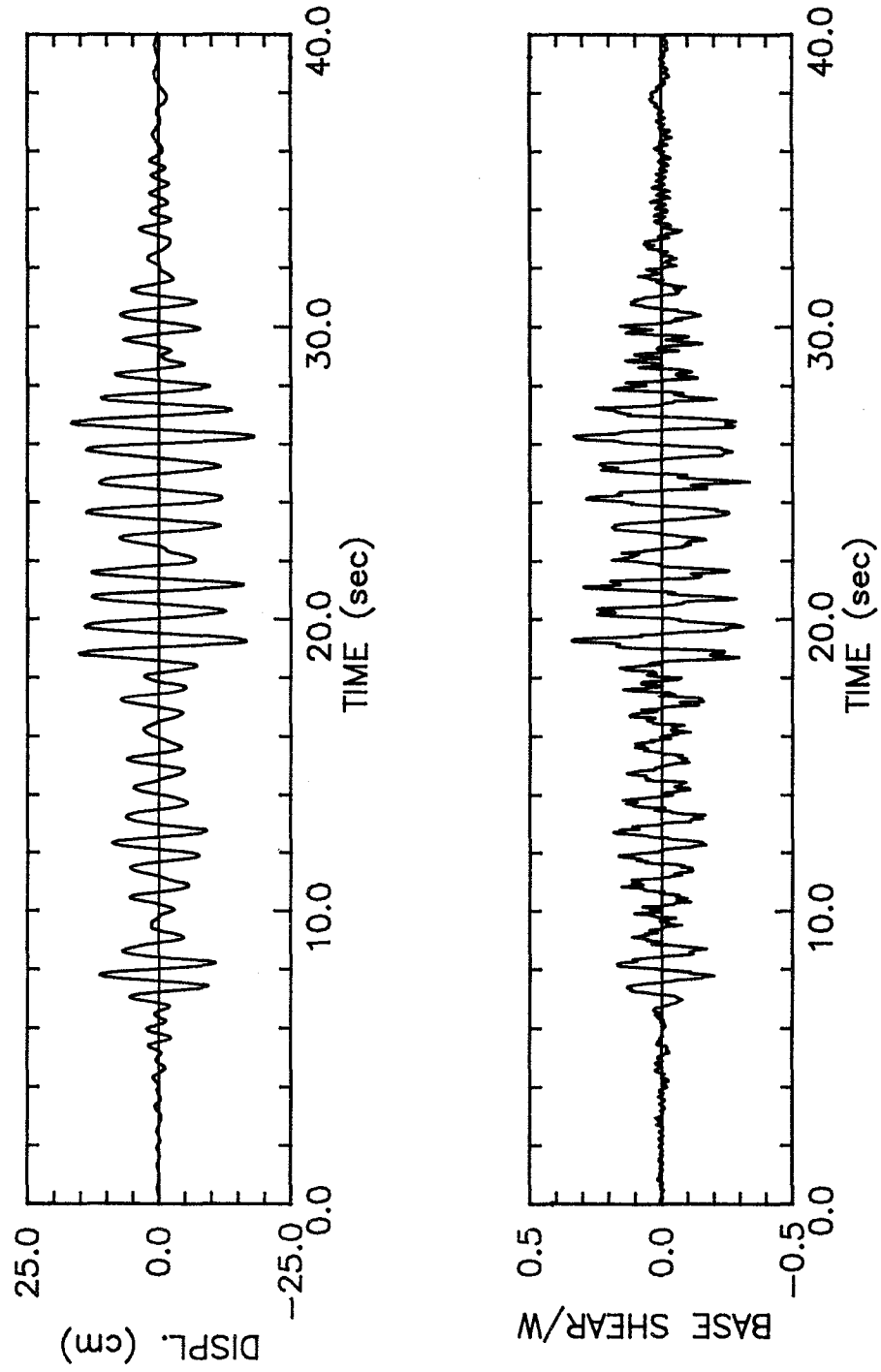


Fig. 7.28 Response History Characteristics — Festival Building

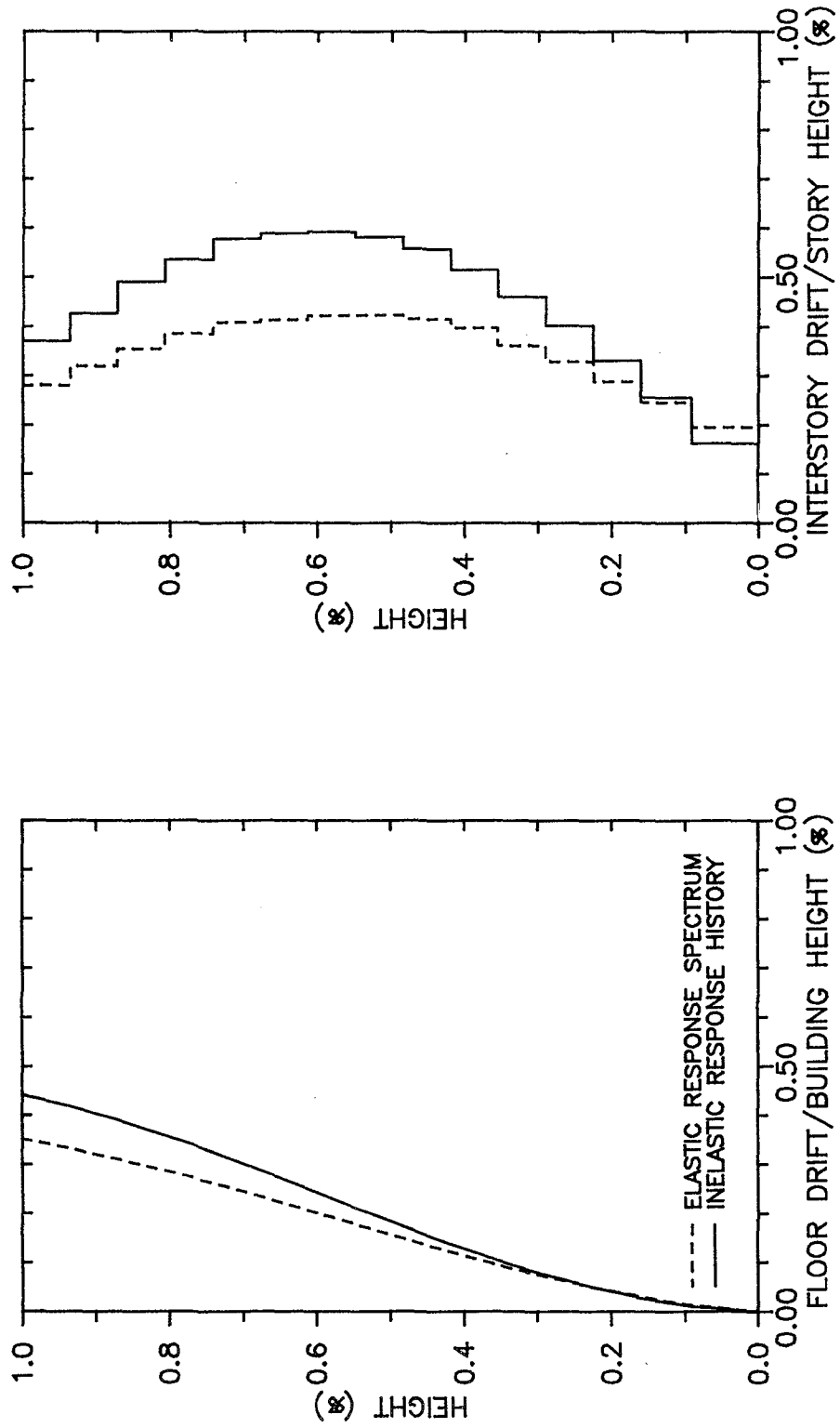


Fig. 7.29 Drift Ratios for Inelastic Analysis - Festival Building

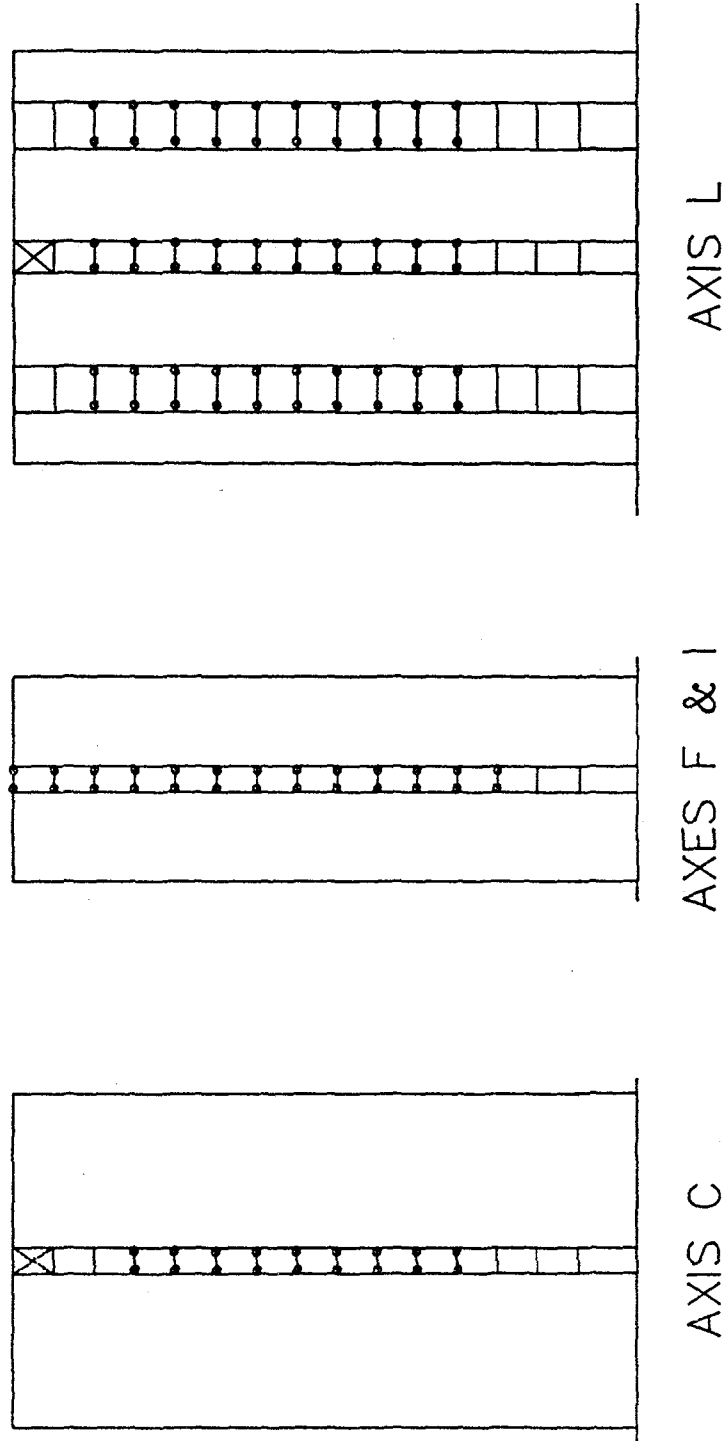


Fig. 7.30 Yielding Pattern for Inelastic Analysis - Festival Building

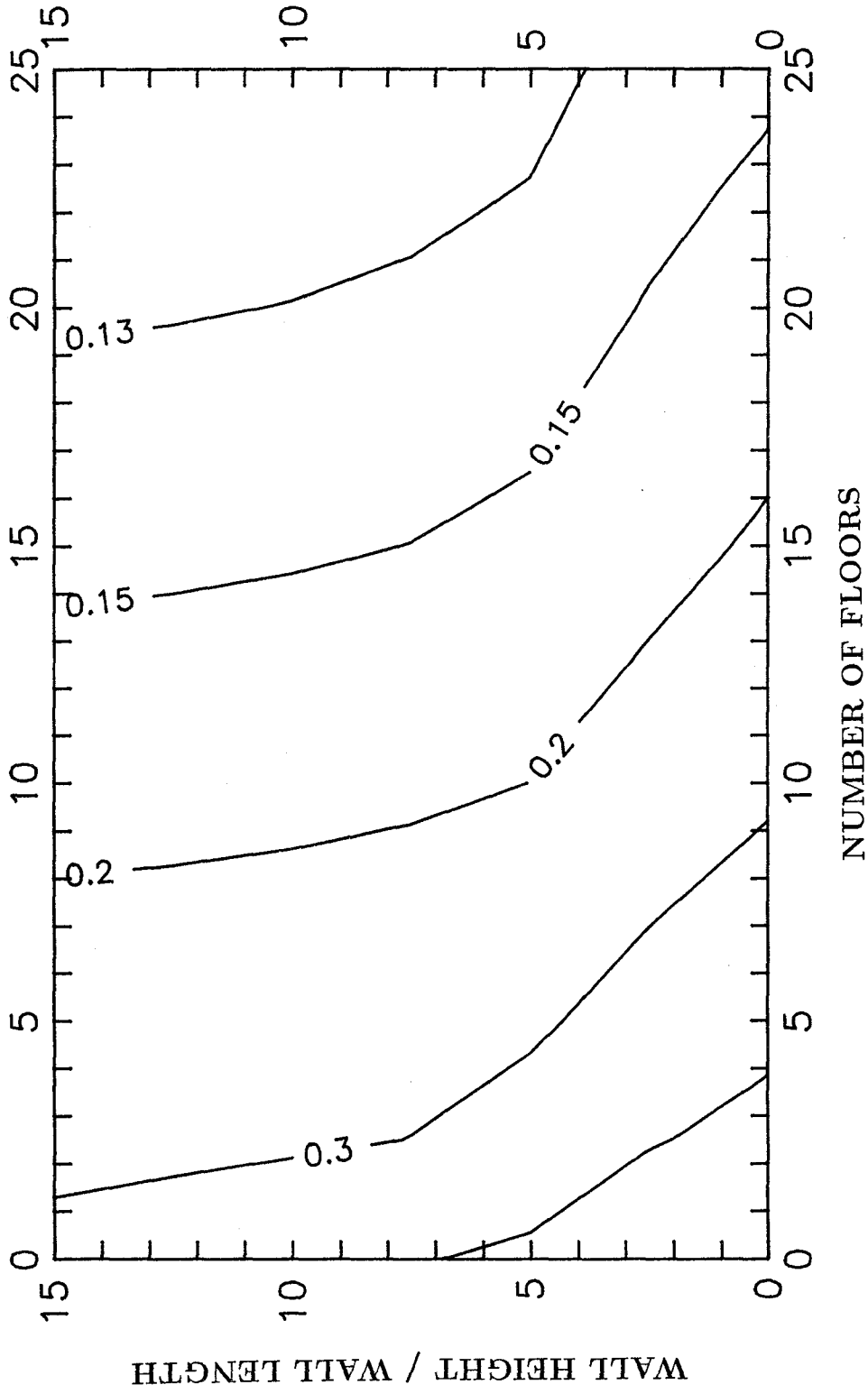


Fig. 8.1 Minimum U.S. Code Strength —  $A_w/A_b=0.005$

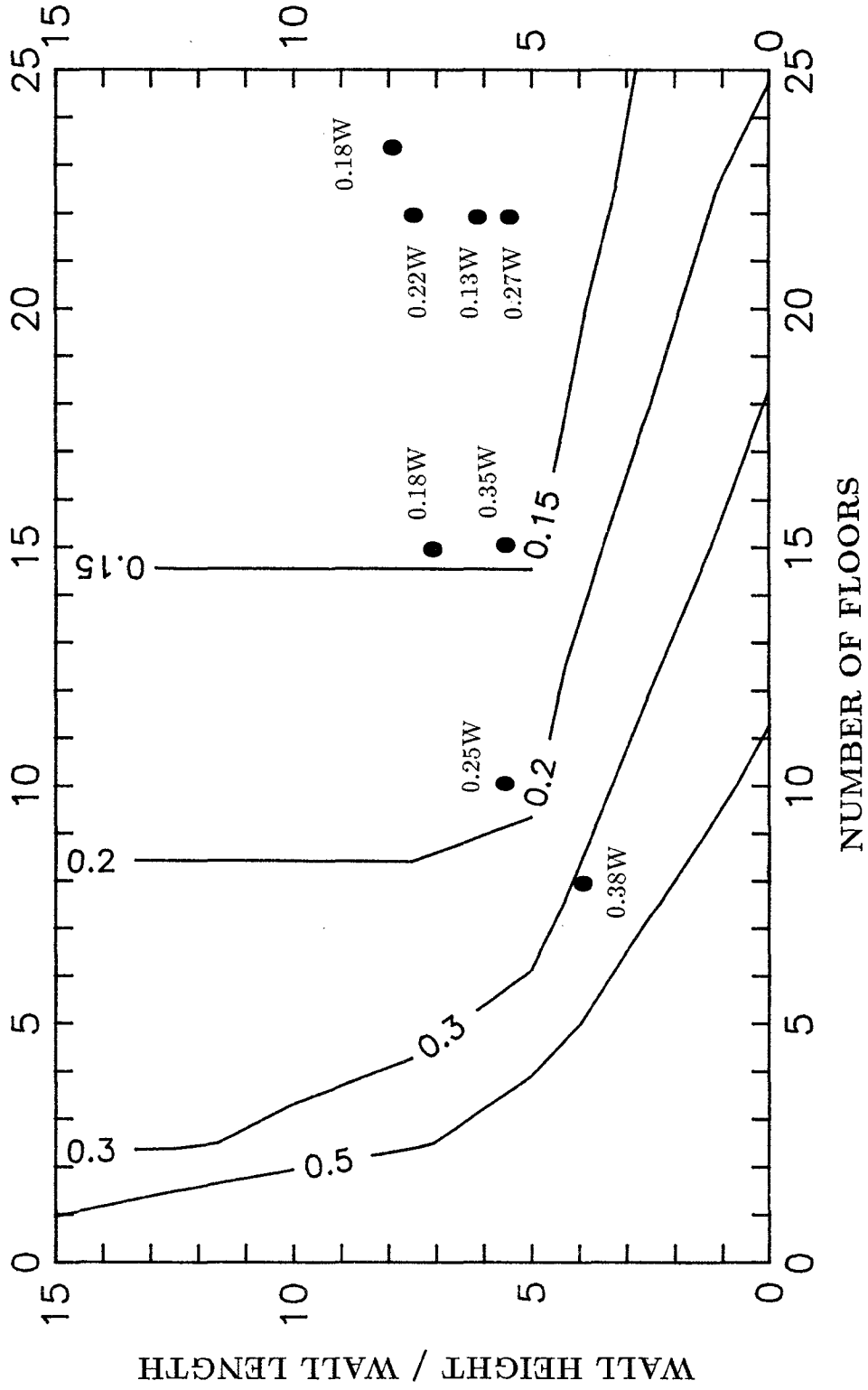


Fig. 8.2 Minimum Chilean Code Strength —  $A_w/A_p=0.025$

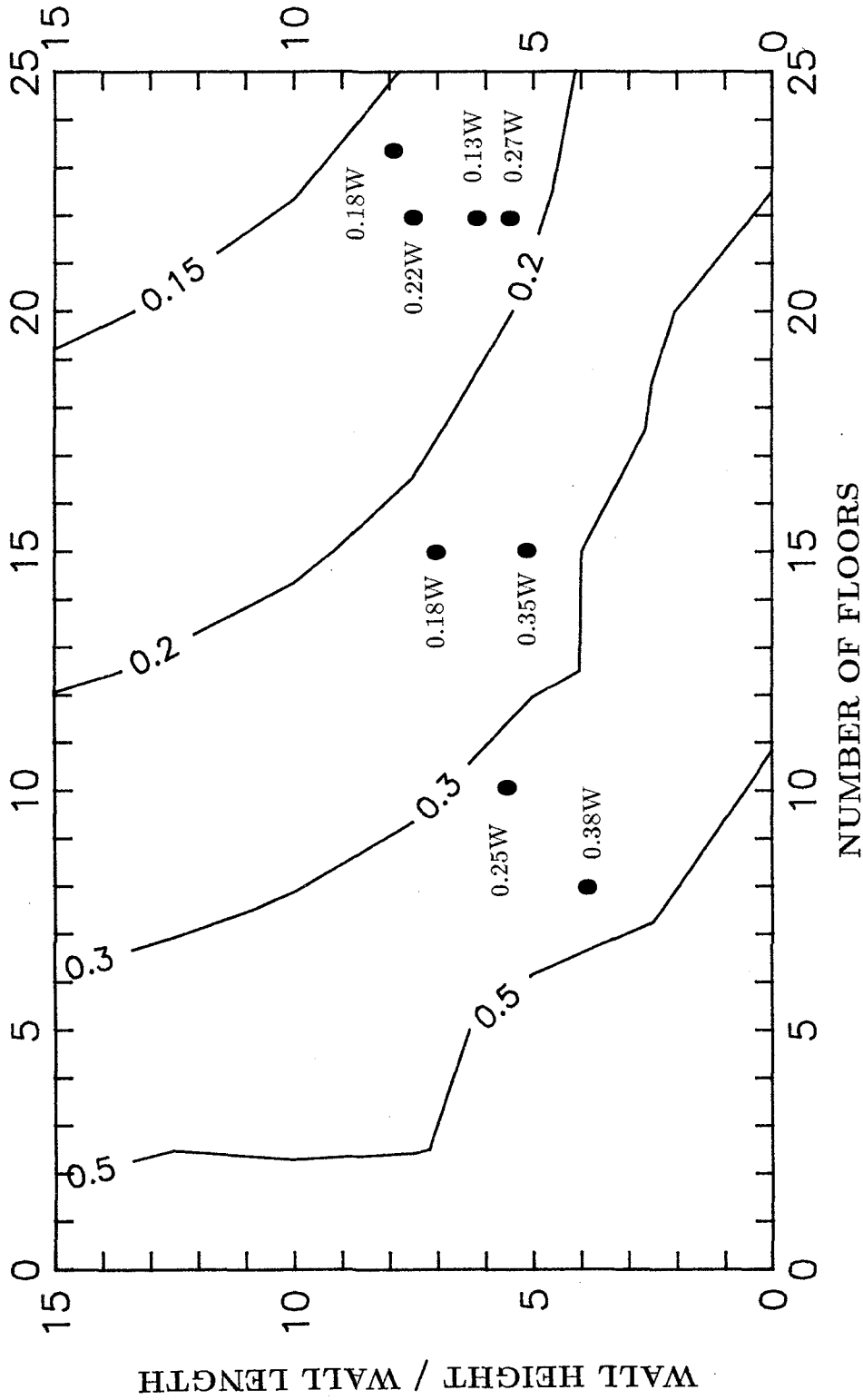


Fig. 8.3 Minimum U.S. Code Strength —  $A_w/A_b=0.025$

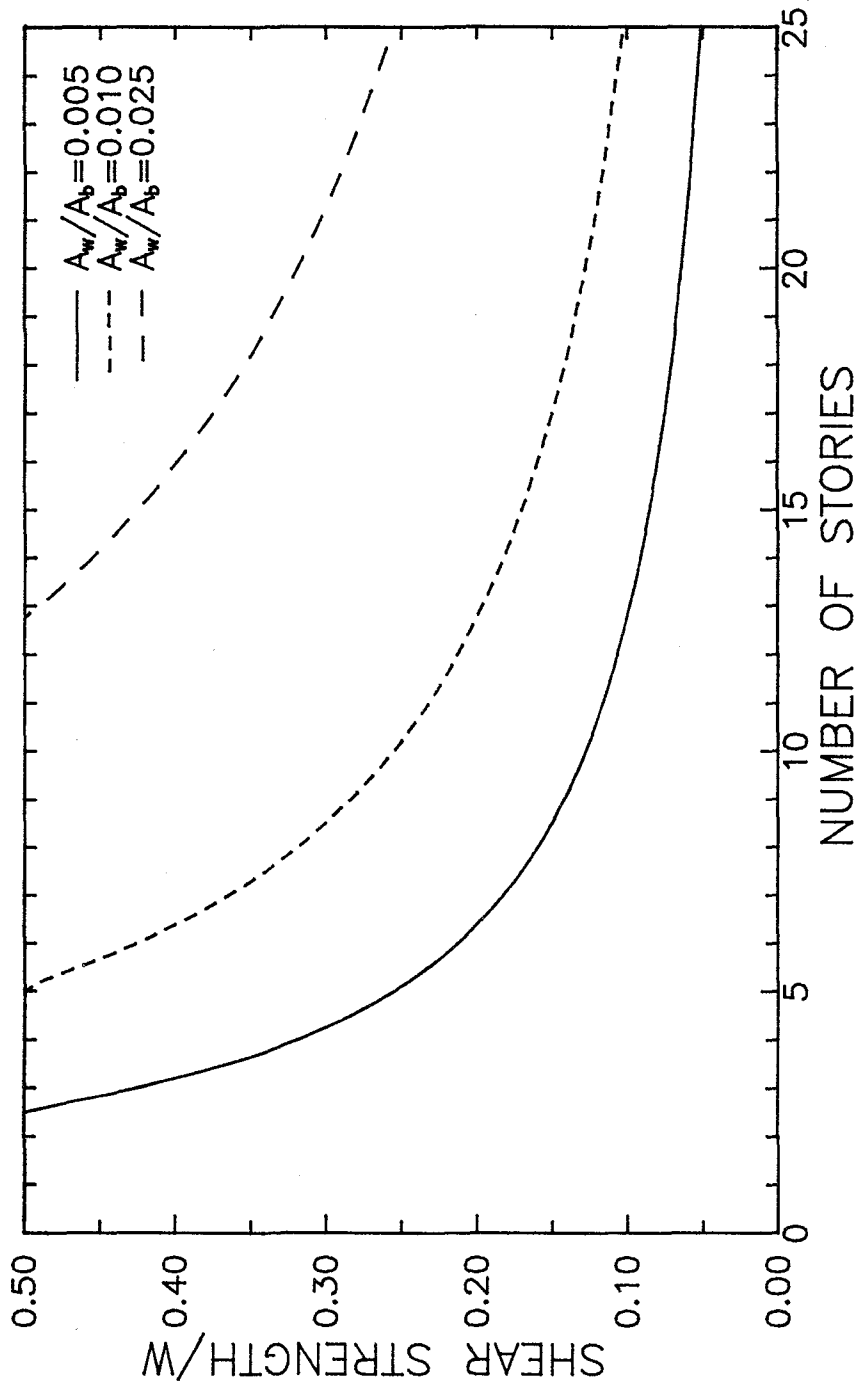


Fig. 8.4 Shear Strength versus Wall Area to Floor Area Ratio

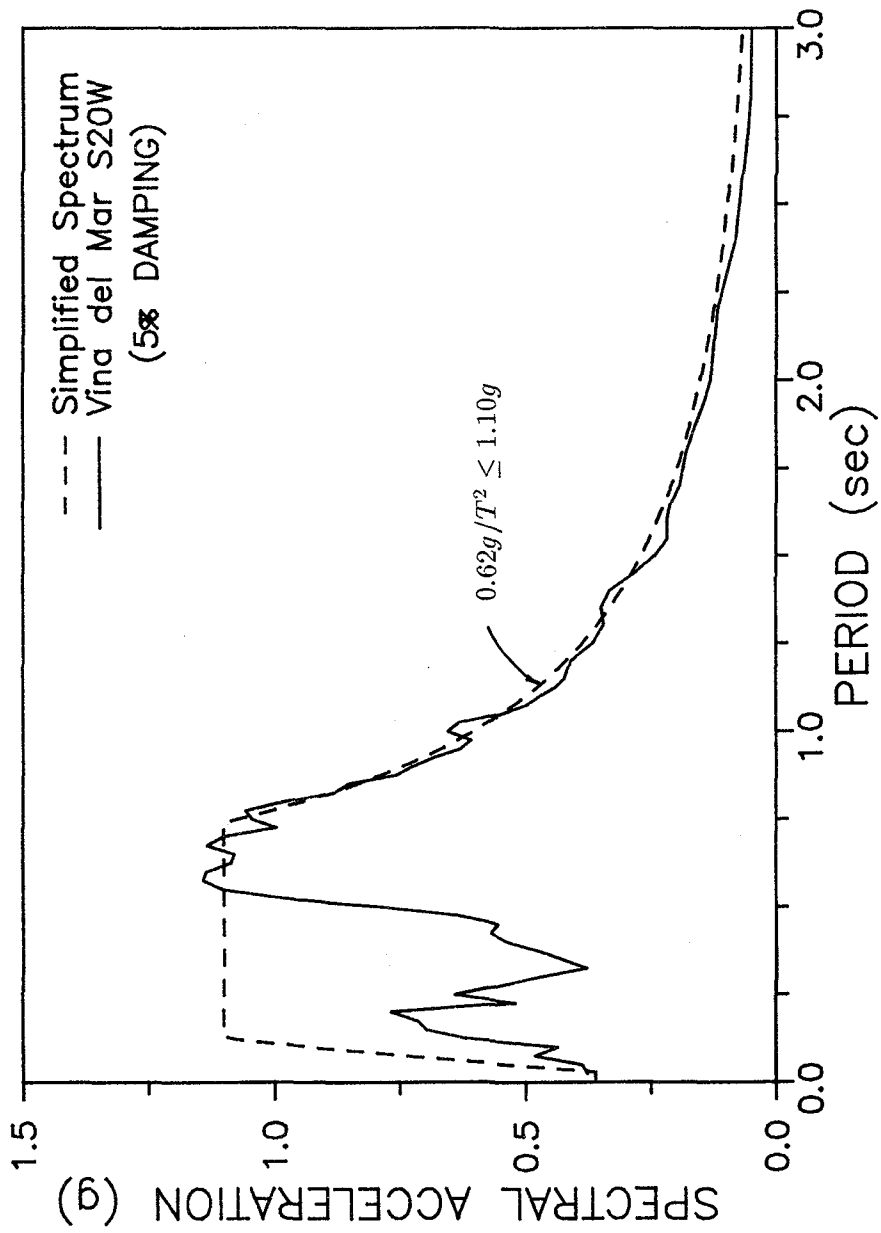


Fig. 8.5.a Acceleration Response Spectrum — Viña del Mar S20W

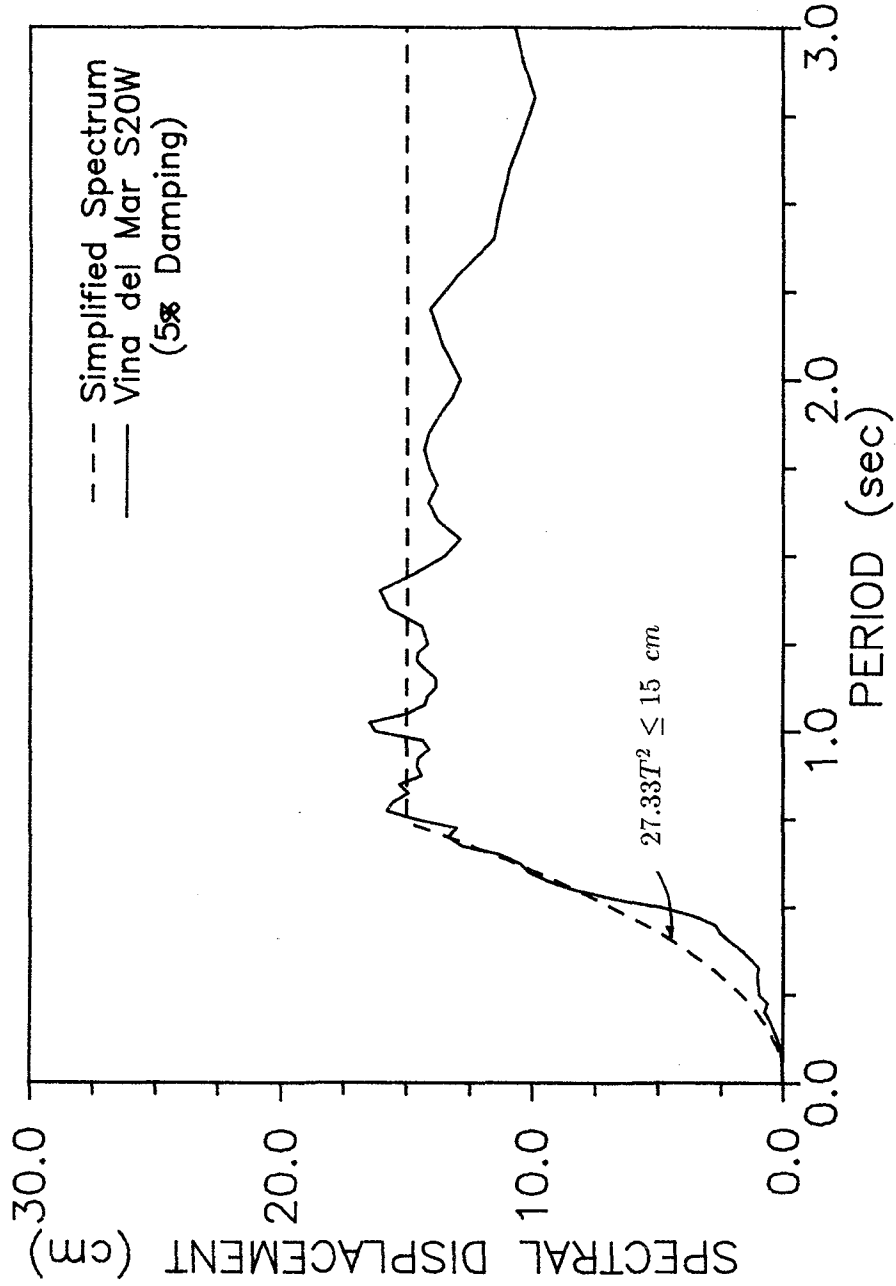


Fig. 8.5.b Displacement Response Spectrum — Viña del Mar S20W

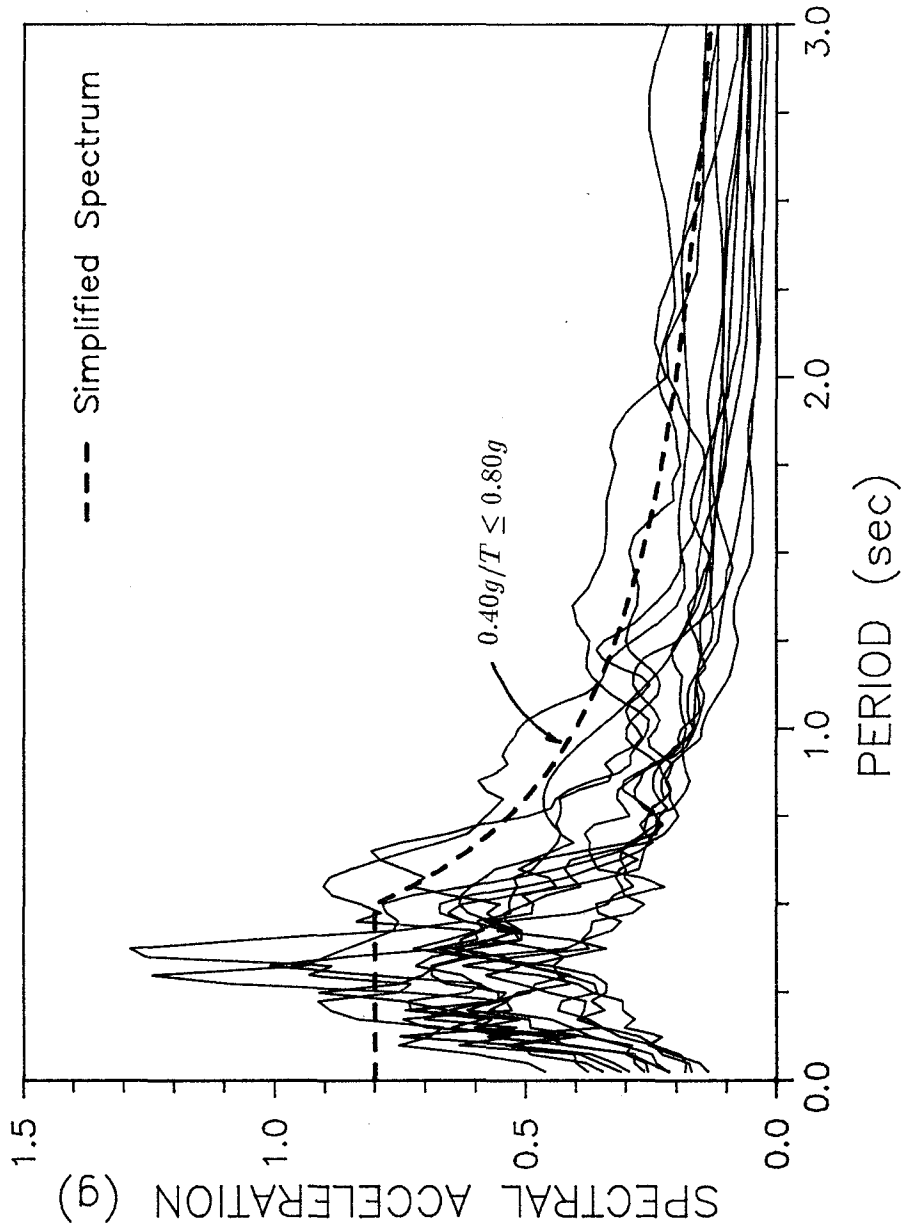


Fig. 8.6.a Acceleration Response Spectrum — Recorded U.S. Motions

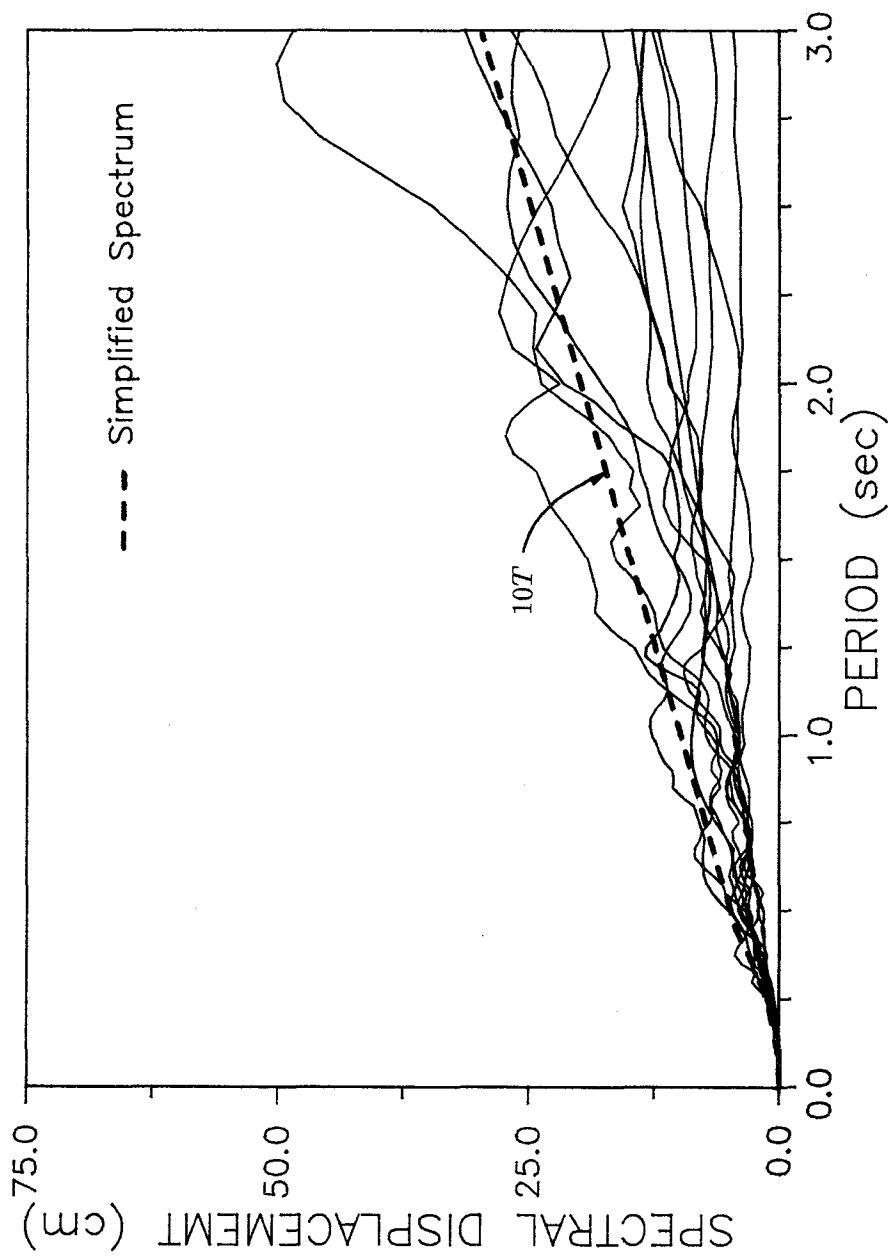


Fig. 8.6.b Displacement Response Spectrum — Recorded U.S. Motions

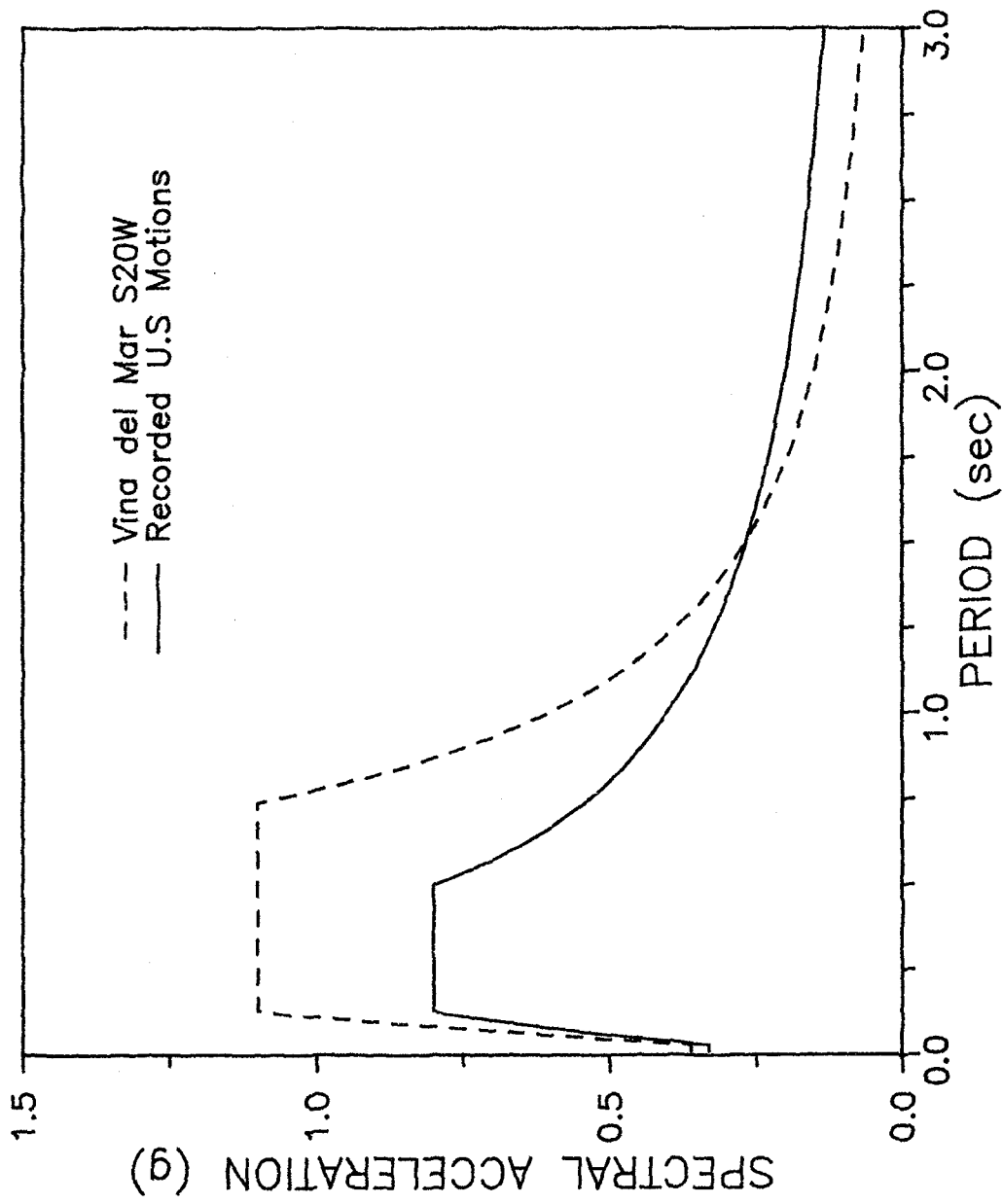


Fig. 8.7.a Comparison of Acceleration Response Spectra  
Recorded U.S. Motions - Viña del Mar S20W

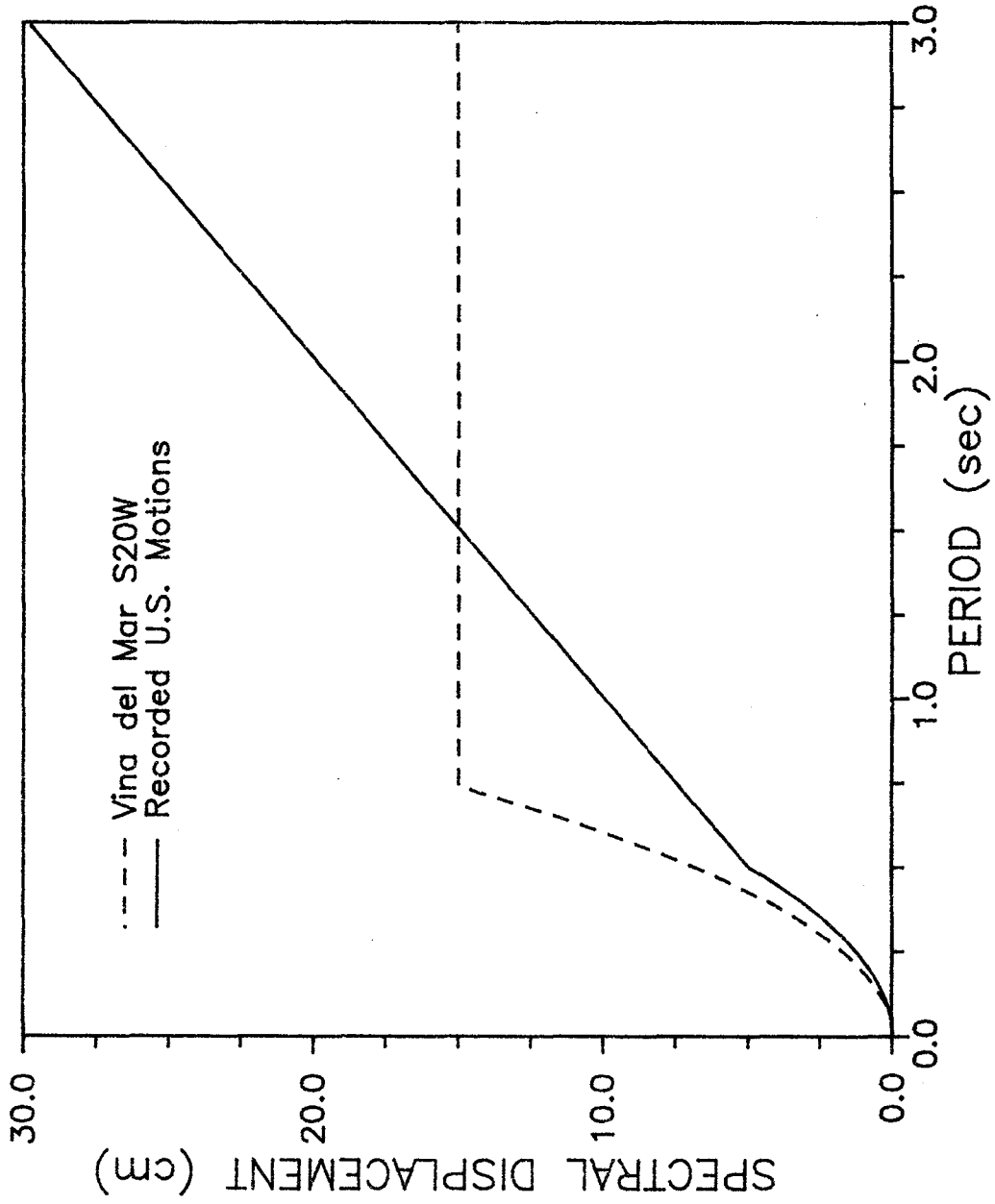


Fig. 8.7.b Comparison of Displacement Response Spectra  
Recorded U.S. Motions - Vina del Mar S20W

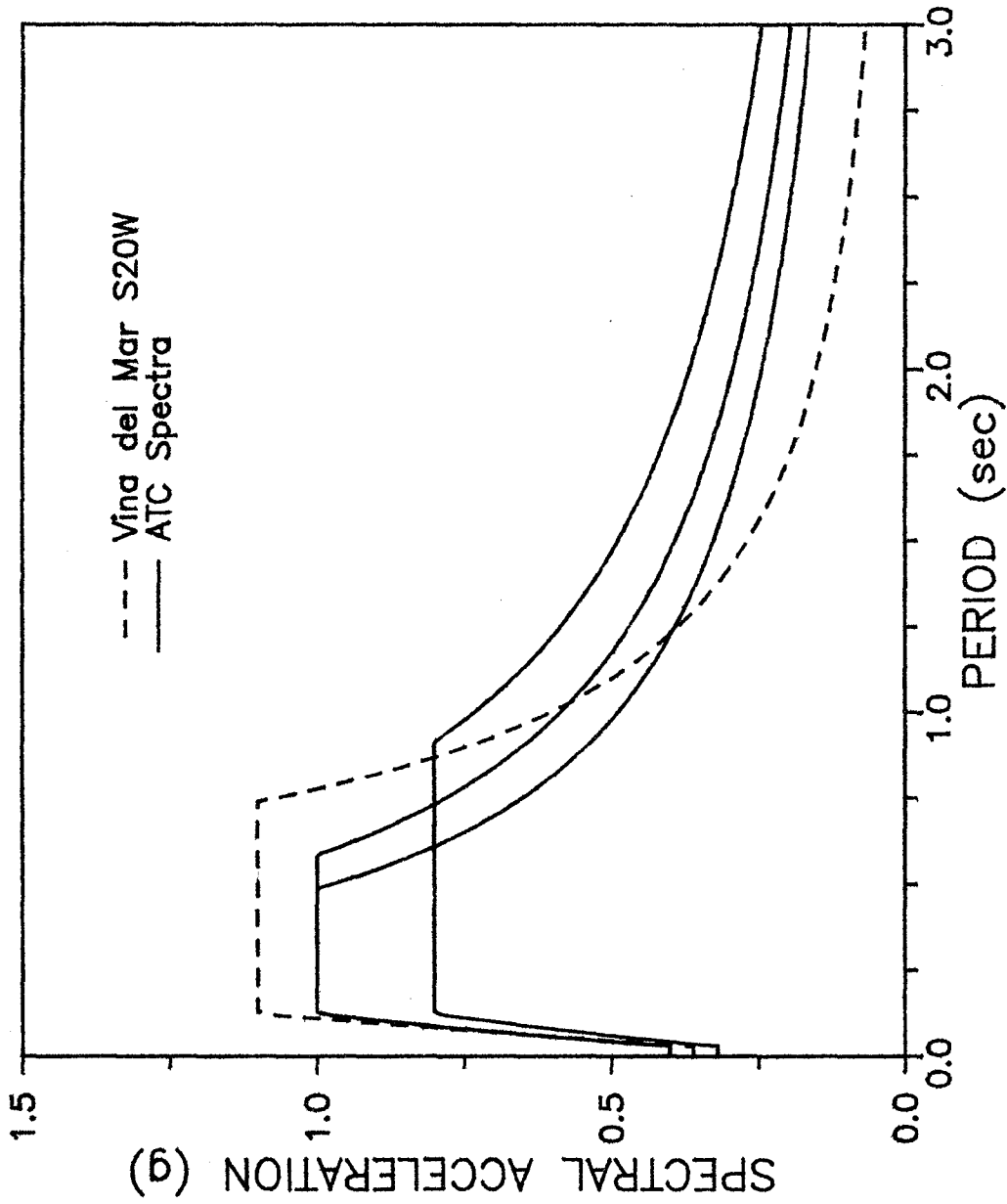


Fig. 8.8.a Comparison of Acceleration Response Spectra  
ATC-3-06 (1978) - Viña del Mar S20W

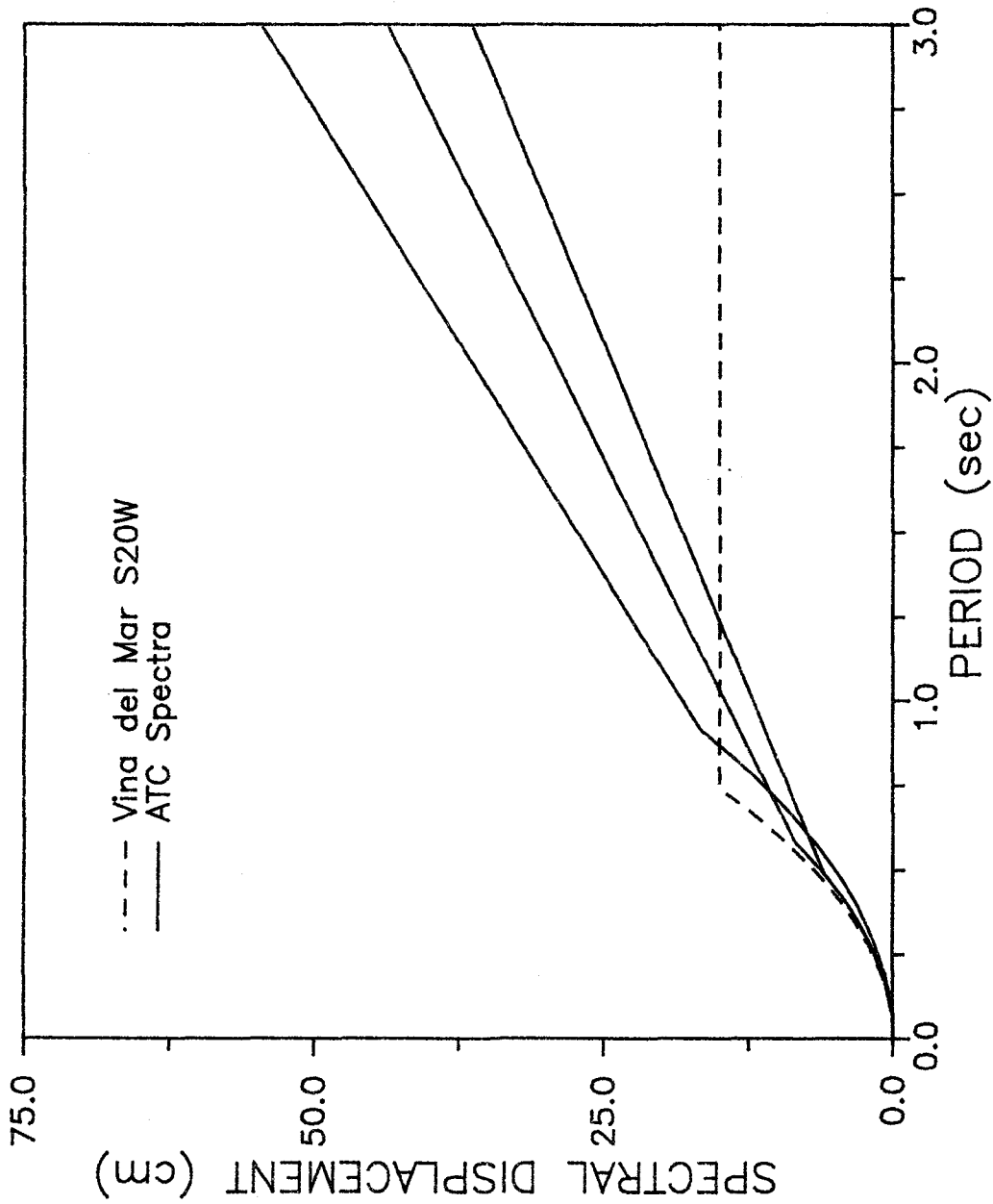


Fig. 8.8.b Comparison of Displacement Response Spectra  
ATC-3-06 (1978) - Vina del Mar S20W

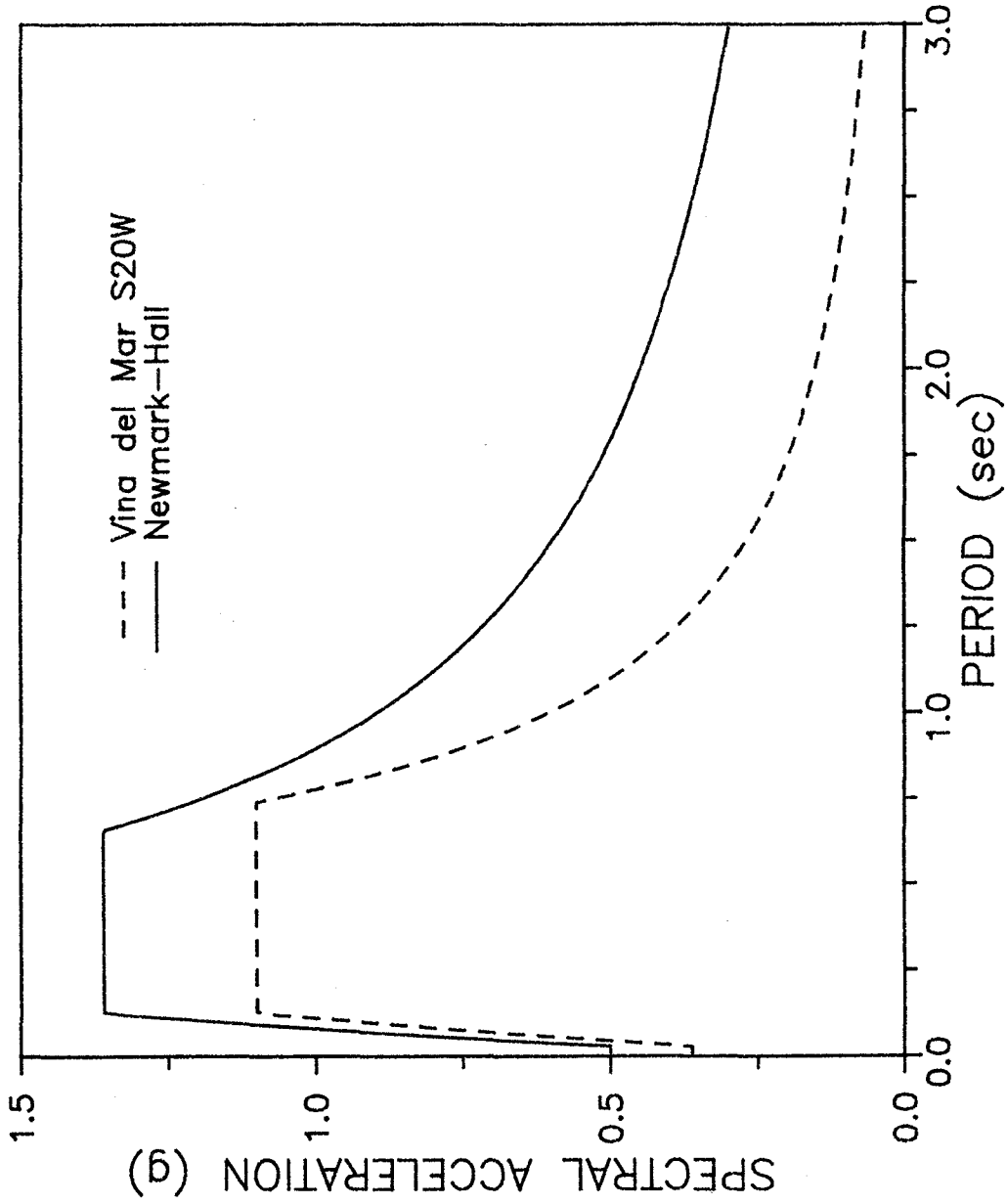


Fig. 8.9.a Comparison of Acceleration Response Spectra.  
Newmark-Hall (1982) - Vina del Mar S20W

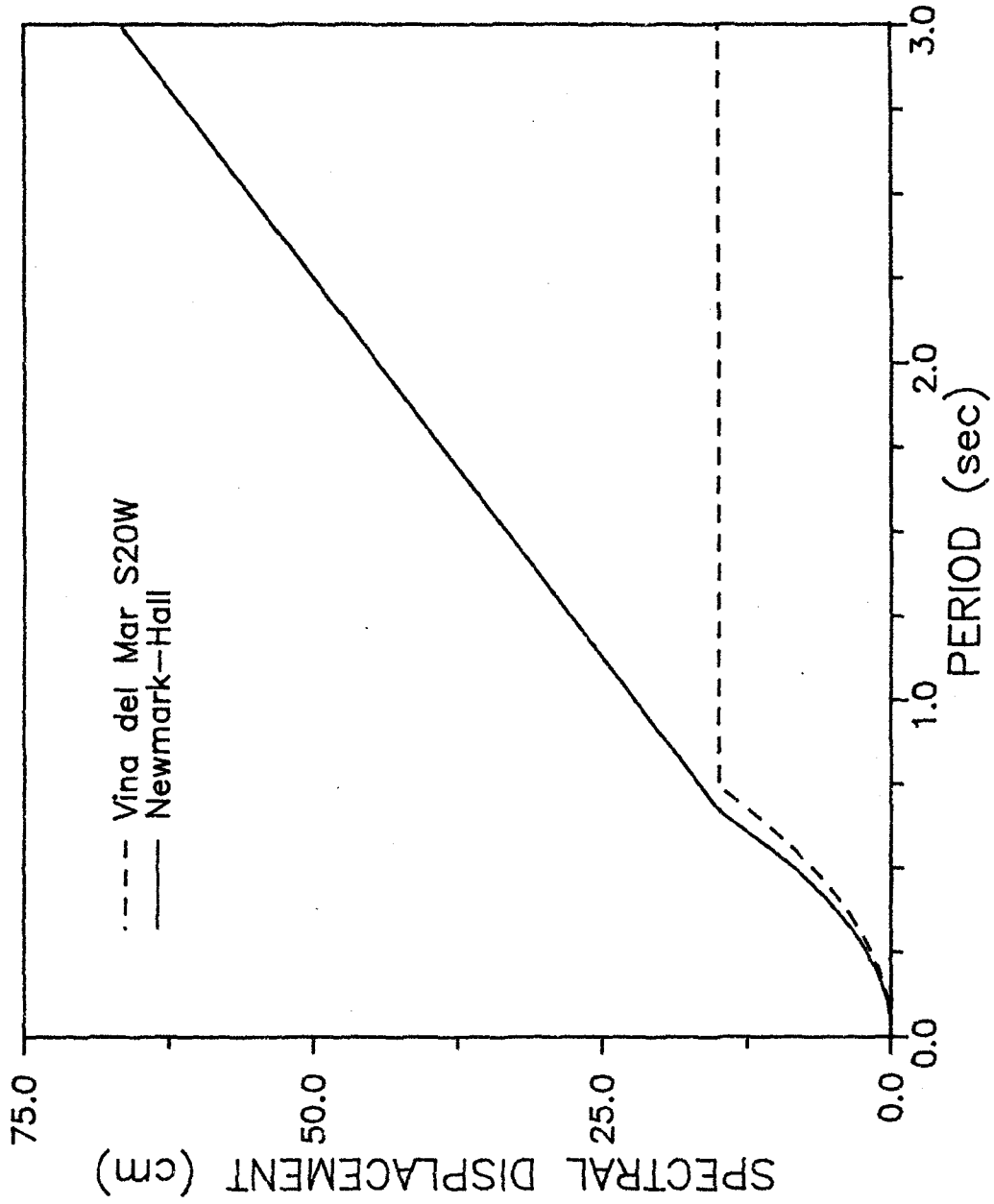


Fig. 8.9.b Comparison of Displacement Response Spectra  
Newmark-Hall (1982) - Viña del Mar S20W

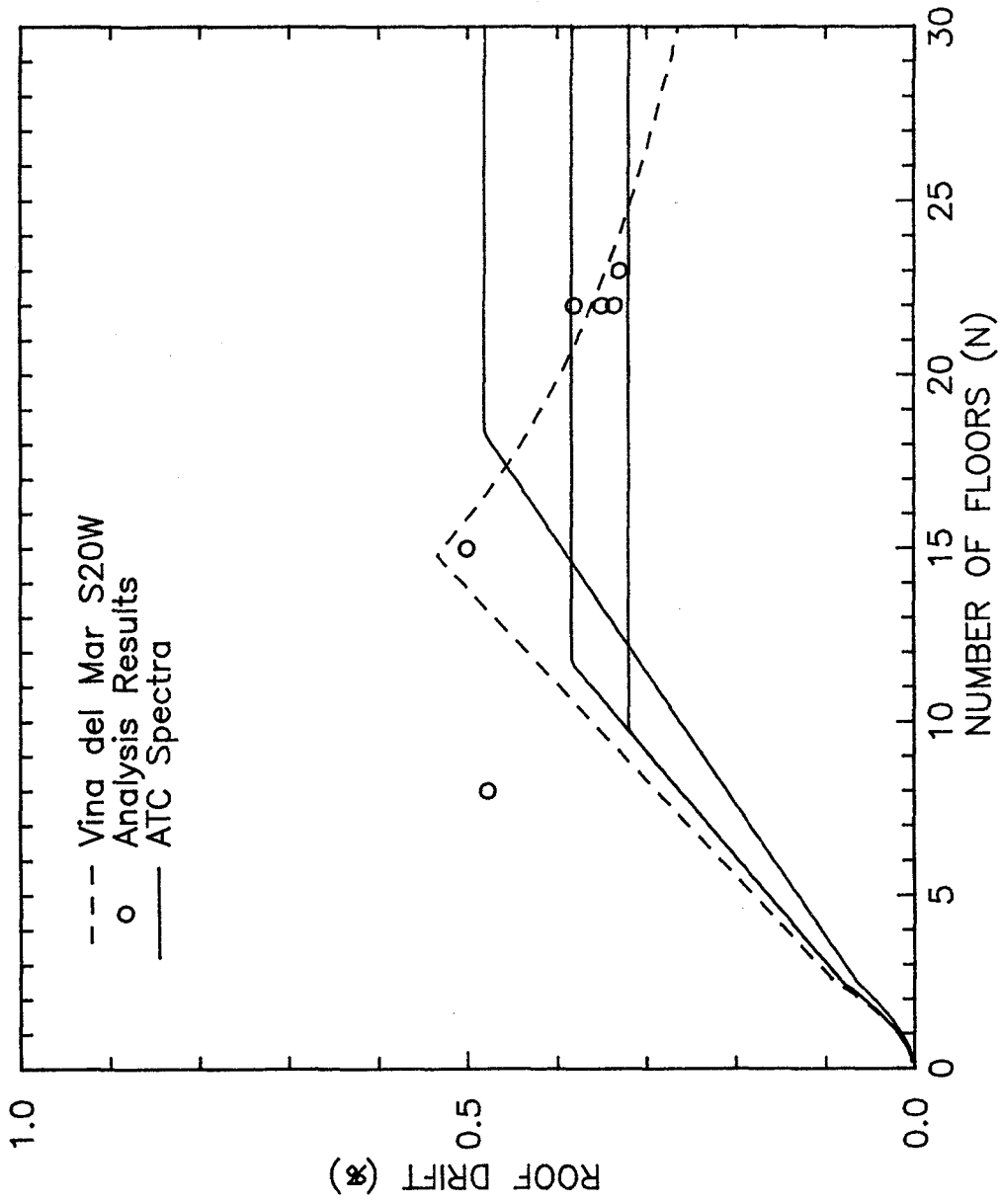


Fig. 8.10 Comparison of Roof Drift versus Number of Floors — Wall Buildings ATC-3-06 (1978) — Viña del Mar S20W

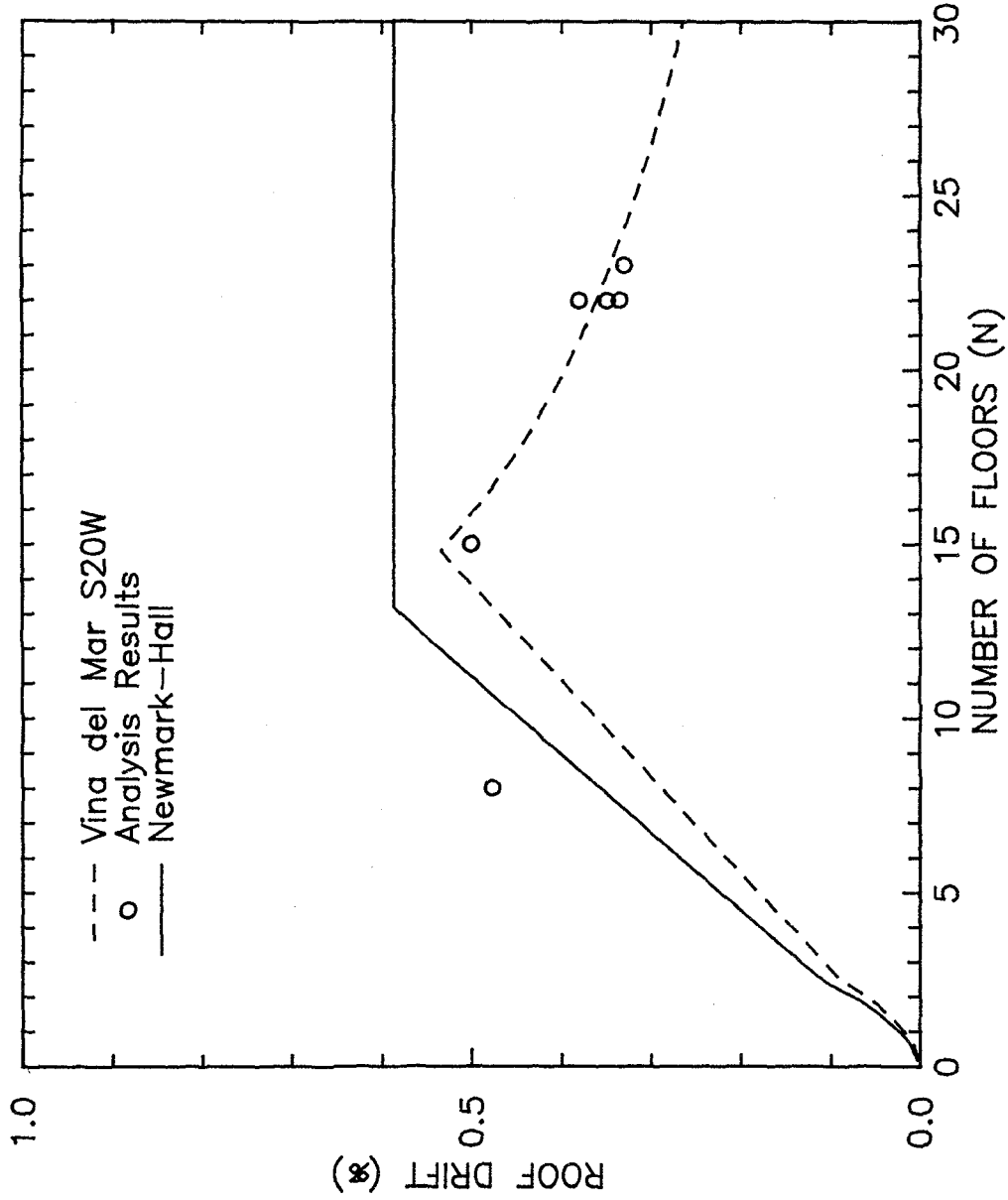


Fig. 8.11 Comparison of Roof Drift versus Number of Floors — Wall Buildings  
Newmark-Hall (1982) — Vina del Mar S20W

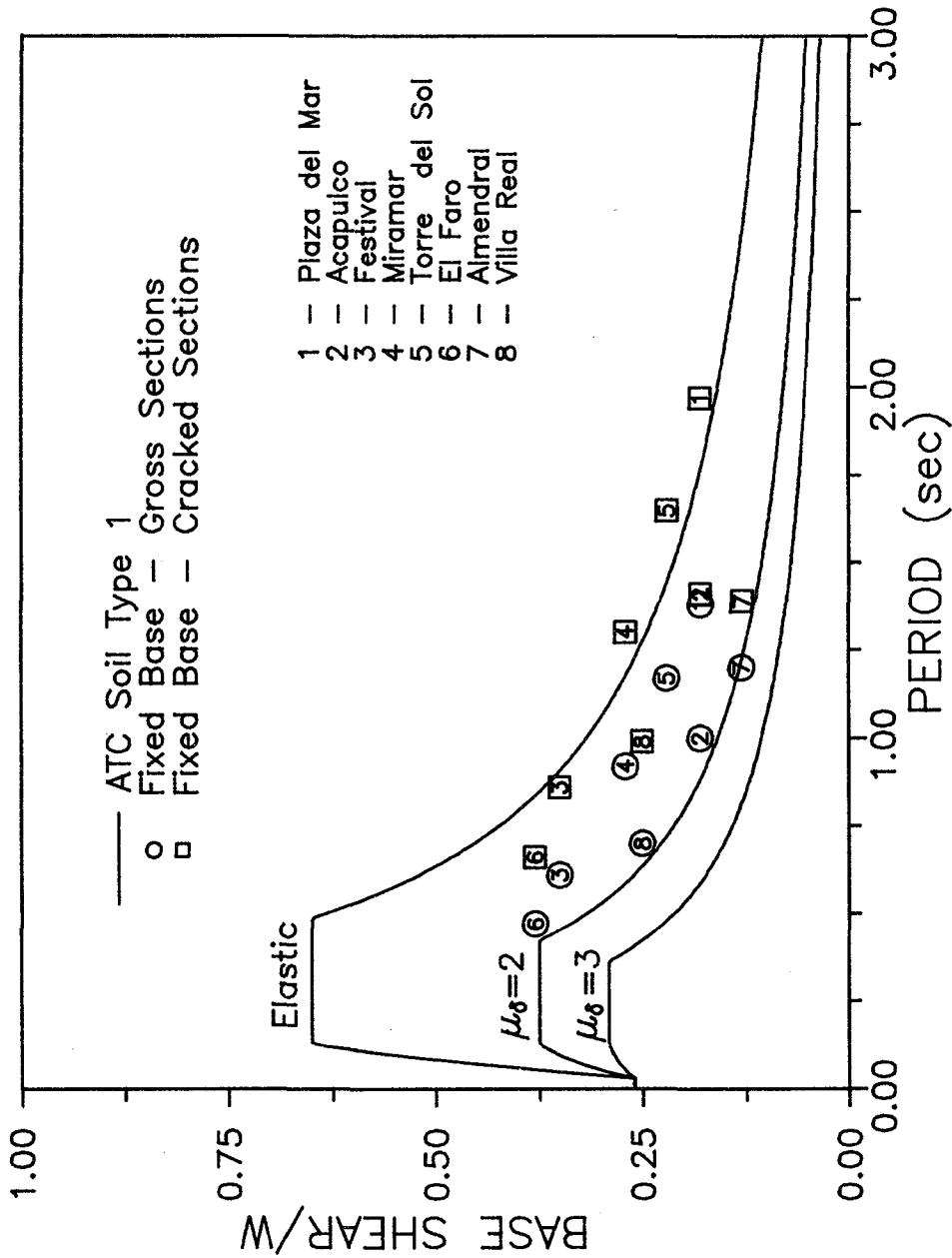


Fig. 8.14 Base Shear versus Period — ATC-3-06 (1978) Soil Type 1  
 Displacement Ductilities,  $\mu_\delta = 1, 2, 3$

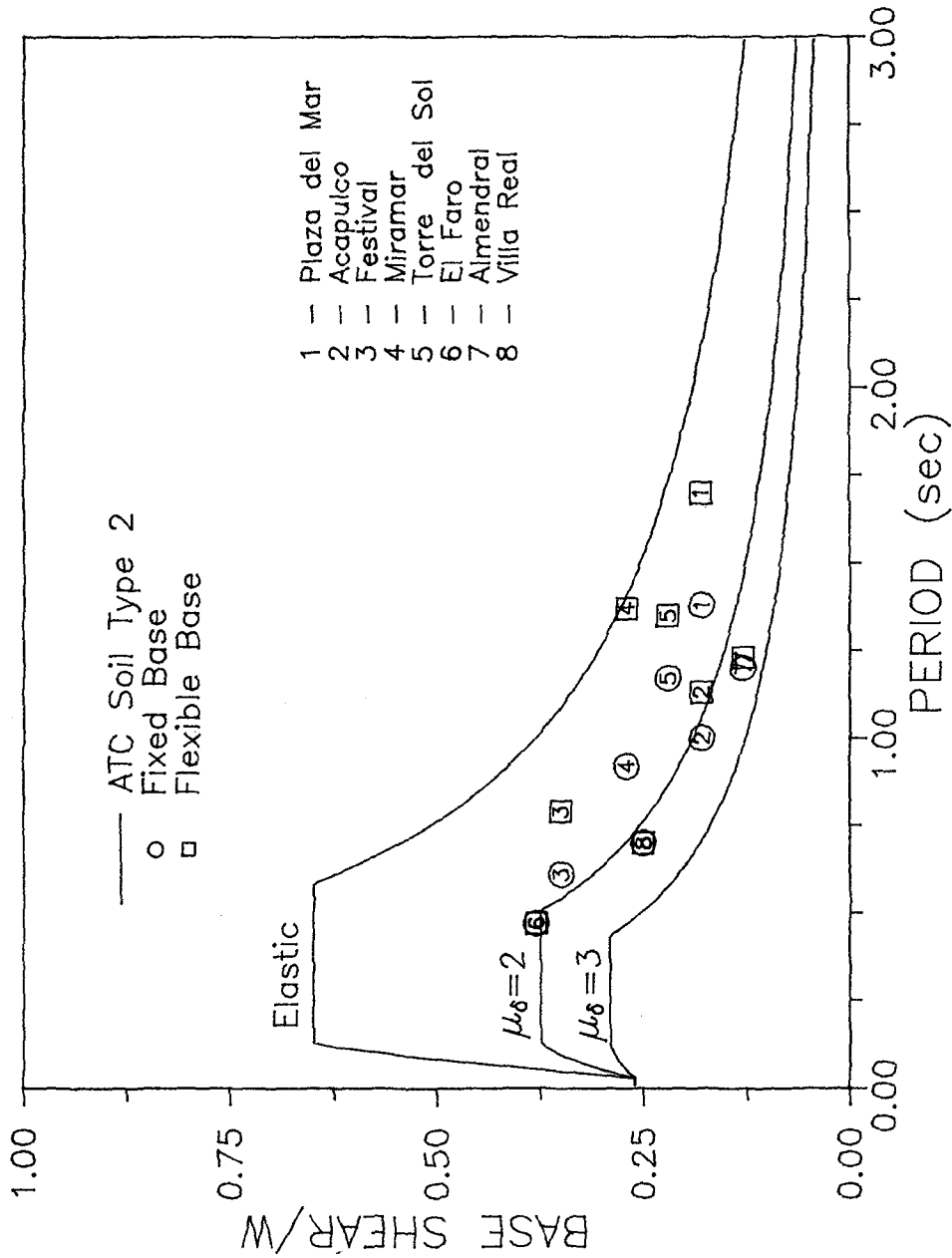


Fig. 8.15 Base Shear versus Period — ATC-3-06 (1978) Soil Type 2  
 Displacement Ductilities,  $\mu_\delta = 1, 2, 3$

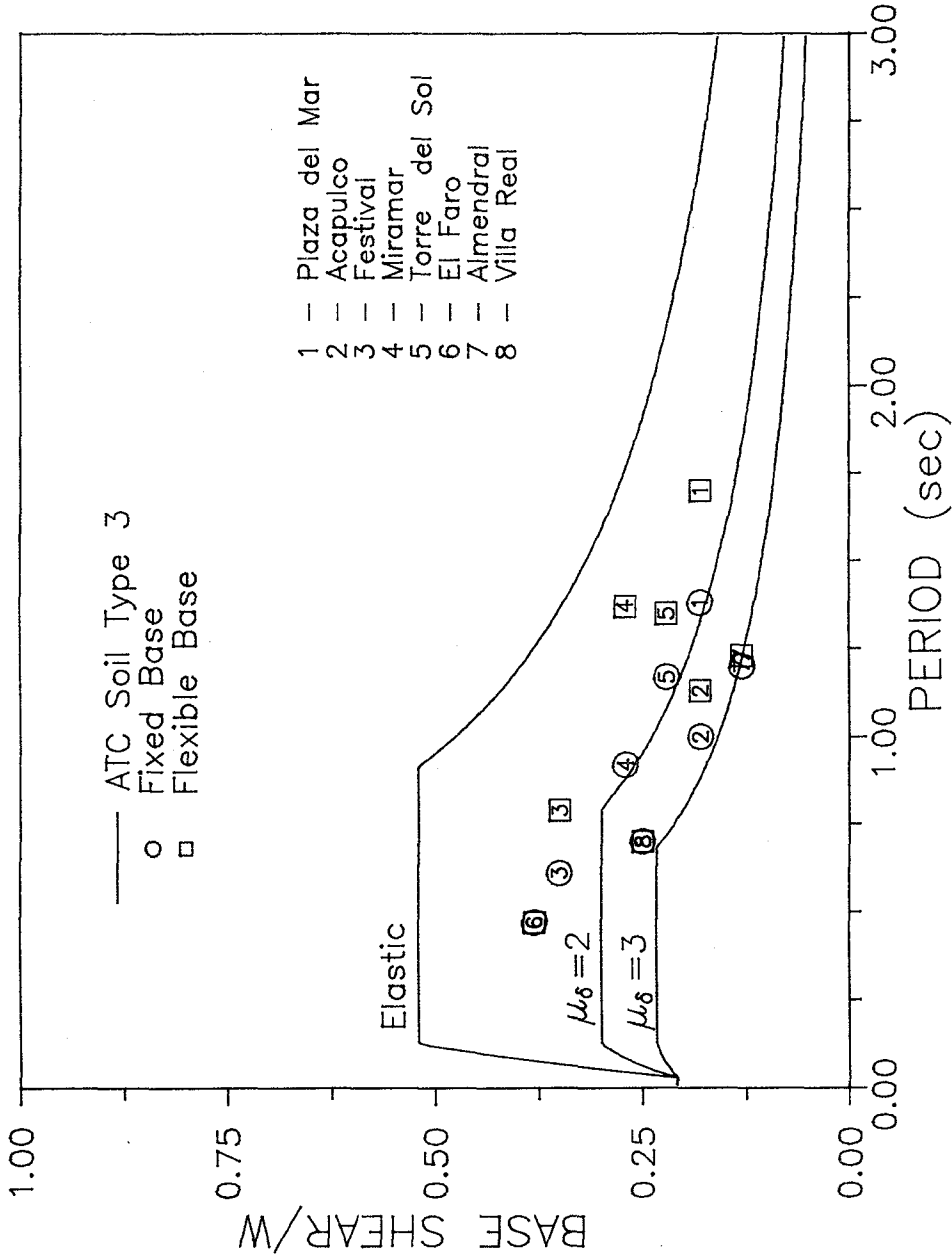


Fig. 8.16 Base Shear versus Period — ATC-3-06 (1978) Soil Type 3  
Displacement Ductilities,  $\mu_\delta = 1, 2, 3$

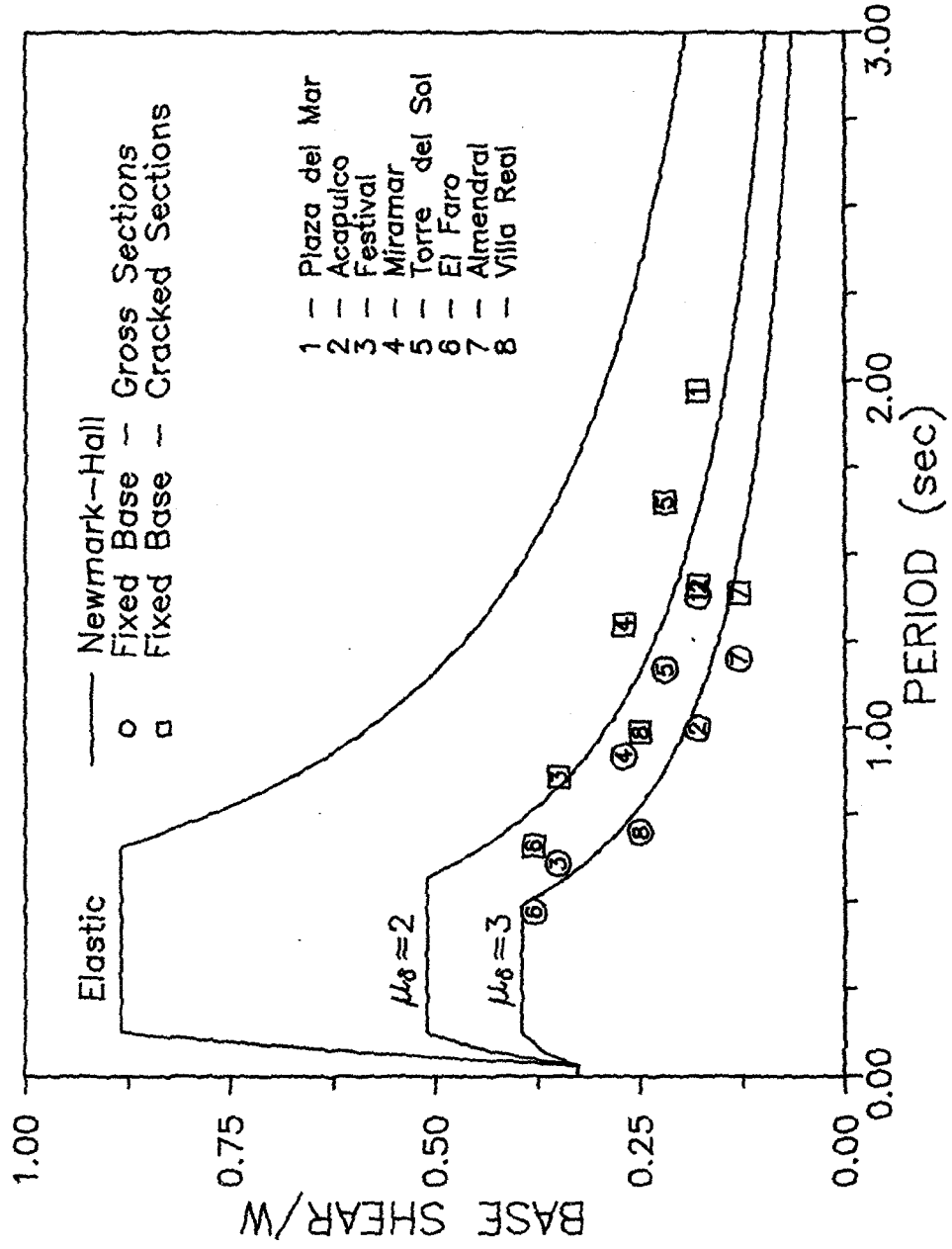


Fig. 8.17 Base Shear versus Period (Firm Ground) --- Newmark-Hall (1982)  
 Displacement Ductilities,  $\mu_s = 1, 2, 3$

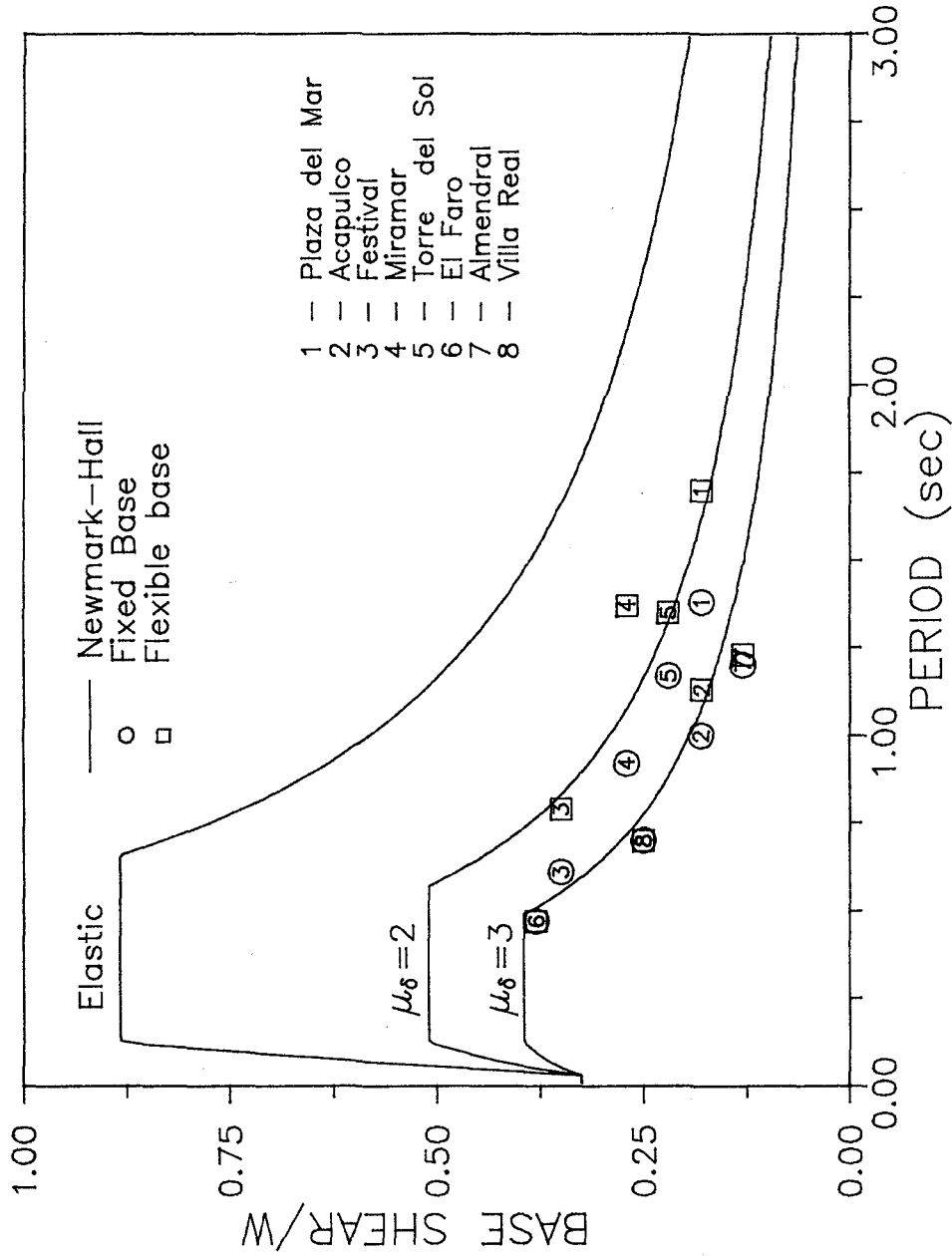


Fig. 8.18 Base Shear versus Period (Flexible Ground) — Newmark-Hall (1982)  
Displacement Ductilities,  $\mu_s = 1, 2, 3$

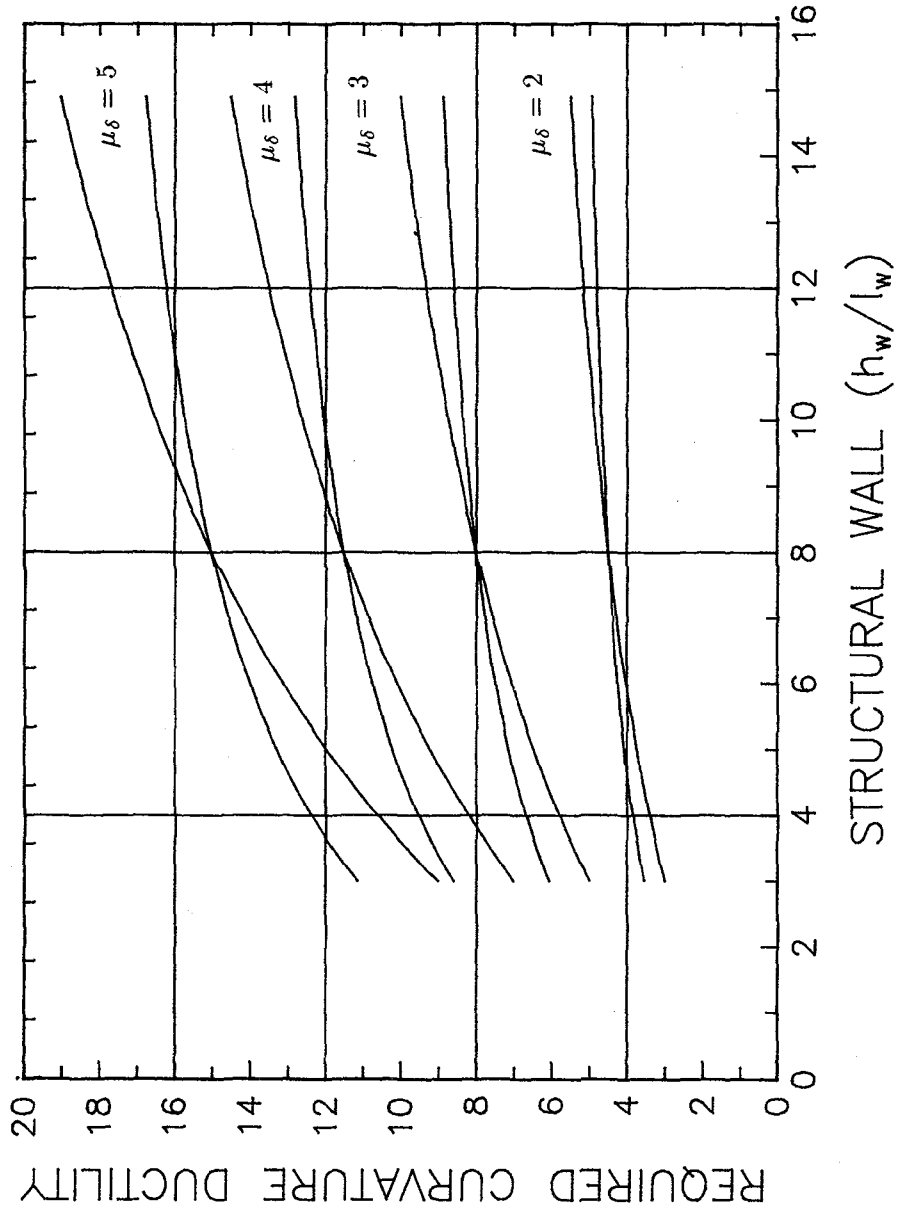


Fig. 8.19 Required Wall Curvature Ductility  
Displacement Ductilities,  $\mu_\delta = 2, 3, 4, 5$

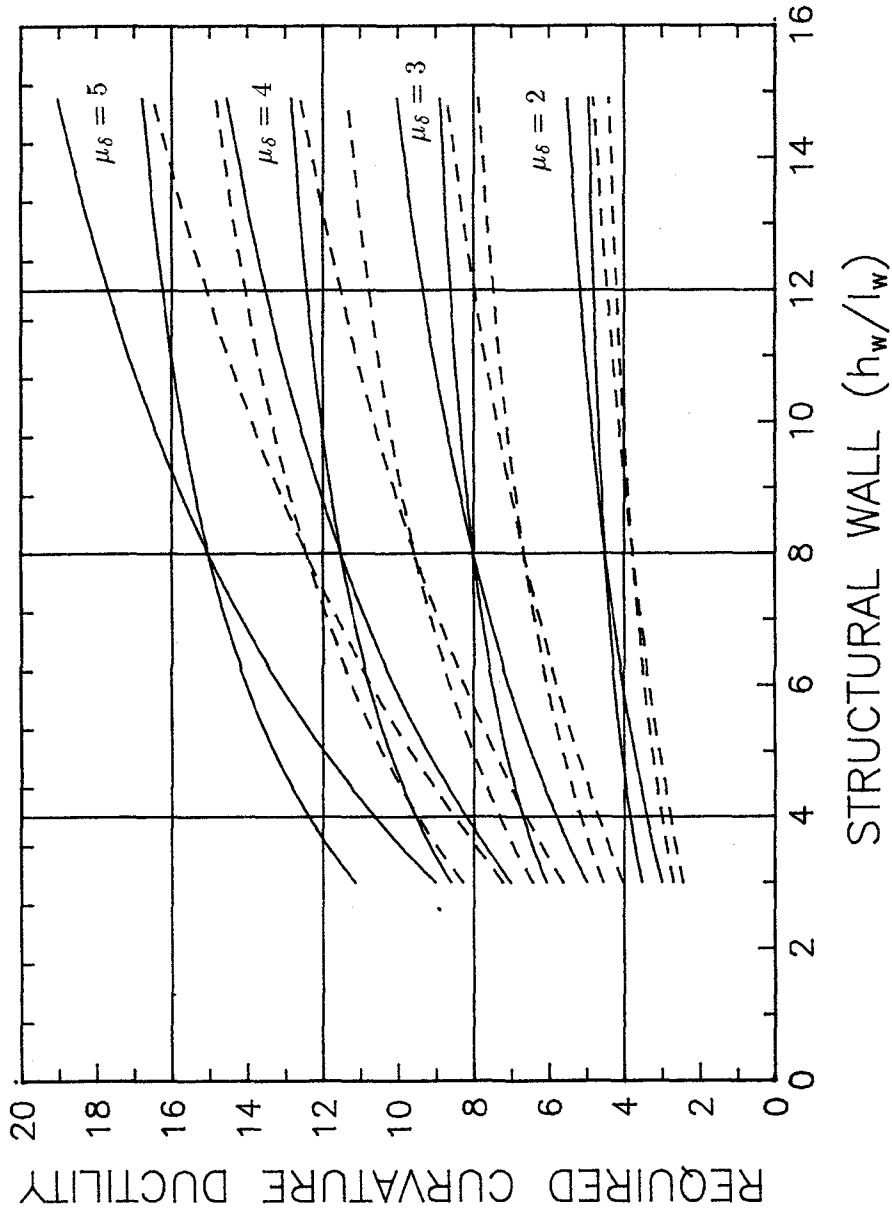


Fig. 8.20.a Effect of Anchorage Pullout on Required Wall Curvature Ductility  
 10 ft Wall — Displacement Ductilities,  $\mu_\delta = 2, 3, 4, 5$

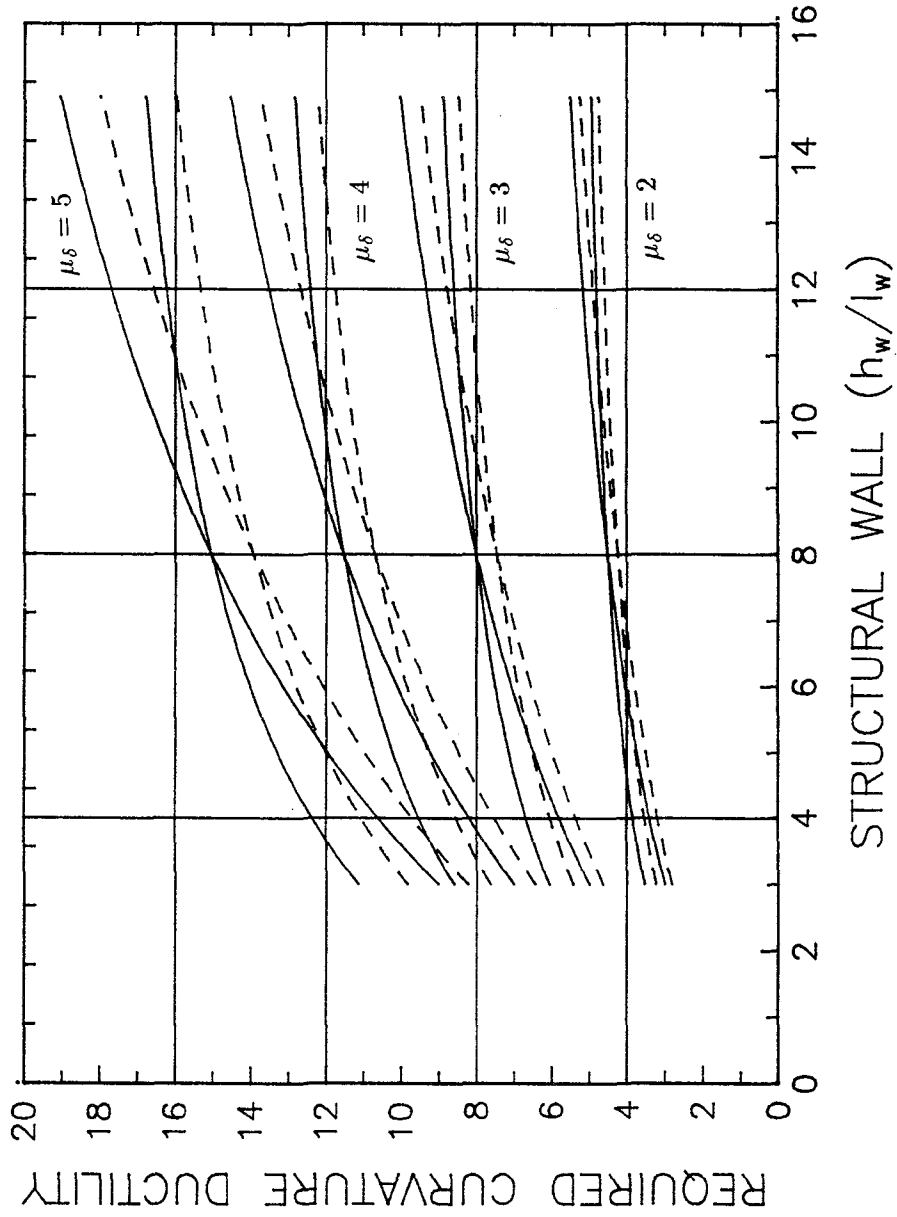


Fig. 8.20.b Effect of Anchorage Pullout on Required Wall Curvature Ductility  
20 ft Wall — Displacement Ductilities,  $\mu_\delta = 2, 3, 4, 5$

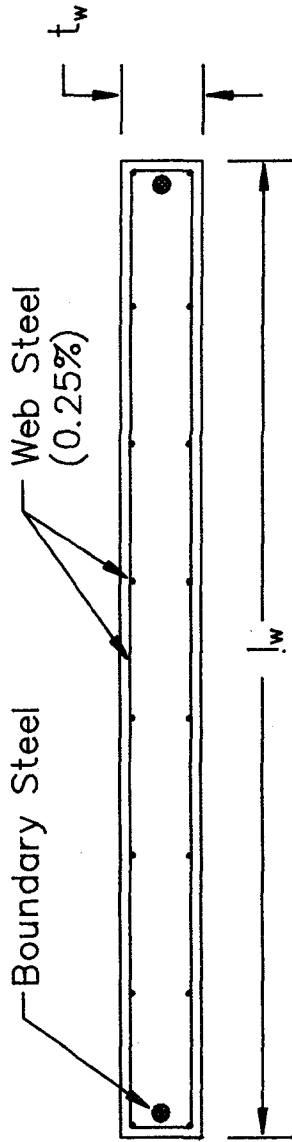


Fig. 8.21 Wall Geometry and Reinforcing Details

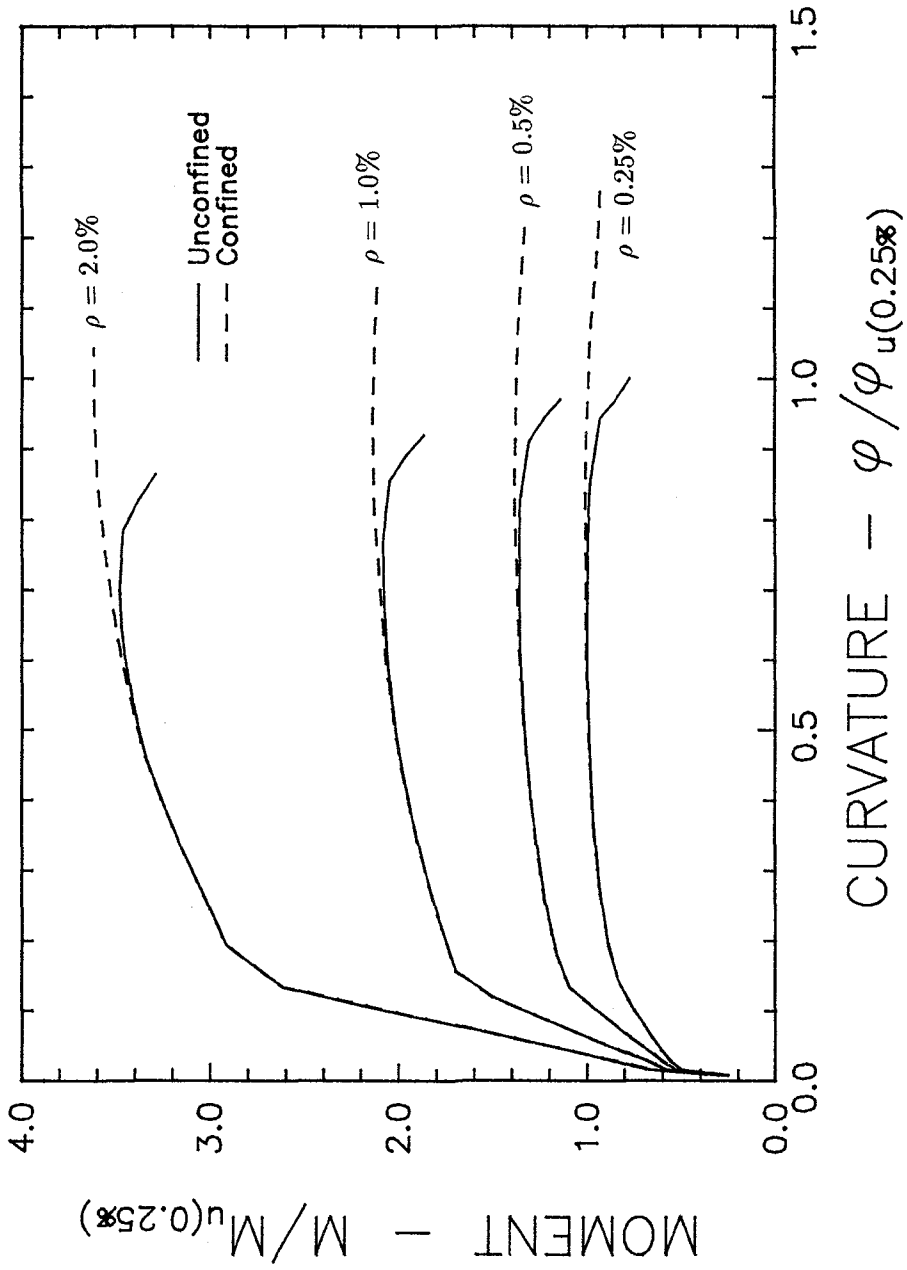


Fig. 8.22.a Computed Wall Curvature — 10 ft Wall  
Steel Ratios — 0.25%, 0.50%, 1.00%, 2.00%

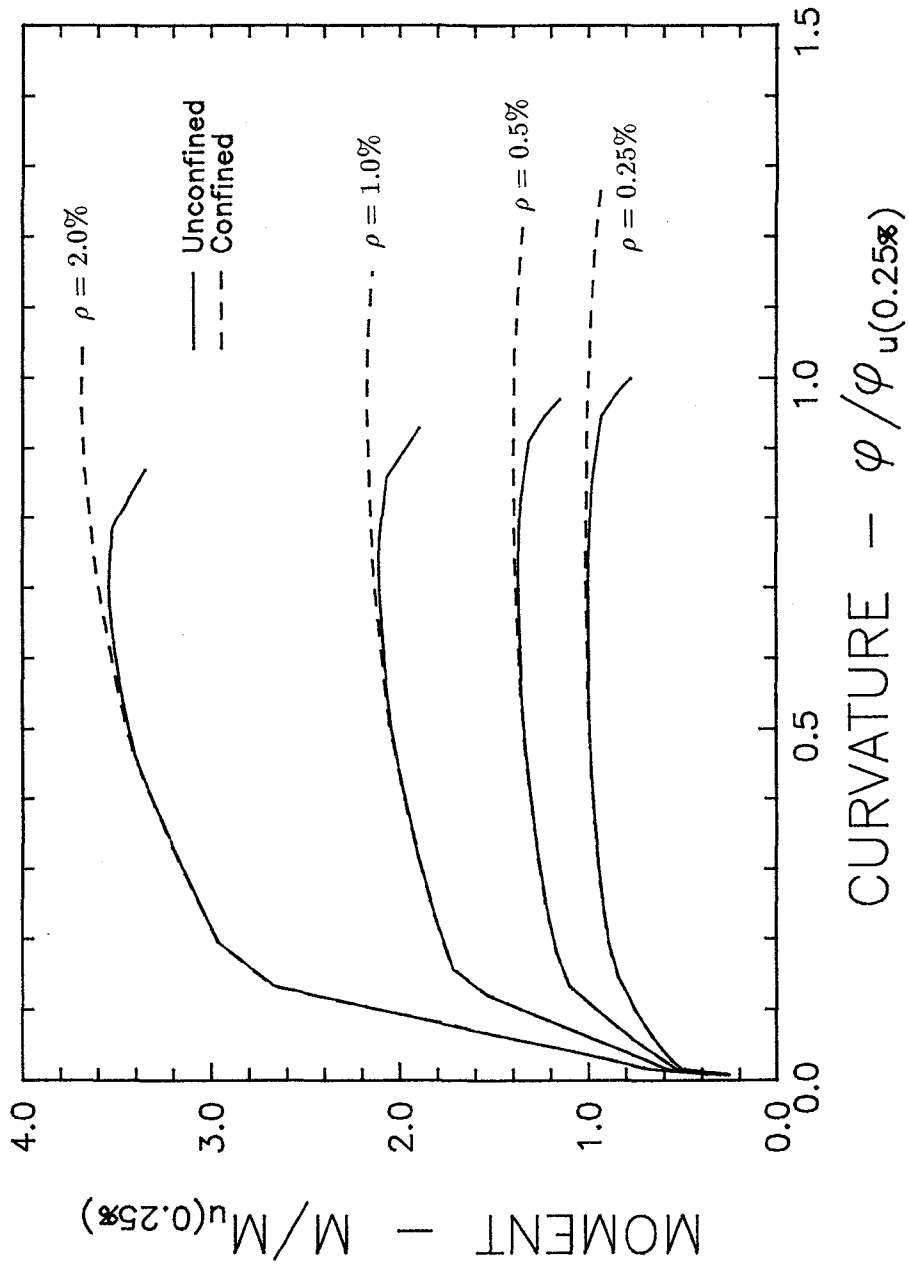


Fig. 8.22.b Computed Wall Curvature — 20 ft Wall  
Steel Ratios — 0.25%, 0.50%, 1.00%, 2.00%

# APPENDIX A

## GEOTECHNICAL CHARACTERISTICS OF SOIL

### IN VIÑA DEL MAR

Detailed soil investigations are not generally conducted because the fairly uniform soil deposits in Viña del Mar are considered to be good foundation materials. The available data indicate that, when required, a typical geotechnical investigation involves the following [Wood et al. (1987)]:

Bore holes	10 – 20 m
Standard penetration tests	8 – 25 m
Dynamic cone tests	8 – 12 m
Grain size analysis	

The results from bore hole and standard penetration tests for eight sites in Viña del Mar are summarized in this Appendix. The characteristic site period is also computed for two of the sites (Borings #1 and #2, and #8). More detailed descriptions of the soil using data from 46 borings in Viña del Mar are presented in Reference 4.8.

The locations of the eight test sites are shown in Fig. A.1. The data obtained at these locations are presented in Fig. A.2–A.9.

Five of the sites are near the beach where the buildings studied in Chapters 6–8 reside. Borings #1 and #2 are close to the site of the Torres de Miramar building. Borings #3 and #5 are close to the Acapulco and Plaza del Mar buildings, and borings #4 and #5 are near the Festival building. The borings indicate that layers of coarse to medium grained sand and fine gravel extend to depths of 20 m. The standard penetration test data indicated the deposits are relatively dense below depths of 2–4 m [4.18]

Boring #8 was obtained just north of the Marga–Marga River within 400 m of the instrument that recorded the 3 March 1985 earthquake. The boring indicated medium to fine grained sands for depths up to about 20 m, with silty sand at greater depths. Standard penetration tests again revealed the sands are relatively dense.

The shear wave velocity can be calculated from the standard penetration test data using equation A.1

$$V_s = 200\sqrt{N_1} \quad (\text{A.1})$$

where  $N_1$  is the blow count corrected for overburden pressure. The characteristic site period can then be calculated from the following expressions [Seed (1975)]

$$T_s = \frac{4H}{\bar{C}_s} \quad (\text{A.2})$$

$$\bar{C}_s = \frac{R_i \sum_{i=1}^n C_{si} H_i}{H} \quad (\text{A.3})$$

$$H = \sum_{i=1}^n H_i \quad (\text{A.4})$$

where  $T_s$  is the characteristic site period,  $H$  is the total depth of the soil deposit to bedrock,  $\bar{C}_s$  is the strain corrected shear wave velocity for an equivalent uniform layer,  $H_i$  is the thickness of soil layer  $i$ , and  $R$  is a factor used to convert the average value of  $C_{si}$  to a velocity consistent with the strain levels of the soil in an earthquake. Table 6.1 presents the values recommended by ATC–3–06 (1978). Values of 0.9 and 0.65 are recommended for moderate and intense ground motions, respectively.

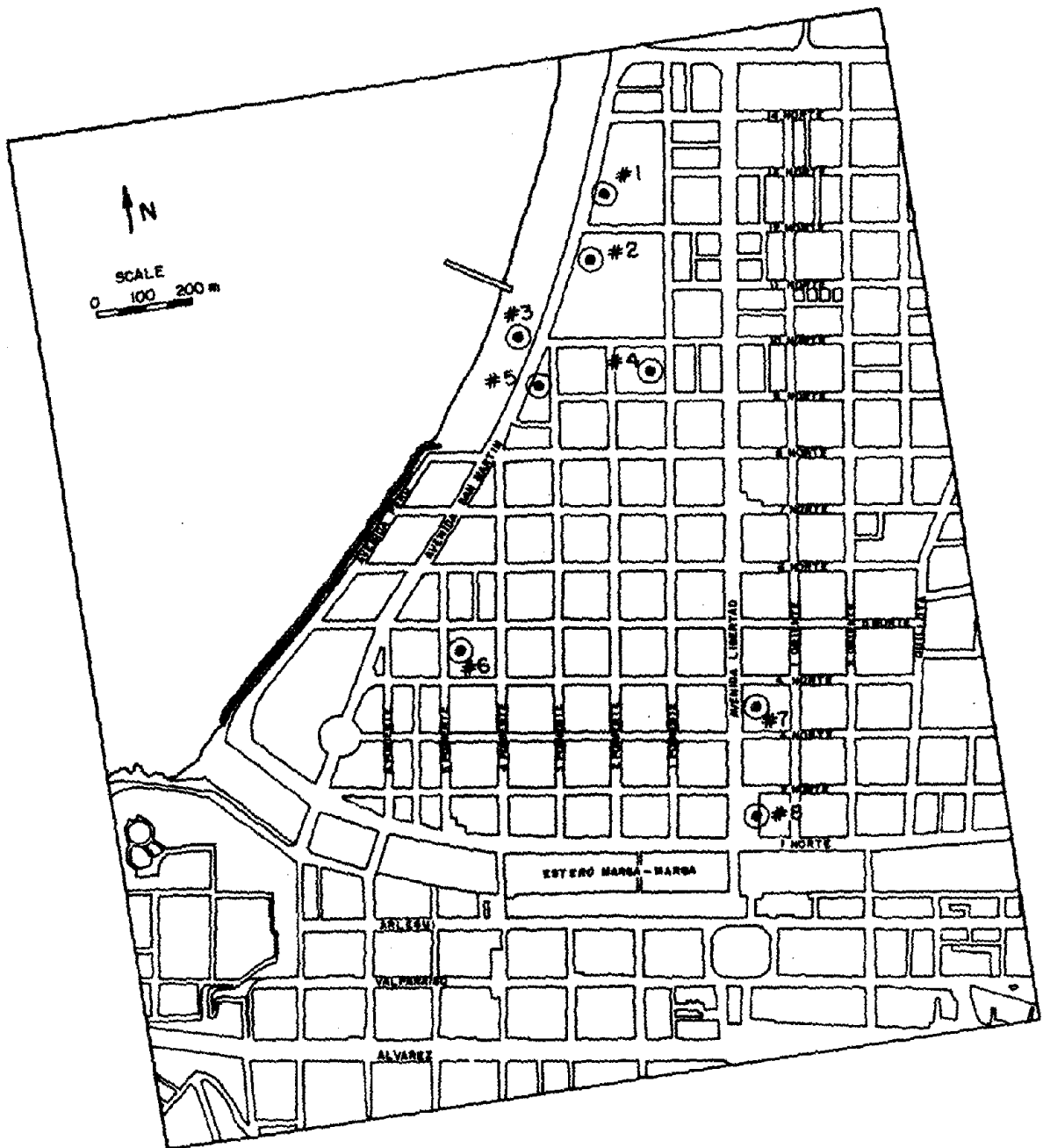
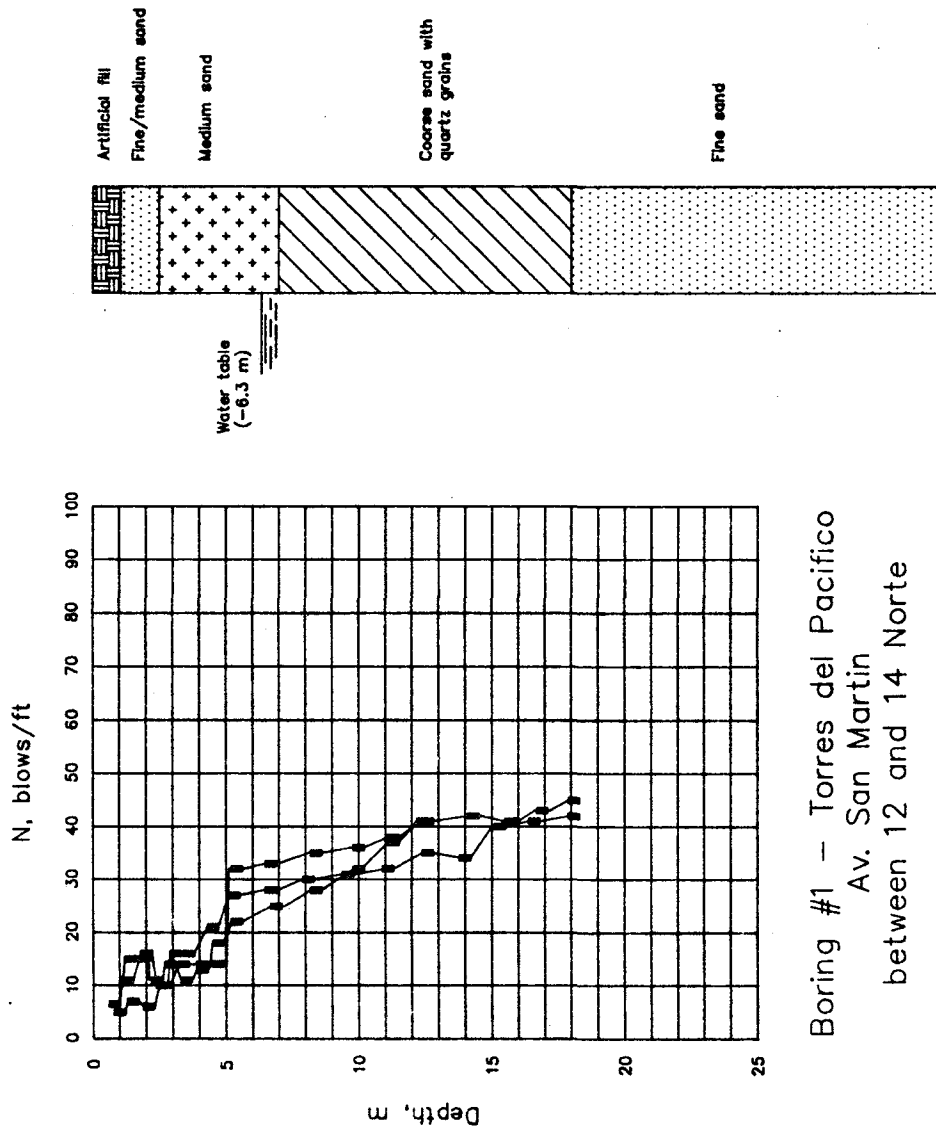


Fig. A.1 Locations of Soil Borings



Boring #1 - Torres del Pacifico  
 Av. San Martin  
 between 12 and 14 Norte

Fig. A.2 Soil Profile and Standard Penetration Test Data for Boring #1

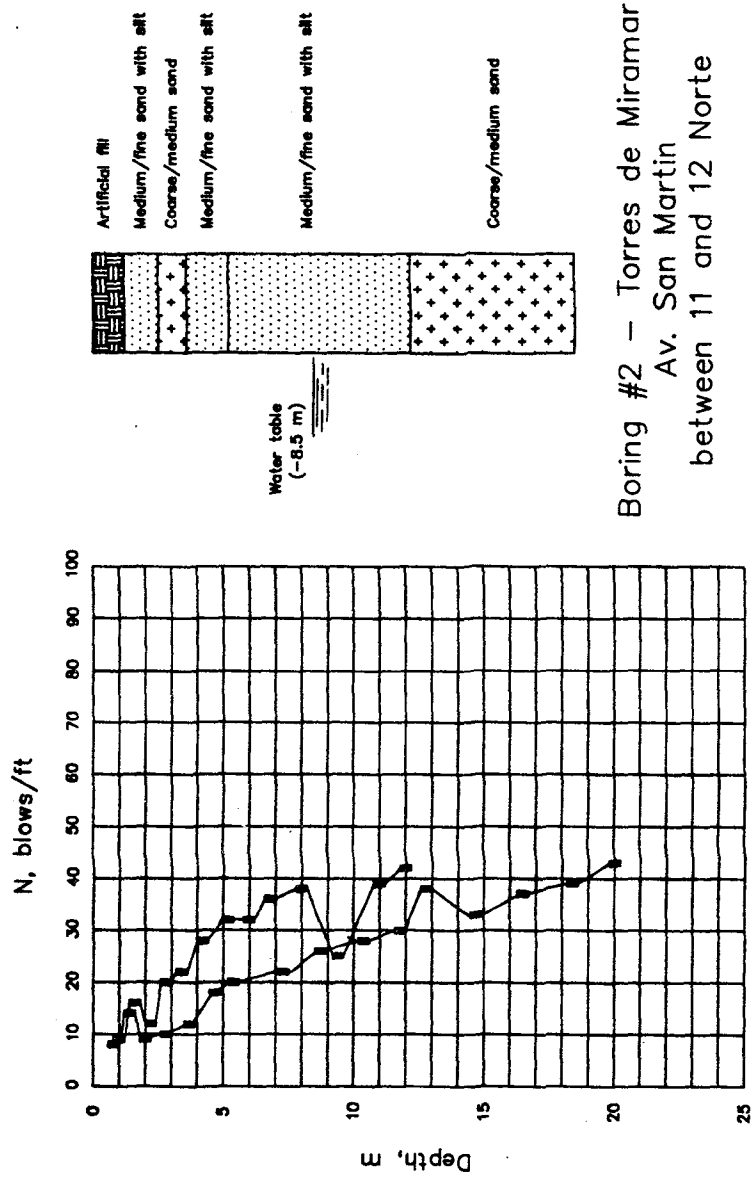
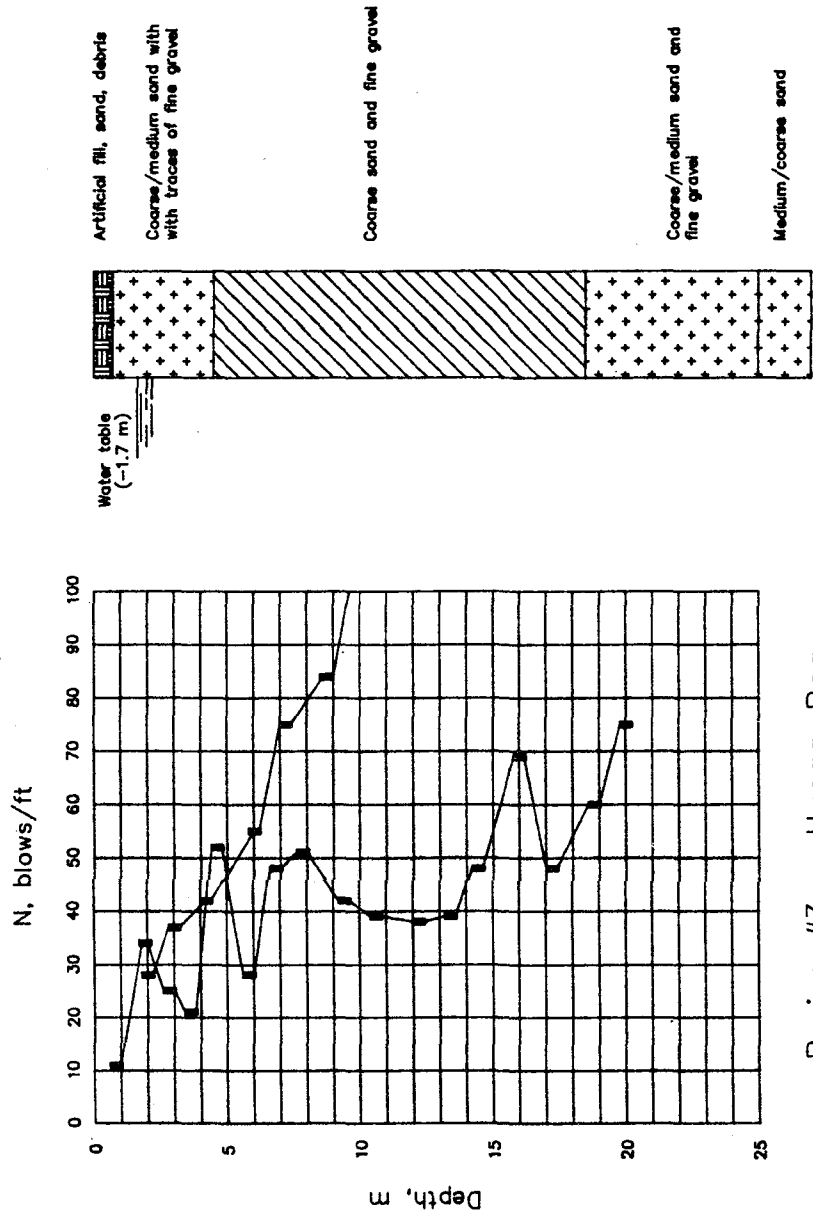


Fig. A.3 Soil Profile and Standard Penetration Test Data for Boring #2



Boring #3 - Hanga-Roa  
Av. San Martin No. 925

Fig. A.4 Soil Profile and Standard Penetration Test Data for Boring #3

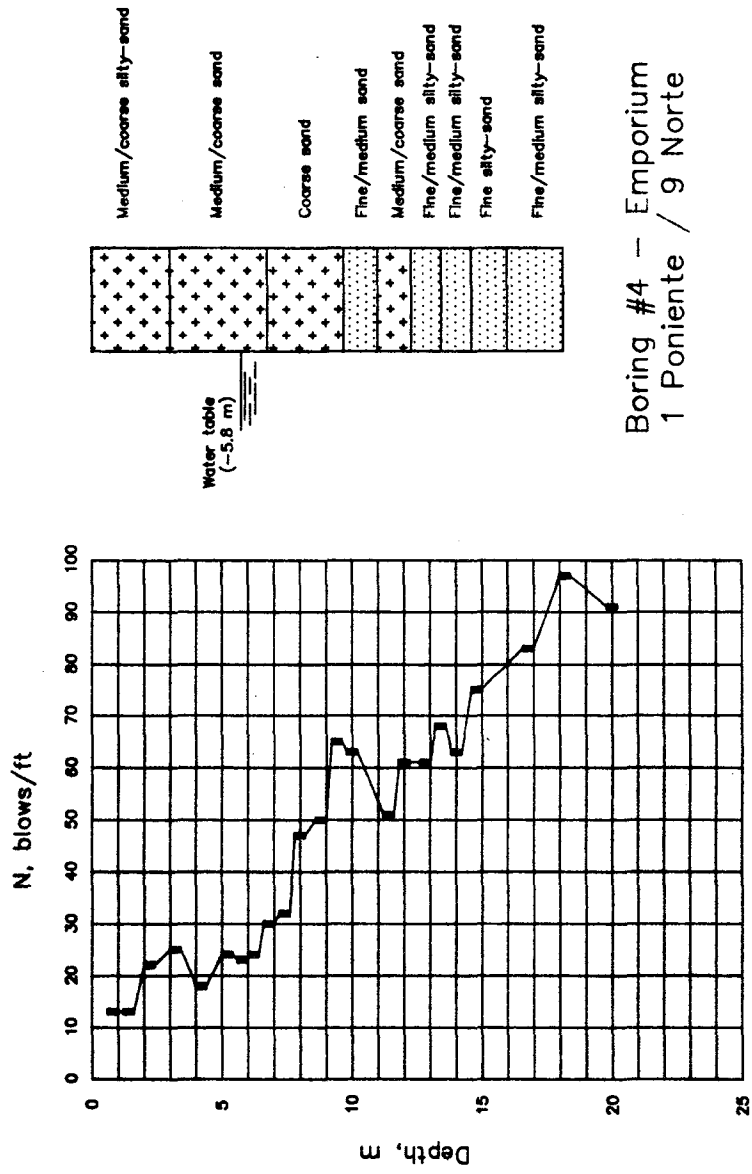
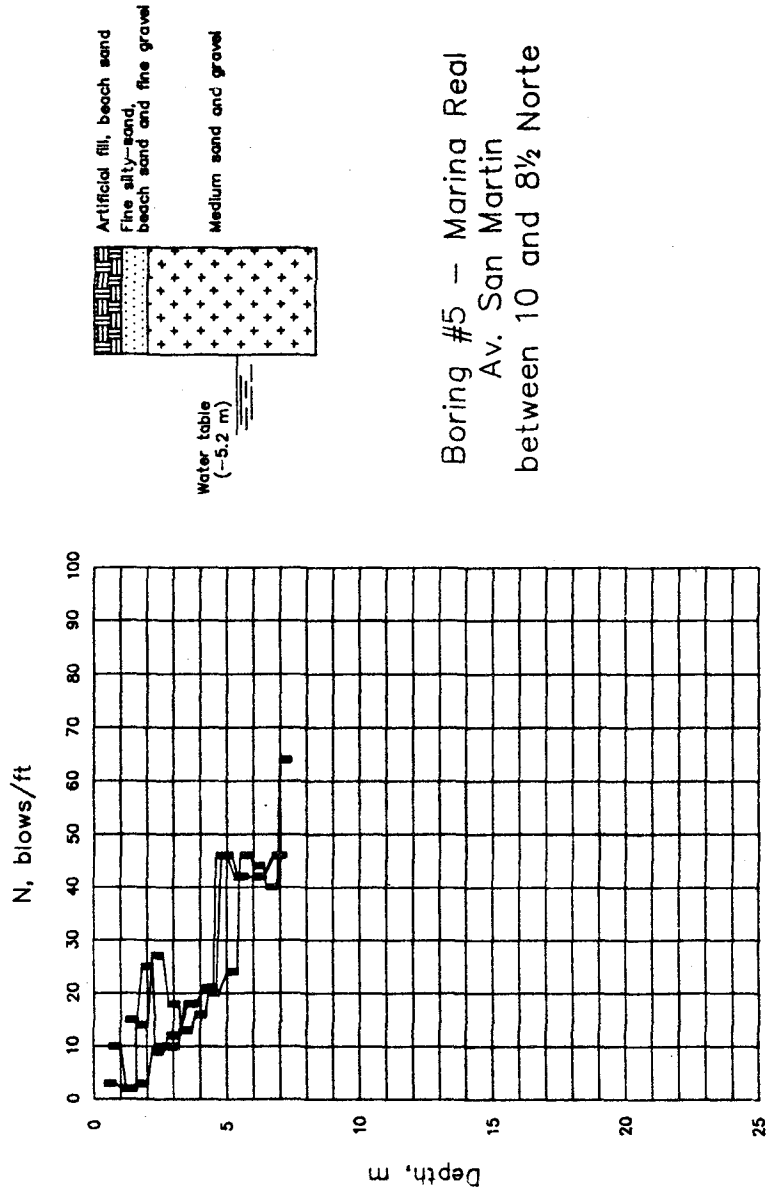
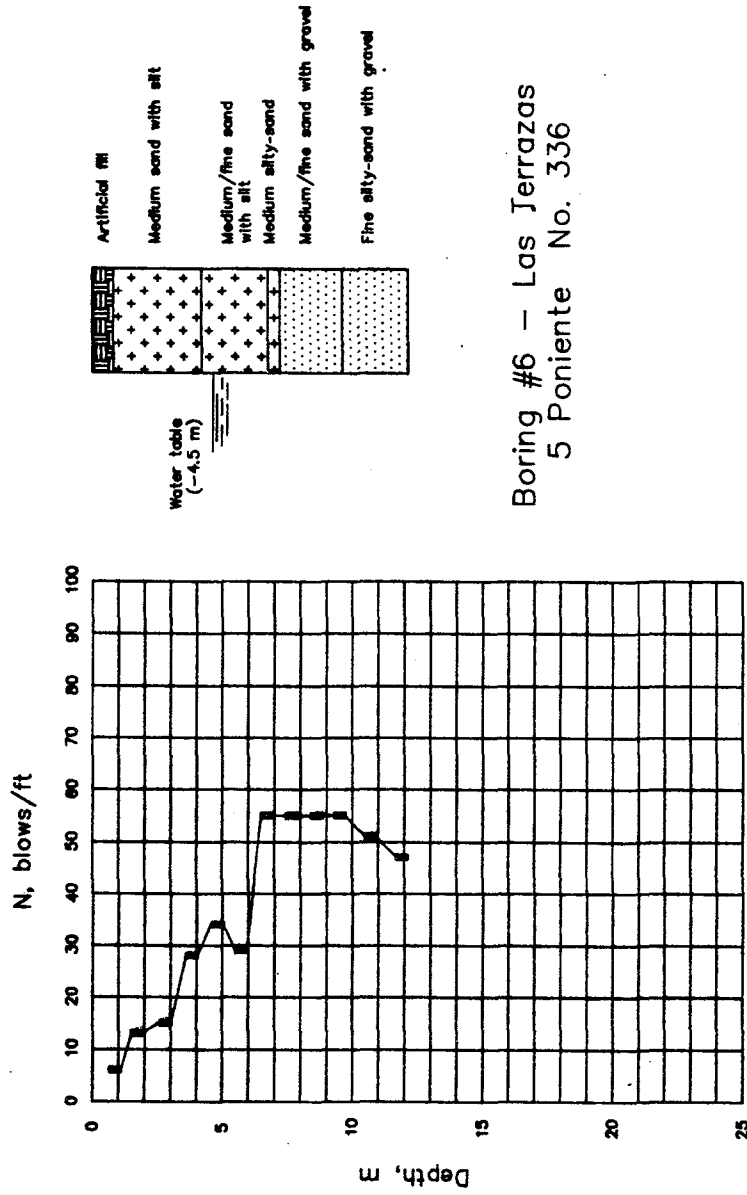


Fig. A.5 Soil Profile and Standard Penetration Test Data for Boring #4



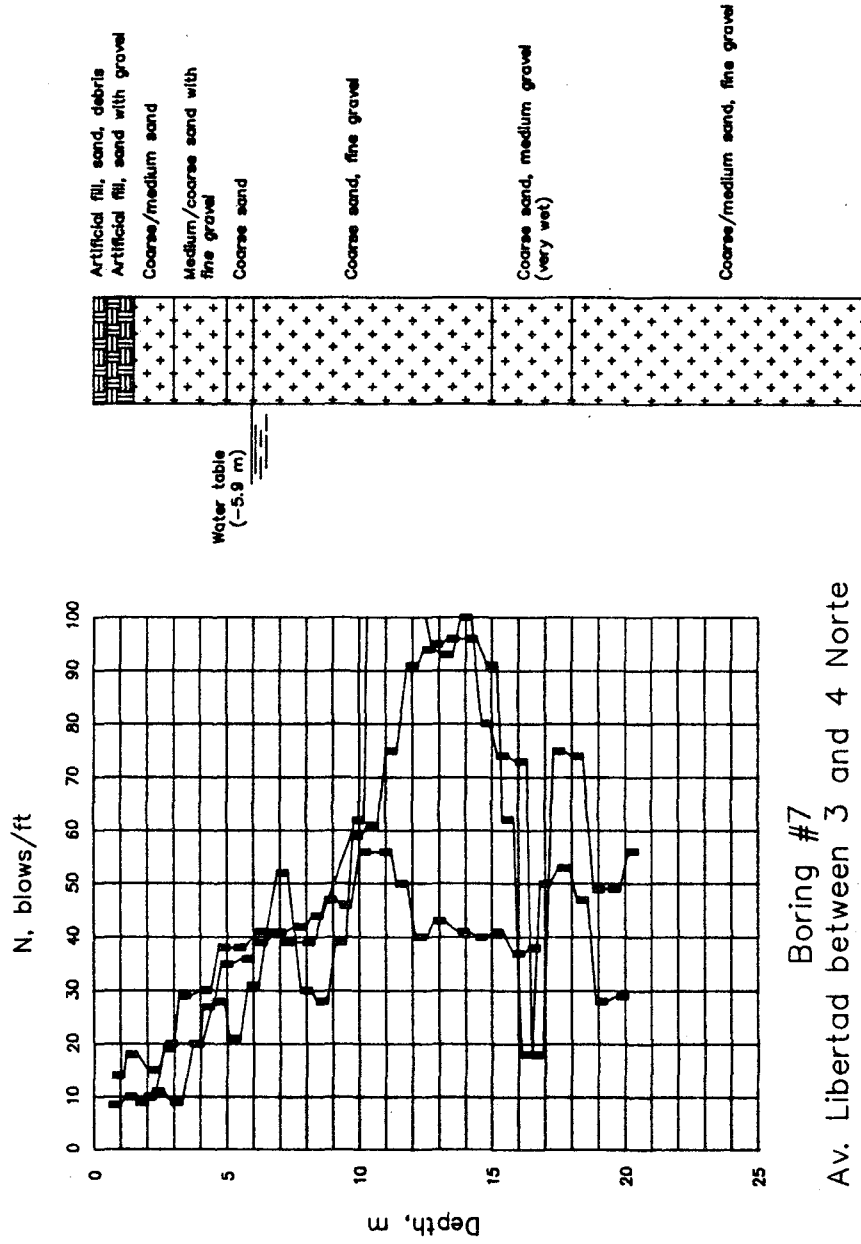
Boring #5 - Marina Real  
Av. San Martin  
between 10 and 8½ Norte

Fig. A.6 Soil Profile and Standard Penetration Test Data for Boring #5



Boring #6 - Las Terrazas  
5 Poniente No. 336

Fig. A.7 Soil Profile and Standard Penetration Test Data for Boring #6



Boring #7  
Av. Libertad between 3 and 4 Norte

Fig. A.8 Soil Profile and Standard Penetration Test Data for Boring #7

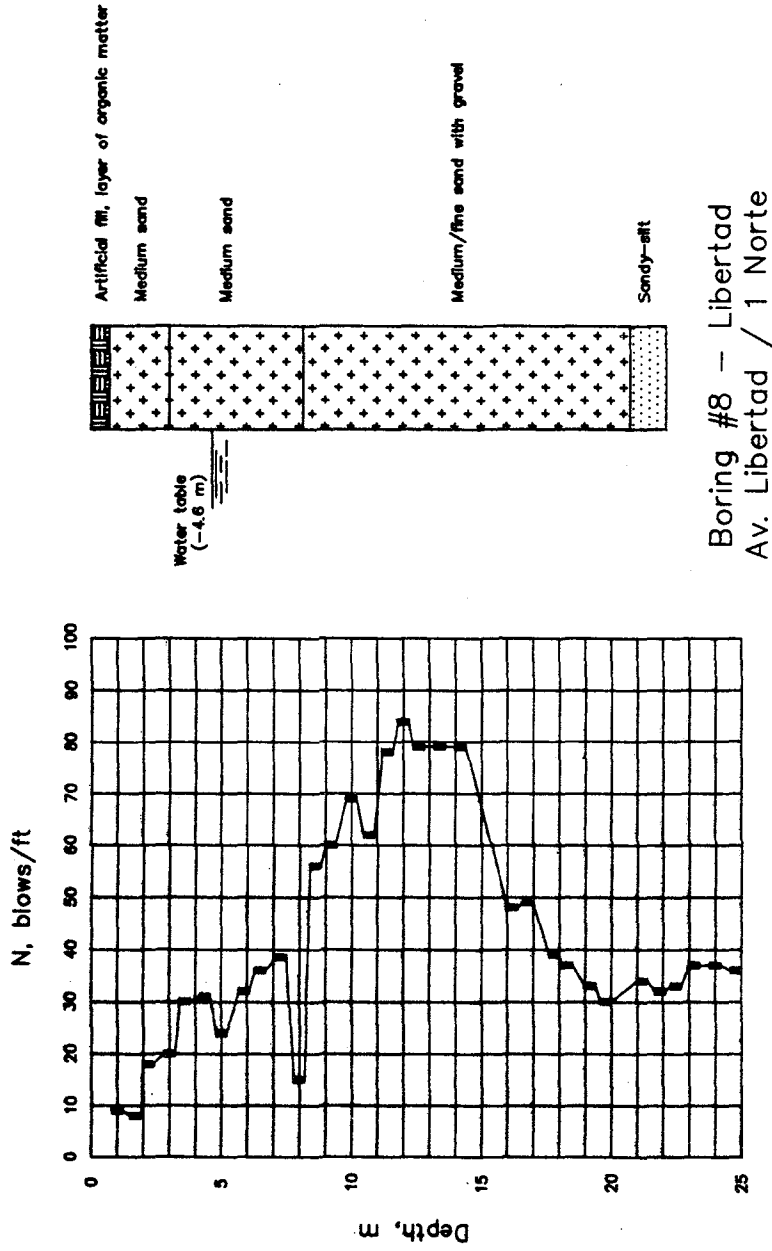


Fig. A.9 Soil Profile and Standard Penetration Test Data for Boring #8

## APPENDIX B

### BUILDING DESCRIPTIONS AND OBSERVED DAMAGE

#### B.1 Plaza del Mar Building

Plaza del Mar, a 23-story apartment building, is the tallest building in Viña del Mar. The building is located on the beach, 100 meters south of the Acapulco building. It was designed in 1980-81, and was fully operational at the time of the earthquake.

A typical floor plan is shown in Fig. 7.2.a. The building comprises two similar portions coupled together at a central staircase by a narrow slab. The building plan is effectively symmetric about the central longitudinal axis. The transverse structural walls are L-shaped, and angled at sixty degrees from the longitudinal corridor to provide ocean views from all units. The transverse walls are coupled directly to the longitudinal walls that form the central hallway. The lintels down the central corridor were precast, and are isolated from the walls. Transverse coupling across the corridor is provided by a thin slab (14 cm).

An elevation of the building is presented in Figure 7.2.b. The wall thickness varies from 30 cm at the base to 20 cm at the roof. All stories have a height of 2.68 m except the first, which is 4.69 m. The superstructure is supported on a 1.5 meter thick cellular-mat foundation 7 m below grade.

The floor area of the building is approximately  $870 \text{ m}^2$  ( $9350 \text{ ft}^2$ ). A mass distribution of  $1000 \text{ kg/m}^2$  (205 psf) was used, yielding a total building mass of 20000 tons (44000 kips) (excluding the basement levels). The ratio of the total cross-sectional area of the structural

walls to the floor area is 6.5%, 5.4%, and 4.3% for floors 1-6, 7-12, and 13-23, respectively. Approximately equal areas exist in the transverse and longitudinal directions.

No structural damage was reported after the earthquake, although minor non-structural damaged occurred [Wood et al. (1987), Arze and Recine Associates (1985)]. Hairline cracks were observed in the corridor slab coupling the building in the transverse direction. Larger cracks (0.4 mm) were located in the slab at the central staircase, apparently due to longitudinal coupling of the similar building portions. Ripples in the plaster (finish material applied over the structural walls) were observed in the transverse walls at the second and fifth floors, but investigation did not reveal any damage in the walls. Cracks were observed in the partition walls near the central staircase, and in the water tank and machine house at the roof level. Some leaking of water from the tank may have occurred. Repairs consisted of cleaning away loose materials and using a grout and epoxy mixture to fill the voids. If necessary, a sealant was to be used in the watertank [Arze and Recine Associates (1985)].

## **B.2 Festival Building**

The Festival building is a 14-story apartment building with a basement level for parking. The structure is supported on a cellular mat foundation. The building plan is I-shaped (Fig. 7.3.a-b) and almost symmetrical. It was designed in 1978.

Structural walls coupled by a 13-cm slab predominate the lateral and vertical load resisting system of the structure. The walls are continuous over the height of the building (Fig. 7.3.c) except at the first and basement levels where large openings were required for access to the parking level. The transverse walls are coupled by deep beams (wall sections)

along axes B and M, and across the corridor at the roof at axes D and K. The longitudinal walls are coupled at the roof level by deep beams between axes B and C, and L and M. The wall thickness is generally 30 cm for stories 1–4, 25 cm for stories 5–9, and 20 cm above the ninth story (Fig. 7.3.c). All stories have a height of 2.65 m except the first, which is 2.80 m, and the parking level which is 3.75 m. The superstructure is supported on a 3.2-meter thick cellular–mat foundation 7 m below grade.

The floor area of the building is approximately 900 m<sup>2</sup> (9700 ft<sup>2</sup>). A mass distribution of 1000 kg/m<sup>2</sup> (205 psf) was used, yielding a total building mass of 13500 tons (30000 kips). The ratio of the total cross-sectional area of the structural walls to the floor area is 5.8%, 4.5%, and 3.5% for floors 1–4, 5–9, and 10–14, respectively. Approximately equal areas exist in the transverse and longitudinal directions.

Structural damage [Bonelli (1986), Wood et al. (1987), Wyllie et al. (1986)] consisted of cracking in the lintels along the major longitudinal axes of the building and diagonal cracks on several of the walls in the transverse direction. Crushing was observed at the boundaries of the walls at axes F and I where the wall boundaries intersected a perimeter retaining wall. Damage was also observed in the parking level due to large openings that were required for garage access. Masonry walls in the bathrooms along the north side of the building collapsed during the earthquake. Crack lengths were measured to be [Municipalidad Viña del Mar (1985)]:

Structural Elements	Nonstructural Elements
Walls 1920 m	Partition Walls 900 m
Beams 330 m	Masonry Walls 560 m
Slabs 110 m	

The cost of structural repairs was approximately 41 million pesos [Municipalidad Viña del Mar (1985)].

### B.3 Acapulco Building

The Acapulco building, a 15-story apartment building on the beach, was the first “high-rise” building in Viña del Mar. It was designed in 1960–62 using hand calculation methods, and constructed in 1962.

A typical floor plan is shown in Fig. 7.4.a and an elevation of the building is presented in Fig. 7.4.b. The building is nearly symmetrical about the central longitudinal axis. In a manner similar to Plaza del Mar, the transverse structural walls are angled at sixty degrees from the longitudinal corridor to provide ocean views from all units. But unlike the Plaza del Mar Building, the transverse walls are coupled to the longitudinal walls with only shallow beams and slabs. A wall thickness of 25 cm is typical for the first two stories, and is reduced to 20 cm for the remaining stories. The typical story height is 2.68 m. The structural walls are coupled by a 12 slab except at locations indicated in Fig. 7.19, where shallow beams couple the walls. The superstructure is supported on a one-meter thick cellular-mat foundation four meters below grade.

The floor area of the building is approximately  $730 \text{ m}^2$  ( $7850 \text{ ft}^2$ ). A mass distribution of  $1000 \text{ kg/m}^2$  (205 psf) was used, yielding a total building mass of 10950 tons (24200 kips). The ratio of the total cross-sectional area of the structural walls to the floor area is 6.9% and 5.8% for the first and third floors, respectively.

The building had been damaged during previous earthquakes in 1965 and 1971 [Husid and Blass (1972), Monge et al. (1965–66), Ortigosa et al. (1972), and Sarrazin (1972)];

however, only cosmetic repairs were made [Bonelli (1986)]. The building was severely damaged during the 3 March 1985 earthquake [Bonelli (1986), Wyllie (1986), and Wood et al. (1987)]. The major damage occurred at the northeast end of the building, at the intersection of axes M and X. Crushing at the wall boundary, buckling of the boundary bars, and slippage along the construction joint were observed at the fourth level. Crushing also occurred at the boundary of wall K at the base. Shear and flexural cracks were observed in most of the walls, and were concentrated in levels 3 through 7. The beams at axis K across the corridor (at the end of the hallway) were also severely damaged. The corridor slab acted as a coupling beam and was cracked over most of the building length. The roof slab was seriously damaged around a water tank located between axes E and F.

#### **B.4 Torres del Miramar Building**

The two identical structures composing the condominium complex Torres del Miramar are one block north of the Acapulco building (Fig. 7.1). Design of the 21-story structures was completed in 1973, and the buildings were constructed in 1974 and 1975. The buildings are triangular in plan (Fig. 6.2.a-b) with equal sides of 34.9 m. The story height is 2.55 m, except for the first and second stories which are 2.89 and 2.72 m, respectively (Fig. 6.2.c). The plan area of the building is reduced at the below the third story (Fig. 6.2.c).

Three channel shaped walls at the building core and nine columns located around the building perimeter provide the lateral and vertical load resisting systems. The openings in the walls over the height of the building are staggered (Fig. 6.2.d). The walls are coupled with a 20-cm slab. Beams span the columns at the perimeter of the building. The columns

are rhombic shaped below the second floor, and triangular above. The superstructure is supported on a continuous footing 6 m below grade.

The floor area of the building is  $530 \text{ m}^2$  ( $5700 \text{ ft}^2$ ) for floors 3–21. The area of the first and second floors is approximately  $300 \text{ m}^2$  ( $3200 \text{ ft}^2$ ). A mass distribution of  $1000 \text{ kg/m}^2$  ( $205 \text{ psf}$ ) was used, yielding a total building mass of 11200 tons (24700 kips) (excluding the basement levels). The ratio of the total cross-sectional area of the structural walls to the floor area is 4.6% for the first and second floors.

No structural damage was observed in either of the buildings. Non-structural damage was localized at the corners of the buildings (which are cantilevered) where some partitions separated from the structure. The soil around the perimeter of both buildings settled as much as 30 cm following the earthquake [Wyllie et al. (1986)]. Backfilled material around foundations is not usually well compacted in Chilean construction [Riddell (1988)], thus settlement is not necessarily indicative of major foundation settlement.

# APPENDIX C

## MATERIAL TESTING DATA

Concrete test data obtained from the Municipality of Viña del Mar is presented for the Plaza del Mar, Festival, and Acapulco buildings in Tables C.1 through C.3.

Batch (No.)	Concrete (Class)	Date	Test (days)	Unit Weight ( $kg/m^3$ )	$R_{Cylinder}$ ( $kg/cm^2$ )	$R_{Cube}$ ( $kg/cm^2$ )	Building Location
1093	E	26.05.82	7	2.43	211	261	Wall
			28	2.44	243	293	(Floor 19)
			28	2.44	254	304	(Axis 10)
1094	E	27.05.82	7	2.43	290	340	Slab
			28	2.43	404	454	(Floor 19)
			28	2.41	416	466	(Axes 3,5)

Table C.1 Concrete Testing — Plaza del Mar Building

Batch (No.)	Concrete (Class)	Date	Test (days)	$R_{Cube}^*$ ( $kg/cm^2$ )	Observations
1	D	10.06.62	7	164	Tabiques y Pilares - 4 piso
2	D	10.06.62	28	155	"
3	D	02.07.62	7	236	"
4	D	02.07.62	28	236	"

\* 20 cm cube strength

Table C.2 Material Testing — Acapulco Building

Batch (No.)	Concrete (Class)	Date	Test (days)	Unit Weight ( $kg/m^3$ )	$R_{Cylinder}$ ( $kg/cm^2$ )	$R_{Cube}$ ( $kg/cm^2$ )	Buiding Location
2373	E (300)	10.11.78	7	2.42	219	270	Wall (Floor 12)
			28	2.38	257	306	
			28	2.38	262	311	
2374	E (300)	11.11.78	7	2.43	199	249	Slab (Floor 12)
			28	2.36	257	306	
			28	2.41	263	313	
2375	E (300)	11.11.78	7	2.39	217	267	Slab (Floor 12)
			28	2.37	272	324	
			28	2.37	268	319	
3110	E (300)	29.11.78	7	2.42	192	239	Slab & Beam (Floor 13) (Depto. #4)
			28	2.38	242	293	
			28	2.39	250	300	
3111	E (300)	29.11.78	7	2.32	181	227	Slab (Floor 13) (Depto. #1)
			28	2.32	239	289	
			28	2.35	237	287	
3114	E (300)	30.11.78	7	2.40	219	269	Slab & Beam (Floor 13) (Depto. #6)
			28	2.37	250	300	
			28	2.37	254	304	
3115	E (300)	30.11.78	7	2.35	188	235	Slab & Beam (Floor 13) (Depto. #5)
			28	2.40	231	281	
			28	2.39	236	285	

Table C.3 Material Testing — Festival Building

## REFERENCES

- ACI-318 (1977), "Building Code Requirements for Reinforced Concrete," *American Concrete Institute*, Detroit, Michigan, 1977.
- ACI-318 (1983), "Building Code Requirements for Reinforced Concrete," *American Concrete Institute*, Detroit, Michigan, 1983.
- Aktan, A. E. and Bertero, V. V. (1985), "RC Structural Walls: Seismic Design for Shear," *Journal of Structural Engineering*, ASCE, Vol. 111, No. 8, August, 1985, pp. 1775-1791.
- Algan, B. (1982), "Drift and Damage Considerations in Earthquake Resistant Design of Reinforced Concrete Buildings," *Ph.D. Thesis, Department of Civil Engineering, University of Illinois*, Urbana, 1982.
- Applied Technology Council (1978), "ATC-03-06: Tentative Provisions for the Development of Seismic Regulations for Buildings," *Applied Technology Council*, Palo Alto, California, 1971.
- Arze and Recine Associates (1985), "Seismic Inspection: Plaza del Mar Building," *Arze and Recine Associates*, Santiago, 18 March 1985.
- Baeza, M. (1963), "Determinación Experimental de Periodos de Oscilación de Edificios de Hormigón Armado," *Revista del IDIEM*, Universidad de Chile, Facultad de Ciencias Físicas y Matemáticas, Vol. 2, No.1, Santiago, April 1963, pp. 27-32.
- Barras para Hormigón Armado, *Compañía de Acero del Pacífico S. A.*, Santiago.
- Bertero, V.V., Popov, E.P., and Viwathanatepa, S. (1978), "Nonlinear Behavior of Reinforced Concrete Spatial Structures," *Contributions to the IASS Symposium*, Vol. 2, 1978.
- Bertling, H. (1956), "Development of Earthquake-Proof Construction in Chile," *Proceedings*, World Conference on Earthquake Engineering, Berkeley, 1956, pp. 20-1 - 20-10.
- Bonelli, P. (1986), "Actividades de Investigación 1986: El Sismo del Marzo del 1985 en Valparaíso y Viña del Mar," *Universidad Técnica Federico Santa María*, Valparaíso, 1986.
- Bongiovanni, G., Celebi, M., and Safak, E. (1987), "Seismic Rocking Response of a Triangular Building Founded on Sand," *Earthquake Spectra*, Vol. 3, No. 4, November 1987.
- Calcagni, J. (1987), "Proposición de un Espectro de Diseño para Zona Epicentral del Terremoto del 3 de Marzo de 1985," *Memoria de título, Universidad de Chile*, Santiago, Chile, April 1987.
- "Cálculo Antisísmico de Edificios - NCh 433-Of.72 (1979), *Instituto Nacional de Normalización*, Santiago, 1979.

- Celebi, M., ed. (1986),** "Seismic Site-Response Experiments Following the March 3, 1985 Central Chile Earthquake (Topographical and Geological Effects)," *United States Department of the Interior, Geological Survey, Open-File Report 86-90*, Menlo Park, California, 1986.
- Charney, F. A. and Bertero, V. V. (1976),** "An Evaluation of the Design and Analytical Seismic Response of a Seven-Story Reinforced Concrete Frame-Wall Structure," *Report No. UCB/EERC-82/08*, Earthquake Engineering Research Center, University of California at Berkeley, August 1976.
- Clough, R. W. and Penzien, J. (1975),** "Dynamics of Structures," *McGraw-Hill, Inc.*, 1975.
- Crempien, J. (1987),** "Personal Communication," 1987.
- De la Llera, J.C. and Riddle R. (1988),** "El Terremoto de 1985 en Chile: Analisis del Edificio Acapulco," *DIE No. 88-1*, Pontificia Universidad Católica de Chile Santiago, Chile, July 1988.
- DIN 1045 (1952)** "Bestimmungen Fur Ausführung von Bauwerken aus Stashbeton," *Deutscher Normenausschuss, DIN 1045*, July, 1952.
- "Earthquake Resistant Regulations-A World List (1980),"** *International Association for Earthquake Engineering*, Tokyo, Japan, 1980.
- Flores, R. and Jimenez (1986),** "Development of Earthquake Engineering in Chile," *Presented at the Workshop on the Chilean Earthquake of 3 March 1985, EERI and ACHISINA*, Instituto de Ingenieros, Santiago, April, 1986.
- Freeman S.A. (1985),** "Drift Limits: Are They Realistic," *Earthquake Spectra*, Vol. 1, No. 2, February 1985.
- Grimme, K. and Alvarez, L. (1964),** "El Suelo de Fundación de Valparaíso y Viña del Mar," *Boletín*, Instituto de Investigaciones Geológicas, Chile, No. 16, 1964.
- Hansen, R., J., ed. (1970),** "Seismic Design for Nuclear Power Plants," *The MIT Press*, 1970, pp. 438-469.
- Herrera, A. (1977),** "Zonificación de Suelos de Viña del Mar," *Departamento de Obras Civiles*, Universidad Técnica Federico Santa María, Valparaíso, Chile, 1977.
- Holtz, R. and Kovacs, W. (1981),** "An Introduction to Geotechnical Engineering," *Prentice-Hall, Inc.*, Englewood Cliffs, N.J., 1981.
- "Hormigón Armado - Part I - NCh 429.EOf57 (1965),"** *Instituto Nacional de Normalización*, Santiago, Chile, 1965.
- "Hormigón Armado - Part II - NCh 430.EOf61 (1965),"** *Instituto Nacional de Normalización*, Santiago, Chile, 1965.
- Housner, G. W. (1959),** "Behavior of Structures During Earthquakes," *Journal of the Engineering Mechanics Division*, ASCE, Vol. 85, No. EM4, October 1959, pp. 108-129.

- Husid, R. and Blass, B. (1972), "Visita a Parte de la Zona Afectada," *Revista del IDIEM*, Universidad de Chile, Facultad de Ciencias Físicas y Matemáticas, Vol. 11, No. 1, Santiago, May 1972, pp.34-38.
- Kannan, A. E. and Powell, G. H. (1973), "DRAIN-2D: A General Purpose Program for Dynamic Analysis of Inelastic Plane Structures," *Report No. UCB/EERC-75/37*, Earthquake Engineering Research Center, University of California at Berkeley, April 1973.
- "Ley y Ordenanza General sobre Construcciones y Urbanización (1949)," *Instituto Nacional de Investigaciones Tecnológicas y Normalización*, November, 1949.
- Lomnitz, C. (1970), "Major Earthquakes and Tsunamis in Chile during the Period 1535 to 1955," *Geologische Rundschau*, Vol. 59, No. 3, 1970, pp. 938-960.
- Moehle, J. P. and Diebold, J. W. (1985), "Lateral Load Response of a Flat-Plate Frame," *Journal of Structural Division*, ASCE, Vol. 111, No. 10, October, 1985, pp. 2149-2164.
- Monge, J., Rosenberg, L., Vives, A., and Yoma, F. (1965-66), "Sismo del 28 de Marzo de 1965, Chile: Informe Sobre Danos en Estructuras", *Anales*, Facultad de Ciencias Físicas y Matemáticas, Universidad de Chile, Vol.22-23, Santiago, 1965-66, pp. 68-80.
- Municipalidad Viña del Mar (1985), "Seismic Inspection: Festival Building," *Director de Obras Municipales*, Municipalidad Viña del Mar, Chile, 4 December 1985.
- Newmark, N. M. (1959), "A Method of Computation for Structural Dynamics," *Journal of the Engineering Mechanics Division*, ASCE, Vol. 85, EM3, July 1959, pp. 69-86.
- Newmark, N. M. and Rosenblueth, E. (1971), "Fundamentals of Earthquake Engineering," *Prentice-Hall*, 1971.
- Newmark, N. M. and Hall W. J. (1982), "Earthquake Spectra and Design," *Engineering Monographs on Earthquake Criteria, Structural Design, and Strong Motion Records*, Earthquake Engineering Research Institute, 1982.
- Ortigosa, P., Acevedo, P., Dobry, R., and Foncea, C. (1972), "Informe Preliminar Sobre Visitas a Algunas Zonas Afectadas por el Sismo del 8 de Julio 1971," *Revista del IDIEM*, Universidad de Chile, Facultad de Ciencias Físicas y Matemáticas, Vol. 11, No. 1, Santiago, May 1972, pp.24-28.
- Pantazopoulou, S. J. (1987), "Modeling Aspects of the Three Dimensional Behavior of Building Structures Subjected to Earthquakes", Ph.D. dissertation submitted to the University of California, Berkeley, 1987.
- Park, R. and Pauley, T. (1975), *Reinforced Concrete Structures*, John Wiley and Sons, Inc., New York, New York, 1975.
- Park, R., Priestley M.J.N. and Gill, W.D., "Ductility of Square-Confined Concrete Columns," *Journal of the Structural Division*, ASCE, Vol. 108, No.108, No. ST4, April 1982, pp. 929-950.

- Paulay, T. (1986),** "The Design of Ductile Reinforced Concrete Structural Walls for Earthquake Resistance," *Earthquake Spectra*, Vol. 2, No. 4, October 1986.
- Paulay, T. and Uzumeri, S.M. (1975),** "A Critical Review of the Seismic Design Provisions for Ductile Shear Walls of the Canadian Code and Commentary," *Canadian Journal of Civil Engineering*, Vol. 2 No. 4, 1975, pp. 592-601.
- Peck, R., W. Hanson, and T. Thornburn (1974),** *Foundation Engineering*, 2nd ed., John Wiley & Sons, New York
- Pecknold, D. A. (1975),** "Slab Effective Width for Equivalent Frame Analysis," *ACI Journal, Proceedings*, Vol. 72, No. 13, April 1975, pp. 135-137.
- Petersen, M. (1986),** "Soil Conditions in Viña del Mar," *Notes from Meetings held during Field Trip*, Viña del Mar, July 1986.
- Petersen, M. and Donoso, J. (1980),** "Estudio de Mecánica de Suelos: Edificio Las Terrazas," Viña del Mar, November 1980.
- Poblete, M. (1982),** "Load-Deformation Properties of Some Chilean Granular Soils," *Primer Congreso Chileno de Ingeniería Geotécnica*, Volume 1, Santiago, August 1982, pp. 42-66.
- Riddell, R. (1988),** "Foundation Construction Practices in Viña del Mar," *Personal Communication*, 1988.
- Riddell, R., Wood, S., and De La Llera (1987),** "The 1985 Chile Earthquake, Structural Characteristics and Damage Statistics for the Building Inventory in Viña del Mar," *Civil Engineering Studies, Structural Research Series No. 534*, University of Illinois, Urbana, April 1987.
- Saragoni, R., Gonzalez, P., and Fresard, M. (1985),** "Análisis de los Acelerogramas del Terremoto del 3 de Marzo de 1985," *Publicación SES I 4/1985 (199)*, Sección Estructuras, Departamento de Ingeniería Civil, Universidad de Chile, Santiago, December 1985.
- Sarazin, M. (1972),** "Algunas Observaciones de Daños Estructurales: Impresiones Recogidas el Día 10 de Julio de 1971," *Revista del IDIEM*, Universidad de Chile, Facultad de Ciencias Físicas y Matemáticas, Vol. 11, No. 1, Santiago, May 1972, pp. 38-40.
- Schnabel, P.B., Lysmer, J. and Seed, H.B. (1972),** "SHAKE: A Computer Program for Earthquake Response Analysis of Horizontally Layered Sites," *Report No. EERC/72-12*, Earthquake Engineering Research Center, University of California, Berkeley, December 1972.
- Seed, H. B. (1975),** "Design Provisions for Assessing the Effects of Local Geology and Soil Conditions on Ground and Building Response During Earthquakes," *New Earthquake Design Provisions, Seminar Papers from ASCE/SEAONC Professional Development Committee Series*, October-November, 1975.
- Seed, H. B. (1987),** "Influence of Local Soil Conditions on Ground Motions and Building Damage During Earthquakes," *Eighth Nabor Carrillo Lecture*, Mexican Society for Soil Mechanics, Mexico, 1987.

- Seed, H. B. and Alonso, J. L. (1974), "Effects of Soil-Structure Interaction in the Caracas Earthquake of 1967," *Proceedings First Venezuelan Conference on Seismology and Earthquake Engineering*, October, 1974.
- Seed, H. B., Wong, R. T., Idriss, I. M., and Tokimatsu, K. (1984), "Moduli and Damping Factors for Dynamic Analysis of Cohesionless Soils," *Report No. UCB/EERC-84/14*, Earthquake Engineering Research Center, University of California, Berkeley, September 1984.
- Seed, H. B., Idriss, I. M., and Arrango, I. (1981), "Evaluation of Liquefaction Potential Using Field Performance Data," presented at the October, 1981 ASCE Convention, held at St. Louis, Mo., pp. 458-482.
- Smith, B. S. and Girgis, A. (1984), "Simple Analogous Frames for Shear Wall Analysis," *Journal of Structural Engineering*, ASCE, Vol. 110, No. 11, November 1984, pp. 2655-2666.
- Stark, R. (1988), "Evaluation of Strength, Stiffness, and Ductility Requirements of Reinforced Concrete Structures using Data from Chile (1985) and Michoacan (1985) Earthquakes," *Ph.D. Thesis, Department of Civil Engineering, University of Illinois, Urbana*, 1988.
- Steinbrugge, Karl V., Schader, and Eugene E. (1973), "Earthquake Damage and Related Statistics: San Fernando, California Earthquake of February 9, 1971," *Leonard M. Murphy, Scientific Coordinator*, U.S. Department of Commerce Washington, D.C., 1973, pp. 691-724.
- Takeda, T., Sozen, M. A., and Nielsen, N. N. (1970), "Reinforced Concrete Response to Simulated Earthquakes," *Journal of the Structural Division*, ASCE, Vol. 96, No. ST12, December 1970, pp. 2557-2573.
- "Uniform Building Code (1985)," *International Conference of Building Officials*, Whittier, California, 1985.
- "Uniform Building Code (1988)," *International Conference of Building Officials*, Whittier, California, 1985.
- Veletsos, A. S. (1977), "Dynamics of Structure-Foundation Systems," *Structural and Geotechnical Mechanics, A Volume Honoring N. M. Newmark (W. J. Hall, Editor)*, Prentice-Hall, Inc., Englewood Cliffs, N. J., 1977, pp. 333-361.
- Wallace, J. W. (1989), "BIAX2: R/C Section Analysis Program," Structural Engineering, Mechanics and Materials, University of California, Berkeley, 1989. In Preparation
- Wight (1988), "Research In Progress," Department of Civil Engineering, University of Michigan, Ann Arbor, 1988.
- Wilson, E. L. (1986), "CAL-86: Computer Assisted Learning of Structural Analysis and The CAL/SAP Development System," *Report No. UCB/SESM-86/05*, Structural Engineering and Structural Mechanics, University of California, Berkeley, August 1986.

- Wilson, E. L., Der Kiureghian, A., and Bayo, E. P. (1981),** "Short Communications: A Replacement for the SRSS Method in Seismic Analysis," *Earthquake Engineering and Structural Dynamics*, Vol. 9, pp. 187-194, 1981.
- Wilson, E. L. (1988),** "SAP-80: Structural Analysis Program", *Computers & Structures Inc.*, Berkeley, California, 1986.
- Wood, S. (1988),** "Shear Strength of Low-Rise Reinforced Concrete Walls," *Structural Journal*, American Concrete Institute, to be published.
- Wood, S., Wight, J., and Moehle, J. (1987),** "The 1985 Chile Earthquake, Observations on Earthquake-Resistant Construction in Viña del Mar," *Civil Engineering Studies, Structural Research Series No 532*, University of Illinois, Urbana, February 1987.
- Wyllie, L. et al. (1986),** "The Chile Earthquake of March 3, 1985," *Earthquake Spectra*, Vol. 2, No. 2 April 1986.



## EARTHQUAKE ENGINEERING RESEARCH CENTER REPORT SERIES

EERC reports are available from the National Information Service for Earthquake Engineering(NISEE) and from the National Technical Information Service(NTIS). Numbers in parentheses are Accession Numbers assigned by the National Technical Information Service; these are followed by a price code. Contact NTIS, 5285 Port Royal Road, Springfield Virginia, 22161 for more information. Reports without Accession Numbers were not available from NTIS at the time of printing. For a current complete list of EERC reports (from EERC 67-1) and availability information, please contact University of California, EERC, NISEE, 1301 South 46th Street, Richmond, California 94804.

- UCB/EERC-80/01 "Earthquake Response of Concrete Gravity Dams Including Hydrodynamic and Foundation Interaction Effects," by Chopra, A.K., Chakrabarti, P. and Gupta, S., January 1980. (AD-A087297)A10.
- UCB/EERC-80/02 "Rocking Response of Rigid Blocks to Earthquakes," by Yim, C.S., Chopra, A.K. and Penzien, J., January 1980. (PB80 166 002)A04.
- UCB/EERC-80/03 "Optimum Inelastic Design of Seismic-Resistant Reinforced Concrete Frame Structures," by Zagajski, S.W. and Bertero, V.V., January 1980. (PB80 164 635)A06.
- UCB/EERC-80/04 "Effects of Amount and Arrangement of Wall-Panel Reinforcement on Hysteretic Behavior of Reinforced Concrete Walls," by Iliya, R. and Bertero, V.V., February 1980. (PB81 122 525)A09.
- UCB/EERC-80/05 "Shaking Table Research on Concrete Dam Models," by Niwa, A. and Clough, R.W., September 1980. (PB81 122 368)A06.
- UCB/EERC-80/06 "The Design of Steel Energy-Absorbing Restrainers and their Incorporation into Nuclear Power Plants for Enhanced Safety (Vol 1a): Piping with Energy Absorbing Restrainers: Parameter Study on Small Systems," by Powell, G.H., Oughourlian, C. and Simons, J., June 1980.
- UCB/EERC-80/07 "Inelastic Torsional Response of Structures Subjected to Earthquake Ground Motions," by Yamazaki, Y., April 1980. (PB81 122 327)A08.
- UCB/EERC-80/08 "Study of X-Braced Steel Frame Structures under Earthquake Simulation," by Ghanaat, Y., April 1980. (PB81 122 335)A11.
- UCB/EERC-80/09 "Hybrid Modelling of Soil-Structure Interaction," by Gupta, S., Lin, T.W. and Penzien, J., May 1980. (PB81 122 319)A07.
- UCB/EERC-80/10 "General Applicability of a Nonlinear Model of a One Story Steel Frame," by Sveinsson, B.I. and McNiven, H.D., May 1980. (PB81 124 877)A06.
- UCB/EERC-80/11 "A Green-Function Method for Wave Interaction with a Submerged Body," by Kioka, W., April 1980. (PB81 122 269)A07.
- UCB/EERC-80/12 "Hydrodynamic Pressure and Added Mass for Axisymmetric Bodies," by Nilrat, F., May 1980. (PB81 122 343)A08.
- UCB/EERC-80/13 "Treatment of Non-Linear Drag Forces Acting on Offshore Platforms," by Dao, B.V. and Penzien, J., May 1980. (PB81 153 413)A07.
- UCB/EERC-80/14 "2D Plane/Axisymmetric Solid Element (Type 3-Elastic or Elastic-Perfectly Plastic)for the ANSR-II Program," by Mondkar, D.P. and Powell, G.H., July 1980. (PB81 122 350)A03.
- UCB/EERC-80/15 "A Response Spectrum Method for Random Vibrations," by Der Kiureghian, A., June 1981. (PB81 122 301)A03.
- UCB/EERC-80/16 "Cyclic Inelastic Buckling of Tubular Steel Braces," by Zayas, V.A., Popov, E.P. and Mahin, S.A., June 1981. (PB81 124 885)A10.
- UCB/EERC-80/17 "Dynamic Response of Simple Arch Dams Including Hydrodynamic Interaction," by Porter, C.S. and Chopra, A.K., July 1981. (PB81 124 000)A13.
- UCB/EERC-80/18 "Experimental Testing of a Friction Damped Aseismic Base Isolation System with Fail-Safe Characteristics," by Kelly, J.M., Beucke, K.E. and Skinner, M.S., July 1980. (PB81 148 595)A04.
- UCB/EERC-80/19 "The Design of Steel Energy-Absorbing Restrainers and their Incorporation into Nuclear Power Plants for Enhanced Safety (Vol.1B): Stochastic Seismic Analyses of Nuclear Power Plant Structures and Piping Systems Subjected to Multiple Supported Excitations," by Lee, M.C. and Penzien, J., June 1980. (PB82 201 872)A08.
- UCB/EERC-80/20 "The Design of Steel Energy-Absorbing Restrainers and their Incorporation into Nuclear Power Plants for Enhanced Safety (Vol 1C): Numerical Method for Dynamic Substructure Analysis," by Dickens, J.M. and Wilson, E.L., June 1980.
- UCB/EERC-80/21 "The Design of Steel Energy-Absorbing Restrainers and their Incorporation into Nuclear Power Plants for Enhanced Safety (Vol 2): Development and Testing of Restraints for Nuclear Piping Systems," by Kelly, J.M. and Skinner, M.S., June 1980.
- UCB/EERC-80/22 "3D Solid Element (Type 4-Elastic or Elastic-Perfectly-Plastic) for the ANSR-II Program," by Mondkar, D.P. and Powell, G.H., July 1980. (PB81 123 242)A03.
- UCB/EERC-80/23 "Gap-Friction Element (Type 5) for the Ansr-II Program," by Mondkar, D.P. and Powell, G.H., July 1980. (PB81 122 285)A03.
- UCB/EERC-80/24 "U-Bar Restraint Element (Type 11) for the ANSR-II Program," by Oughourlian, C. and Powell, G.H., July 1980. (PB81 122 293)A03.
- UCB/EERC-80/25 "Testing of a Natural Rubber Base Isolation System by an Explosively Simulated Earthquake," by Kelly, J.M., August 1980. (PB81 201 360)A04.
- UCB/EERC-80/26 "Input Identification from Structural Vibrational Response," by Hu, Y., August 1980. (PB81 152 308)A05.
- UCB/EERC-80/27 "Cyclic Inelastic Behavior of Steel Offshore Structures," by Zayas, V.A., Mahin, S.A. and Popov, E.P., August 1980. (PB81 196 180)A15.
- UCB/EERC-80/28 "Shaking Table Testing of a Reinforced Concrete Frame with Biaxial Response," by Oliva, M.G., October 1980. (PB81 154 304)A10.
- UCB/EERC-80/29 "Dynamic Properties of a Twelve-Story Prefabricated Panel Building," by Bouwkamp, J.G., Kollegger, J.P. and Stephen, R.M., October 1980. (PB82 138 777)A07.
- UCB/EERC-80/30 "Dynamic Properties of an Eight-Story Prefabricated Panel Building," by Bouwkamp, J.G., Kollegger, J.P. and Stephen, R.M., October 1980. (PB81 200 313)A05.
- UCB/EERC-80/31 "Predictive Dynamic Response of Panel Type Structures under Earthquakes," by Kollegger, J.P. and Bouwkamp, J.G., October 1980. (PB81 152 316)A04.
- UCB/EERC-80/32 "The Design of Steel Energy-Absorbing Restrainers and their Incorporation into Nuclear Power Plants for Enhanced Safety (Vol 3): Testing of Commercial Steels in Low-Cycle Torsional Fatigue," by Spanner, P., Parker, E.R., Jongewaard, E. and Dory, M., 1980.

- UCB/EERC-80/33 "The Design of Steel Energy-Absorbing Restrainers and their Incorporation into Nuclear Power Plants for Enhanced Safety (Vol 4): Shaking Table Tests of Piping Systems with Energy-Absorbing Restrainers," by Stiemer, S.F. and Godden, W.G., September 1980, (PB82 201 880)A05.
- UCB/EERC-80/34 "The Design of Steel Energy-Absorbing Restrainers and their Incorporation into Nuclear Power Plants for Enhanced Safety (Vol 5): Summary Report," by Spencer, P., 1980.
- UCB/EERC-80/35 "Experimental Testing of an Energy-Absorbing Base Isolation System," by Kelly, J.M., Skinner, M.S. and Beucke, K.E., October 1980, (PB81 154 072)A04.
- UCB/EERC-80/36 "Simulating and Analyzing Artificial Non-Stationary Earth Ground Motions," by Nau, R.F., Oliver, R.M. and Pister, K.S., October 1980, (PB81 153 397)A04.
- UCB/EERC-80/37 "Earthquake Engineering at Berkeley - 1980," by , September 1980, (PB81 205 674)A09.
- UCB/EERC-80/38 "Inelastic Seismic Analysis of Large Panel Buildings," by Schricker, V. and Powell, G.H., September 1980, (PB81 154 338)A13.
- UCB/EERC-80/39 "Dynamic Response of Embankment, Concrete-Gavity and Arch Dams Including Hydrodynamic Interaction," by Hall, J.F. and Chopra, A.K., October 1980, (PB81 152 324)A11.
- UCB/EERC-80/40 "Inelastic Buckling of Steel Struts under Cyclic Load Reversal," by Black, R.G., Wenger, W.A. and Popov, E.P., October 1980, (PB81 154 312)A08.
- UCB/EERC-80/41 "Influence of Site Characteristics on Buildings Damage during the October 3,1974 Lima Earthquake," by Repetto, P., Arango, I. and Seed, H.B., September 1980, (PB81 161 739)A05.
- UCB/EERC-80/42 "Evaluation of a Shaking Table Test Program on Response Behavior of a Two Story Reinforced Concrete Frame," by Blondet, J.M., Clough, R.W. and Mahin, S.A., December 1980, (PB82 196 544)A11.
- UCB/EERC-80/43 "Modelling of Soil-Structure Interaction by Finite and Infinite Elements," by Medina, F., December 1980, (PB81 229 270)A04.
- UCB/EERC-81/01 "Control of Seismic Response of Piping Systems and Other Structures by Base Isolation," by Kelly, J.M., January 1981, (PB81 200 735)A05.
- UCB/EERC-81/02 "OPTNSR- An Interactive Software System for Optimal Design of Statically and Dynamically Loaded Structures with Nonlinear Response," by Bhatti, M.A., Ciampi, V. and Pister, K.S., January 1981, (PB81 218 851)A09.
- UCB/EERC-81/03 "Analysis of Local Variations in Free Field Seismic Ground Motions," by Chen, J.-C., Lysmer, J. and Seed, H.B., January 1981, (AD-A099508)A13.
- UCB/EERC-81/04 "Inelastic Structural Modeling of Braced Offshore Platforms for Seismic Loading," by Zayas, V.A., Shing, P.-S.B., Mahin, S.A. and Popov, E.P., January 1981, (PB82 138 777)A07.
- UCB/EERC-81/05 "Dynamic Response of Light Equipment in Structures," by Der Kiureghian, A., Sackman, J.L. and Nour-Omid, B., April 1981, (PB81 218 497)A04.
- UCB/EERC-81/06 "Preliminary Experimental Investigation of a Broad Base Liquid Storage Tank," by Bouwkamp, J.G., Kollegger, J.P. and Stephen, R.M., May 1981, (PB82 140 385)A03.
- UCB/EERC-81/07 "The Seismic Resistant Design of Reinforced Concrete Coupled Structural Walls," by Aktan, A.E. and Bertero, V.V., June 1981, (PB82 113 358)A11.
- UCB/EERC-81/08 "Unassigned," by Unassigned, 1981.
- UCB/EERC-81/09 "Experimental Behavior of a Spatial Piping System with Steel Energy Absorbers Subjected to a Simulated Differential Seismic Input," by Stiemer, S.F., Godden, W.G. and Kelly, J.M., July 1981, (PB82 201 898)A04.
- UCB/EERC-81/10 "Evaluation of Seismic Design Provisions for Masonry in the United States," by Sveinsson, B.I., Mayes, R.L. and McNiven, H.D., August 1981, (PB82 166 075)A08.
- UCB/EERC-81/11 "Two-Dimensional Hybrid Modelling of Soil-Structure Interaction," by Tzong, T.-J., Gupta, S. and Penzien, J., August 1981, (PB82 142 118)A04.
- UCB/EERC-81/12 "Studies on Effects of Infills in Seismic Resistant R/C Construction," by Brokken, S. and Bertero, V.V., October 1981, (PB82 166 190)A09.
- UCB/EERC-81/13 "Linear Models to Predict the Nonlinear Seismic Behavior of a One-Story Steel Frame," by Valdimarsson, H., Shah, A.H. and McNiven, H.D., September 1981, (PB82 138 793)A07.
- UCB/EERC-81/14 "TLUSH: A Computer Program for the Three-Dimensional Dynamic Analysis of Earth Dams," by Kagawa, T., Mejia, L.H., Seed, H.B. and Lysmer, J., September 1981, (PB82 139 940)A06.
- UCB/EERC-81/15 "Three Dimensional Dynamic Response Analysis of Earth Dams," by Mejia, L.H. and Seed, H.B., September 1981, (PB82 137 274)A12.
- UCB/EERC-81/16 "Experimental Study of Lead and Elastomeric Dampers for Base Isolation Systems," by Kelly, J.M. and Hodder, S.B., October 1981, (PB82 166 182)A05.
- UCB/EERC-81/17 "The Influence of Base Isolation on the Seismic Response of Light Secondary Equipment," by Kelly, J.M., April 1981, (PB82 255 266)A04.
- UCB/EERC-81/18 "Studies on Evaluation of Shaking Table Response Analysis Procedures," by Blondet, J. M., November 1981, (PB82 197 278)A10.
- UCB/EERC-81/19 "DELIGHT.STRUCT: A Computer-Aided Design Environment for Structural Engineering," by Balling, R.J., Pister, K.S. and Polak, E., December 1981, (PB82 218 496)A07.
- UCB/EERC-81/20 "Optimal Design of Seismic-Resistant Planar Steel Frames," by Balling, R.J., Ciampi, V. and Pister, K.S., December 1981, (PB82 220 179)A07.
- UCB/EERC-82/01 "Dynamic Behavior of Ground for Seismic Analysis of Lifeline Systems," by Sato, T. and Der Kiureghian, A., January 1982, (PB82 218 926)A05.
- UCB/EERC-82/02 "Shaking Table Tests of a Tubular Steel Frame Model," by Ghanaat, Y. and Clough, R.W., January 1982, (PB82 220 161)A07.

- UCB/EERC-82/03 "Behavior of a Piping System under Seismic Excitation: Experimental Investigations of a Spatial Piping System supported by Mechanical Shock Arrestors," by Schneider, S., Lee, H.-M. and Godden, W. G., May 1982, (PB83 172 544)A09.
- UCB/EERC-82/04 "New Approaches for the Dynamic Analysis of Large Structural Systems," by Wilson, E.L., June 1982, (PB83 148 080)A05.
- UCB/EERC-82/05 "Model Study of Effects of Damage on the Vibration Properties of Steel Offshore Platforms," by Shahrivar, F. and Bouwkamp, J.G., June 1982, (PB83 148 742)A10.
- UCB/EERC-82/06 "States of the Art and Practice in the Optimum Seismic Design and Analytical Response Prediction of R/C Frame Wall Structures," by Aktan, A.E. and Bertero, V.V., July 1982, (PB83 147 736)A05.
- UCB/EERC-82/07 "Further Study of the Earthquake Response of a Broad Cylindrical Liquid-Storage Tank Model," by Manos, G.C. and Clough, R.W., July 1982, (PB83 147 744)A11.
- UCB/EERC-82/08 "An Evaluation of the Design and Analytical Seismic Response of a Seven Story Reinforced Concrete Frame," by Charney, F.A. and Bertero, V.V., July 1982, (PB83 157 628)A09.
- UCB/EERC-82/09 "Fluid-Structure Interactions: Added Mass Computations for Incompressible Fluid," by Kuo, J.S.-H., August 1982, (PB83 156 281)A07.
- UCB/EERC-82/10 "Joint-Opening Nonlinear Mechanism: Interface Smeared Crack Model," by Kuo, J.S.-H., August 1982, (PB83 149 195)A05.
- UCB/EERC-82/11 "Dynamic Response Analysis of Techí Dam," by Clough, R.W., Stephen, R.M. and Kuo, J.S.-H., August 1982, (PB83 147 496)A06.
- UCB/EERC-82/12 "Prediction of the Seismic Response of R/C Frame-Coupled Wall Structures," by Aktan, A.E., Bertero, V.V. and Piazzo, M., August 1982, (PB83 149 203)A09.
- UCB/EERC-82/13 "Preliminary Report on the Smart 1 Strong Motion Array in Taiwan," by Bolt, B.A., Loh, C.H., Penzien, J. and Tsai, Y.B., August 1982, (PB83 159 400)A10.
- UCB/EERC-82/14 "Shaking-Table Studies of an Eccentrically X-Braced Steel Structure," by Yang, M.S., September 1982, (PB83 260 778)A12.
- UCB/EERC-82/15 "The Performance of Stairways in Earthquakes," by Roha, C., Axley, J.W. and Bertero, V.V., September 1982, (PB83 157 693)A07.
- UCB/EERC-82/16 "The Behavior of Submerged Multiple Bodies in Earthquakes," by Liao, W.-G., September 1982, (PB83 158 709)A07.
- UCB/EERC-82/17 "Effects of Concrete Types and Loading Conditions on Local Bond-Slip Relationships," by Cowell, A.D., Popov, E.P. and Bertero, V.V., September 1982, (PB83 153 577)A04.
- UCB/EERC-82/18 "Mechanical Behavior of Shear Wall Vertical Boundary Members: An Experimental Investigation," by Wagner, M.T. and Bertero, V.V., October 1982, (PB83 159 764)A05.
- UCB/EERC-82/19 "Experimental Studies of Multi-support Seismic Loading on Piping Systems," by Kelly, J.M. and Cowell, A.D., November 1982.
- UCB/EERC-82/20 "Generalized Plastic Hinge Concepts for 3D Beam-Column Elements," by Chen, P. F.-S. and Powell, G.H., November 1982, (PB83 247 981)A13.
- UCB/EERC-82/21 "ANSR-II: General Computer Program for Nonlinear Structural Analysis," by Oughourlian, C.V. and Powell, G.H., November 1982, (PB83 251 330)A12.
- UCB/EERC-82/22 "Solution Strategies for Statically Loaded Nonlinear Structures," by Simons, J.W. and Powell, G.H., November 1982, (PB83 197 970)A06.
- UCB/EERC-82/23 "Analytical Model of Deformed Bar Anchorages under Generalized Excitations," by Ciampi, V., Elgehausen, R., Bertero, V.V. and Popov, E.P., November 1982, (PB83 169 532)A06.
- UCB/EERC-82/24 "A Mathematical Model for the Response of Masonry Walls to Dynamic Excitations," by Sucuoglu, H., Mengi, Y. and McNiven, H.D., November 1982, (PB83 169 011)A07.
- UCB/EERC-82/25 "Earthquake Response Considerations of Broad Liquid Storage Tanks," by Cambra, F.J., November 1982, (PB83 251 215)A09.
- UCB/EERC-82/26 "Computational Models for Cyclic Plasticity, Rate Dependence and Creep," by Mosaddad, B. and Powell, G.H., November 1982, (PB83 245 829)A08.
- UCB/EERC-82/27 "Inelastic Analysis of Piping and Tubular Structures," by Mahasuverachai, M. and Powell, G.H., November 1982, (PB83 249 987)A07.
- UCB/EERC-83/01 "The Economic Feasibility of Seismic Rehabilitation of Buildings by Base Isolation," by Kelly, J.M., January 1983, (PB83 197 988)A05.
- UCB/EERC-83/02 "Seismic Moment Connections for Moment-Resisting Steel Frames," by Popov, E.P., January 1983, (PB83 195 412)A04.
- UCB/EERC-83/03 "Design of Links and Beam-to-Column Connections for Eccentrically Braced Steel Frames," by Popov, E.P. and Malley, J.O., January 1983, (PB83 194 811)A04.
- UCB/EERC-83/04 "Numerical Techniques for the Evaluation of Soil-Structure Interaction Effects in the Time Domain," by Bayo, E. and Wilson, E.L., February 1983, (PB83 245 605)A09.
- UCB/EERC-83/05 "A Transducer for Measuring the Internal Forces in the Columns of a Frame-Wall Reinforced Concrete Structure," by Sause, R. and Bertero, V.V., May 1983, (PB84 119 494)A06.
- UCB/EERC-83/06 "Dynamic Interactions Between Floating Ice and Offshore Structures," by Croteau, P., May 1983, (PB84 119 486)A16.
- UCB/EERC-83/07 "Dynamic Analysis of Multiply Tuned and Arbitrarily Supported Secondary Systems," by Igusa, T. and Der Kiureghian, A., July 1983, (PB84 118 272)A11.
- UCB/EERC-83/08 "A Laboratory Study of Submerged Multi-body Systems in Earthquakes," by Ansari, G.R., June 1983, (PB83 261 842)A17.
- UCB/EERC-83/09 "Effects of Transient Foundation Uplift on Earthquake Response of Structures," by Yim, C.-S. and Chopra, A.K., June 1983, (PB83 261 396)A07.
- UCB/EERC-83/10 "Optimal Design of Friction-Braced Frames under Seismic Loading," by Austin, M.A. and Pister, K.S., June 1983, (PB84 119 288)A06.
- UCB/EERC-83/11 "Shaking Table Study of Single-Story Masonry Houses: Dynamic Performance under Three Component Seismic Input and Recommendations," by Manos, G.C., Clough, R.W. and Mayes, R.L., July 1983, (UCB/EERC-83/11)A08.
- UCB/EERC-83/12 "Experimental Error Propagation in Pseudodynamic Testing," by Shiing, P.B. and Mahin, S.A., June 1983, (PB84 119 270)A09.
- UCB/EERC-83/13 "Experimental and Analytical Predictions of the Mechanical Characteristics of a 1/5-scale Model of a 7-story R/C Frame-Wall Building Structure," by Aktan, A.E., Bertero, V.V., Chowdhury, A.A. and Nagashima, T., June 1983, (PB84 119 213)A07.

- UCB/EERC-83/14 "Shaking Table Tests of Large-Panel Precast Concrete Building System Assemblages," by Oliva, M.G. and Clough, R.W., June 1983, (PB86 110 210/AS)A11.
- UCB/EERC-83/15 "Seismic Behavior of Active Beam Links in Eccentrically Braced Frames," by Hjelmstad, K.D. and Popov, E.P., July 1983, (PB84 119 676)A09.
- UCB/EERC-83/16 "System Identification of Structures with Joint Rotation," by Dimsdale, J.S., July 1983, (PB84 192 210)A06.
- UCB/EERC-83/17 "Construction of Inelastic Response Spectra for Single-Degree-of-Freedom Systems," by Mahin, S. and Lin, J., June 1983, (PB84 208 834)A05.
- UCB/EERC-83/18 "Interactive Computer Analysis Methods for Predicting the Inelastic Cyclic Behaviour of Structural Sections," by Kaba, S. and Mahin, S., July 1983, (PB84 192 012)A06.
- UCB/EERC-83/19 "Effects of Bond Deterioration on Hysteretic Behavior of Reinforced Concrete Joints," by Filippou, F.C., Popov, E.P. and Bertero, V.V., August 1983, (PB84 192 020)A10.
- UCB/EERC-83/20 "Correlation of Analytical and Experimental Responses of Large-Panel Precast Building Systems," by Oliva, M.G., Clough, R.W., Velkov, M. and Gavrilovic, P., May 1988.
- UCB/EERC-83/21 "Mechanical Characteristics of Materials Used in a 1/5 Scale Model of a 7-Story Reinforced Concrete Test Structure," by Bertero, V.V., Aktan, A.E., Harris, H.G. and Chowdhury, A.A., October 1983, (PB84 193 697)A05.
- UCB/EERC-83/22 "Hybrid Modelling of Soil-Structure Interaction in Layered Media," by Tzong, T.-J. and Penzien, J., October 1983, (PB84 192 178)A08.
- UCB/EERC-83/23 "Local Bond Stress-Slip Relationships of Deformed Bars under Generalized Excitations," by Eligehausen, R., Popov, E.P. and Bertero, V.V., October 1983, (PB84 192 848)A09.
- UCB/EERC-83/24 "Design Considerations for Shear Links in Eccentrically Braced Frames," by Malley, J.O. and Popov, E.P., November 1983, (PB84 192 186)A07.
- UCB/EERC-84/01 "Pseudodynamic Test Method for Seismic Performance Evaluation: Theory and Implementation," by Shing, P.-S.B. and Mahin, S.A., January 1984, (PB84 190 644)A08.
- UCB/EERC-84/02 "Dynamic Response Behavior of Kiang Hong Dian Dam," by Clough, R.W., Chang, K.-T., Chen, H.-Q. and Stephen, R.M., April 1984, (PB84 209 402)A08.
- UCB/EERC-84/03 "Refined Modelling of Reinforced Concrete Columns for Seismic Analysis," by Kaba, S.A. and Mahin, S.A., April 1984, (PB84 234 384)A06.
- UCB/EERC-84/04 "A New Floor Response Spectrum Method for Seismic Analysis of Multiply Supported Secondary Systems," by Asfura, A. and Der Kiureghian, A., June 1984, (PB84 239 417)A06.
- UCB/EERC-84/05 "Earthquake Simulation Tests and Associated Studies of a 1/5th-scale Model of a 7-Story R/C Frame-Wall Test Structure," by Bertero, V.V., Aktan, A.E., Charney, F.A. and Sause, R., June 1984, (PB84 239 409)A09.
- UCB/EERC-84/06 "R/C Structural Walls: Seismic Design for Shear," by Aktan, A.E. and Bertero, V.V., 1984.
- UCB/EERC-84/07 "Behavior of Interior and Exterior Flat-Plate Connections subjected to Inelastic Load Reversals," by Zee, H.L. and Moehle, J.P., August 1984, (PB86 117 629/AS)A07.
- UCB/EERC-84/08 "Experimental Study of the Seismic Behavior of a Two-Story Flat-Plate Structure," by Moehle, J.P. and Diebold, J.W., August 1984, (PB86 122 553/AS)A12.
- UCB/EERC-84/09 "Phenomenological Modeling of Steel Braces under Cyclic Loading," by Ikeda, K., Mahin, S.A. and Dermitzakis, S.N., May 1984, (PB86 132 198/AS)A08.
- UCB/EERC-84/10 "Earthquake Analysis and Response of Concrete Gravity Dams," by Fenves, G. and Chopra, A.K., August 1984, (PB85 193 902/AS)A11.
- UCB/EERC-84/11 "EAGD-84: A Computer Program for Earthquake Analysis of Concrete Gravity Dams," by Fenves, G. and Chopra, A.K., August 1984, (PB85 193 613/AS)A05.
- UCB/EERC-84/12 "A Refined Physical Theory Model for Predicting the Seismic Behavior of Braced Steel Frames," by Ikeda, K. and Mahin, S.A., July 1984, (PB85 191 450/AS)A09.
- UCB/EERC-84/13 "Earthquake Engineering Research at Berkeley - 1984," by , August 1984, (PB85 197 341/AS)A10.
- UCB/EERC-84/14 "Moduli and Damping Factors for Dynamic Analyses of Cohesionless Soils," by Seed, H.B., Wong, R.T., Idriss, I.M. and Tokimatsu, K., September 1984, (PB85 191 468/AS)A04.
- UCB/EERC-84/15 "The Influence of SPT Procedures in Soil Liquefaction Resistance Evaluations," by Seed, H.B., Tokimatsu, K., Harder, L.F. and Chung, R.M., October 1984, (PB85 191 732/AS)A04.
- UCB/EERC-84/16 "Simplified Procedures for the Evaluation of Settlements in Sands Due to Earthquake Shaking," by Tokimatsu, K. and Seed, H.B., October 1984, (PB85 197 887/AS)A03.
- UCB/EERC-84/17 "Evaluation of Energy Absorption Characteristics of Bridges under Seismic Conditions," by Imbsen, R.A. and Penzien, J., November 1984.
- UCB/EERC-84/18 "Structure-Foundation Interactions under Dynamic Loads," by Liu, W.D. and Penzien, J., November 1984, (PB87 124 889/AS)A11.
- UCB/EERC-84/19 "Seismic Modelling of Deep Foundations," by Chen, C.-H. and Penzien, J., November 1984, (PB87 124 798/AS)A07.
- UCB/EERC-84/20 "Dynamic Response Behavior of Quan Shui Dam," by Clough, R.W., Chang, K.-T., Chen, H.-Q., Stephen, R.M., Ghanaat, Y. and Qi, J.-H., November 1984, (PB86 115177/AS)A07.
- UCB/EERC-85/01 "Simplified Methods of Analysis for Earthquake Resistant Design of Buildings," by Cruz, E.F. and Chopra, A.K., February 1985, (PB86 112299/AS)A12.
- UCB/EERC-85/02 "Estimation of Seismic Wave Coherency and Rupture Velocity using the SMART 1 Strong-Motion Array Recordings," by Abrahamson, N.A., March 1985, (PB86 214 343)A07.

- UCB/EERC-85/03 "Dynamic Properties of a Thirty Story Condominium Tower Building," by Stephen, R.M., Wilson, E.L. and Stander, N., April 1985, (PB86 118965/AS)A06.
- UCB/EERC-85/04 "Development of Substructuring Techniques for On-Line Computer Controlled Seismic Performance Testing," by Dermitzakis, S. and Mahin, S., February 1985, (PB86 132941/AS)A08.
- UCB/EERC-85/05 "A Simple Model for Reinforcing Bar Anchorages under Cyclic Excitations," by Filippou, F.C., March 1985, (PB86 112 919/AS)A05.
- UCB/EERC-85/06 "Racking Behavior of Wood-framed Gypsum Panels under Dynamic Load," by Oliva, M.G., June 1985.
- UCB/EERC-85/07 "Earthquake Analysis and Response of Concrete Arch Dams," by Fok, K.-L. and Chopra, A.K., June 1985, (PB86 139672/AS)A10.
- UCB/EERC-85/08 "Effect of Inelastic Behavior on the Analysis and Design of Earthquake Resistant Structures," by Lin, J.P. and Mahin, S.A., June 1985, (PB86 135340/AS)A08.
- UCB/EERC-85/09 "Earthquake Simulator Testing of a Base-Isolated Bridge Deck," by Kelly, J.M., Buckle, I.G. and Tsai, H.-C., January 1986, (PB87 124 152/AS)A06.
- UCB/EERC-85/10 "Simplified Analysis for Earthquake Resistant Design of Concrete Gravity Dams," by Fenves, G. and Chopra, A.K., June 1986, (PB87 124 160/AS)A08.
- UCB/EERC-85/11 "Dynamic Interaction Effects in Arch Dams," by Clough, R.W., Chang, K.-T., Chen, H.-Q. and Ghanaat, Y., October 1985, (PB86 135027/AS)A05.
- UCB/EERC-85/12 "Dynamic Response of Long Valley Dam in the Mammoth Lake Earthquake Series of May 25-27, 1980," by Lai, S. and Seed, H.B., November 1985, (PB86 142304/AS)A05.
- UCB/EERC-85/13 "A Methodology for Computer-Aided Design of Earthquake-Resistant Steel Structures," by Austin, M.A., Pister, K.S. and Mahin, S.A., December 1985, (PB86 159480/AS)A10.
- UCB/EERC-85/14 "Response of Tension-Leg Platforms to Vertical Seismic Excitations," by Liou, G.-S., Penzien, J. and Yeung, R.W., December 1985, (PB87 124 871/AS)A08.
- UCB/EERC-85/15 "Cyclic Loading Tests of Masonry Single Piers: Volume 4 - Additional Tests with Height to Width Ratio of 1," by Sveinsson, B., McNiven, H.D. and Sucuoglu, H., December 1985.
- UCB/EERC-85/16 "An Experimental Program for Studying the Dynamic Response of a Steel Frame with a Variety of Infill Partitions," by Yanev, B. and McNiven, H.D., December 1985.
- UCB/EERC-86/01 "A Study of Seismically Resistant Eccentrically Braced Steel Frame Systems," by Kasai, K. and Popov, E.P., January 1986, (PB87 124 178/AS)A14.
- UCB/EERC-86/02 "Design Problems in Soil Liquefaction," by Seed, H.B., February 1986, (PB87 124 186/AS)A03.
- UCB/EERC-86/03 "Implications of Recent Earthquakes and Research on Earthquake-Resistant Design and Construction of Buildings," by Bertero, V.V., March 1986, (PB87 124 194/AS)A05.
- UCB/EERC-86/04 "The Use of Load Dependent Vectors for Dynamic and Earthquake Analyses," by Leger, P., Wilson, E.L. and Clough, R.W., March 1986, (PB87 124 202/AS)A12.
- UCB/EERC-86/05 "Two Beam-To-Column Web Connections," by Tsai, K.-C. and Popov, E.P., April 1986, (PB87 124 301/AS)A04.
- UCB/EERC-86/06 "Determination of Penetration Resistance for Coarse-Grained Soils using the Becker Hammer Drill," by Harder, L.F. and Seed, H.B., May 1986, (PB87 124 210/AS)A07.
- UCB/EERC-86/07 "A Mathematical Model for Predicting the Nonlinear Response of Unreinforced Masonry Walls to In-Plane Earthquake Excitations," by Mengi, Y. and McNiven, H.D., May 1986, (PB87 124 780/AS)A06.
- UCB/EERC-86/08 "The 19 September 1985 Mexico Earthquake: Building Behavior," by Bertero, V.V., July 1986.
- UCB/EERC-86/09 "EACD-3D: A Computer Program for Three-Dimensional Earthquake Analysis of Concrete Dams," by Fok, K.-L., Hall, J.F. and Chopra, A.K., July 1986, (PB87 124 228/AS)A08.
- UCB/EERC-86/10 "Earthquake Simulation Tests and Associated Studies of a 0.3-Scale Model of a Six-Story Concentrically Braced Steel Structure," by Uang, C.-M. and Bertero, V.V., December 1986, (PB87 163 564/AS)A17.
- UCB/EERC-86/11 "Mechanical Characteristics of Base Isolation Bearings for a Bridge Deck Model Test," by Kelly, J.M., Buckle, I.G. and Koh, C.-G., November 1987.
- UCB/EERC-86/12 "Effects of Axial Load on Elastomeric Isolation Bearings," by Koh, C.-G. and Kelly, J.M., November 1987.
- UCB/EERC-87/01 "The FPS Earthquake Resisting System: Experimental Report," by Zayas, V.A., Low, S.S. and Mahin, S.A., June 1987.
- UCB/EERC-87/02 "Earthquake Simulator Tests and Associated Studies of a 0.3-Scale Model of a Six-Story Eccentrically Braced Steel Structure," by Whitaker, A., Uang, C.-M. and Bertero, V.V., July 1987.
- UCB/EERC-87/03 "A Displacement Control and Uplift Restraint Device for Base-Isolated Structures," by Kelly, J.M., Griffith, M.C. and Aiken, I.D., April 1987.
- UCB/EERC-87/04 "Earthquake Simulator Testing of a Combined Sliding Bearing and Rubber Bearing Isolation System," by Kelly, J.M. and Chalhoub, M.S., 1987.
- UCB/EERC-87/05 "Three-Dimensional Inelastic Analysis of Reinforced Concrete Frame-Wall Structures," by Moazzami, S. and Bertero, V.V., May 1987.
- UCB/EERC-87/06 "Experiments on Eccentrically Braced Frames with Composite Floors," by Ricles, J. and Popov, E., June 1987.
- UCB/EERC-87/07 "Dynamic Analysis of Seismically Resistant Eccentrically Braced Frames," by Ricles, J. and Popov, E., June 1987.
- UCB/EERC-87/08 "Undrained Cyclic Triaxial Testing of Gravels-The Effect of Membrane Compliance," by Evans, M.D. and Seed, H.B., July 1987.
- UCB/EERC-87/09 "Hybrid Solution Techniques for Generalized Pseudo-Dynamic Testing," by Thewalt, C. and Mahin, S.A., July 1987.
- UCB/EERC-87/10 "Ultimate Behavior of Butt Welded Splices in Heavy Rolled Steel Sections," by Bruneau, M., Mahin, S.A. and Popov, E.P., July 1987.
- UCB/EERC-87/11 "Residual Strength of Sand from Dam Failures in the Chilean Earthquake of March 3, 1985," by De Alba, P., Seed, H.B., Retamal, E. and Seed, R.B., September 1987.

- UCB/EERC-87/12 "Inelastic Seismic Response of Structures with Mass or Stiffness Eccentricities in Plan," by Bruneau, M. and Mahin, S.A., September 1987.
- UCB/EERC-87/13 "CSTRUCT: An Interactive Computer Environment for the Design and Analysis of Earthquake Resistant Steel Structures," by Austin, M.A., Mahin, S.A. and Pister, K.S., September 1987.
- UCB/EERC-87/14 "Experimental Study of Reinforced Concrete Columns Subjected to Multi-Axial Loading," by Low, S.S. and Moehle, J.P., September 1987.
- UCB/EERC-87/15 "Relationships between Soil Conditions and Earthquake Ground Motions in Mexico City in the Earthquake of Sept. 19, 1985," by Seed, H.B., Romo, M.P., Sun, J., Jaime, A. and Lysmer, J., October 1987.
- UCB/EERC-87/16 "Experimental Study of Seismic Response of R. C. Setback Buildings," by Shahrooz, B.M. and Moehle, J.P., October 1987.
- UCB/EERC-87/17 "The Effect of Slabs on the Flexural Behavior of Beams," by Pantazopoulou, S.J. and Moehle, J.P., October 1987.
- UCB/EERC-87/18 "Design Procedure for R-FBI Bearings," by Mostaghei, N. and Kelly, J.M., November 1987.
- UCB/EERC-87/19 "Analytical Models for Predicting the Lateral Response of R C Shear Walls: Evaluation of their Reliability," by Vulcano, A. and Bertero, V.V., November 1987.
- UCB/EERC-87/20 "Earthquake Response of Torsionally-Coupled Buildings," by Hejal, R. and Chopra, A.K., December 1987.
- UCB/EERC-87/21 "Dynamic Reservoir Interaction with Monticello Dam," by Clough, R.W., Ghanaat, Y. and Qiu, X-F., December 1987.
- UCB/EERC-87/22 "Strength Evaluation of Coarse-Grained Soils," by Siddiqi, F.H., Seed, R.B., Chan, C.K., Seed, H.B. and Pyke, F., December 1987.
- UCB/EERC-88/01 "Seismic Behavior of Concentrically Braced Steel Frames," by Khatib, I., Mahin, S.A. and Pister, K.S., January 1988.
- UCB/EERC-88/02 "Experimental Evaluation of Seismic Isolation of Medium-Rise Structures Subject to Uplift," by Griffith, M.C., Kelly, J.M., Coveney, V.A. and Koh, C.G., January 1988.
- UCB/EERC-88/03 "Cyclic Behavior of Steel Double Angle Connections," by Astaneh-Asl, A. and Nader, M.N., January 1988.
- UCB/EERC-88/04 "Re-evaluation of the Slide in the Lower San Fernando Dam in the Earthquake of Feb. 9, 1971," by Seed, H.B., Seed, R.B., Harder, L.F. and Jong, H.-L., April 1988.
- UCB/EERC-88/05 "Experimental Evaluation of Seismic Isolation of a Nine-Story Braced Steel Frame Subject to Uplift," by Griffith, M.C., Kelly, J.M. and Aiken, I.D., May 1988.
- UCB/EERC-88/06 "DRAIN-2DX User Guide," by Allahabadi, R. and Powell, G.H., March 1988.
- UCB/EERC-88/07 "Cylindrical Fluid Containers in Base-Isolated Structures," by Chalhoub, M.S. and Kelly, J.M., April 1988.
- UCB/EERC-88/08 "Analysis of Near-Source Waves: Separation of Wave Types using Strong Motion Array Recordings," by Darragh, R.B., June 1988.
- UCB/EERC-88/09 "Alternatives to Standard Mode Superposition for Analysis of Non-Classically Damped Systems," by Kusainov, A.A. and Clough, R.W., June 1988.
- UCB/EERC-88/10 "The Landslide at the Port of Nice on October 16, 1979," by Seed, H.B., Seed, R.B., Schlosser, F., Blondeau, F. and Juran, I., June 1988.
- UCB/EERC-88/11 "Liquefaction Potential of Sand Deposits Under Low Levels of Excitation," by Carter, D.P. and Seed, H.B., August 1988.
- UCB/EERC-88/12 "Nonlinear Analysis of Reinforced Concrete Frames Under Cyclic Load Reversals," by Filippou, F.C. and Issa, A., September 1988.
- UCB/EERC-88/13 "Implications of Recorded Earthquake Ground Motions on Seismic Design of Building Structures," by Uang, C.-M. and Bertero, V.V., September 1988.
- UCB/EERC-88/14 "An Experimental Study of the Behavior of Dual Steel Systems," by Whittaker, A.S., Uang, C.-M. and Bertero, V.V., September 1988.
- UCB/EERC-88/15 "Dynamic Moduli and Damping Ratios for Cohesive Soils," by Sun, J.I., Golesorkhi, R. and Seed, H.B., August 1988.
- UCB/EERC-88/16 "Reinforced Concrete Flat Plates Under Lateral Load: An Experimental Study Including Biaxial Effects," by Pan, A. and Moehle, J., November 1988.
- UCB/EERC-88/17 "Earthquake Engineering Research at Berkeley - 1988," by EERC, November 1988.
- UCB/EERC-88/18 "Use of Energy as a Design Criterion in Earthquake-Resistant Design," by Uang, C.-M. and Bertero, V.V., November 1988.
- UCB/EERC-88/19 "Steel Beam-Column Joints in Seismic Moment Resisting Frames," by Tsai, K.-C. and Popov, E.P., September 1988.
- UCB/EERC-88/20 "Base Isolation in Japan, 1988," by Kelly, J.M., December 1988.
- UCB/EERC-89/01 "Behavior of Long Links in Eccentrically Braced Frames," by Engelhardt, M.D. and Popov, E.P., January 1989.
- UCB/EERC-89/02 "Earthquake Simulator Testing of Steel Plate Added Damping and Stiffness Elements," by Whittaker, A., Bertero, V.V., Alonso, J. and Thompson, C., January 1989.
- UCB/EERC-89/03 "Implications of Site Effects in the Mexico City Earthquake of Sept. 19, 1985 for Earthquake-Resistant Design Criteria in the San Francisco Bay Area of California," by Seed, H.B. and Sun, J.I., March 1989.
- UCB/EERC-89/04 "Earthquake Analysis and Response of Intake-Outlet Towers," by Goyal, A. and Chopra, A.K., July 1989.
- UCB/EERC-89/05 "The 1985 Chile Earthquake: An Evaluation of Structural Requirements for Bearing Wall Buildings," by Wallace, J.W. and Moehle, J.P., July 1989.